

K⁺ Channels: Function-Structural Overview

Carlos González,¹ David Baez-Nieto,¹ Ignacio Valencia,¹ Ingrid Oyarzún,¹ Patricio Rojas,² David Naranjo,¹ and Ramón Latorre^{*1}

ABSTRACT

Potassium channels are particularly important in determining the shape and duration of the action potential, controlling the membrane potential, modulating hormone secretion, epithelial function and, in the case of those K⁺ channels activated by Ca²⁺, damping excitatory signals. The multiplicity of roles played by K⁺ channels is only possible to their mammoth diversity that includes at present 70 K⁺ channels encoding genes in mammals. Today, thanks to the use of cloning, mutagenesis, and the more recent structural studies using x-ray crystallography, we are in a unique position to understand the origins of the enormous diversity of this superfamily of ion channels, the roles they play in different cell types, and the relations that exist between structure and function. With the exception of two-pore K⁺ channels that are dimers, voltage-dependent K⁺ channels are tetrameric assemblies and share an extremely well conserved pore region, in which the ion-selectivity filter resides. In the present overview, we discuss in the function, localization, and the relations between function and structure of the five different subfamilies of K⁺ channels: (a) inward rectifiers, Kir; (b) four transmembrane segments-2 pores, K_{2P}; (c) voltage-gated, Kv; (d) the Slo family; and (e) Ca²⁺-activated SK family, SKCa. © 2012 American Physiological Society. *Compr Physiol* 2:2087-2149, 2012.

Introduction

It is most probable that K⁺ channels started to evolve from the moment that life appeared on earth, as the presence of more than 200 potassium channel-related proteins in archaea and bacteria attest. Once K⁺ channels were identified in bacteria (485), the dream of many biophysicists, to have large quantities of channel protein to produce crystals amenable to x-ray analysis, became a reality. This feat was performed by MacKinnon's group (115) when they crystallized the K⁺ channel (KcsA) from the bacterium *Streptomyces lividans*. This primitive K⁺ channel is a tetramer composed of four identical subunits consisting in two transmembrane (TM) domains connected by a pore region, in which the ion-selectivity filter resides. The exquisite K⁺ selectivity of this class of ion channels is conferred by amino acids located in the pore region, the signature sequence T/SXGXGX (193).

This structure of the pore present in KcsA channels is retained in all the K⁺ channels known to date, including those present in fungi, protozoans, and metazoans but although the pore structure did not evolved considerably, other parts of the channel sequence show considerable structural diversity. Thus, we have organized the present overview by dividing K⁺ channels in three structural classes (157, 181, 280, 377, 467, 569) (Fig. 1): (i) the inward rectifier (Kir) family that follows the same structural pattern of the KcsA channel, their subunits contain two TM segments flanking the pore-forming domain and they assemble as tetramers. In mammals, Kir channels are encoded by 15 different genes grouped into 7 subfamilies, Kir1.x to Kir7.x and this diversity has been greatly increased by the identification of 6 alternative splicing isoforms in the

case of Kir1.1 and the ability of the proteins inside the subfamilies to form heteromultimers (203, 436); (ii) the two-pore four TM segments K⁺ channels (K_{2P}) family, which in contrast to the other families we discuss in the present article, their subunits assemble as dimers. Fifteen different genes of this family has been found in mammals and surprisingly this class of channels has 46 genes in the worm *Caenorhabditis elegans*; (iii) the six TM (S1-S6) segments K⁺ channels with one pore domain (S5-P-S6) that include the subfamily of voltage-gated channels, Kv1.x to Kv4.x (corresponding to Shaker, Shab, Shaw, and Shal channels, respectively, in *Drosophila*). Consisting of eight different genes the Kv1.x (*Shaker*) subfamily is the largest in this structural class of K⁺ channels. Voltage-dependent K⁺ channels are characterized by containing a voltage-sensor domain (VSD; S1-S4) in which the S4 contains positively charged amino acids that constitute the voltage-sensing elements. The six TM domains class also includes the KCNQ (Kv7.x), ether-a-go-go (Kv10.x; gated by voltage and cyclic nucleotides), erg (Kv11.x), and elk (Kv12.2) subfamilies.

Despite the fact that Kv5, Kv6, Kv8, and Kv9 share the same general structure with other members of the Kv

*Correspondence to ramon.latorre@uv.cl

¹ Centro Interdisciplinario de Neurociencia de Valparaíso, Facultad de Ciencias, Universidad de Valparaíso, Valparaíso, Chile

² Departamento de Química y Biología, Universidad de Santiago de Chile, Santiago, Chile

Published online, July 2012 (comprehensivephysiology.com)

DOI: 10.1002/cphy.c110047

Copyright © American Physiological Society

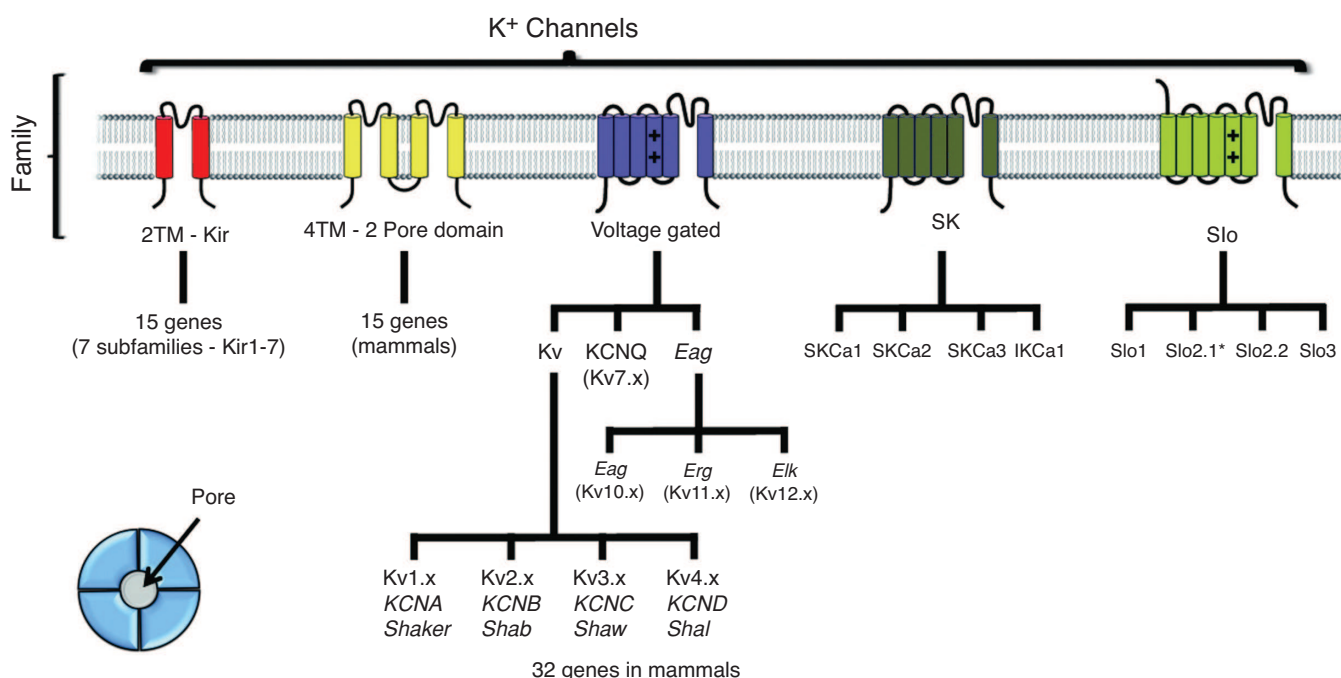


Figure 1 Potassium channel families arranged according to their subunit structure. Potassium channel families can be grouped in those having two transmembrane segments (2TM; Kir), 4TM (2-pore domain), 6TM (voltage gated and SK), and 7TM (Slo). Note that for the sake of simplicity the large-conductance Slo channel family includes the Slo2.x channels, which have only six transmembrane domains. The 6TM domain class can be divided into four families: Voltage-gated Kv, voltage-gated KCNQ-type (KCNQ); ether- α -go-go (Eag), and Ca²⁺-activated channels (SK). Subdivisions of the voltage-gated Kv channels into four subfamilies and Eag into three subfamilies are also named according to the *Drosophila melanogaster* genes. In the SK family IKCa1 stands for intermediate conductance Ca²⁺-activated K⁺ channel.

family, they do not form functional channels. These proteins have been denominated silent (KvS) subunits. However, by forming heterotetrameric channels with Kv2 and Kv3 α -subunits they modulate the biophysical properties and inhibit the expression of these outward rectifier channels (181, 224, 408, 472).

To this extended six TM domains family, we must add the small conductance (SKCa) Ca²⁺-activated K⁺ channels (271, 569) and the Slo channel subfamily. SKCa channels, although containing two arginines in the S4 segment, are voltage insensitive and gated by submicromolar levels of intracellular Ca²⁺. On the other hand, the Slo channel subfamily α -subunits (466, 569) consist of four members; Slo1 and Slo3, unlike the other K⁺ channels, contain seven TM segments α -subunits and hence their N-terminus faces the extracellular medium. The other two members of this subfamily, Slo2.1 and Slo2.2 (Slick and Slack, respectively) have; however, α -subunits containing six TM domains.

After this bird's-eye look on K⁺ channel diversity, several questions arise: why is there such a large diversity of K⁺ channels? What role does each of them play? How their activity is regulated? What are the relations between structure and function? Precisely, because of this huge channel diversity, it would be impossible to give a detailed response to all these questions, either because the answer to each of them will require a treatise or simply because the answer is unknown. Given this complex scenario, our choice has been to give an

overview of what (arbitrarily), we think is important to know about this superfamily of ion channels that may be considered the guardians of the cellular electrical homeostasis.

Kir Channels Family

The seven Kir channel subfamilies (Fig. 2A) can be classified into four functional groups [Hibino et al. (203)]: (i) classical Kir; (ii) G-protein-gated channels (Kir3.x); (iii) ATP-sensitive K⁺ channels (Kir6.x); and (iv) K⁺-transport channels.

Function and localization

In 1949, Bernard Katz (255) reported in muscle the presence of a potassium current that behave “anomalously” when compared with the outwardly rectifying K⁺ like the one present in the squid axon. Depending of the electrochemical gradient, K⁺ current was flowing inwardly (Fig. 2B). This was the first Kir channel characterized and since this K⁺ conductance only develops at voltages negative to the equilibrium potential for K⁺ (E_K), it will become important in setting the resting potential near E_K (185). In Kir channels, the inward arises from a voltage-dependent block induced by Mg²⁺ or polyamines (319, 320, 358, 557). Not all Kir channels show the same degree of inward rectification. There are “weak” (Fig. 2C) and “strong” Kir (Fig. 2D) channels and the molecular nature of the differences between these two types of

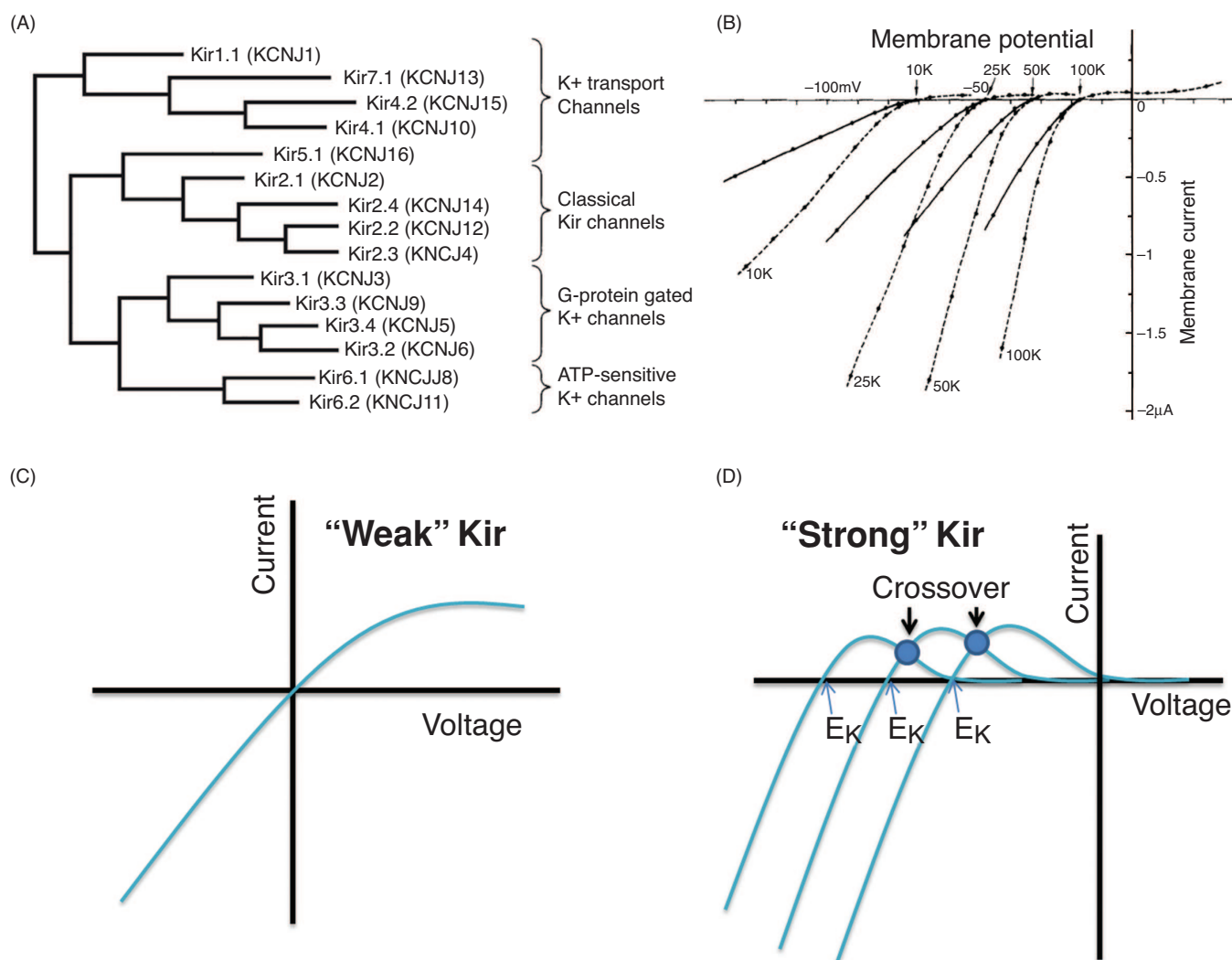


Figure 2 Phylogenetic tree of Kir channels and their current-voltage curves. (A) Amino acid sequence alignments and phylogenetic analysis for the 15 known members of the human Kir family. International Union of Pharmacology and Hugo Gene Nomenclature Committee names of the genes are shown. The subunits were classified into four functional groups following Hibino et al. (2003). (B) Inward rectification and conductance are strongly external K⁺ concentration-dependent. I-V relationships are of the starfish egg cell membrane at four different K_{ext} concentrations in Na⁺-free media. Continuous and broken line indicates instantaneous and steady-state current, respectively (adapted, with permission, from reference 185). Notice that K⁺ conductance develops at voltages negative to the equilibrium potential for K⁺ (E_K). (C) I-V relationship characteristic of a "weak" inward rectifier. (D) In "strong" inward rectifiers K⁺ conductance tends to zero as the membrane potential is depolarized and contrary to expectations the crossover phenomena produces an increase in K⁺ conductance at voltages larger than the crossover voltage despite the decrease in the K⁺ driving force.

channels will be discussed later when we look at the Kir channel structure. Gating in Kir channels is also modulated by nucleotides such as adenosine-tri-phosphate (ATP) and adenosine-di-phosphate (ADP), phosphorylation, G-proteins, and phosphatidyl-inositol-4,5-bisphosphate (PIP₂). It is important to note here that in the absence of PIP₂ a large number of different Kir channels [e.g., Kir2.1, Kir6.2/SUR2A, and Kir3.x; (530)] suffer a pronounced rundown suggesting that this lipid is essential for normal channel functioning. In the absence of PIP₂, current rundown is complete in the whole Kir3.x subfamily (GIRK).

Kir channels are blocked by Ba²⁺ and Cs⁺ but some of the classical K⁺ channels inhibitors like tetraethylammonium

(TEA) or 4-aminopyridine (4-AP) have little effect on Kir channels [e.g., Hibino et al. (2005)]. However, the sensitivity to external Ba²⁺ depends, on the type of Kir channels. We can find large differences in Ba²⁺ sensitivity within a subfamily and in between different Kir subfamilies. Kir2.2 is about 65-fold more sensitive to Ba²⁺ than Kir2.4 (545), and Kir3.x channels are approximately 100-fold less sensitive than Kir2.1 when tested under similar experimental conditions (303,496). Tertiapin, a toxin present in the honeybee venom, is able to block Kir3.x and Kir1.1 channels at nanomolar concentrations and the oxidation-resistant product known as tertiapinQ is able to specifically block Kir3.x channels (241,242).

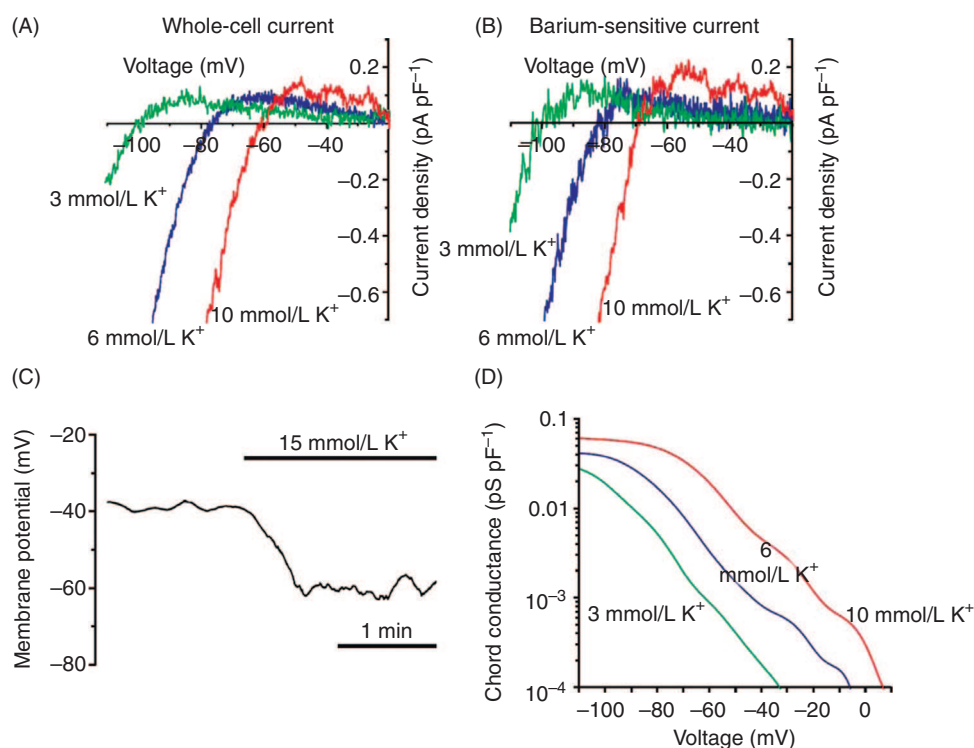


Figure 3 Kir2.1 induces a smooth muscle cell hyperpolarization when K_{ext} increases. (A) The average current densities at three different $[K_{\text{ext}}]$ were obtained in response to a voltage ramp from -130 to 0 mV lasting for 140 ms. (B) Ba^{2+} -sensitive currents densities recorded in the same condition as in A. (C) Elevation of K_{ext} from 3 mmol/L to 15 mmol/L caused a membrane potential hyperpolarization of smooth muscle cells [adapted, with permission, from Filosa et al. (139)]. (D) Chord conductance-voltage curve at the same experimental conditions as in B. Notice that there is an appreciable increase in smooth muscle cells Kir conductance as the $[K_{\text{ext}}]$ is raised at physiological membrane potentials (-50 to -40 mV).

The seven Kir channel subfamilies (Fig. 2A) can be classified into four functional groups [Hibino et al. (203)].

Classical Kir (Kir2.x)

These channels exhibit a strong inward rectification, are constitutively active, and are most prominent in ventricular tissue. In cardiac myocytes, they give origin to the background current, I_{K1} , and stabilize the resting potential (≈ -90 mV) near the K⁺ equilibrium potential [E_K (8)]. This background current becomes negligible at $V > E_K$ and the absence of I_{K1} at depolarizing potentials results in a maintained depolarization that shapes the plateau of the cardiac action potential. I_{K1} is induced by Kir2.1/Kir2.2 heteromeric channels (633). It is important to note here that about 50% of the background current is lost in the Kir2.2 knockout mice whereas removal of the Kir2.1 channel promotes the complete disappearance of I_{K1} (617). Unlike wild-type ventricular myocytes that are quiescent, ventricular myocytes isolated from the heart of Kir2.1 knockout mice show spontaneous activity and broader action potentials. These observations strongly suggest that Kir2.1 commands the I_{K1} currents in the heart.

Classical Kirs, mainly Kir 2.2 (133), are also present in endothelial cells and smooth muscle cells where they play an important role in setting the vascular tone. In endothelial cell, by setting a negative resting potential, they provide the driving force for Ca^{2+} to enter the cell and activate the metabolic machinery that produces the vasorelaxant, NO (288,571). In vascular smooth muscle cells (VSMCs), contrary to expectations and as a consequence of the crossover effect (Figs. 2D and 3A and B), Kir2.1 (617) hyperpolarize the cells in response to an increase in the external K⁺ concentration (Fig. 3C; e.g., reference 268) promoting *dilation* of rat coronary and cerebral arteries. This is the result of an increase in Kir-dependent conductance (Fig. 3D). In the brain, the perivascular space K⁺ concentration can be elevated due to K⁺ secretion mediated by Slo1 channels (see the Slo family channel section) present in the astrocytic bouton, a secretion promoted by neuronal activity. Therefore, the presence of a strong Kir in the VSMC, allows that the increase in K⁺ couples neuronal activity to vasodilation in the brain (139).

All classical Kir channels are expressed in the brain and their expression is restricted to neurons, soma, and dendrites where they are important in determining the resting potential

and in the control neuronal excitability (106). Interestingly, Kir2.1 and Kir2.3 are located in the microvilli of Schwann cells where they can play the role of “keepers” of the external potassium concentration by absorbing the excess of K⁺ secreted by the neurons during excitation (366).

In the kidney, we found classical Kir (Kir2.3) channels localized in the basolateral membrane of the cortical collecting duct where they maintain the membrane potential at a value that suffices to drive the K⁺ flux from the basolateral to the apical side (192).

G-protein-gated channels (Kir3.x)

These channels (K_G also known as GIRK), which are gated by membrane-bound G proteins as first reported by Kurachi et al. (286), are formed by a variety of combinations of the four subunits, Kir3.1-Kir3.4, that give origin to this functional group of Kir channels (234, 270, 276, 303, 332). Actually, Kir3.1 and Kir3.3 subunits are unable to form independently functional channels but can coassemble forming Kir3.1/Kir3.3 and Kir3.2/Kir3.3 heterotetrameric channels.

K_G channels are activated by the βγ-subunits (G_{βγ}) of pertussis toxin-sensitive guanosine triphosphate (GTP)-activated proteins (G_i or G_o-type G protein. (285, 315, 574). The dissociation of the βγ-subunits from the α-subunit of the G protein is induced by binding of agonists [acetylcholine, adenosine, γ-aminobutyric acid type B (GABA_B), dopamine] to G protein-coupled receptors (GPCRs) in the presence of GTP. The βγ-subunits bind to both N- and C-terminus of K_G channel subunits (191, 231, 504). G_{βγ} is unable to activate K_G channels in the absence of PIP₂ since if Kir3.1/Kir4.1 channels are allowed to rundown completely, they are not activated by addition of G_{βγ}, but addition of PIP₂ rapidly restores K_G channel-induced currents (223, 521). Several other modulators are able to activate K_G channels, including internal Na⁺ and phosphorylation mediated by protein kinase A [PKA; (207, 363, 380, 520)]. The channels GIRK2 (Kir3.2) and GIRK4 (Kir3.4) are sensitive to intracellular Na⁺, where the aspartate in the sequence DXRXXH is coordinating the sodium ion.

K_G channels show a basal activity even in the absence of receptor activation by agonists, activity due to the direct binding of the G_α a result supporting the hypothesis that GPCRs, G-proteins, regulatory proteins [G protein signaling (RGS) protein] and sorting nexin (SNX27) and K_G channels reside together in a signaling microdomain [Fig. 4A (145, 426)].

K_G channels are inhibited by a number of excitatory transmitters or hormones (e.g., acetylcholine, substance P, thyroid-stimulating hormone (TSH)-releasing hormones] (269, 301, 529). These transmitters or hormones by interacting with a GPCR coupled to a *pertussis toxin-insensitive* G protein (G_q) induce the activation of phospholipase C (PLC) (301, 494, 529). The depletion of PIP₂ induced by the activation of PLC mediates the inhibitory/desensitization effect

of some neurotransmitters on K_G channels [(102, 269, 301); see Fig. 4A]. The activation of PLC also promotes the activation of protein kinase C (PKC) and the PKC-dependent phosphorylation of K_G channels (Kir3.1/Kir3.4) underlies the inhibition of K_G channels by substance P (347).

In the heart, Kir3.1 and Kir3.4 subunits (276) form the K_{ACh} channel that, activated by the ACh released from the vagal nerve, decelerates the heartbeat (reviewed in reference 8). However, we should point out here that the data of reference 34 may suggest that the subunit stoichiometry of this type of channels may vary since homotetrameric Kir3.4 can be expressed in rat atrial myocytes. *I*_{K_{ACh} is most prominent in atrial tissue and in sino atrial node (SAN) and current rectification is “weak” compared to that shown by the *I*_{K1}.}

Atrial fibrillation (AF) is the most common cardiac arrhythmia in clinical practice. AF can become persistent due to remodeling of atrial electrophysiology. Electrical remodeling in AF patients causes an increase in constitutively active component of *I*_{K_{ACh} and a decrease of its ACh-induced component (112). This switch from a ligand-gated current to constitutively active behavior would lead K_G/Kir3.x channels to shorten atrial action potential duration and refractory period in cAF patients.}

In the pancreas, catecholamines and somatostatin suppress insulin secretion from β-cells (232, 451, 501, 604) by activating K_G-mediated currents. In pancreatic islets, Kir3.2 and Kir3.4 DNAs were identified and homo and heterotetramers of these two types of K_G channel subunit are probably originating the G protein-gated currents than regulate hormone secretion from islet cells (53, 136).

Present in a number of brain regions, K_G channels localized in dendritic spines, in the postsynaptic density as well as extra synaptic sites are involved in the generation of slow inhibitory postsynaptic potential [sIPSP; (331, 503); reviewed in references 203, 330, and 332]. Different types of K_G channels are, however, found in synaptic and extrasynaptic regions of neurons. Kir3.2 is present in the postsynaptic density of neurons of the *substantia nigra pars compacta*, while Kir3.1 and Kir3.2 can be detected in the extrasynaptic membrane of CA1 hippocampal pyramidal neurons (275). At extrasynaptic sites of Purkinje cells K_G channels are formed by Kir3.1/Kir3.2/Kir3.3, postsynaptic densities contain Kir3.2/Kir3.3 heterotetrameric channels, and dendritic shafts contain Kir3.1/Kir3.3 (134).

Receptor activation of K_G channels mediate at least three different changes in electrical signaling in the nervous system (332). We consider first the case of the low-threshold spiking (LTS) in neocortical neurons that possess a form of long-lasting self-inhibition mediated by endocannabinoids (22). Endocannabinoids release from dendrites activates cannabinoid receptor 1 which is coupled to K_G of the same dendrite resulting in a long-lasting hyperpolarization. Second, in CA1 hippocampal pyramidal neurons K_G channels colocalize with and are functionally coupled to γ-aminobutyric acid type B (GABA_B) receptors (275). This proximity allows

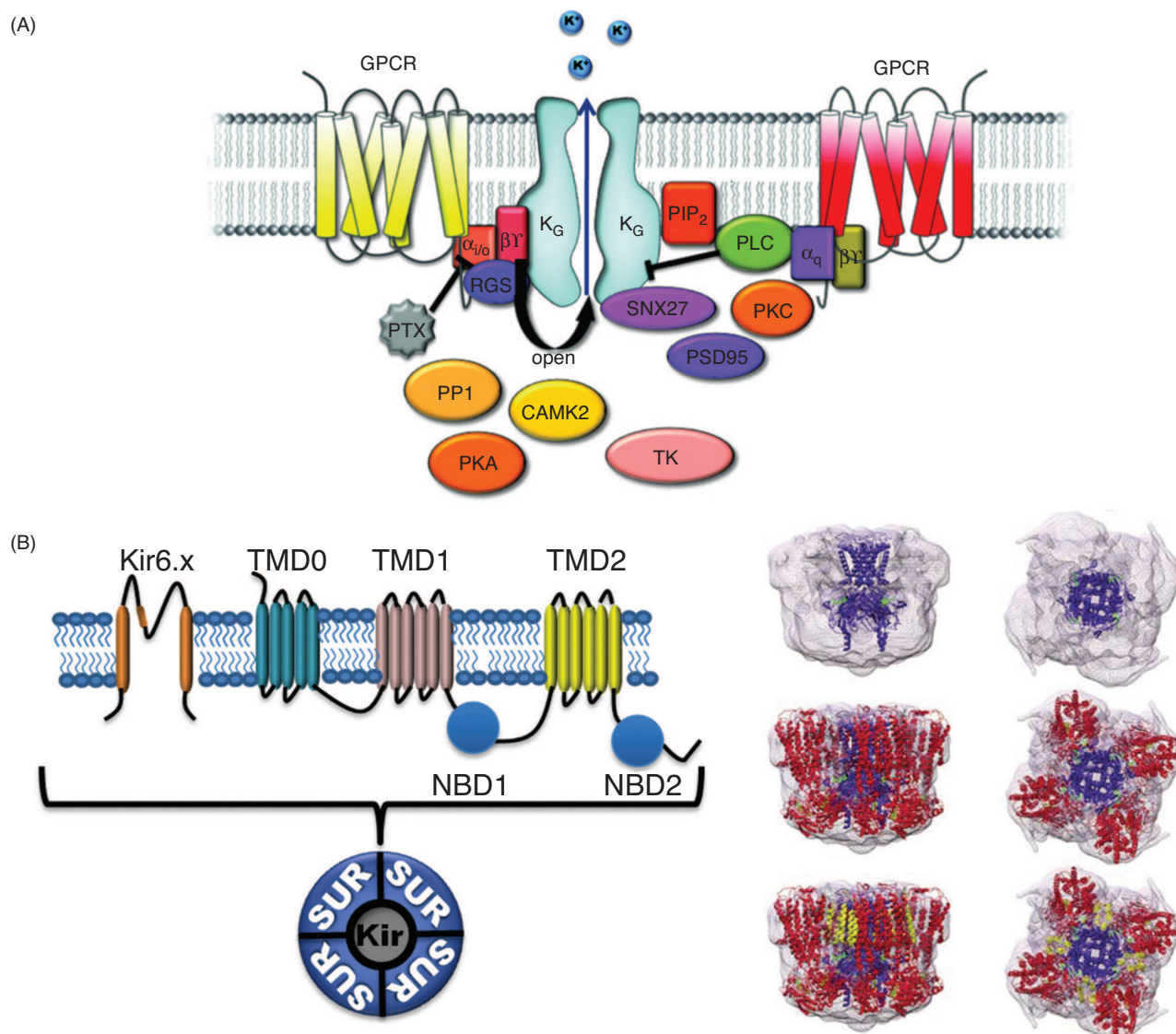


Figure 4 Dual modulation of K_G channels by G protein-coupled receptor (GPCR) and the topology and structure of Kir6.x. (A) Agonist activation of GPCR coupled to pertussis (PTX)-sensitive α_{i/o}-type of G protein promotes activation of K_G channels. Activation of K_G channels is induced by binding to the channel-forming protein of the βγ complex of the G protein. Agonist binding to α_q-type of G protein results in channel inhibition that is a consequence of the activation of phospholipase C (PLC), which in turn hydrolyses phosphatidyl-inositol-4,5-bisphosphate (PIP₂). Other modulators include tyrosine kinase (TK), Ca²⁺-calmodulin-dependent kinase 2 (CAMK2), and protein phosphatase (PP1). Modified, with permission, from reference 332. For more details, see text. (B) SUR subunits contain 17 transmembrane segments assembled in three domains, TMD0-2, and containing two nucleotide-binding domains (NBD) contained between TMD1 and TMD2 (NBD1) and in the C-terminus (NBD2). The structures show top and side views of the entire K_{ATP} channel complex analyzed at 18 Å resolution. Blue represents Kir6.x. Red represents the rest of SUR and yellow represents TMD0 of SUR [adapted, with permission, from Mikhailov et al. (367)].

the activation of K_G induced by GABAB diffusion from nearby inhibitory synaptic contacts, which end result is the sIPSP crucial in the control of rhythmic hippocampal activity (479). Third, K_G channels are also involved in large-scale neuronal network modulation through a process known as volume transmission whereby the neurotransmitter release from many neurons diffuses to activate K_G channels on target neurons. The net result of the elevation of the ambient concentration of neurotransmitters is to reduce network activity of neurons (reviewed in reference 332).

ATP-sensitive K⁺ channels (Kir6.x)

K_{ATP} channels were discovered in cardiac tissue where they are present in the sarcolemmal membranes in high density (399). These channels show a weak inward rectification and, as the classical Kir2.x channels, they have constitutive activities—in excised patches, K_{ATP} channels open spontaneously, openings that are inhibited by internal ATP. Composed of four Kir6.x and four sulfonylurea receptor (SUR1, SUR2A, and SUR2B) subunits, these channels have an

octameric stoichiometry (Fig. 4B) (81, 500). The Kir subunits form the ion channel pore and are responsible for the internal ATP channel inhibition whereas the SUR subunits, containing two nucleotide-binding domains, bind nucleotide diphosphates (NDPs; e.g., ADP) and activate K_{ATP} channels.

An array of inhibitory and stimulatory substances binds to SUR. The sulfonylureas (e.g., chlorpropamide) act as K_{ATP} channel inhibitors whereas agents such as pinacidil work as K⁺ channel openers (KCOs) (see references 18 and 116). In pancreatic β -cells, K_{ATP} channels, made up of Kir6.2 and SUR1 subunits (226, 227), play a crucial role not only in setting the resting potential but also in modulating insulin secretion (19). The small cytoplasmic ATP concentration kept by low levels of blood glucose allows the opening of K_{ATP} channels which, under those conditions are able to maintain the resting potential. As the blood glucose concentration increases, the influx of glucose produces an increase in the internal β -cell ATP concentration and K_{ATP} channels closed. The closing of K_{ATP} channels depolarizes the β -cell causing the opening of L-type voltage-dependent Ca²⁺ (VDCC) channels. The influx of Ca²⁺ through VDCC induces the fusion of insulin-containing vesicles to the plasma membrane with the consequent hormone release. Thus, K_{ATP} channels play the important role of coupling blood glucose concentration to insulin secretion.

K_{ATP} channels in the heart, due to the high internal ATP concentration in this tissue, are quiescent but they open in response to metabolic insult such as ischemia. Opening of K_{ATP} channels will shorten the cardiac action potential, reducing the Ca²⁺ influx through VDCC (252, 390, 399). Thus, in the heart, K_{ATP} channels provide protection against the insult of ischemia. These channels are directly involved in the protective role that brief periods of ischemia (preconditioning) have on a subsequent severe ischemic insult (172). The importance of Kir6.2 in determining the protection against severe ischemic insult has become clear since preconditioning disappears in the Kir6.2 knockout mice (178). K_{ATP} channels also play a protective role during acute exercise stress avoiding the cytosolic Ca²⁺ overload induced by hyperadrenergic conditions. Supporting the protective role that K_{ATP} channels play in stress adaptation, the Kir6.2 knockout mice is unable to shorten the cardiac action potential upon adrenergic stress (632).

It is of importance to mention here that K_{ATP} channel are present in the SAN and that metabolic inhibition antagonizes pacemaker activity by activating this type of channels. Activation of K_{ATP} channels in SAN may have dramatic effects on the rate of diastolic depolarization (188).

In hypothalamic glucose-sensitive neurons extracellular glucose removal causes a cell hyperpolarization and an inhibition of action potential firing. Kir6.2 channels are involved in the generation of the glucose-sensitive K⁺ current in neurons indicating that the increase in neuronal excitation observed when the concentration of external glucose raises is due to closure of K_{ATP} channels (368, 618). However, some glucose-sensitive neurons (e.g., neurons in the rat ventrome-

dial hypothalamus) express K_{ATP} channels formed by Kir6.1 and SUR1 (298).

K⁺-transport channels (Kir1.1, Kir4.x, Kir5.x, and Kir7.1)

Kir1.1 Previously known as ROMK1, Kir1.1 is a weak Kir having six alternative splicing isoforms (reviewed in reference 203). Kir1.1 channels are found in numerous different types of cells and, in particular, in polarized cells (e.g., kidney cells) they play an important physiological role not only in setting the resting membrane potential, but located in the apical or in basolateral membranes, they are involved in the regulation of the K⁺ concentration as well as in the Na⁺ and Cl⁻ concentration (e.g., references 192 and 566). For example, the efflux of K⁺ mediated by Kir1.1, located in the apical membrane of thick ascending limb cells, promotes the necessary K⁺ recycling for the activation of the Na⁺-K⁺-2Cl⁻ cotransporter needed for about 25% of the reabsorbed Na⁺ (51).

Kir4.x and Kir5.1 Most expressed in glial cells, Kir4.1 controls neuronal function by exerting a K⁺-buffering capacity (389). Kir4.1 can form homotetramers or heterotetramers with Kir5.1 (55, 202, 429, 536). However, Kir5.1 is unable to form functional homotetramers and only play physiological roles in combination with Kir 4.1 or Kir4.2 albeit with different biophysical properties. Kir 4.1 shows an intermediate inward rectification that turns into a strong inward rectification when forming heteromers with Kir5.1. Kir4.1/Kir5.1 channels are activated by internal Na⁺ a property conferred to the channel by aspartate205 in the Kir5.1 subunit, a residue not conserved in Kir4.1 (454).

Situated in the basolateral side of distal convoluted tubule cells, Kir4.1/Kir5.1 plays an important role in Na⁺ reabsorption (192). Kir4.1/Kir5.1 channels supply the necessary external K⁺ to the Na⁺-K⁺-ATPase pump that, coupled with epithelial Na⁺ channels in the apical membrane, allows the Na⁺ movement from the apical to the basolateral side of the epithelium. Since the pump internalizes the K⁺ supplied by the K⁺ efflux mediated by the Kir4.1/Kir5.1 channel, this process is called "K⁺ recycling."

Kir 4.1 plays several others important physiological roles. Expressed in the apical membrane of intermediate cells in the cochlear *stria vascularis* (7) is the molecular component in charge of the K⁺ secretion that maintains the high K⁺ concentration in the endolymph and sets the endocochlear positive potential (~80 mV) with reference to the perilymph (204, 393, 531). Kir4.1 knockout mice are deaf, the endocochlear potential is near 0 mV and the K⁺ concentration in the endolymph is reduced by approximately 50% (350). In glial cells, on the other hand, Kir4.1 is fundamental in the clearance of the excess of external K⁺ produced by neuronal activity (e.g., reference 388 and 538). However, it is important to point out here, that in cortical astrocytes of the brain Kir4.1 and Kir4.1/Kir5.1 channels are expressed in perisynaptic

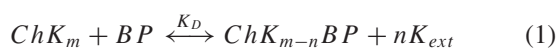
processes whereas Kir4.1/Kir5.1 are only expressed at the end feet (310). It is possible to interpret these results by assuming that in astrocytes external K⁺ is taken up by Kir4.1 and Kir4.1/Kir5 channels and secreted only by Kir4.1.

Kir7.1 Only one isoform of Kir7.1 has been isolated and although its physiological role is largely unknown, colocalize with the Na⁺-K⁺-ATPase pump in epithelial cells suggesting that, like Kir1.1 and Kir 4.1, may play a role in K⁺ recycling (see reference 203).

Kir channels structure-function relationships

Molecular determinants of inward rectification

As discussed before, inward rectification in Kir channels is a consequence of a voltage-dependent block by Mg²⁺ or polyamines and is not due to the movement of gating charges intrinsic to the channel-forming protein. The displacement of a blocking ion within the electric field produces a voltage-dependent block that according to Woodhull (581) depends of the location of the blocker-binding site inside the electric field. For example, if a polyamine having a valence of 2 “sees” the whole voltage drop across the pore (defined as an electrical distance, δ , of 1), the valence, $z\delta$, of the voltage-dependent reaction should reach a *maximum* value of 2. How is possible then that alkyl bis- and mono-amines carrying 1 or 2 positives charges are able to generate a voltage dependence with a $z\delta$ as large as 4 with increasing chain length? The most economical explanation to this anomalous large voltage dependence is to assume a strong coupling between polyamines or Mg²⁺ block and K⁺ movements through a long pore (179, 320, 325, 421). In this case, the voltage dependence of the block arises, not as a consequence of the blocking ion moving within the electric field but rather the blocker, entering the long pore from the cytoplasmic side, forces multiple K⁺ ions to move in a queue in front of the blocker (Fig. 5A). Thus a channel containing m K⁺ ions will become one containing $m - n$ K⁺ ions after the blocking particle (BP that can be Mg²⁺ or a polyamine) is in its equilibrium position inside the pore according to the reaction



where K_D is the dissociation constant.

The proposed mechanism to explain the large voltage dependence of spermine block needs; therefore, a single file of at least 5 K⁺ ions contained in a pore toward the cytoplasmic side of the selectivity filter (497). The elucidation at 1.8 Å resolution of the crystal structure of the protein originated from the intracellular N- and C-termini of a bacterial Kir Kir3.1 (GIRK1) by Nishida and MacKinnon (395) gave the first structural confirmation to the long-pore hypothesis. The structure of the N- and C-terminus of Kir3.1 consisting of 14 β -strands and 2 α -helices, contains a pore, dubbed the cytoplasmic pore that forced a K⁺ ion to travel more than 60 Å from the extracellular side to the end of the C-terminus

(284, 395) (Fig. 5B). In this journey, the K⁺ ion would have to diffuse about 30 Å in the membrane and another 30 Å in the cytoplasmic pore before reaching the internal solution, a distance nearly twice that found in other K⁺ channels. The long-pore characteristic of Kir channels was soon confirmed by Kuo et al. (284) who elucidated the crystal structure of a prokaryotic Kir channel, KirBac1.1. The KirBac1.1 structure was crystallized in the closed configuration characterized by an ion conduction pathway blocked by the side chains of phenylalanine 146 localized near the C-terminus of TM2 (see Fig. 5B). This residue is highly conserved in the Kir channel family and defines a closed helix bundle gate since replacement of the bulky Phe (F181 in Kir3.1 and F187 in Kir3.4) with Ala or Ser converted channels from agonist activation to constitutive active (80).

The entire Kir channel assembly showed a conduction machinery possessing a well-conserved selectivity filter with the characteristic T-X-G-Y-G signature sequence, and a central cavity, not different from other K⁺ channels (for more structural details about the selectivity filter, see section on Kv channels). However, it should be mentioned here that in the canonical selectivity filters the last glycine of the GYG motif is followed by an aspartate whereas in most Kir channels there is a phenylalanine in that position. The crystal structure of Kir2.2 shows that this phenylalanine projects directly into the external solution. This together with the fact that the Kir2.2 turrets are larger and come closer together makes the pore external entryway much narrower when compared to that of Kv1.2 (539). Since other K⁺ channels present a flat surface surrounding the external aspect of the selectivity filter opening, the protrusion created by the phenylalanines and the large turret hinder toxin docking and are important factors in determining the insensitivity of Kir channels to toxins (539).

With the exception of Kir 7.1, the conductance of Kir channels increases with the square root of the external K⁺ concentration (207, 277) a result in agreement with the multi-ion pore nature of this type of channels. Moreover, Lopatin and Nichols (321) showed that even in the absence of Mg²⁺ and polyamines, Kir2.1 also exhibits the square root dependence of the external K⁺ suggesting that this is a property of the open pore. Nishida et al. (394) using a Kir3.1-prokaryotic Kir channel chimera showed that, as in KcsA, four K⁺ ion positions were observed in the selectivity filter and one in the channel cavity. However, in contrast to KcsA channels, two ions were localized in the cytoplasmic pore (Fig. 5B). Although confirming the existence of K⁺ ions localized in the cytoplasmic pore, their number is insufficient to explain the voltage dependence of Kir channels found experimentally. More recently, Xu et al. (594) solved the crystal structure of the isolated cytoplasmic pore of the Kir3.1 channels at 2 Å resolution. Using Na⁺ as a K⁺ surrogate, they were able to show the presence of five ions in sites denominated S7-S11 (Fig. 5C), most of them coordinated by the side chains of polar or negatively charged amino acids with the exception of S10, a site consisting of a ring of four phenylalanines (Phe255) implying that in this case the central ion is stabilized by

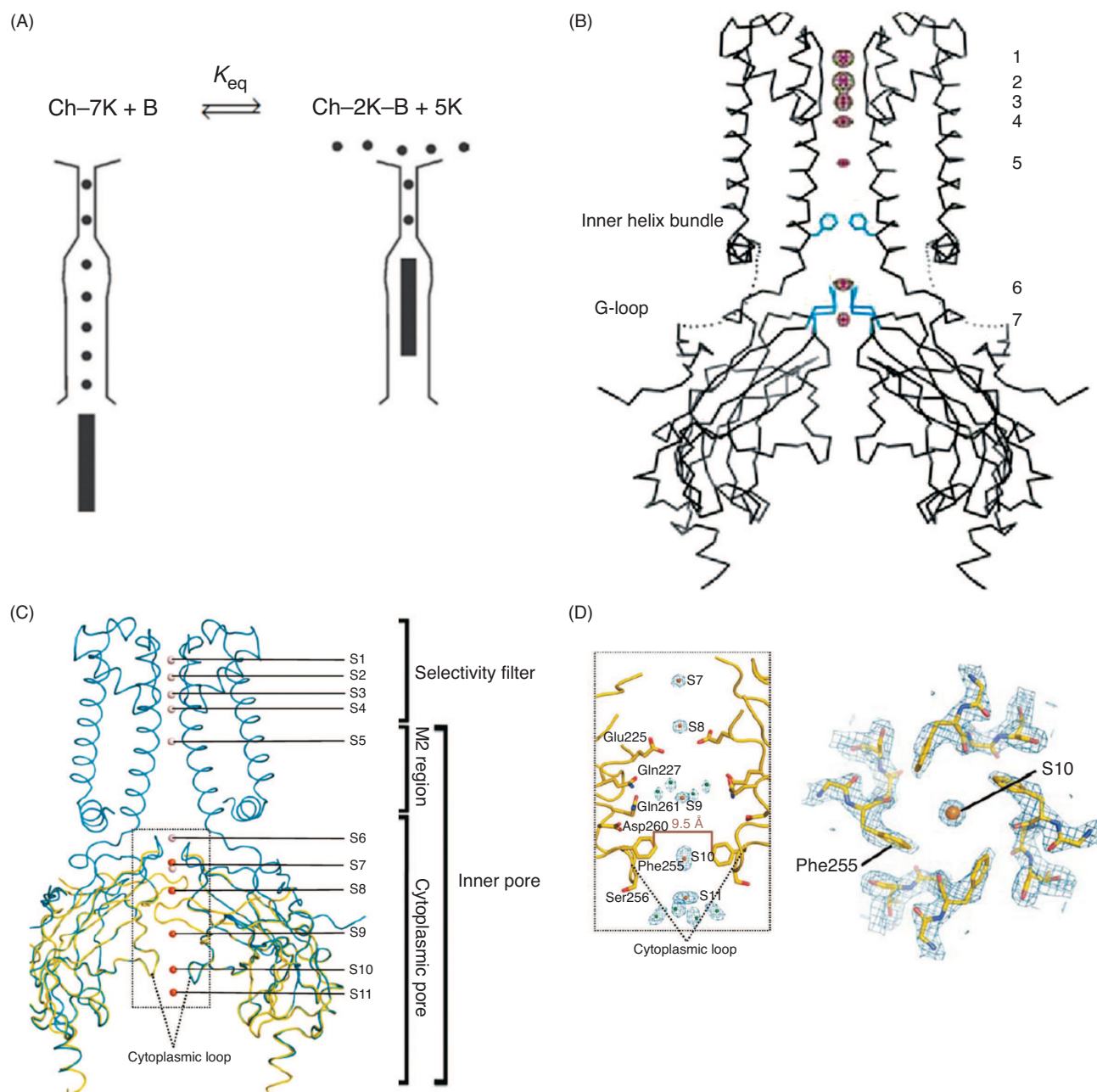


Figure 5 Kir channel crystal structure and cation-binding sites. (A) Voltage dependence in Kir channels arises as a consequence of the movement of K⁺ ions contained in the cytoplasmic pore. (B) Crystal structure of a Kir3.1-prokaryotic Kir channel chimera determined at 2.2 Å. Seven Rb⁺ ions were located in the conduction pore. Two constriction sites, F181 side chain and residues 302-309 C α atoms in the G-loop are colored in blue. For the sake of clarity only two subunits are shown [adapted, with permission, from Nishida et al. (394)]. (C) Crystal structure of the cytoplasmic pore of S225E mutant of Kir3.1 (yellow) and the Kir chimera (308) (cyan). Na⁺ ions are represented by orange spheres and Rb⁺ ions by pink spheres. (D) Crystal structure model of the cytoplasmic pore of S225E mutant Kir3.1 corresponding to the boxed region in A. The residues, Q225, G227, G261, D260, F255, and S256, interact directly or through water molecules with the Na⁺ ions located at S8-S11. The positions of the phenylalanines coordinating the Na⁺ through π -cation interactions at site S10 are shown [adapted, with permission, from Xu et al. (594)].

π -cations interactions (Fig. 5D). These findings demonstrates that there are enough ions in the cytoplasmic pore as to account for the strong voltage dependence of Kir channels and the presence of a constriction near the intracellular end of the cytoplasmic pore ensures an obligatory outward movement of the K⁺ ions file induced by the entrance of the polyamine.

Acidic residues in M2 and the cytoplasmic pore determine inward rectification

The cloning, expression and mutagenesis of Kir channels gave the first clues about the possible location of the residues important in determining blocker affinity. Three different groups

found in the same year that an aspartate (D172 in Kir2.1) in TM2 is critical in conferring strong inward rectification (328,510,573). Moreover, a Kir channel like Kir1.1 that shows a weak inward rectification can be converted into a strong Kir if N171 (corresponding to D172 in Kir2.1) is replaced by an acidic residue (328). Blockade is electrostatically tuned since replacement of neutral residues by acidic residues in a number of positions of M2 confers high affinity for blocking ions and that a histidine replacement of D172 makes inward rectification pH dependent (179,328,329).

Taglialetela et al. (528) found that replacement of the C-terminus of the weak Kir Kir1.1 for the C-terminus of Kir2.1

transformed the former channel into a channel showing strong inward rectification. This result was a clear indication that the C-terminus is also a structural determinant of the affinity of Kir channels for intracellular blocking ions, and soon it was demonstrated that acidic amino acids in the cytoplasmic pore are also crucial for the underlying affinity of Kir channels for blocking ions. In Kir2.1 residue E224 is important in determining the degree of inward rectification (Fig. 6A and B) (281,598). On the basis of the crystal structure of the cytoplasmic domain of Kir2.1 and electrophysiological studies a diaspertate cluster on the distal end of the cytoplasmic pore (D255/D259) and a glutamate 299 important in the

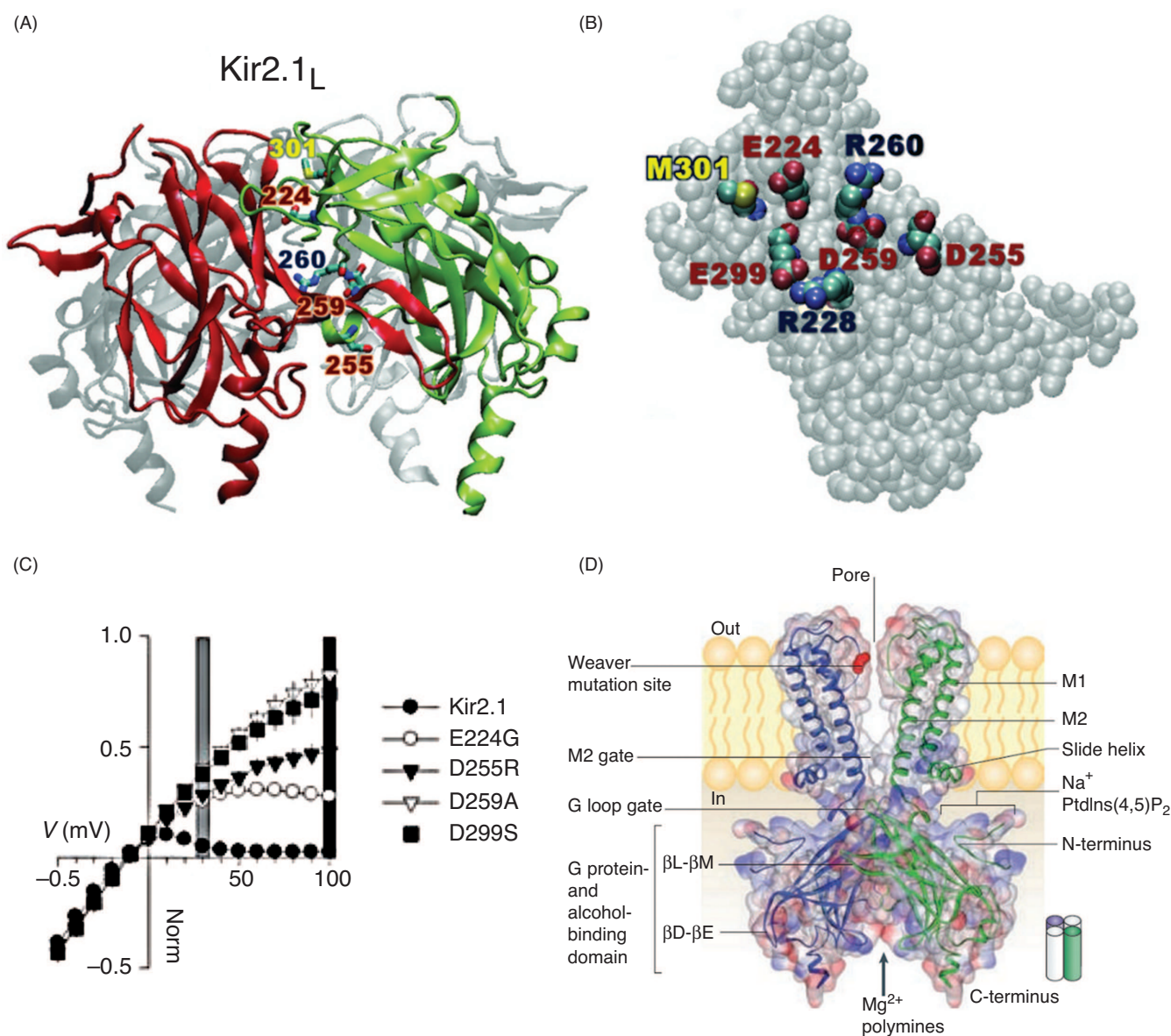


Figure 6 Molecular determinants of inward rectification and location of modulators binding sites in the cytoplasmic domain of K_G channels. (A, B) Amino acid residues in the cytoplasmic pore determining inward rectification in Kir2.1 channels. (C) Current-voltage relationships for different Kir2.1 point mutants [adapted, with permission, from Pegan et al. (425)]. (D) The structure shown contains the cytoplasmic domains of Kir3.1 a G protein-gated channel and the transmembrane domains and pore region of the chimeric Kir channel. The regions implicated in Na⁺, PIP₂, G protein, and alcohol binding are shown [adapted, with permission from Luscher and Slensinger (332)].

modulation of inward rectification were identified (Fig. 6A-C) (425). The crystal structure of Kir2.2, on the other hand, revealed several cation-binding sites in the conduction machinery of this channel; One in the TM pore (formed by D173) and two in the cytoplasmic pore constituted by a double ring of charges (upper ring, E225/E300) and a lower ring of charges (D256) (539). Interestingly, all three sites show a preference for Sr²⁺ over Rb⁺, selectivity that due to the large diameter of the sites is likely to be electrostatic in origin. This brings the total number of acidic amino acids determining the Kir2.1 channel high affinity for Mg²⁺ and polyamines to 4-5. However, number *and* position of the negatively charged amino acids are important in determining the degree of inward rectification. For example, although Kir4.1 has only three negatively charged residues in the long pore, it shows strong inward rectification but Kir 1.1 containing the same number of acidic amino acids at sites implicated in rectification, shows a weak rectification (132, 328).

Some structural inferences about gating induced by agonists

The crystal structures of the cytoplasmic domains of Kir2.1 and the G-protein-gated Kir3.1 revealed that the cytoplasmic pore has four loops (the G-loop) that form a structure that in the case of Kir2.1 completely occludes the path of ions (425). The girdle formed by the G-loops is located near the junction between the cytoplasmic and TM pore domains (Figs. 5B and 6D). This a flexible structure and its conformational changes, induced for example by PIP₂ or other agonists, may modulate gating. In fact, mutations in the G-loop disrupt gating and inward rectification. The crystal structure of a chimeric Kir channel in which most of the pore domain belongs to the prokaryotic KirBac1.3 channel and the remainder including the slide helix and cytoplasmic pore are from the mouse Kir3.1 gave a strong support to the hypothesis that the G-loop behaves as a gate in the cytoplasmic pore (394). Two different structures for the chimeric channel were found in which the cytoplasmic pore adopted different conformations. In one the girdle formed by the G-loops is constricted (equivalent to a closed state of the channel) whereas in the other is dilated (open state). The dilated conformation leaves a pore sufficiently wide to permit the passage of mostly hydrated K⁺ ions. The constricted conformation of the G-loop, on the other hand, is so narrow that even a dehydrated K⁺ ion is unable to pass through this region.

As discussed previously, the activity of Kir channels depends critically on the interaction of the channel with PIP₂. Positively charged amino acid residues located in the C- and N-terminus of Kir channels were identified as essential for PIP₂ channel activation (e.g., references 323 and 551). It is possible then that the chemical energy of binding of PIP₂ to these residues, all located in the external surface of the cytoplasmic pore, may be allosterically coupled to conformational changes of the G-loop gate (Fig. 6D) (394). In agreement with this hypothesis, Ma et al. (334) found that a mutation of one

of the amino acid located in the G-loop (V302M) profoundly alters the PIP₂ sensitivity of Kir2.1 channels.

Amino acid residues located in the external aspect of the cytoplasmic domains are involved in both agonist-independent and receptor-induced Gβγ activation of Kir3.x channels (283, 332, 504). A leucine (L333) residue located in the C-terminal domain of Kir3.1 (βL-βM sheet; corresponding to L344 and L339 in Kir3.2 and Kir3.4, respectively) plays a vital role in the Gβγ-dependent activation (Fig. 6D) (191). Importantly, direct binding of Gβγ to fragments of Kir3.x subunits shows that mutations of this important leucine do not reduce the binding of Gβγ suggesting that this residue is part of the coupling system involved in the transduction of the energy of binding to the mechanical energy necessary to open the channel (231). Riven et al. (447) using fluorescence resonance energy transfer (FRET) showed that the conformational rearrangement of the channel induced by Gβγ is consistent with a rotation and a widening of the cytoplasmic domains, movements that may be coupled to the G-loop or bundle crossing gates.

Two-Pore Domain Potassium Channels (K_{2P}) Family

Leak conductances also called background conductances, like inward rectifying K⁺ channels, mediate resting membrane potentials, and alter action potential height and duration (225, 430). Goldstein et al. (158) searched the DNA database for sequences homologous to the P-domain of previously cloned K⁺ channels and found a gene in the budding yeast *Saccharomyces cerevisiae*, named TOK1. The discovery of TOK1 started a search for other two-pore domain K⁺ channel (K_{2P}) genes. In comparison with previously described K⁺ channels this type of channels were novel in two aspects: (1) the TOK1 channel-forming protein contains two pore-forming regions; and (2) TOK1 was the first cloned example of a new functional type of outward rectifier K⁺ channel. In 1996, another K_{2P} human K⁺ channel gene (*TWIK-1*) with four-TM segments was identified (304) and soon after, the cloning of nerves and muscles genes of *Drosophila melanogaster* resulted in the isolation of *Ork1*, the product of which was denominated K_{2P0} (158, 225, 257, 430). From further electrophysiological studies, it became evident that these channels formed a single pore by making a *dimer* of two subunits, leaving both N- and C-termini facing the cytosol. The four-TM channels cloned and expressed are all selective to K⁺ presenting some small rectification. Given these characteristics these channels prove to be important in setting the resting potential, regulating cellular excitability, and in increasing K⁺ permeability of cells that need to transport K⁺ ions (354, 534).

K_{2P0} has a linear current-voltage relationship under symmetrical K⁺ conditions; however, significant outward currents are seen only under physiological conditions with high internal K⁺ and low external K⁺. After this first functional

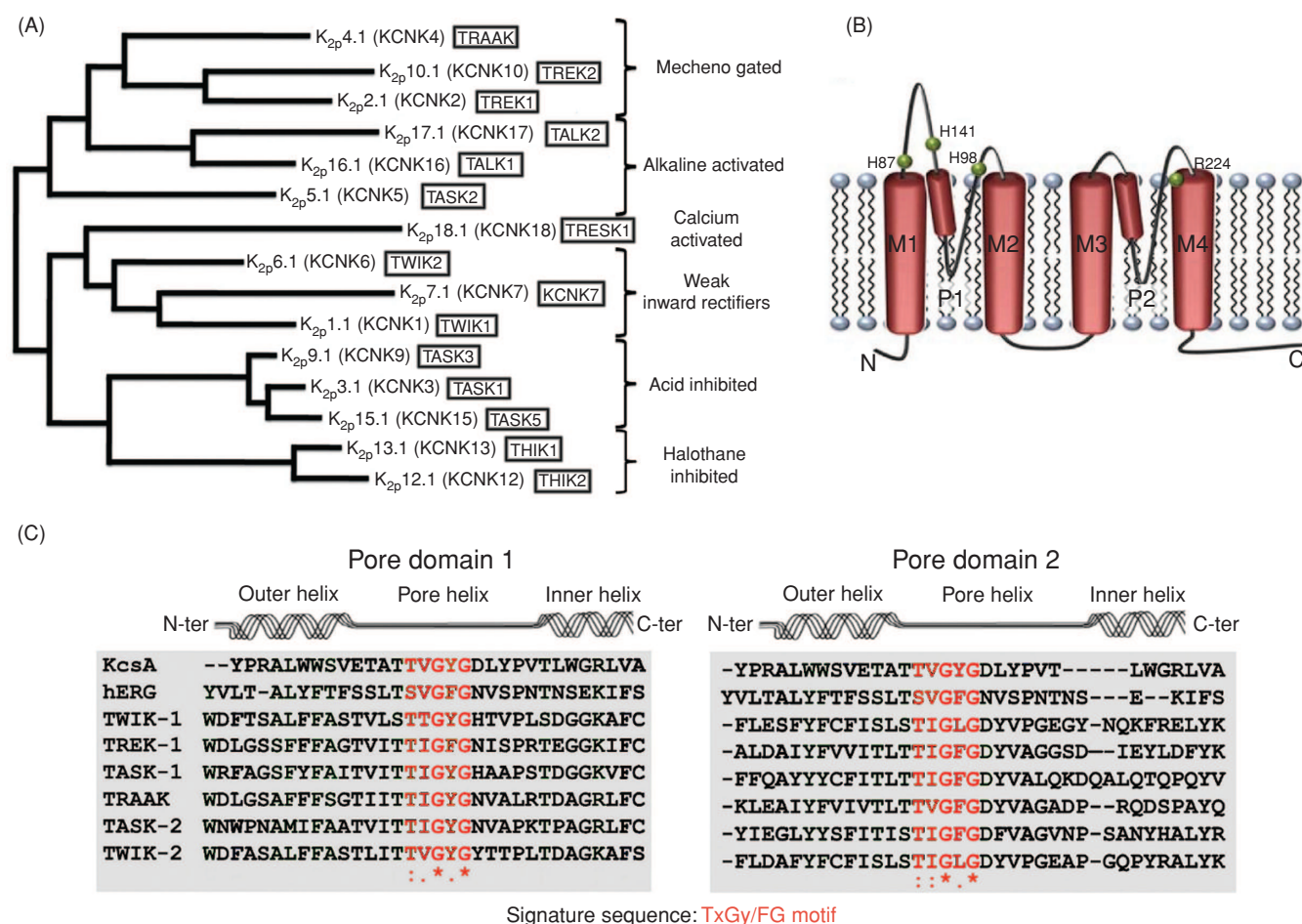


Figure 7 Diversity of 2-pore (2P)-domain K⁺ channel (K_{2P}) subunits and membrane topology. (A) The alignment was made using the web tool: Phylogeny.fr (109), with different sequences of human two pore K⁺ channels obtained from gene bank accession numbers from KCNK1 to KCNK18: NP_002236, NP_055032, NP_002237.1, NP_201567.1, NP_003731.1, NP_004814.1, NP_005705.1, NP_057685.1, NP_066984.1, NP_071338.1, NP_071337.2, NP_071753.1, NP_115491.1, NP_113648.2, and NP_862823.1. (B) Putative membrane topology of the two-pore domain K⁺ channels. Green spheres indicate pH sensing residues and their predicted location in the first turret loop and M4 transmembrane domain. (C) Multiple sequence alignment of the outer and inner helix region of KcsA, hERG, and several K_{2P} K⁺ channels. Amino acid residues colored in red show the K⁺ channel signature sequence, corresponding to the selectivity filter.

characterization, the K_{2P} mammalian channels were formally named K_{2P}1, K_{2P}2, etc., and the encoding genes named accordingly, *KCNK1*, *KCNK2*, etc. (128, 203). Since their discovery, 15 human K_{2P} members have been identified, and most of them behave as pure leak or background K⁺ channels (Fig. 7A), whose main function is to maintain the resting level of membrane potential (94, 354). Although, the K_{2P} channel subunits display the same structural motif (Fig. 7B), they share only moderate sequence homology outside their pore regions (Fig. 7C). In addition, to the four putative TM segments and the two P-domains, the more relevant structural features are: the short N-terminal, the long C-terminal, and a long extracellular loop between TM1 and P1 (305, 417) (Fig. 7B).

K_{2P} channel subfamilies

The K_{2P} channels are regulated by an extensive variety of stimuli: for example, pH, temperature, and membrane stretch.

For example, an increase in the low basal activity of K_{2P} channels in response to sumoylation, and dephosphorylation, or to changes in physicochemical parameters including temperature, intracellular/extracellular pH, oxygen tension, and changes in osmolarity and/or membrane stretch enable rapid and significant changes in ion fluxes (430, 534). Evidence is accumulating for the potential importance of targeting and altering the activity of K_{2P} channels in a number of therapeutic situations in the nervous system, including neuroprotection, neuropathic pain, depression, anaesthesia, and epilepsy (27, 29, 213, 314, 459). Due to the diversity of responses when confronted to different stimuli, members of the K_{2P} family were divided into six subfamilies (Fig. 7A): (i) mechanogated; (ii) alkaline-activated; (iii) Ca²⁺-activated; (iv) weak Kirs; (v) acid-inhibited; and (vi) halothane-inhibited channels (213).

Other genes such as *KCNK6* and *KCNK7* code for silent subunits that probably require a partner to form functional

channels (29, 95, 305). Although the members of the different subfamilies show relatively low sequence similarity, (TWIK-1 and TREK-1 show only a 28% of identity at the protein level) all members of the background potassium channel family are characterized by the same general molecular architecture (Fig. 7B).

K_{2P} channels topology and stoichiometry

Lesage et al. showed that TWIK-1 self associates to form disulfide-bridged homodimers (306) and that this assembly involves a 44-amino acid region sufficient to promote the self-dimerization and located in the TM1-P1 interdomain. Therefore, unlike the assembly of Kv or Kir subunits that form noncovalently associated tetramers, K_{2P} channel subunits require the formation of a stabilizing interchain disulfide bridge (305, 306). It has been suggested that the domain that is essential for the dimerization in K_{2P} channels might function as a regulatory region possibly by binding extracellular ligands (305). All mammalian K_{2P} channel subunits possess four TM segments; the 4TM/2P structure defines the membership in the K_{2P} channel family. Based on the pioneer characterization of the oligomeric state of TWIK-1, a dimeric structure has been assumed for all the other K_{2P} channels. Furthermore, all the cloned subunits, except TASK-1, contain a cysteine residue at a position equivalent to cysteine 69 of TWIK-1, and all these subunits (except TASK-1) are able to form covalent homodimers when heterologously expressed in insect or CV-1 (simian) cells, and carrying the SV40 genetic material (COS) cells. In addition, the covalent dimerization of TREK-1 and TRAAK was also observed in synaptic membranes (305). In this family, the K⁺ channel signature sequence GYG is replaced by GFG in TREK-1, in both P motifs of the subunit, and in one P motif in Task-1, TASK-2, and TASK-3 (Fig. 7C). In TWIK1, and TWIK2 one of the P motifs the signature sequence GYG is replaced by GLG. Furthermore, in KCNK6 and KCNK7 (silent subunits) a glutamic residue GLE is found instead of the strictly conserved glycine residue (273, 305).

TREK and TRAAK channels

The first cloned K_{2P} mammalian mechanogated K⁺ channels were named TREK and TRAAK. They are considered mechanosensitive ion channels since at atmospheric pressure their open probability is low, and channel activity is elicited by increasing the mechanical pressure applied to the cell membrane (Figs. 8A and 9A) (95, 417). The TREK/TRAAK is a subfamily of polymodal K⁺ channels since is regulated by several stimuli such as: stretch, osmolarity, pH, temperature, polyunsaturated FAs, lysophospholipids, neuroprotective agents, cationic amphipaths, volatile anaesthetics, and phosphorylation triggered by G-coupled receptors and other intracellular cascades (see Fig. 8B) (95, 147, 214, 282, 305, 417).

TASK-1: The perfect background K⁺ channel

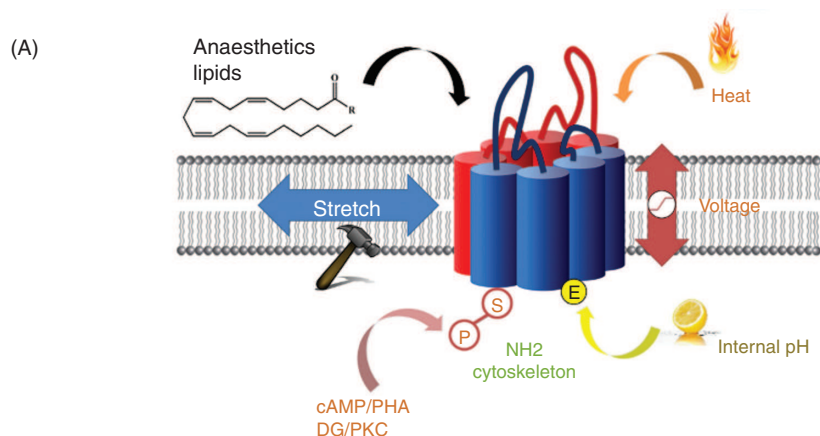
TASK-1 was the first cloned mammalian K⁺ channel to produce time-independent currents with all the characteristics of

a background or baseline conductance. This channel found in myelinated nerve, is insensitive to the classical K⁺ channel blockers TEA, 4-AP, and Cs⁺. TASK-1 current-voltage relationship curves are well fitted by the constant field theory (Goldman-Hodgkin-Katz rectification or open rectification) for simple electrodiffusion through an open K⁺ selective pore (305). Since both, TASK-1 and TASK-2 are constitutively active, they are predicted to contribute to the maintenance of the resting membrane potential, and/or to K⁺ transport associated with recycling or secretion. Moreover, these channels are present in nonexcitable cells, with the exception of TASK-1 that is present in brain and heart (122, 262, 302). TASK channels respond to variety of extracellular calcium-mobilizing receptor agonists and are inhibited by antagonists such as extracellular acidosis, anandamide, volatile anaesthetics, and other stress processes such as hypoxia (Fig. 8C).

Compared with TASK channels, TREK-1 and TRAAK currents have a low basal activity when expressed in heterologous expression systems. This family is relatively insensitive to TEA and other K⁺ channel blockers, and sensitive to the known blockers of stretch-sensitive ion channels, such as amiloride and Gd³⁺. At the single channel level, TREK and TRAAK channels are highly flickering (see Fig. 9B and C), and their cord conductances in symmetric 150 mmol/L KCl are 100 and 45pS, respectively. Single-channel recordings from TRAAK show spike-like openings due to an extremely short mean open time (see Fig. 9B and C) and can be easily distinguished from TREK-1 and TREK-2, in symmetric K⁺, by their linear current-voltage relationship (147, 187, 260, 305). In spite of the fact that TREK and TRAAK are both activated by membrane stretch, changes in pH have a differential effect. Particularly, TREK channels are activated by intracellular acidosis (Fig. 9D, top), converting TREK mechanogated into constitutively active channels. Lowering the intracellular pH shifts the pressure-activation relationship of TREK-1 toward positive values and ultimately leads to channel opening at atmospheric pressure. TRAAK, on the other hand, opens upon intracellular alkalosis (95, 147, 417). The channel sensor for stretch, acidosis, and temperature (at least in TREK-1) is on the C-terminus and the extracellular TM1-P1 loop (214, 345).

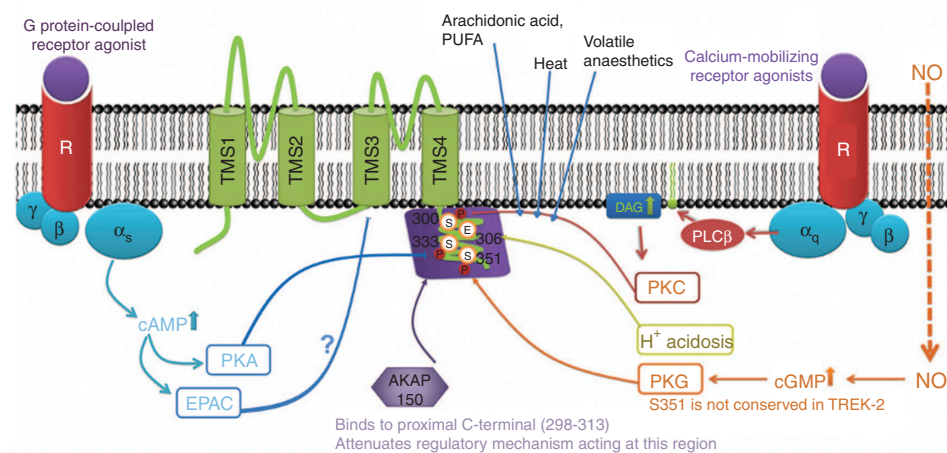
General TREK/TRAAK channels tissue distribution

TREK and TRAAK have been shown to be located in human peripheral organs and tissues of the central nervous system (CNS). However, they have different subcellular locations; for instance, TRAAK is mainly present in soma and, to a lesser degree, in axons and dendrites, whereas TREK-1 is concentrated in dendrites in almost all neuronal types expressing this channel [(197, 305, 362, 534); for review, see Talley et al. (533)]. The widespread distribution of TREK-1 in CNS might suggest that this channel participates in a number of potential physiological roles. For instance, TREK-1 is located throughout the brain and spinal cord but with specific areas appearing to be particularly enriched in TREK-1 protein, such as the



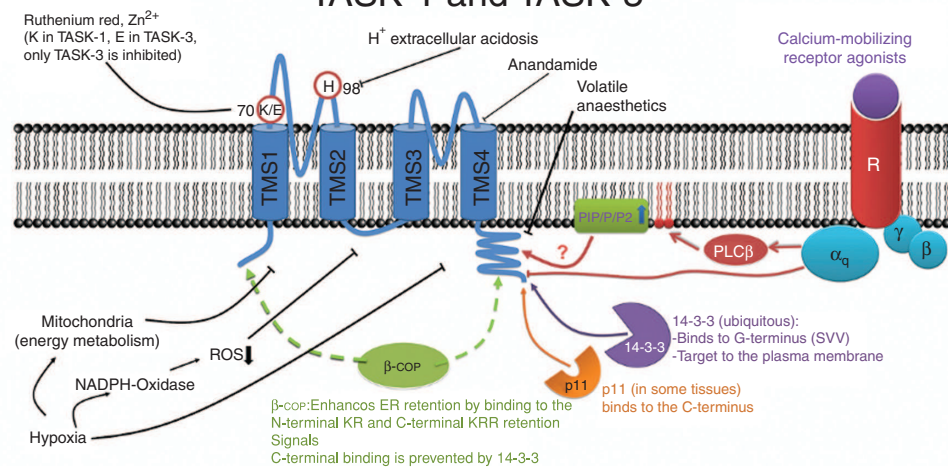
(B)

TREK-1 and TREK-2



(C)

TASK-1 and TASK-3



cortex, hippocampal formation, thalamus, geniculate nuclei, hypothalamus, basal ganglia, periaqueductal gray, and the gray matter of the spinal cord. In addition, the fact that TREK-1 and TRAAK are expressed in cortex, hippocampus, and thalamic nuclei along with the presence of riluzole and polyunsaturated FAs (both known for their neuroprotective effects) is consistent with the idea that these channels may play a crucial role in the prevention of epileptic seizures (197). There are some inconsistencies in the literature regarding the location of some of the K_{2P} channel members. For instance, Talley et al. (534) found that the highest expression of TREK-1 is in the striatum, CA2 of the hippocampus, and layer IV of the neocortex. While Lazdunski laboratory (140) reported that TREK-1 levels in the striatum were unremarkable, and there was uniform labeling of hippocampal pyramidal neurons and in the various cortical laminae. TREK-2, was found to be primarily restricted to the cerebellum (534). In addition, the highest levels of TRAAK were localized in the cerebral cortex, and TWIK-1 is mainly present in the cerebellum and cortex.

Thermosensitivity

When expressed in heterologous systems, TREK-1 shows low activity at room temperature (253). Raising the temperature increases channel activity and a maximal response is observed in the 37 to 42°C range (Fig. 9C). This result suggests that TREK-1 is highly active at physiological temperature and contributes significantly to the background K⁺ conductance in native conditions (95,253,343). Recently, Kang et al. (253) showed that not only TREK-1 is thermosensitive, but also TREK-2 and TRAAK (Fig. 9C), channels that, as TREK-1, have a high probability of opening at physiological temperatures. Therefore, TREK-1, TREK-2, and TRAAK contribute to the background K⁺ conductance that helps to stabilize the resting membrane potential at physiological temperatures (253). Once it was established that the TREK/TRAAK subfamilies were tightly regulated by temperature, it became relevant to unveil the mechanism that promotes channel opening by temperature. Based on the observation that channel activity closely follows rapid changes in temperature, Kang et al. (253) ruled out the involvement of newly synthesized heat-inducible proteins. In addition, Maingret et al. (343) suggested

that the temperature sensor could be a molecule closely associated with TREK-1, TREK-2, and TRAAK, but such a molecule has not been identified yet (253,343). Deletion of 106 amino acids of the distal part of the C-terminus of TREK-1 generates a mutant that has a rather weak response to heat. Also, a chimeric channel in which the TREK-1 C-terminus was replaced with that of TASK-1 was found to be rather insensitive to heat (343). Thus, the C-terminus of TREK-1 plays an important role in providing the temperature sensitivity phenotype. It is noteworthy that, the mean open-time duration of TREK-1 was differentially affected by temperature in different cells. The reason of these differences is at present unknown but they can be due to the different membrane lipid composition of these cells (253). Since TREK-1 and TREK-2 are expressed along with several transient receptor potential (TRP) channels in the hypothalamus and dorsal root ganglion neurons, they might act in concert in the transduction of temperature and nociception. Kang et al. (253) have suggested that TREK channels could act as suppressors of the excitation elicited by the activation of TRP channels.

Anaesthetics

General anaesthetics are compounds that produce loss of consciousness and pain relief when breathed in through the lungs. Indeed, the first anaesthetics that were used in clinical practice were the inhalational agents diethyl ether and nitrous oxide. The most commonly used inhalational anaesthetics are halogenated ethers (isoflurane, sevoflurane, and desflurane) or halothane (147). Despite the over 150 years of use, there is little consensus on how general volatile anaesthetics act at the molecular level. Several targets have been proposed over the years but the relative nonselectivity and low potency of inhalational anaesthetics has made it difficult to identify which molecular targets are pharmacologically relevant. It has been suggested that anaesthetics might reduce neuronal excitability by opening K⁺ channels, along with the already established role of certain ligand-gated ion channels (147). In 1999, Maingret et al. (345) established that TREK channels, unlike TRAAK, are reversibly opened by clinical concentrations of volatile anaesthetics such as chloroform, diethyl ether, halothane, and isoflurane (Fig. 9E) The opening of TREK

Figure 8 Polymodal nature of K_{2P} channels receptors. (A) TREK-1 channels are modulated by stretch, heat, intracellular acidosis, depolarization, lipids, general anaesthetics, and tonically inhibited by the actin cytoskeleton [adapted, with permission, from Patel and Honoré (417)]. (B) Polymodal regulation of TREK-1 and TREK-2. Activation of the Gs/cAMP/protein kinase A (PKA) and the Gq/phospholipase C (PLC)/Diacyl Glycerol (DAG)/protein kinase C (PKC) signaling pathway inhibit TREK channels by phosphorylating serine residues present on the C-terminal. TREK-1 is activated via the NO/cGMP/Protein kinase G (PKG) pathway, but the PKG phosphorylation consensus site is missing in TREK-2. (Arrows indicate stimulation; lines with T ending represent inhibition.) [Modified, with permission, from Enyedi and Czirják (128).] (C) Regulation of TASK-1 and TASK-3. The channels are inhibited by extracellular acidification (EC) acidification as a result of protonation of histidine98 in the second extracellular loop. Anandamide inhibits both TASK-1 and TASK-3. Hypoxia inhibits TASK current indirectly. TASK channels are activated by halothane and isoflurane but they are not influenced by chloroform or ether. The polycation ruthenium red and Zn²⁺ allow pharmacological distinction between the two closely related channel subunits. Dashed lines represent effects on targets; arrows indicate stimulation; lines with T ending represent inhibition. [Modified, with permission, from Enyedi and Czirják (128).]

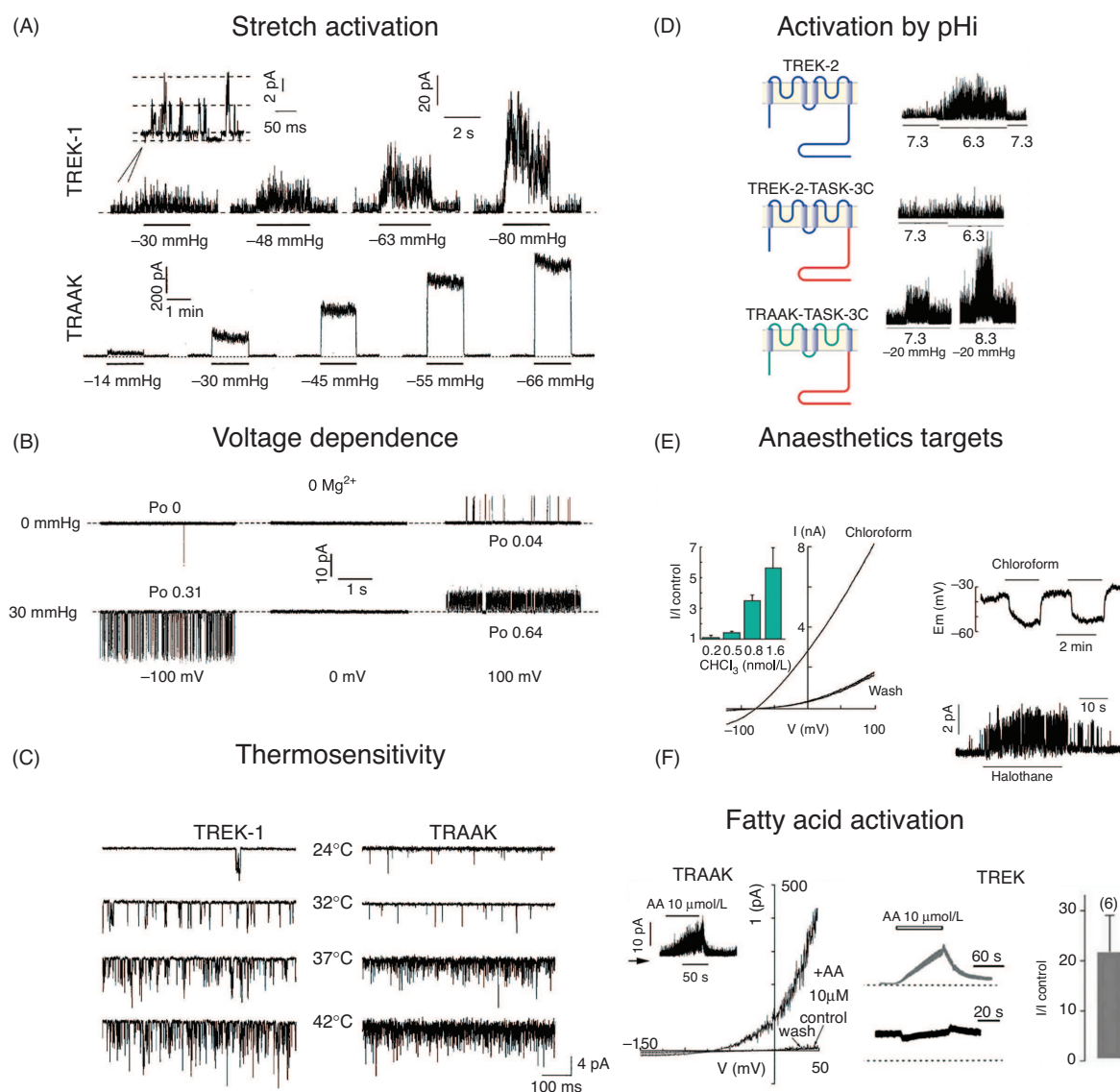


Figure 9 K²P channel activation by different stimuli. (A) Top: TREK-1 activation was graded with membrane stretch in a cell-attached patch from oocytes expressing TREK-1. The inset shows channel openings with an enlarged time scale. In this patch, a small conductance endogenous channel was also present. Bottom: graded reversible negative pressure activation of hTRAAK in physiological K⁺ conditions. The patch was held at 0 mV and the zero current is indicated by a dashed line [from Paté et al. (418) and Lesage and Lazdunski (305)]. (B) TREK-1 channels show outward rectification. Single-channel currents recorded in absence of Mg²⁺ at -100 mV (left trace), 0 mV (middle trace), and 100 mV (right trace) at atmospheric pressure (top traces) and at a steady pressure of -30 mm Hg (bottom traces). Po denotes open probability [adapted, with permission, from Maingret et al. (342)]. (C) Thermosensitivity. Cell-attached patches from COS-7 cells incubated at different bath temperatures are shown for TREK-1 and TRAAK [adapted, with permission, from Kang et al. (253)]. (D) The C-terminus of TREK-2 is required for sensitivity to fatty acids and pH. (Top) Wild-type TREK-2 expressed in COS-7 cells is robustly activated by a decrease in intracellular pH. Middle. The pH sensitivity is abolished in a chimeric mutant that consists of the core transmembrane segments of TREK-2 and the C-terminus of TASK-3 (red) (chimera TREK-2-TASK-3C) indicating that C-terminus of TREK-2 is required for pH sensitivity. (Bottom) The sensitivity of a TRAAK-TASK-3C chimera to pH is similar to wild-type TRAAK, which indicates that the C-terminus of TRAAK is unlikely to mediate activation by pH [adapted, with permission, from Kim (260)]. (E) Left. TREK-1 is reversibly opened by chloroform (0.8 mmol/L). Voltage was linearly depolarized with a voltage ramp from -120 to 100 mV. Current becomes zero at a membrane potential equal to the equilibrium potential for K⁺ (-80 mV). Inset: stimulation of the K⁺ current by chloroform (CHCl₃) is concentration dependent and observed at pharmacologically relevant concentrations. Right top. Chloroform (0.8 mmol/L) induces reproducible membrane hyperpolarizations. Right bottom. Halothane (1 mmol/L; 0 mV) induces TREK-1 single-channel activity characterized by rapid flickering between closed and open states [modified, with permission, from Franks and Honore (147)]. (F) Fatty acid activation of TRAAK and TREK in COS cells. (Left side) Current-voltage relationships obtained in an inside-out patch with voltage ramps ranging from -150 to +50 mV, 500 ms in duration, before (control), after 3 min perfusion with 10 μmol/L AA and after the wash. Inset: effects of 10 μmol/L AA on TRAAK currents recorded in an inside-out patch clamped at +20 mV. The zero current level is indicated by an arrow. (Right side) Inside out patch currents were recorded at 0 mV from transfected COS cells. The zero current levels are indicated by a dotted line. The histograms represent the ratio of the mean currents recorded before (I_{control}) or after 10 μmol/L of AA application (I), gray and black color denotes absence or coexpression of A-kinase anchoring protein (AKAP150), respectively [adapted, with permission, from Sandoz et al. (468) and Fink et al. (141)].

channels by these anaesthetics induces cell hyperpolarization (95, 147, 282, 417). The fact that the effect of volatile anaesthetics is independent of cell integrity in excised patches, and the lack of effect of volatile anaesthetics on TRAAK, indicates that an indirect membrane effect of volatile anaesthetics is unlikely (147). The use of TREK1 knockout mice has provided the most direct evidence for the role of TREK-1 in anesthesia. In these animals, the gene encoding TREK-1 was disrupted without interfering with brain mRNA expression of other members of the K_{2P} channel family or of the GABA receptor. These knockout mice did not display an abnormal phenotype; on the contrary both reflex and cognitive functions were not altered. However, under the presence of volatile agents such as chloroform, halothane, sevoflurane, and desflurane TREK-1 knockout mice showed a marked decrease in anesthetic sensitivity. In addition, to the longer time required to put TREK-1^{-/-} mice under anesthesia, the concentrations required to reach loss of righting reflex and the failure to respond to a painful stimulus were significantly higher in knockout animals compared to wild type animals. It is also important to mention here that, there was no difference between knockout and wild-type animals following the administration of the barbiturate pentobarbital, which does not affect TREK-1, showing that the decrease in sensitivity to volatile anaesthetics of the knockout mice was unlikely to be due to a generalized increase in excitability (147).

Membrane stretch and lipid effect on the TREK-TRAAK subfamily

By inducing blebs without cytoskeletal elements, Zhang et al. (626), carefully established the role of membrane proteins as mechanotransducers studying mechanosensitive channels in the complex cell surface of *Xenopus* oocytes. Hyposmolarity promotes TREK/TRAAK channel opening and hyperosmolarity has the opposite effect, suggesting that these channels can be modulated by the cellular volume. These channels can be also activated by application of stretch or negative pressure to the cell membrane (Fig. 9A); the pressure to induce half-maximal activation is -36 mmHg for TREK-1 and -46mmHg for TRAAK (345). Similar to other eukaryotic mechanosensitive channels, disruption of the cytoskeleton by either biological (colchicine, cytochalasin) or mechanical agents (membrane excision) potentiates channel opening by membrane stretch. These results suggest that the mechanical force generated by osmotic changes and transmitted directly to the channel via the lipid bilayer is tonically repressed by the cytoskeleton. Moreover, agents that alter the cell shape by preferential insertion in one of the leaflets of the membrane modify the activity of these channels (147, 253, 305, 417-419).

The TREK/TRAAK subfamilies are also stimulated by polyunsaturated fatty acids (PFAs; Fig. 9F), lysophospholipids containing large polar heads and by intracellular lysophosphatidic acid (LPA) either directly on the channel protein or via a membrane effect. The activation by arachidonic acid (AA) is reversible and concentration-dependent;

moreover, channel activity does not decrease when the AA perfusion is supplemented with a mixture of inhibitors of the AA metabolism pathway. This supports the idea that the AA effect is direct and not due to another eicosanoid, either by interaction with the channel protein or as a consequence of partitioning into the lipid bilayer and indirectly affecting channel gating. This effect can be also induced by other unsaturated FAs, such as oleate, linoleate, arachidonate, eicosapentaenoate, and docosahexaenoate, but not by saturated FAs like palmitate, stearate, or arachidate. In the particular case of LPA, TRAAK channels can be reversibly activated by intracellular LPA at atmospheric pressure and shows the highest sensitivity to intracellular LPA, compared with TREK-1 and TREK-2. Intracellular LPA shifts the mechanosensitivity of TRAAK toward lower tension values, leading to channel opening at atmospheric pressure (95, 147, 260, 305, 417, 419).

Since PKA-mediated phosphorylation of Ser333 in the C-terminus promotes channel closing, this enzyme is able to reverse the effect of lipids on TREK-1. TREK-1 activity is also inhibited by the protein kinase C pathway, although the phosphorylation site remains to be identified (417).

Arachidonic acid

AA is a PFA with 20 carbons and four *cis* double bonds that make this molecule extremely flexible. This acid affects the behavior of biological systems in two ways: First, the liberation of this FA from the cell membrane, via receptor-mediated activation of phospholipases, leads to the generation of biologically active AA metabolites that could account for the activation of K⁺ channels; and Second, AA and FAs themselves elicit a second class of direct responses and not through metabolic pathways (405). Even before K_{2P} channels were cloned and identified, Kim and Clapham (261) found two types of K⁺ selective channels activated by intracellular AA in neonatal rat atrial cells. They reported that in inside-out patches AA along with other FAs opened outwardly rectifying K⁺ selective channels. Also Ordway et al. (405) reported that both AA and certain other FAs, at concentrations similar to those required for both metabolic-mediated and direct effects of a FAs, directly activated specific K⁺ channels in smooth muscle cells isolated from the *Bufo marinus* stomach. With these results they were able to suggest that channel activation may be mediated by a FA-induced alteration of the physical properties of the membrane. In spite of the fact that a clear link could not be established between leak K⁺ channels and the ones that were reported in the previously mentioned studies, they had enough data to propose an explanation for the role of these K⁺ selective channels in the increase of K⁺ conductance observed in ischemic cells. Ischemia or hypoxia can reduce the duration of the action potential and thereby cause an early repolarization of cardiac cells. The opening of these channels would cause a rapid hyperpolarization of the cell and limit additional entry of Ca²⁺ via voltage-sensitive Ca²⁺ channels as well as minimize energy consumption by conserving ATP. Furthermore, a decrease in intracellular pH together with

the opening of the K⁺ channels by AA would contribute to the cell hyperpolarization, further protecting the cells from ischemic damage. Another possible role for FA-sensitive K⁺ channels might be to monitor the level of free FA and protons in the cell, thus providing a protective mechanism by reducing cell excitability. When metabolic inhibition occurs due to pathological processes, such as ischemia and hypoxia, the intracellular pH decreases, the cytosolic concentrations of free FAs and Ca²⁺ increase, phospholipases are activated, and neurons swell. All these alterations will contribute to open TREK, at both presynaptic and postsynaptic sites and the resulting hyperpolarization will inhibit the activation of the presynaptic voltage-gated Ca²⁺ channels and limit glutamate release. At postsynaptic level, hyperpolarization will enhance the Mg²⁺ block of the N-methyl D-aspartate (NMDA) glutamate receptors at negative membrane potentials, reduce Ca²⁺ influx, and thus lower glutamate transmission and excitotoxicity. The opening of TREK-1 at the postsynaptic level will also tend to antagonize the depolarization induced by the activation of the ionotropic Alpha-amino-3-hydroxy-5-methyl-4-isoxazolepropionic acid (AMPA)/kainate glutamate receptors. On the other hand, stimulation of the metabotropic glutamate receptors will close TREK-1 and reduce neuroprotection. Thus, it is possible to suggest that the opening of TREK-1 is consistent with the action of an antagonist of metabotropic glutamate receptors to produce maximal neuroprotection (147, 201, 260). On the other hand, the finding that TRAAK knockout mice do not have an increased sensitivity to either ischemia or epilepsy, in spite of the fact that polyunsaturated FAs and lysophospholipids open this channel, implies that TRAAK channels do not play a significant role in neuronal protection. In addition, this negative result further demonstrates that the increased vulnerability that was found in the TREK-1 knockout mice is specific, and not due to a general increase in excitability (147, 201).

A chimeric channel in which the entire C-terminus of TREK-2 was replaced with that of TASK-3 preserves mechanosensitivity, but is neither activated neither by free FAs nor by protons (Fig. 9D). This result not only indicates that activation of TREK-2 by free FAs is dependent on the C-terminus, but also that membrane stretch involves distinct molecular mechanisms, and rules out the idea that increased tension of the lipid membrane activates K⁺ channels by releasing free FAs (264). In TREK-1, a glutamate residue in a region closed to the fourth TM segment acts as a proton sensor that also tunes mechano- and lipid sensitivity. Mutation of this glutamate to an alanine produces gain-of-function mutant channels, which are trapped in the active state (260).

Lysophosphatidic acid

LPA is a lipid-derived second messenger very abundant in cells and it exerts multiple biological effects. LPA elicits growth cone collapse, neurite retraction, cortical neurogenesis, and cell rounding in various neurons, thus mediating a role in axonal growth and path finding (71, 148, 602). Extracellular

LPA evokes biological responses that are mediated through the activation of three G-protein-coupled receptors. Since TREK-1, TREK-2, and LPA are all present in the brain at high levels, it is hypothesized that these channels are involved in the response of the CNS to hemorrhagic brain injury given that under this type of brain damage the concentration of LPA in the cerebrospinal fluid is increased (94). Intracellular LPA is a potent regulator of the TREK/TRAAK K_{2P} channels, since it converts the voltage-sensitive K⁺ channel TREK-1 into a leak conductance. Thus opening of these K_{2P} channels by intracellular LPA directly links the lipid status to cell electrogenesis. LPA preferentially activates TREK-1 only when applied intracellularly (344). LPA activation is dependent on the presence of the phosphate head group and the acyl chain; the lack of the phosphate at position 3 of the glycerol renders the lipid completely ineffective (94). Intracellular LPA activation neither involves the C-terminal domain of TREK-1 nor the N-terminus. Thus, AA, intracellular pH, and LPA open TREK-1 by different mechanisms. Interestingly, when the TM1-TM3 intracellular loop of TREK-1 is exchanged with the loop of TRESK1 (another K_{2P} channel that is not stimulated by intracellular LPA) the stimulatory effect of intracellular LPA is strongly reduced. However, it cannot be ruled out that this effect could be due to the effect that the substitution has *per se*, and the question about what region of TREK-1 senses intracellular LPA is still open. It is important to keep in mind that TREK-1, TREK-2, and TRAAK are mechanosensitive, so it is possible that LPA mechanism might involve a membrane effect. Such a mechanism was proposed for the control of synaptic vesicle formation by endophilin I in presynaptic neurons in (94). Endophilin is a membrane-associated protein required for endocytosis of synaptic vesicles, which is thought to induce a negative membrane curvature. This effect might be product of the conversion of the inverted cone-shape lipid LPA to the cone-shape lipid phosphatidic acid in the cytoplasmic leaflet of the bilayer, thus promoting vesicle formation. It seems that the shape of the lipids is important for TREK-1 activation, as intracellular phosphatidic acid weakly stimulates TREK-1 compared with LPA. Furthermore, intracellular phosphatidic acid reversibly inhibits TREK-1 channel activity after AA stimulation. Thus, it is possible that TREK-1 activation can rely on a membrane effect by intracellular LPA, but the existence of a possible LPA-binding site, and an interaction between the cytosolic domain and the TM segments cannot be entirely rule out at present (94).

Activation gate of K_{2P} channels

Kollewe et al. (273) developed a structural model of K_{2P} channel (KCNK0) based on the Kv 1.2 crystal structure and the identification of pairs of sites that display electrostatic compensation (Fig. 10A). The systematic addition of a charge in the pore loop 1 (P1) or P2 promoted the restoration of channel function. The model supports the hitherto widely held assumption that K_{2P} channels form functional dimers with each subunit contributing two P regions to the pore. Also, this

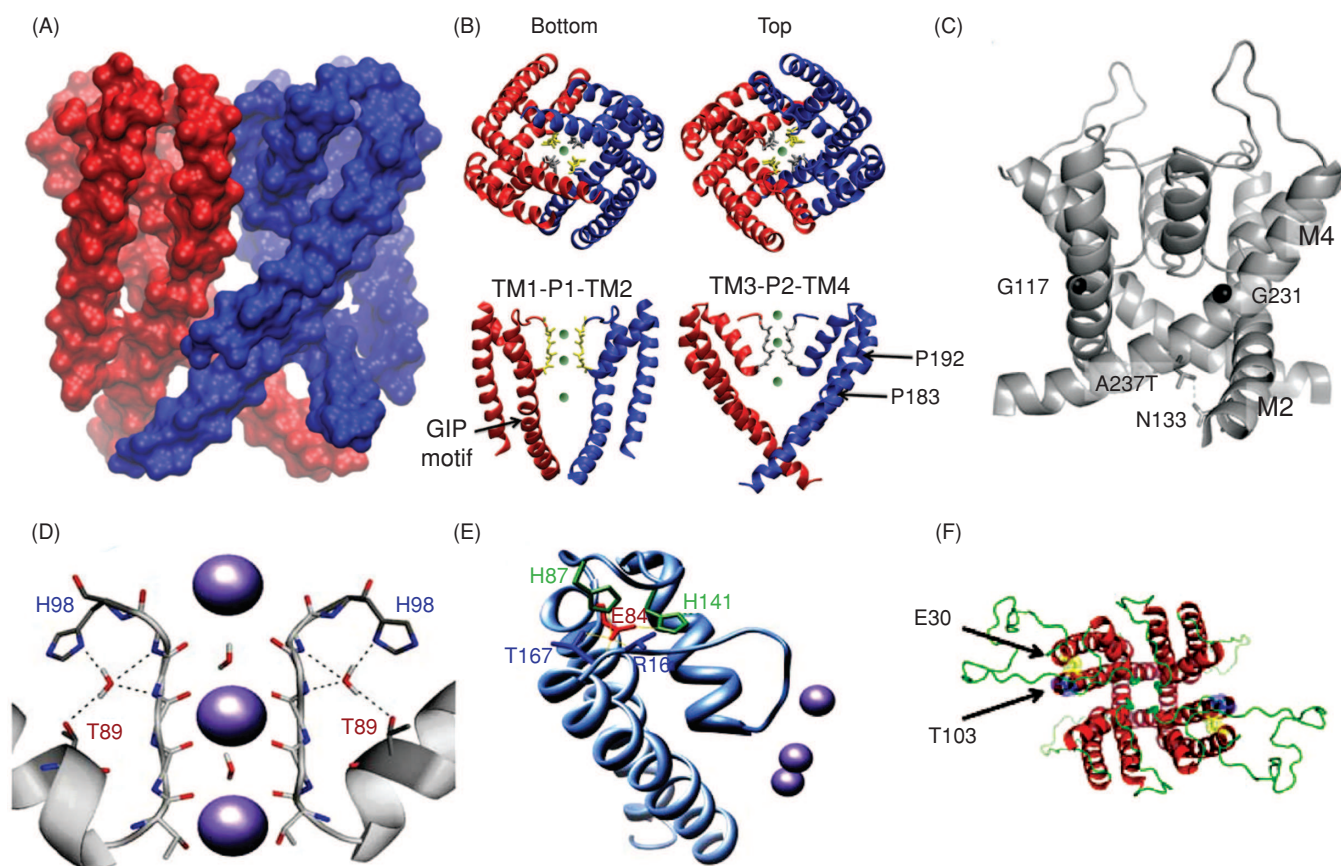


Figure 10 K_{2P} channel structure. (A) Homology model for $\Delta K2P\emptyset$ (K_{2P} \emptyset channel variant lacking AA from 299 to 1000) channel shows bilateral symmetry with a 4-fold symmetric selectivity filter. Color red indicates monomer A (from residue 1 to 152) and color blue monomer B (from residue 174 to 276). (B) Extracellular (top) and cytoplasmic (bottom) sides reveals overall symmetry like a parallelogram. The model includes residues 1 to 276 without the TM1-P1 loop (residues 30–91), TM2-TM3 linker (residues 153–173), and TM2-P2 loop (residues 225–238). (Bottom) Side view of domain I of both subunits. The glutaminase interacting protein (GIP) motif (G129–I130–P131) in TM2 is indicated. Side view of domain II of both subunits. Proline residue 183 and 192 in TM3 are indicated. (C) Structure of a mutant TASK-3 channel modeled in an open state, using the structure of KvAP [adapted, with permission, from Jiang et al. (238)] as template. It is hypothesized that channels open through flexion of M2 and M4 around hinge glycines G117 and G231. The positions of these hinge glycines are indicated as spheres in the helices M2 and M4. Gain of function mutants stabilizes the open state through altered side chain-side chain interactions between residues. A possible H-bond between Thr in position 237 of M4 (in mutant A237T) and N133, which may contribute to stabilizing the open state, is indicated. The model gives a bond length of 3.2 Å. (D) K2P3.1 model, illustrating the interactions of a water molecule with the backbone of Tyr-96 and Gly-97 and the side chains of Thr-89 and His-98 in the unprotonated form of His-98, according to molecular dynamic simulations, based on Yuill et al. (608). (E) pH-sensing mechanism of human K2P2.1. Ribbon representation of one subunit of the bacterial KcsA potassium channel, based on the published structure [Doyle et al. (115)]. Predicted hydrogen bonds between KcsA residues are presented as orange lines. The side chain of Glu-51 is predicted to form hydrogen bonds with the backbone amide groups of Val-84 and Thr-85 and the side chain hydroxyl group of Thr-85. The homologous K2P2.1 residues are Glu-84 (red), Arg-166, and Thr-167 (blue), respectively. KcsA Ala-54 and Leu-59 were replaced in this presentation by histidines, as present at the homologous positions in K2P2.1 [i.e., His-87 and His-141 (green), respectively] based on Cohen et al. (82). (F) Homology model of the TASK-3 K2P channel. Illustrating the proximity of the two E30 (yellow) and two T103 (blue) residues (view looking from the top down). The model was created using Modeller 9v7 (465) based on the KcsA structure as template [originally solved by Doyle et al. (115)].

model showed the glycine hinge residues present in almost all K⁺ and implicated in channel opening (237). This glycine residue is present in the M2 regions of K_{2P} channels within the glutaminase interacting protein (GIP) motif (glycine 129–isoleucine 130–proline 131) but not in the M4 regions (273). While K_{2P} channels are 4-fold symmetrical in the selectivity filter region, below this region they are only bilaterally symmetrical reflecting the low amino acid identity between M2 and M4 (Fig. 10B).

K_{2P} channels have a lower activation gate (glycine residues) and an upper slow inactivation gate (33,83). In contrast with Kv channels where these two gates are negatively

coupled, lower and upper gates in K_{2P} channels are positively coupled, with the opening of the lower activation gate signaling the opening of the upper inactivation gate. However, for full-length mammalian K_{2P}s the resting P_o is relatively low and mutations in residues close to the activation gate (A237T) can increase the open probability several folds. It has been suggested that the introduced threonine in M4 stabilizes the open state of the channel through altered side chain interaction between amino acid residues in M2. Channel activity may either increase or decrease through the action of regulators that influence this gate. Anesthetic activation, methanandamide inhibition and GPCR-mediated inhibition of TASK-1

and TASK-3 suggest that this introduced threonine residue in M4 stabilizes the open state of the channel through altered side-chain interactions between residues, possibly with N133 in M2 (see Fig. 10C). The results suggest that the alanine residue stabilizes the closed state of the channel through an interaction with residue L128 in M2 (20).

Voltage-dependent gating

TREK-1 is voltage-gated when S348 is phosphorylated by PKA or substituted with an aspartate to mimic phosphorylation. On the other hand, when TREK-1 is dephosphorylated by intracellular alkaline phosphatase or an alanine mutation (mimicking dephosphorylation), it behaves as a voltage-independent leak K⁺ channel. It is possible that voltage- and mechanogating might be functionally linked because progressive deletion of the C-terminal region and chimera mutants that affect voltage-dependency, also dramatically impair mechanogating, and the pressure-response curve is affected (toward more negative pressure values) (52,342). It has been previously described that cell depolarization changes the membrane curvature and induces membrane tension, and this tension is enough to activate mechanosensitive ion channels (154,623). Thus, the existence of this phenomenon led Maingret et al. (342) to suggest that depolarization might be able to stimulate TREK-1 opening through an alteration in membrane curvature and tension. Since there are several clusters of charges in the C-terminal domain, it is possible that this domain may act as a voltage sensor, independently of the mechanogating mechanism. However, to be able to sense the TM voltage the C-terminus has to be deeply inserted into either the lipid bilayer or into the ionic pore (342).

Inactivation gate of K_{2P} channels

In KcsA channels hydrogen bonds between residues in the selectivity filter and its adjacent pore helix determine the degree of C-type inactivation process (84,85,92). This type of gating mechanism appears to be also present in K_{2P} channels. For example, in TASK-1 and TASK-3, primarily by binding to a histidine (H98) next to the selectivity filter, protons inhibit the K⁺ currents (Fig. 10D) (263,322,439). In TASK-1, the residues in the outer pore mouth contribute to ion selectivity and the protonation of H98 initiates a C-type gating response that involves a conformational change in the selectivity filter of TASK-1 (see also reference 391).

Finally, a conserved glutamate residue (E28), located at the end of the first TM domain of the channel at the extracellular side of the membrane, has been shown to be important for gating in KCNK0 channel (631) and the equivalent residue (E418) in *Shaker* is a molecular determinant for C-type inactivation (294). The homologous residue in TASK-3 channels is E30 while in TREK-1 channels it is E84 (Fig. 10E). E28 stabilizes the open configuration of the channel by forming a hydrogen bond with amino acid residues in the pore region of the channel. For TASK-3 channels, mutation of the equivalent

amino acid residue E30 to cysteine also reduces the current amplitude (see Fig. 10F).

The Structural Family of Voltage-Dependent (Kv) Channels

This family is composed by two structural and functional types of members: 36 genes of six TM K⁺ channels (6TM) Kv: *KCNA* (Kv1 family), *KCNB* (Kv2), *KCNC* (Kv3), and *KCND* (Kv4), *KCNQ* (Kv7), *KCNH* (Kv10, Kv11, and Kv12, including ether-a-go-go-related gene (EAG) and human ether-a-go-go-related gene (ERG)], and the nonconducting group of gating modulator: *KCNF* (Kv5), *KCNG* (Kv6), *KCNV* (Kv8), and *KCNS* (Kv9). The phylogenetic tree for Kv channels depicted in Figure 11 shows the major classes of voltage-dependent K⁺ channels.

To be fully functional, Kv channels require a minimal tetrameric organization, with the ion conduction pore lying in the axis of a 4-fold symmetric structure (115,194,337). The primary sequence of these hydrophobic segments shows similarities between all Kv α -subunits, including a voltage-sensing domain (VSD) formed by TM segments S1 to S4 (or S0-S4 in the Slo family) and the pore domain comprising S5 to S6 (Fig. 12).

Several crystal structures of two Kv channel α -subunits have been uncovered in Rod Mackinnon's lab: the structure of KvAP channel from *Aeropyrum pernix* (238), the Shaker relative Kv1.2 (316) and a more refined chimera of Kv1.2 with the "paddle" segment of Kv2.1 (318) (Fig. 12).

All they show a pore domain with structural features conserved with other channel of the 2TM design as the bacterial KcsA, or MthK channels or the Kir channels (115,236,394,395).

Physiological function

The vertebrate α -subunit of voltage-gated K⁺ delayed rectifier family (Kv channels) is composed of twelve members (K_v1–K_v12) according to amino acid sequence similarity (Fig. 11). K_v1.1 is the vertebrate homolog of the fruit fly *Drosophila Shaker*. In flies lacking the fast transient Shaker K⁺ current in presynaptic terminals, the release of neurotransmitter is increased due to longer lasting action potential compared to the wild-type *Drosophila*.

To make a comprehensive description of Kv channel physiology based solely on their family diversity is impractical because the large variety of potassium channels type that arises from several factors (see later), makes a moderately complete description of Kv channels functional repertoire an encyclopedic task by itself. Thus, this revision must necessarily be taken as a "primer" on the subject.

In general terms, potassium currents can be classified into showing A-type (inactivating) or delayed rectifier behavior (noninactivating). However, at the molecular level, functional diversity in different cells types stems from the expression

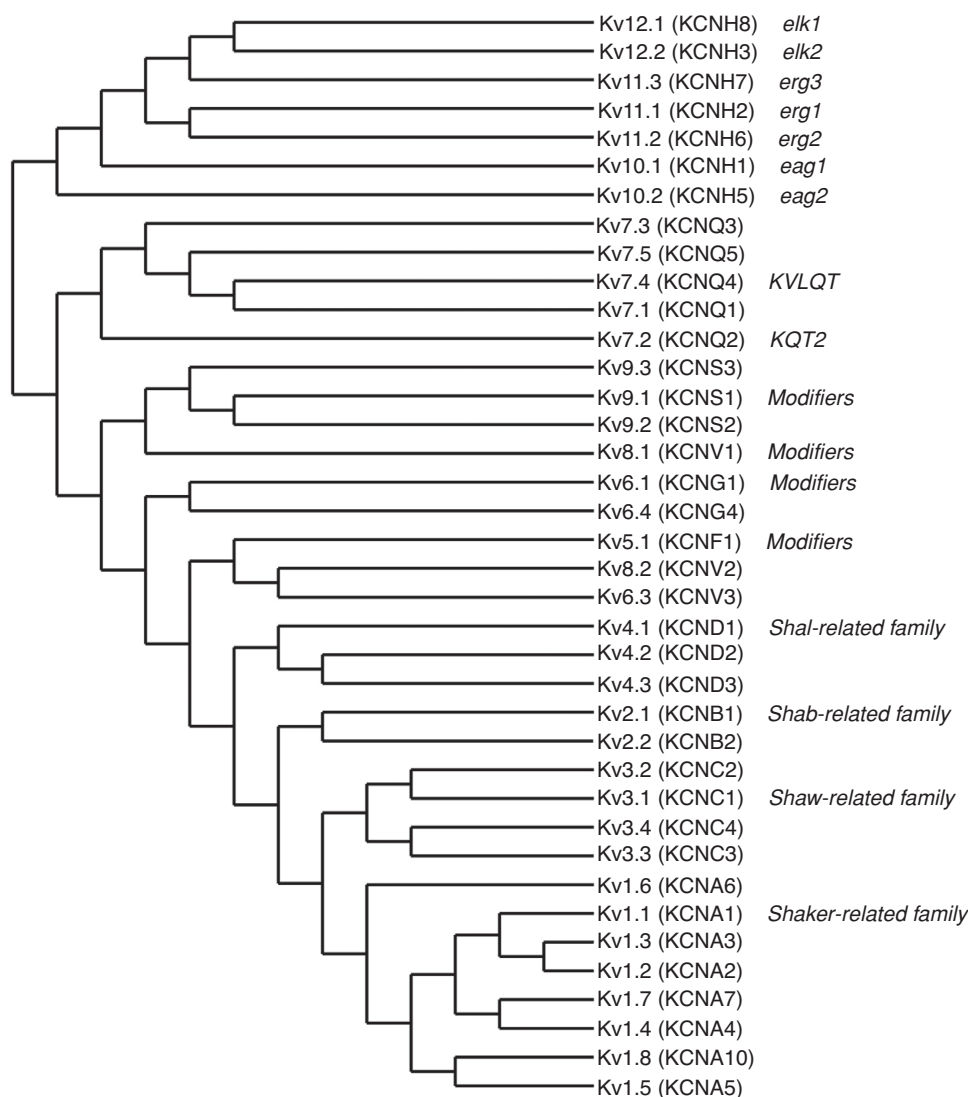


Figure 11 Organization of the voltage-dependent K⁺ channel superfamily. Phylogenetic tree for the Kv1-12 families. Amino acid sequence alignments of the human channel Kv proteins were created using CLUSTALW. Only the hydrophobic cores (S1-S6) were used for analysis. The IUPHAR and HGNC names are shown together with the genes' chromosomal localization and other commonly used name. The alignment was made using the web tool: Phylogeny.fr (109), with different sequences of human two pore K⁺ channels obtained from gene bank accession numbers: KCNH1: NM_002238.3, KCNH2: NP_000229.1., KCNH3: NP_036416.1., KCNH5: NP_647479.2., KCNH6: NP_110406.1., KCNH7: NP_150375.2., KCNH8: NP_653234.2., KCNQ1: NP_000209.2., KCNQ2: NP_004509.2., KCNQ3: NP_004510.1., KCNQ4: NP_004691.2., KCNQ5: NP_062816.2., KCNS1: NP_002242.2., KCNS2: NP_065748.1., KCNS3: NP_002243.3., KCNV1: NP_055194.1., KCNG1: NP_002228.2., KCNG4: NP_758857.1., KCNF1: NP_002227.2., KCNV2: NP_598004.1., KCNG3: NP_579875.1., KCND1: NP_004970.3., KCND2: NP_036413.1., KCND3: NP_004971.2., KCNB1: NP_004966.1., KCNB2: NP_004761.2., KCNC1: NP_004967.1., KCNC2: NP_631874.1., KCNC3: NP_004968.2., KCNC4: NP_004969.2., KCNA1: NP_000208.2., KCNA2: NP_004965.1., KCNA3: NP_002223.3., KCNA4: NP_002224.1., KCNA5: NP_002225.2., KCNA6: NP_002226.1., KCNA7: NP_114092.2., KCNA10: NP_005540.1.

of a subset of the approximately 35 genes of K_v channels. The multiplicity of K_v channels is further increased through: (i) heteromultimerization in which different gene products of the same family, as is the case of the Kv1, Kv7, and Kv10 families, form heterotetramers with novel functional properties not seen in the parental channels. (ii) Heteromultimerization with silent subunit families. For example, Kv2 family-form heterotetramers with novel properties with Kv5,

Kv6, and Kv8, subunits that do not form functional channels as homotetramers (181). (iii) Multimerization of K_vα tetramers with accessory β-subunits. For example, Kv1.1, Kv1.2, Kv1.3, and Kv1.5 are delayed rectifiers but when expressed with Kvβ1.1, become rapidly inactivating as the Shaker channel in *Drosophila* (195, 446) (Fig. 13). Together with Kvβ1 and Kvβ2, other auxiliary subunits modify function of K_v channels: (a) KCHIP1 by interacting with the N-terminal

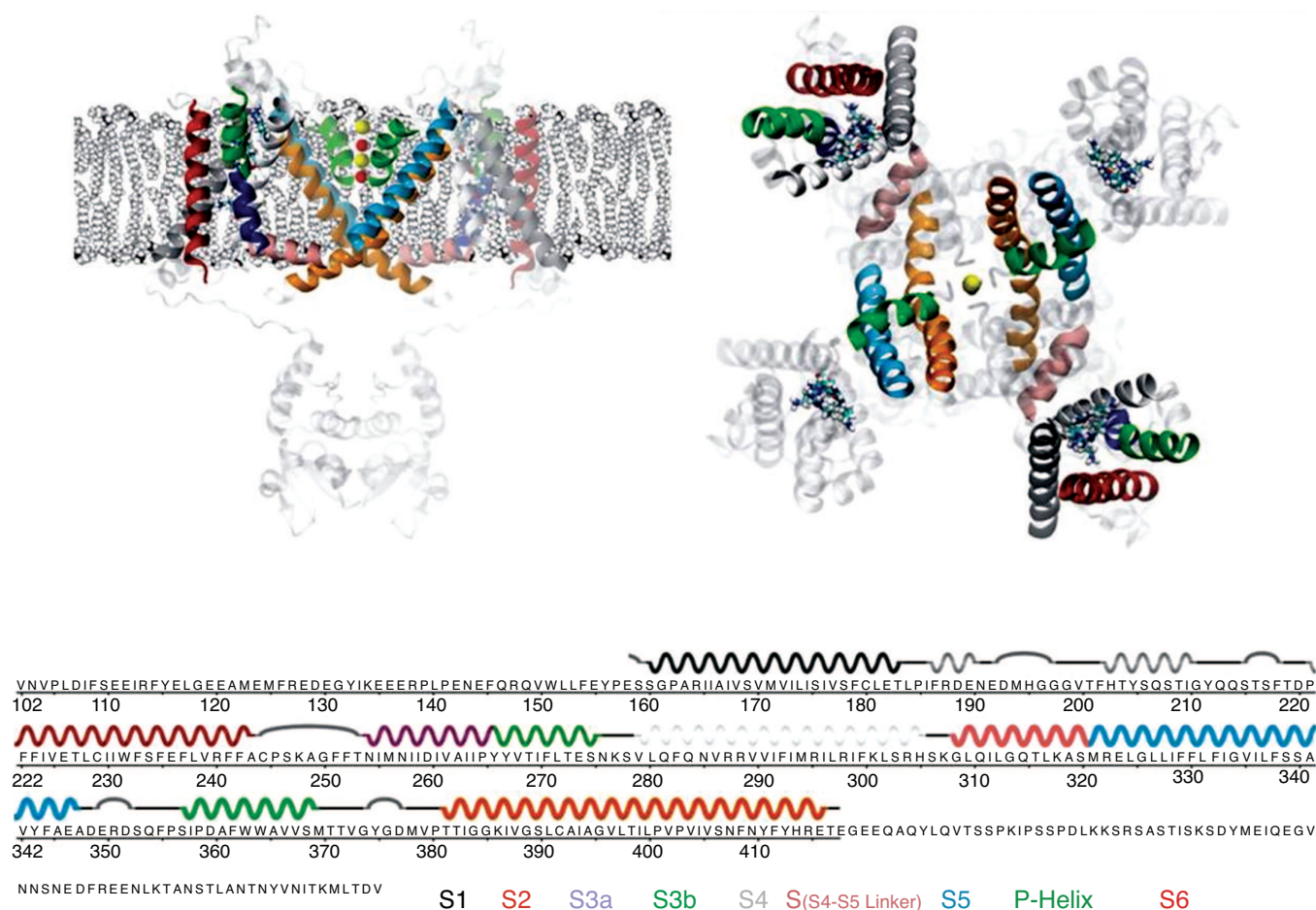


Figure 12 Organization and structure of the Kv1.2/Kv2.1 chimeric channel (PDB.ID: 2RAR). Lateral (left) and top (right) views of the protein embedded in the membrane. Arginine residues important for voltage dependence are shown in sticks. For clarity, two monomers are shown in light gray. The secondary structure of the amino acid sequence (below) is color coded to match the respective transmembrane and functional segments of the protein. Potassium ions are represented in green and the oxygen of water molecules in red. The cytosolic structure hanging from the main protein body is the tetramerization domain, T.

domain of Kv4.x channels modulates this class of ion channels surface expression and gating; (b) Ca²⁺/calmodulin inhibits Kv10; and (c) minK greatly modifies the gating kinetics of Kv11 (181,567). (iv) Alternative splicing: Several families Kv3, Kv4, Kv6, Kv7, Kv9 Kv10, and Kv11 can be subject to alternative splicing (181). (v) mRNA editing by hydrolytic deamination of adenosine to inosine by adenosine to deaminase acting on RNA (609). mRNA editing of Kv1.1

channels changes the kinetics of Kvβ1-induced inactivation (45). (vi) Posttranslational modifications as phosphorylation, palmitoylation, ubiquitinylation, etc.

A-type currents

After a sustained positive going voltage pulse, A-type potassium channels activate and then inactivate, producing a

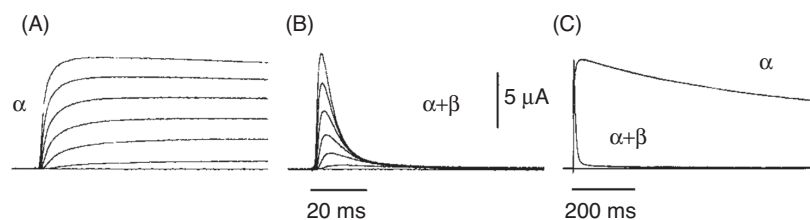


Figure 13 Kvβ1 inactivate currents of a Kv1 channel. (A) Delayed rectifier currents elicited by voltage steps in the absence of Kvβ-subunit. (B) Coexpression with Kvβ (α+β). (C) A single-voltage pulse shown in a large time scale. More details in reference 446.

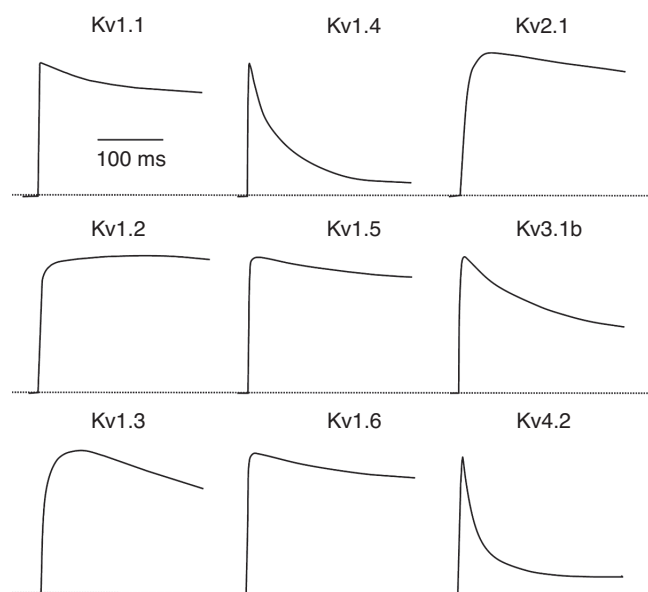


Figure 14 K⁺ currents diversity in Kv channels family. The indicated rat Kv channels were transiently expressed in HEK 293 cells. For each channel, whole-cell K⁺ currents at +40 mV were measured in similar physiological conditions. Modified, with permission, from reference 62.

transient response. Fast inactivation may play a role in setting the action potential interval because the Kv-dependent repolarization phase gets shorter if Kv channels inactivate and the neuron (or any excitable cell) is ready to fire a new action potential. Typical inactivating channels are Kv1.4, Kv3.3, and Kv3.4 and Kv4.1, Kv4.2, and Kv4.3 (Fig. 14). A complex formed by Kv4.2, Kv4.3, and KChIP2 may underlie the fast transient outward current (I_{to} fast) in cardiac muscle, while Kv1.4 may underlie a slower transient outward current (I_{to} slow) (180, 420). Kv 4.2 also encodes A-type K⁺ currents in dendrites of CA1 pyramidal neurons where they antagonize the back propagation of centrally generated action potentials, impeding the development of Long Term Potentiation (LTP) (100). On the other hand, Kv3.3 appears to block either excitability or Ca²⁺ signal propagation in cerebellum Purkinje cells (611) and mutations in Kv3.3 cause spinocerebellar ataxia in humans (SCA13) (138).

Kv1 channels are the *Shaker* counterparts of *Drosophila*, of which Kv1.4 α -subunit is the only member containing a N-type inactivation domain as *Shaker*. Kv1.4 can coassemble with other Kv1.x subunits to form Kv1-only heterotetramers. Kv1.4/Kv1.2 heteromultimers may underlie the presynaptic A-type K-current. Kv1.4 associate with accessory subunits such as Kv β -subunits, and with PSD96, SAP97, KChAP among others. CaMKII/calcineurin regulation through phosphorylation/dephosphorylation induces a Ca²⁺-dependent inactivation. Kv1.4 homotetramers are sensitive to micromolar 4-AP, riluzole, quinidine, and nanomolar UK78282 and nifedipine. Kv1.4 expresses in brain (mainly olfactory bulb, corpus striatum), lung-carcinoid, skeletal muscle, heart, and pancreatic islet. Kv1.4 expression increases in ventricular

myocytes after myocardial infarction and induction of diabetes (181).

Kv4 channels are *Shal* counterparts of *Drosophila*. This family is composed of three members, Kv4.1, Kv4.2, and Kv4.3 being able to form Kv4 heterotetramers. In humans all three genes contains six exons, and splice variants could modify their activity (181). They associate with other proteins as Kv β -subunits that assist them in the plasma membrane expression and enhance inactivation, while KChIPs enhances channel expression and delays inactivation. Kv4.1 and Kv4.2 are responsible for the somatodendritic A-type currents. For example, in different neuron types KV4 channels prolong the latency to the first spike in a train of action potentials, slow repetitive spike firing, shorten action potentials, and attenuate back propagating action potentials (86). KChIP1 increases KV4.1 current densities, accelerates inactivation time course and recovery from inactivation, and shifts steady-state inactivation to more depolarized potentials (181). Coexpression of KChIP1 with Kv4.2 results in increased current densities, slowed onset of inactivation, and accelerated recovery from inactivation (448).

Classical delayed rectifier

This name was used by Hodgkin and Huxley (HH) to describe the giant squid axon mostly outward K⁺-current that activated later than the Na⁺ currents (208). This current does not show inactivation in the millisecond time scale. According to this classical view, these channels not only terminate the action potential, restoring the dominant potassium permeability of the resting membrane but they also shape it. Several members of the voltage gated K⁺ channels underlie noninactivating currents. Most of the following description and references can be found well organized in the Gutman et al. compendium (181).

Unlike their *D. Shaker* counterpart, in the absence of β -subunits most members of the Kv1 channel family are not inactivating and only Kv1.4 inactivates with fast kinetics (195) (see Fig 14). Kv1 can coassemble with other Kv1 subunits only because they share the same T1 tetramerization domain (279, 308). They associate with the β -subunits, Kv β 1, Kv β 2, or Kv β 3, that confer inactivation to noninactivating subunits and play a role in channel membrane recruitment. Also, most Kv1.x channels associate to synaptic protein as PSD95, SAP97, or Dlg. Kv1.5 can also associate to *Src* tyrosine kinase.

A detailed pharmacological study comparing several delayed rectifiers including Kv1.1, Kv1.2, Kv1.3, and Kv1.5, found that all have submillimolar sensitivity to 4-AP and flaccinide; tens of micromolar sensitivity to capsaicin, nifedipine, diltiazem, and resiniferatoxin (171). They have different sensitivity to external TEA, with EC₅₀ ranging from 0.3 to 560 mmol/L in Kv1.1 and Kv1.2, respectively. Both, Kv1.1 and Kv1.2 have low nanomolar sensitivity to dendrotoxin (DTX). Kv1.2 and Kv1.3 have low nanomolar sensitivity to charybdotoxin (CTX) and noxiustoxin (NTX). Kv1.1 and

Kv1.3 have nanomolar and picomolar affinity to kalitoxin (KTX), respectively. Also, Kv1.1, Kv1.3, and Kv1.6 have picomolar sensitivity to the sea anemone toxin, ShK (93, 249).

In rats, Kv1.1 expresses in brain, heart, retina, skeletal muscle (31, 552), and their malfunction is associated to episodic ataxia type 1 with myokymia (104). Kv1.2 is expressed in brain (mostly in pons, medulla, cerebellum, and inferior colliculus), spinal cord, Schwann cells, atrium, ventricle, islet, retina, and smooth muscle where participate in contractile tone regulation. Kv1.3 is expressed in brain (mostly in inferior colliculus, olfactory bulb, and pons), lungs, islets, thymus, spleen, lymph nodes, fibroblasts, B and T lymphocytes, pre-B cells, tonsils, macrophages, microglia, oligodendrocytes, osteoclasts, platelets, and testis. Because it could be a therapeutic target for immunosuppressant, its role in T-cell activation has been intensely studied. Kv1.3 inhibitors inhibit calcium signaling, cytokine production, and proliferation of T-cells *in vitro*, and T-cell-motility *in vivo* (444). Kv1.5 is expressed in aorta, colon, kidney, stomach, smooth muscle, whole embryo, hippocampus, and cortex (oligodendrocytes, microglia, and Schwann cells), pituitary, and pulmonary artery. Kv1.5 has properties similar to the ultra rapidly activating I_{K_{ur}} current in the heart. It has potential use in management of AF via blockade of I_{K_{ur}}. Information on Kv1.6, Kv1.7, and Kv1.8 is sparser.

Kv2.x channels are the counterparts of *Shab* in *Drosophila*. This family is composed of Kv2.1, the mayor delayed rectifier present in CNS neurons (372), and Kv2.2 expressed abundantly in localized GABAergic neurons (196). Although, many tissues express both types of channels, and an approximately 90% identity in the N-terminus, there is very little evidence indicating heteromultimerization among them. Expression of these two types of channel appears to be spatially segregated within cells (381, 550) and Kv2.1/Kv2.2 coexpression apparently does not form functional heterotetramers (346). Recently, Kv2.1/Kv2.2 multimerization has been described in neurons expressing an approximately 100-residue longer form of Kv2.2 (259). However, Kv2.1 form heterotetramers with Kv5, Kv6, Kv8, and Kv9 subunits, showing a very complex landscape of functional diversity (181). Kv2.1 function can be modulated by phosphorylation (372) and inhibited by hanatoxin binding to its voltage sensor apparatus (525). Some chronic pulmonary hypertension decreases the expression of Kv2 (181).

Kv3.x channels are the counterparts of the *Drosophila* Shaw channel. While Kv3.3 and Kv3.4 produce A-type of currents, Kv3.1 and Kv3.2 are delayed rectifiers expressed prominently in the brain. Kv3 subunits form Kv3 heterotetramers. Because their fast activation and deactivation kinetics, Kv3 delayed rectifier channels are found in some neurons that are specialized to fire very short action potentials at high rates, such as those of the auditory system. They are found in cerebellum (in fast spiking neurons), skeletal muscle, arterial smooth muscle, and germ cells. They are blocked by micromolar 4AP and TEA and, in particular, Kv3.2 channels are block by verapamil and the toxin from the sea anemone

Stichodactyla helianthus (ShK). Kv3.2 knockout mice are susceptible to epileptic seizures (181).

The Kv7 channels are also known as the KCNQ subfamily in humans. The *KCNQ1* (Kv7.1) gene was the first member of the KCNQ subfamily to be isolated. Mutations in this gene give rise to the most common form of long QT syndrome, LQT1. Kv7.1 in association with KCNE3 [minK-related peptide 2 (MiRP2)] and minK (KCNE1), a single TM domain β -subunit, are the major determinants of the cardiac I_{K_s} current, which is involved in the repolarization of ventricular action potential (24, 470). *KCNQ1* mRNA is abundant in the heart, but also is found in the pancreas, kidney, lung, placenta, and ear.

Kv 7.2 (KCNQ2) and Kv7.3 (KCNQ3) have overlapping tissue distribution. Antibodies directed against Kv7.2 are able to coimmunoprecipitate Kv7.3, and vice versa. The heteromeric channel Kv7.2/Kv7.3 determine subthreshold excitability and corresponds to the M-channel found in neurons. They are sensitive to external pH (Fig. 15A and B) and are widely distributed throughout the brain, sympathetic and dorsal root ganglia (DRG), and expressed at high levels in hippocampus, chordate nucleus, and amygdala. Mutations in the *KCNQ2/KCNQ3* genes give rise to an idiopathic form of epilepsy (181).

KCNQ4 (Kv7.4) is expressed in outer hair cells (OHCs) and neurons of the auditory system and VSM. Kv5, Kv6, Kv8, and Kv9 channels are not functional alone; they coassemble with Kv2 subunits and modify their function.

The Eag family

The *Eag* channel family derives its name from a *Drosophila* behavioral mutant, ether-à-go-go, having enhanced neurotransmitter release at the neuromuscular junction. Known as the *KCNH* gene family in humans, it consists of three closely related subfamilies of genes defined by sequence homology, Kv10 (truly *Eag*), Kv11 (*Erg*), and Kv12 (127), where *Erg* stands for *ether-à-go-go related gene*, and *Elk* for *ether-à-gogo-like K-channel*. They all produce slowly activating currents (Fig. 15C).

The Kv10 family has two members, Kv10.1 and Kv10.2 having a restricted distribution. Kv10.1 has been found almost exclusively in brain, slightly in placenta and transiently in myoblasts, and in several tumor cell types, while Kv10.2 has been found in the CNS only (181). Kv10.1 has a potential as tumor marker and in cancer therapy (413).

Kv11 family is composed of three members, Kv11.1, Kv11.2, and Kv11.3, all capable to form Kv11 heteromultimers. Kv11.1 channels are ubiquitous; transcripts have been found in heart, brain, kidney, liver, testis, uterus, and prostate. The C-type inactivation of the ionic currents of the human counterpart, human ether-a-go-go-related gene (HERG) is orders of magnitude faster than the time course of activation (Fig. 15C). These properties are evidenced in characteristic outward going tails upon return to negative voltages. HERG underlies the cardiac Kir current known as I_{K_r} and is

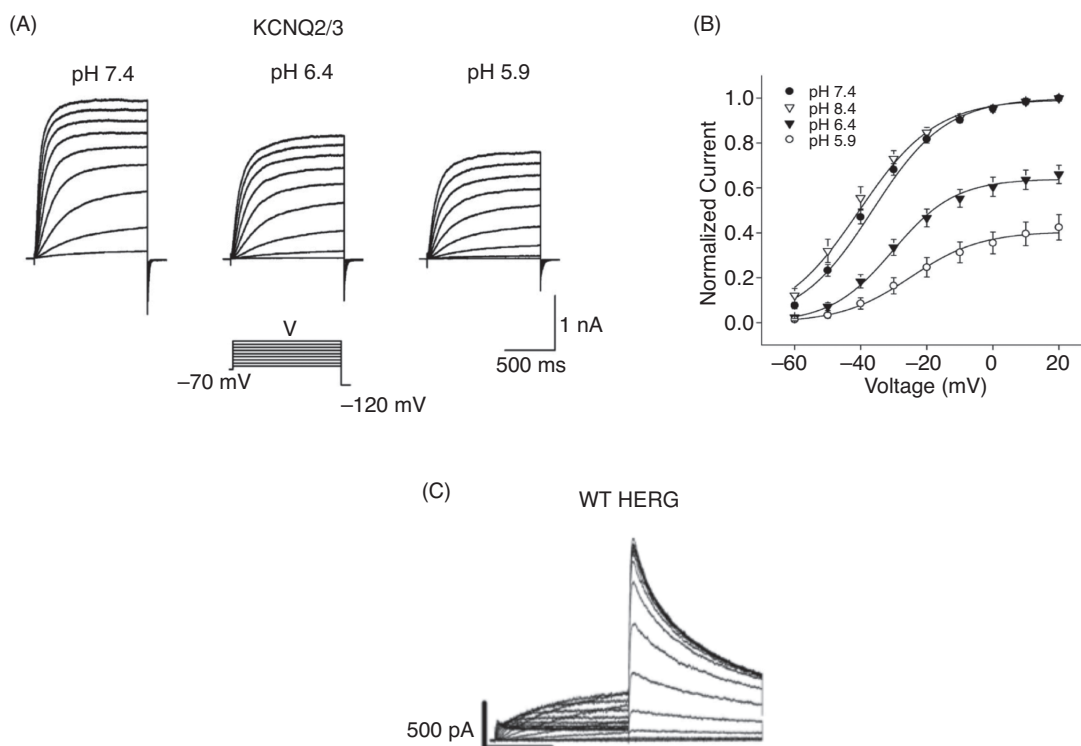


Figure 15 K currents from Kv7 and EAG families. Modulation of heteromeric KCNQ2/3 current by extracellular H⁺ ions. (A) Whole-cell KCNQ2/3 currents from a HEK-293 cell in bathing solutions of differing pH were elicited by depolarizing voltage steps (1.5 s duration) from a holding potential of -70 mV. (B) Whole-cell KCNQ2/3 current activation curves in bathing solutions of different pHs (437). (C) Isochronal activation of human ether-a-go-go-related gene (HERG) channels. Membrane potential was stepped from -80 mV to a test potential between -70 and 100 mV, in intervals of 10 mV, for 2 s, followed by step to -50 mV. The HERG characteristic rapid rise in the tails of current account for a very fast recovery from inactivation and a slower inactivation (378).

responsible for ending the plateau phase of the cardiac action potential (471). Nonfunctional mutations or deletion produce type 2 long QT syndrome (LQT2) not linked to deafness. Patients are prompt to fibrillation and sudden cardiac death (181). Kv11.1 homotetramer are blocked by nanomolar concentrations of astemizole, ergotxin, sertindole, dofetilide, cisapride, pimozide, terfenadine, halofantrine, and micromolar concentrations of CT haloperidol, imipramine, cocaine, and ketoconazole. Kv11.2 can be found in brain, uterus, and in some tumor cells as neuroblastoma and leiomyosarcoma. Kv11.3 can be found in brain (CA pyramidal neurons, lactotrophs, and rat pituitary), pituitary derived GH3 cells, and sympathetic ganglia. Kv11.3 is blocked by nanomolar concentrations of sertindole and pimozide (181).

Recently, Kv11.1 activators have gained interest as potential therapeutic agents mainly as a potential treatment of certain types of cardiac arrhythmias (111, 292). Two of these compounds have markedly different modes of action. NS1643 has been shown to increase Kv11.1 currents primarily by rightward shifting the inactivation curve and by slowing the fast inactivation process (76, 189). In contrast, RPR260243 almost exclusively acts by slowing the deactivation process of the channels (254).

Kv12 family is composed of three members, Kv12.1, Kv12.2, and Kv12.3 that are able to form Kv12-only heterotetramers (634). They are expressed primarily in the nervous system and produce a slowly activating and deactivating current. They contain a light, oxygen, or voltage (LOV) flavin mononucleotide and cyclic nucleotide-binding domains. Kv12.1 is expressed in brain, sympathetic ganglia, testis, colon, and lung. Kv12.2 is expressed in brain, (eye, cortex, amygdala, hippocampus CA1 and CA3, and dentate gyrus) peripheral nervous system, and lymphocytes. Blockade by 1-(2-chloro-6-methylphenyl)-3-(1,2-diphenylethyl) thiourea (CX4) or genetic deletion of Kv12.2 reduce the firing threshold in hippocampal pyramidal neurons. Also, Kv12.2^{-/-} mice show persistent neuronal hyperexcitability, spontaneous seizures, and increased sensitivity to convulsants (624). Little is known about Kv12.3 except that appear to be expressed in brain, esophagus, lung, and pituitary gland (181).

Kinetic models consistent with Kv gating

The Hodgkin and Huxley model

To explain voltage-dependent ion permeability, HH proposed that it arises “from the effect of the electric field on the

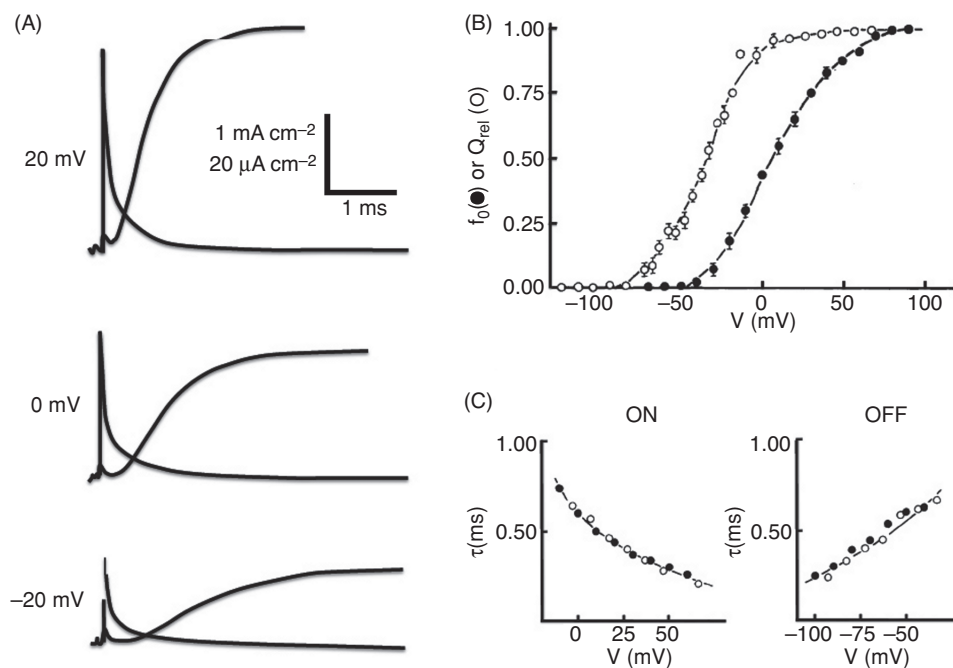


Figure 16 Gating currents elicited by the squid potassium channels. (A) Superimposed 10 ms traces of gating and ionic currents recorded at three different voltages taken at 20°C degrees. Na⁺-gating currents are missed because at this temperature they are too fast for the recording system (modified, with permission, from reference 44). (B) Voltage dependency of the gating charge (open symbols) and the ionic conductance (filled symbols). (C) Kinetics of the gating and ionic currents (B and C modified, with permission, from reference 572).

distribution or orientation of molecules with a charge or dipole moment” (209). Currently, there is a consensus that voltage dependency in K⁺ channels is mostly due to charge movement instead of displacement of dipoles. The probability of finding the charge in either side of the electric field (or the membrane) must follow a Boltzmann distribution, which is a function describing the probability (P_o) of finding a charged particle with valence z in a electric field of intensity V , such that:

$$P_o = \frac{1}{1 + e^{\frac{-zF(V-V_o)}{RT}}}$$

where F , R , and T have their usual meanings and V_o is the voltage at which $P_o = 0.5$. We must emphasize here that the effective valence z is actually the product of the actual valence times the fractional distance the charges move across the electric field.

HH applied a Boltzmann distribution to describe the K⁺ conductance as function of the applied TM voltage (see, for example, the curve f_o vs. V in Fig. 16B). Notice that when V is sufficiently negative, equation becomes:

$$P_o = K e^{zFV/RT} \quad (2)$$

where K is constant. In this limit HH found for that the K⁺ conductance increased an e -fold increase every 4 mV. Their

conclusion was that the particles controlling the K⁺ conductance were endowed with at least six electronic charges that move across the electric field.

One key observation was that after a square voltage pulse from a negative voltage, where K⁺ conductance was at rest (or closed), the activation of the K⁺ currents followed a sigmoidal time course (Fig. 16A). In other words, there is a lag in the ionic currents after the voltage pulse is applied. This particular kinetic attribute suggested that the structure governing the K⁺ conductance undergo several nonconductive steps before reaching the active state. On the other hand, after returning to the resting voltage, the relaxation of the currents did not show a delay and was well described with an exponential time course. Thus, the system governing K⁺ conductance had several nonconductive states but only one or few conductive states.

Following HH, we can assume that four identical and independent charged particles control the K⁺-permeability. The particle moves across the electric field between two positions, *active* and *resting*. The probability for the potassium channels to be in the active conformation is proportional to the joint probability that all four charged particles are in the active position. If n is the probability of each particle to be in the active position, $1 - n$ is the probability of being at resting. Thus the probability of finding K-channels conducting is proportional to n^4 . Then, the reaction:

$$n \leftrightarrow 1 - n \quad (3)$$

must be a simple first order chemical reaction such that in the presence of a perturbation (for example, a change in membrane voltage) reaches a new equilibrium according to:

$$\frac{dn}{dt} = -\beta n + \alpha(1 - n) \quad (4)$$

where α and β are the backward and forward rate constants, respectively. The solution of this equation describes how the n -particle relaxes to a new equilibrium, n_∞ , from the previous pre-perturbation equilibrium, n_0 and is given by:

$$n(t) = n_\infty + (n_0 - n_\infty)e^{-\frac{t}{\tau}} \quad (5)$$

where $n_\infty = \alpha/(\alpha + \beta)$ and $n_0 = \alpha_0/(\alpha_0 + \beta_0)$. At $t = 0$, $n(t) = n_0$, the initial value, which relaxes exponentially to reach n_∞ as $t \rightarrow \infty$. The time constant of this exponential relaxation is $\tau = 1/(\alpha + \beta)$. Because four independent particles in the active position are needed to activate K-permeability, a general expression for the potassium current (I_K) is:

$$I_K = g_K n(t)^4 (V - E_K) \quad (6)$$

where g_K is the maximal K-conductance, V is the membrane potential, and E_K is the equilibrium potential for K⁺.

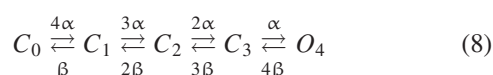
Fitzhugh's expansion of the HH model

The expansion of the HH model, as recognized by Clay Armstrong in his seminal 1975 review (11), is due to Richard Fitzhugh an influential biophysicist that developed several conceptual and educational advances in our understanding of the HH model (142, 143).

If the activating particles distribute randomly, at a given membrane potential, the total number of nonconductive configurations and their proportion, is given by the binomial distribution and by the geometrical arrangement of the particles. If none of the geometrical configurations are equivalent, the number of all possible configurations having less than four active n particles ϕ_i is given by:

$$\sum_{i=0}^3 \phi_i; \quad \text{where} \quad \phi_i = \frac{4!}{i!(4-i)!} \quad (7)$$

For four particles, the maximal number of nonconductive states is $\phi_0 + \phi_1 + \phi_2 + \phi_3 = 15$, producing a complex kinetic scheme. But if geometry is not important, the number of nonconductive states becomes reduced to four, having 0, 1, 2, or 3 active n particles, and yielding a more simple kinetics:



where C and O represent closed and open states of the channel, respectively, and the subindexes represent the number of active n particles in each population. This kinetic scheme, which is in fact the expansion of the HH model (11), reproduces the basic kinetic and steady-state features of the potassium conductance in the squid axon. Due to the transit of the K⁺ channel among several closed states, it reproduces the sigmoidal activation of the currents, and the monoexponential deactivation because there is only one open state (209).

The HH model made two additional predictions that were tested only 20 years later (12, 13, 41, 42). Because of the charged nature of the *voltage-sensing* particle it could be possible to detect the movement of the n particles as a nonionic current. With a high-enough number of channels on the membrane or with high-enough sensitivity, it would be possible to measure the current produced by the intramembrane charge displacement of the voltage sensing particles, the *gating currents*. The gating currents, I_g , can be predicted from the HH model assuming that each n particle has a charge z and that they are proportional to the rate of movement of N particles

$$I_g = Nze \frac{dn}{dt}$$

Because, most of the transitions in scheme 8 occur among closed states, upon positive voltage pulses, these gating currents should follow an exponential relaxation time course with a time constant equals to $1/\alpha$ preceding the activation of the ionic currents. On the other hand, upon returning to the resting voltage, the gating currents should be four times slower than the ionic currents because the channel closes with 4β while the n -particle returns with a rate constant β . These predictions were tested for K⁺ currents about 30 years later (13, 44, 258).

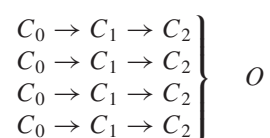
For K⁺ channels, the gating currents show a very fast rising phase followed by an exponential decay (Fig. 16A) and indicating that most of the sensing charge displacement occurs among closed states, the voltage activation of the gating charge (Q_{rel}) is shifted toward negative voltages compared to the K⁺ conductance (f_o), (Fig. 16B). However, both activation and deactivation kinetics of the gating currents were similar to those of the ionic currents (Fig. 16C). These results indicated that leaving the deeper closed states is rate limiting for activation and leaving the open states could be also rate limiting for the deactivation and gating charge return (44, 572).

The ZHA kinetic model

After the molecular cloning of voltage gated K⁺ channels during the late 1980s, the preferred model for structure-function studies on voltage gated ion channels was the Shaker K⁺ channel. This protein is the alternative splicing product of a complex gene in *Drosophila*, extending approximately 130 kb (250, 412).

The tetrameric structure of potassium channels put forward for Shaker K-channels (311, 337) reinforced the idea of four gating particles, each one in each subunit. Aldrich and

co-workers proposed a kinetic scheme for Shaker K-channels, the ZHA model (220,613,614) is consistent with macroscopic currents, gating currents, and single channel recordings. The key observation on the channel behavior was that the effective valence was large, 12 to 13 electronic charges (e_0), but no single process, as activation or deactivation, showed a large voltage dependence. To describe the latency of the current activation required a minimum of eight transitions between closed states. Thus, the voltage-dependent activation must involve a large number of states, each one moving a small number of charges. The resulting scheme has some of the features of the original n -particle model from HH, but includes two voltage-dependent transitions per subunit (613).



Each subunit displaces approximately 3 e_0 in two transitions, suggesting three conformations for the voltage sensor (Eq. 9). This scheme introduces a concerted opening transition when the last voltage sensor reaches the C2 state. The rate constant describing the channel closing is 10-fold slower than the other backward rates departing from C2. This explains in a most economical manner why the kinetics of the OFF gating currents is similar to that of deactivation of the ionic currents as was observed by White and Bezanilla (572).

However, the ZHA model has the caveat of strictly tying the last forward transition of the voltage sensor to channel opening. There is ample evidence for the existence of an activated-not-open conformation present in several types of voltage gated K⁺ channels (see, for example, reference 15). More complete kinetic models that incorporate the existence of activated nonopen state and a concerted opening transition have been developed by Sigworth and co-workers (483,627).

Structure-function relations in voltage-dependent K⁺ channels

Gating in the Kv channels is conferred through the attachment of VSDs to the pore. The basic function of this domain is to perform mechanical work that allows the ion conduction pore to change its conformation between closed and open states. In voltage-dependent channels, the VSD converts the energy stored in the membrane electric field into mechanical work. There is strong evidence that the positive charges contained in S4 are the voltage-sensing elements (3,490). Thus, Kv channel gating is essentially an electromechanical coupling between a voltage sensing unit and a pore unit.

The crystal structure of a mammalian voltage-dependent K⁺ channel (Kv1.2), suggested to be in a relaxed state (see section on *VSD conformation during slow inactivation*), had initially been resolved at 2.9 Å and further improved to 2.4 Å using a chimeric Kv1.2-Kv2.1 channel. In the latter case,

the channel was crystallized in complex with lipids. These structures showed that the helices of the ion conduction pore (S5-S6) related to the helices of the voltage sensor domain (S1-S4) in a special way. The voltage sensor domain of one subunit is located near the pore domain of an adjacent subunit (Fig. 12). The connection between the pore and the voltage-sensor domain is made by the S4-S5 linker helix, which runs parallel to the intracellular membrane surface.

Voltage sensitivity

The tetrameric organization of voltage-dependent K⁺ was demonstrated early after the almost simultaneous molecular cloning of the *D. Shaker* K-channels (311,337). Each monomer is formed by two well-defined structural and functional domains, the pore domain and the VSD (see Fig. 17A) (238,307,523). The pore domain is structurally related to the Kir channels family. As in the KcsA K⁺ channel, this protein module should contain two TM α -helices and a reentrant loop composed of a four-turn pore helix flanking a selectivity filter lined by the carbonyl groups of six residues unfolded in an extended conformation (115). The operation of the pore main access gate is under the control of the VSD, which is a separate structural domain formed by four TM segments [named S1 to S4 (238,307,458)].

There are several lines of evidence indicating that the VSD of voltage-gated K⁺ channels is a separate structural domain *per se*. *First*, The VSD from the bacterial (*A. pernix*) voltage-gated K channels, KvAP, can be synthesized, purified, and folded separately showing similar crystallographic structure to the channel-attached domain (238,458). *Second*, it can be added to pore domain only K⁺ channels, such as KcsA, transferring VSD-gated voltage sensitivity (326) to the chimeric channel. *Third*, there are functionally different membrane proteins consisting of only a voltage-sensor domain. For example, a voltage-gated proton channel (161,401,442,476) and a voltage-sensitive phosphatase discovered in the ascidian *Ciona intestinalis*, Ci-VSP, which consist in a VSD functionally linked to an inositol phosphatase. This protein displays channel-like “gating” currents and directly translates changes in membrane potential into the turnover of phosphoinositide (215,382,401). The physiological activity persists after functional detachment of the phosphatase domain (559).

When Numa and co-workers first cloned a voltage-gated ion channel (398), they proposed that the unusually charged fourth TM segment (S4), hosted the molecular determinant for the voltage sensitivity. In voltage-gated K⁺ channels, S4 contains a highly conserved sequence array of 6-8 basic amino acids periodically spaced by two hydrophobic residues. With individual charge-neutralizing mutations of charged residues in the VSD of Shaker K⁺ channels, only E293 an acidic residue in S2 (G1 in Fig. 17A), and R262, R365, R368, and R371 (R1 to R4, respectively in Fig. 17A) in S4 contributed significantly to the gating charge or to the voltage sensitivity. Individual neutralization of each of these charged residues led

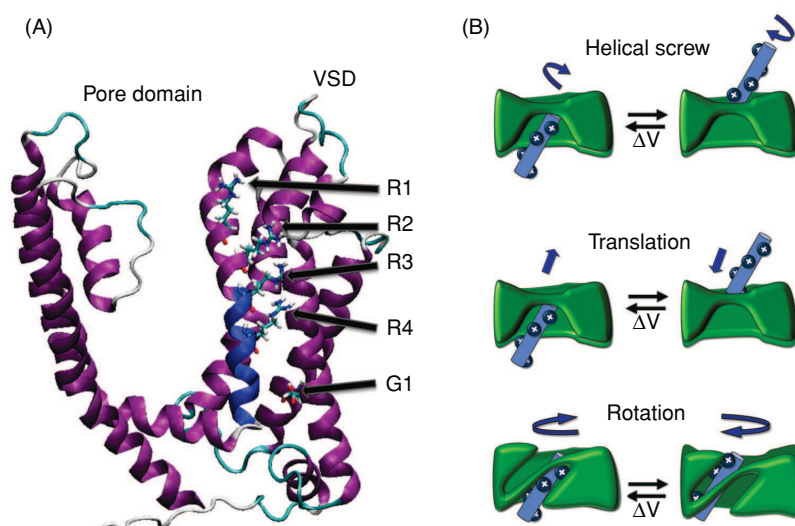


Figure 17 Structural determinants for the voltage sensitivity in voltage-gated K⁺ channels. (A) Structure of a single monomer depicting the voltage-sensor domain (VSD) and the pore domain. Arginines R1, R2, R3, and R4 (corresponding to Shaker R362, R365, R368, and R371) are represented in stick form. (B) Possible trajectories for the gating charges (for more details see text).

to large decreases ($\sim 4 e_o$ each) in the gating charge and in the effective valence of the voltage dependence (z in Eq. 1) (3, 490). This agreement indicates that most, if not all, the charge transferred during activation is energetically coupled to channel opening.

However, the simple arithmetical addition of the contribution of each individual charge neutralization reaches over $20 e_o$, a figure much larger than the total number of 12 to 14 e_o charges per channel determined by either gating currents (3, 490) or by the limiting slope analysis (160, 229, 482, 614). This paradox can be solved if it is assumed that neutralization of some of the charges not only changes the total number of gating charges but also is modifying the local electric field. This disparity also indicates that each charge does not contribute independently to the voltage dependence and their contribution must depend on the specific protein sequence nearby the voltage-sensing residues. For example, the introduction of charged side chains into conserved hydrophobic positions in the S4 reduces dramatically the effective gating charge (160).

Physical displacements in the VSD

The individual contribution of each of the S4 arginines R362, R365, R368, and R371 (named R1–R4 in Fig. 17A) of the Shaker K⁺ channel to the gating charges is close to 4 electronic charges (e_o) (3, 490). A straightforward interpretation to these results, imply that each one of the four arginines side chains move across most of the electric field. If the electric field decays along the thickness of the membrane, each voltage-sensing arginine should move 30 to 40 Å. Following an strategy designed in Richard Horn's lab for the sodium

channel, a few labs measured activation-dependent internal and external solvent accessibility of cysteine residues introduced to replace R1 to R4, one at a time (293, 600, 609). Chemical modification of residue 362 by membrane impermeant thiol reagents was possible from the extracellular side in the active state and, to a much lesser extent, in the closed state. For residues 365 and 368 changes in accessibility were more dramatic; they were internally accessible in the closed state and accessible to thiol reagent from the external side in the open state. Thus, these results not only revealed significant movements of S4, but also a short hydrophobic septum in the closed state, since 362 was accessible from the external side as 368 was it from the internal side (i.e., only 6 amino acid residues, which if conforming a α -helix implies a septum of ~ 9 Å). Thus, water crevices must surround the voltage sensor very deep into the protein, focusing the electric field in a short stretch of low dielectric material (293). The elegant histidine substitution studies of Bezanilla's group (511–513) gave further support to the structural model that considered the S4 contained in water-lined crevices separated by a short hydrophobic septum. Histidines introduced in R2 and R3 transport protons down the proton gradient each time the voltage sensor moves from the resting to the activated state indicating that R2 and R3 traverse the full length of the electric field. Histidines replacing R2 and R4, on the other hand behaves as voltage-dependent proton channels, which allow proton fluxes only when the voltage sensor is in the resting and the active state, respectively. The fact that replacement of R1 and R4 by histidines form proton pores in both the open and the closed state is a strong evidence of the existence of a short hydrophobic septum in the resting and active state of the voltage sensor.

Because the size of the gating charge decreases at low ionic strength, part of the electric field must fall across these water crevices (230). From this reduction, an intracellular conical cavity of 20 to 24-Å depth and 12-Å aperture, and a smaller extracellular cavity of 3-Å depth and the same aperture could be estimated, leaving a septum with an expected thickness of 3 to 7 Å. Consistent with this figure, using a series of permanently charged methanethiosulfonate (MTS) reagents with alkyl tethers ranging from methyl to hexyl, Ahern and Horn (5) found that short adducts (<3CH₂) added to R362C could be dragged across the electric field during activation to carry charge across it; however, charged adducts with six CH₂ or longer linkers could not be dragged across the septum, suggesting that these linkers were long enough to stretch with the voltage-sensor movement without shuttling the charge across the field. Thus, the low dielectric septum must be only 4 Å across (5).

Consistent with a very short septum, amino acid replacement in some of the voltage-sensing positions make the voltage sensor behave as cationic pore at negative voltages (in the resting conformation) (72, 512, 542, 543). The histidine scanning mutagenesis studies and these results indicate that a single amino acid replacement can disorganize entirely the dielectric septum transforming it into an ion channel.

The trajectory of the voltage-sensing charges

From the previous description, a small “vertical” movement should be necessary to shuttle the sensing charges across the electric field. In fact, Bezanilla’s lab made measurements with luminescence resonance energy transfer (LRET) of distance changes between the voltage sensors of each Shaker subunit and between voltage sensors and a pore-bound scorpion toxin during activation. They proposed a small vertical displacement of 2 Å or less (91, 155, 433) (see Fig. 17B). On the other hand, the KvAP structure (238, 240, 457) suggested that S4 together with the second half of S3 (S3b) formed a helical hairpin structure located rather intracellular that MacKinnon and colleagues named the “paddle.” They attached a biotin molecule, through a 17 Å linker, to paddle residues and then probed for their activation-dependent internal and external accessibility to streptavidin. The accessibility pattern to streptavidin suggested that the paddle would traverse most of the membrane thickness, that is, 25 to 35 Å. (240). Alternatively, S4 could also slide up in a helical screw trajectory along S3 (78, 182) (Fig. 17B top). By cutting short the Shaker K-channel S3-S4 linker to restrict S4 movement (163, 357) it was found that S4 require to slide 3 to 5 Å with respect to S3 in a rotational trajectory (162, 164). However, a disulfide bond between Shaker residues 325 in S3 and 360 in S4 can be formed in the closed state, while a bond between 325 and 366 can be formed in the open state, a result consistent with a helical trajectory of 9–16 Å of S4 (63). Discrepancies may arise from the use of different channels (bacterial vs. mammalian) as well as from the use of different experimental approaches [see (39, 524)].

The molecular determinants of the hydrophobic septum have been further elucidated by substituting residues I241 and I287 in S1 and S2, respectively by histidines in the Shaker K⁺ channel (72). Mutants I241H and I287H generate inward currents at negative applied voltages indicating that these residues are part of the hydrophobic plug. Replacement of I241 and I287 by cysteines showed that under oxidizing conditions and at hyperpolarized voltages, these residues are able to form disulfide bonds and metal (Cd²⁺) bridges positioning in an unambiguously manner the position of the S4 segment relative to S1 and S2. Importantly, these results open for the possibility of predicting the trajectory followed by the S4 segment in going from the closed to the open state. To satisfy these constraints, the S4 rotates (~180°) and undergoes a vertical movement of about 6.5 Å (72).

The environment surrounding the voltage-sensing charges is aqueous

S4 is an unusually charged TM segment, having a strictly conserved sequence array of six to eight basic amino acids periodically spaced by two hydrophobic residues (see supplementary material in reference 299).

Some of S4 basic residues seem to be stabilized by a network of negatively charged residues in S2 and S3. Intragenic suppression strategy with charge reversal mutations in Shaker suggested activation-dependent electrostatic interactions between E283 (S2) and R3 and R4, and between K374 in S4 with E293 in S2 and D316 in S3 (540, 541). The other charged arginine side chains could be stabilized by hydration shells protruding into the core of the membrane (5, 243, 244, 278, 549) or by counter charges provided by phosphate groups of the polar head of phospholipids (200, 316, 318, 338, 443, 481, 524, 593). The counter charges mechanism must be specific for *basic* residues; in contrast, hydration could stabilize charges independently of their sign. Consistent with this latter expectation, S4 tolerates additional charged side chains, negative and positive, added in a number of positions in S4 (4, 160). These results argue in favor of hydration as the charge stabilization mechanism. This mechanism would shape the protein-lipid-water interfaces, providing a molecular explanation for the formation of the aqueous crevices surrounding S4 (160, 244, 278, 549).

The K⁺ selective pore domain

The K⁺ selective pore is located in a structurally homologous locus of the protein as voltage-gated Na⁺ and Ca²⁺ channels, and share a common mechanism of ion transport too: they can hold several permeant ions in single file (125, 199, 385, 445). K channels are endowed of a highly K⁺ selective pore that allows fluxes of K⁺ ranging from 10⁶ to 10⁸ ions/s in physiological conditions (in terms of conductance, it is equivalent to ~3 pS to ~300 pS). Voltage-gated K⁺ channels constitute one of the most diverse membrane protein family (467) but all of them encoded an extremely conserved signature sequence

of seven amino acidic residues, TTVGYGD (193) that forms the structure of the ion selectivity filter.

Potassium channels conduct K⁺ ions with high selectivity over other cations. In general, they prefer K⁺ ions hundreds times over the Na⁺ ions having only an approximately 0.4 Å smaller radius. This high selectivity was expected if oxygen atoms inside the pore replace K⁺ hydration shell with a separation between oxygen so critical that Na⁺ does not fit comfortable (40). When the crystal structure of a bacterial K channel KcsA at 3.2 Å resolution became available from the MacKinnon lab (115), it showed a snapshot of several permeant ions in single file inside the conduction pathways as was anticipated in 1955 by Hodgkin and Keynes for the giant axon (210). The structure of this ion channel showed two zones that K⁺ ions must transit in their trajectory through the pore; the selectivity filter, containing two cations, and the internal vestibule or “cavity,” having one cation beneath the entrance of the selectivity filter (Fig. 18A). MacKinnon and colleagues proposed that the oxygen atoms of the peptide backbone carbonyl groups, in perfect 4-fold symmetry, stabilized dehydrated K⁺ ions by acting as water “surrogate,” as Bezanilla and Armstrong had proposed earlier (40). The transit of the ions in the selectivity filter could be restricted to jumps between well-defined binding sites (zones of larger electron densities in the crystallographic data), while in the

cavity, cations would have to diffuse from the internal entrance to the deep end to reach the cavity-binding site.

In a surprising example on how a static/stable structure of the selectivity filter determined at 2 Å resolution (629) revealed details of a dynamic process as ion conduction, this structure shows in detail a remarkable machinery appearing to be optimized not only to conduct ions but also to exquisitely discriminate between K⁺ from other cations (Fig. 18B). The structure revealed seven K⁺-binding sites in single file in the pore with alike electron densities (i.e., energetically similar). The two antipodal K⁺, at the external end of the selectivity filter and at the cavity, were fully hydrated with eight water molecules around the pore's axis of symmetry, four on top and four on the bottom of the K⁺, suggesting that the energetic cost of dehydrating K⁺ ions inside the pore is close to zero. The second K⁺, counting from the external site at the external entrance shows partial dehydration, as if during the snapshot it was being stripped from its solvating water as it enters the pore. Because the distance between the binding sites is too small (~3.5 Å) to overcome electrostatic repulsive interaction between sites neighboring K⁺, it is unlikely that, in addition to the cavity site, all six binding sites are simultaneously occupied by K⁺ ions. Instead, the similarities in electron densities could be revealing two alternating and energetically equivalent ion configurations within the

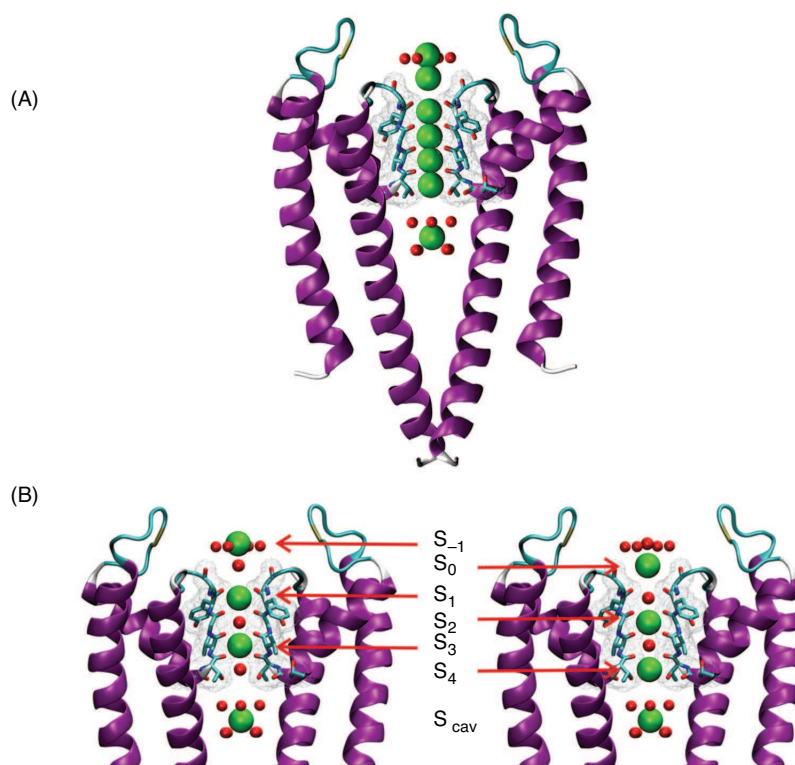


Figure 18 Structural design of the K⁺ conduction system. (A) Ions in the pore of the KcsA bacterial channel (PDB.ID: 1K4C). All possible K⁺-binding sites are shown. Hydration water molecules are shown in red with a Van der Waal radius of 0.5 Å. (B) Ion conduction is due to two alternating and energetically equivalent configurations in ion occupancy (for more details see text).

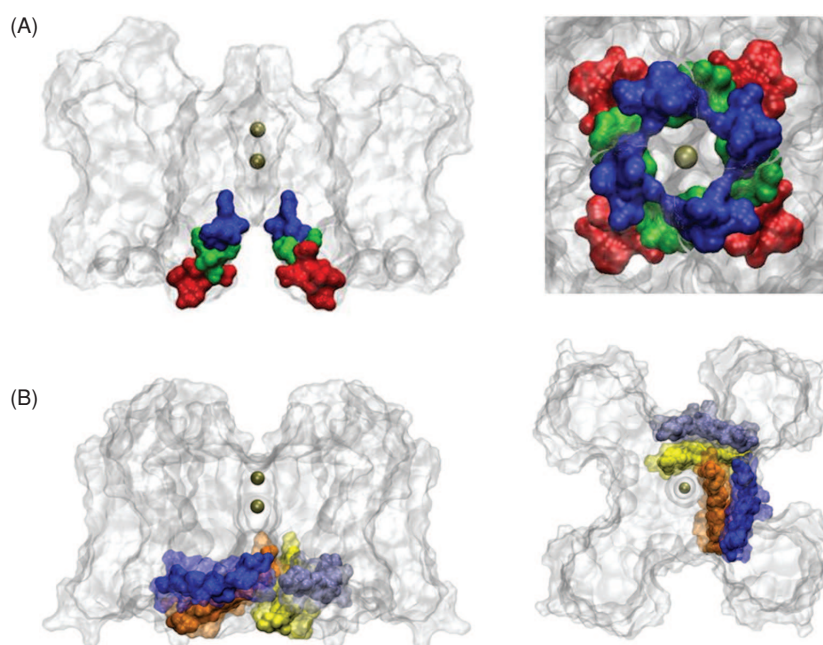


Figure 19 Mechanical movements of the voltage-sensitive pore opening. (A) Side and enlarged bottom views of the residues that change in accessibility during the opening of the Shaker activation gate (residues 470-474; in blue), that do not change in accessibility during gating (residues 481-486, in red), and residues that may form the gate (residues 475-479; in green). After reference 313. (B) Allosteric surface proposed for the interaction between the S4 and S5 linker (in blue and gray) with the S6 C-terminal half of two adjacent subunits (in yellow and orange).

selectivity filter, each having only three K⁺ ions. One configuration occupies the sites -1 , 1 , and 3 (s_{-1} , s_1 , and s_3 in Fig. 18B), while the other configuration fills sites 0 , 2 , and 4 . Thus, ionic conduction in the selectivity filter is pictured as concerted transitions between these two conformations, both energetically equivalent to diffusion (375). The occupancy of s_4 favors s_{-1} , s_1 , s_3 configuration because of electrostatic repulsion with the ion in s_3 , in an electric equivalent of the transference of kinetic energy in the Newton swinging balls, in which the strike of the swinging ball to the last ball in the row expels the first one almost instantaneously (369).

Coupling between VSD and the K-selective pore

The pioneering work of Clay Armstrong revealed that only open channels allowed the entrance of large tetraalkylammonia ions into the pore from the intracellular side (9). Moreover, this type of ions could be trapped inside the pore by forcing the blocked channel to close (10). These classical experiments revealed for the first time the existence of an internal gate able to hinder the passage of ions through K⁺ channels.

Using internal thiol reagent to modify cysteine residues that were introduced in several locations of Shaker's S6, Gary Yellen's lab showed that chemical modification in position 470 to 474 was possible by activation and inhibited by tetrabutylammonium (TBA). Meanwhile, cysteine residues located at 481 to 486 were always highly accessible and could

not be protected by TBA (107, 211, 313). Thus, the intermediate residues, 475 to 480, would form the access gate to the pore. Other work extended the gate between 473 and 481 (184) (see Fig. 19A).

The movement of the voltage sensor that makes possible the opening of the pore appears to require physical interaction between residues 475 and 480 in S6 with residues in the S4 and S5 linker (326, 327). In fact, the structure of Shaker mammalian ortholog, Kv1.2, shows a surface of intimate contact between these two helical segments, in the same, and neighboring, subunits, suggesting an allosteric communication between the VSD and the pore domain (see Fig. 19B) (317). Such a picture is in agreement with current kinetic models as those proposed by Aldrich and Sigworth groups (483, 613), if we assume they represent the late stages in the activation pathway (see Section "The ZHA Kinetic Model"). This structure and that of the Kv1.2/Kv2.1 chimera shows all voltage sensors in the active position and the pore open. In the closed state, this interaction surface probably persists because the open probability in Shaker K⁺ channels maintains a tight coupling to the voltage sensor, not showing hints of becoming less voltage dependent, even at open probabilities as low as 10^{-8} (160, 229, 482). Asymptotic reduced voltage dependence at low P_o is the expected outcome of an allosteric model (218). Thus, the allosteric binding energy between the S4 and S5 linker and the C-end of S6 remains high in the closed-resting state, being at least 11 kcal/mol.

Inactivation mechanisms

N-type inactivation

At the beginning of the nineties, both the Aldrich's and Yellen's labs proposed what is the classical view of potassium channel inactivation. They described two types of inactivation processes in Shaker, the N-type and the C-type inactivation, each having different molecular bases. The N-type inactivation occurs when a movable 22-residue segment localized at the N-terminus of the protein blocks the pore by binding to the internal entrance of the pore in the open conformation (108, 219). Removal of part of the N-terminus of Shaker abolish N-type inactivation and the addition of the isolated 22-residue peptide back into the internal solution restores the inactivation in a dose-response manner (14, 612).

C-type inactivation

The removal of the N-type inactivation to Shaker uncovers another, slower, inactivation process reminiscent of the one observed in the squid axon (43), the so-called C-type inactivation (219). Structural determinants of this inactivation appear to be localized toward the external entrance of the selectivity filter (see Fig. 1 in reference 404), and toward the N-terminus of the sixth TM segment of the protein (221). In the conventional view, the C-type inactivated state is produced by a localized constriction of the external mouth of the channel, which thereby interrupts K⁺ ion conduction. Such conformational change is antagonized by the extracellular addition of K⁺ ions or tetraethylammonium (TEA) (26, 103, 324, 373, 603). Based on crystals of KcsA obtained in different K⁺ concentrations, several structural propositions have emerged to account for such conformational change in the selectivity filter (87, 628, 629).

Other inactivation types

At present, other slow inactivation processes have been described for Shaker, Kv1.5, Kv2.1, Kv3.1 and Kv4.2 K-channels (113, 159, 266, 287). An inactivation process having an opposite voltage dependence to that of C-type inactivation, rendering U-shaped voltage-dependent channel availability. This slow inactivation is not antagonized by external K⁺ or external TEA but is delayed by internal TEA, suggesting the presence of an intracellular molecular determinant intervening in its development. In agreement with this, mutations at the internal mouth of the pore severely alter the slow inactivation rate (104, 212, 265). Moreover, during deactivation or slow inactivation, Kv1.4 extrudes similar volumes of water toward the cytosolic side, suggesting comparable conformational changes (235). For Shaker and Kv4.2 a mechanism has been proposed similar to the ultraslow inactivation in Na-channels or the so called voltage desensitization present in HCN channels that imply the re-closing of the activation gate (113, 159, 469, 498). Thus, it wouldn't be surprising if several members

of the voltage-gated ion channel family were endowed of a common repertoire of non conducting conformations.

VSD conformation during slow inactivation

The gating charge-voltage (Q-V) curves from slow inactivated channels are shifted to more negative voltages (~ -60 mV) as compared with the Q-V curves obtained from non slow-inactivated channels (159, 402). Thus, slow inactivation correlates with the appearance of a highly stable conformational state of the voltage sensor. Such a conformational change induced by voltage appears to be an intrinsic property of the VSD, since the shift in the Q-V curve that is seen in slow-inactivated channels can be also observed when gating currents are measured using the isolated VSD (560). Periodicity analysis suggests a S4 transition from a mostly 3_{10} helical packing at resting to mostly α -helical at positive voltages (a relaxed state). This latter packing being the observed in the structure of Kv channels, crystallized in the absence of electric field.

The slo (KCa) Family of K⁺ Channels

Function and localization

This family, encoded by the *slo* genes, is characterized by K⁺ channels having an unusually large conductance (466). In particular, Slo1, that with a 250 pS single-ion conductance in 100 mmol/L symmetrical K⁺, has also been dubbed "big" potassium (BK) channels and also maxi-K channels. The first member of this family was cloned from the *Drosophila* mutant *slowpoke* (*Slo*) (2, 21) and was found to code for a voltage- and Ca²⁺-activated channel. Four genes encode the Slo family of ion channels in mammals (Fig. 20A): *Slo1* (*KCa1.1*; KCNMA1 in humans); the mammalian *slo* orthologue was cloned using a low-stringency DNA hybridization of a mammalian cDNA using the *Drosophila slo* cDNA (69). Slo1 is activated by Ca²⁺ and voltage; *Slo2* (*KCa4*) cloning was possible thanks to the genomic sequencing in *C. elegans* that revealed a gene coding for a channel able to be activated by internal Ca²⁺ and Cl⁻ (605). In mammals two *Slo2* paralogs, *Slo2.1* (*KCa4.2*, KCNT2, *Slick*) and *Slo2.2* (*KCa4.1*, KCNT1, *Slack*), were found but in contrast to the *C. elegans* Slo2 channel, in mammals Slo2 is activated by Na⁺ and Cl⁻ (47, 605). *Slo3* (*KCa5.1*, KCNU1) was identified by performing a computer search that lead to the identification of an expressed sequence tag (EST) with homology to part of the C-terminus of mSlo1 (484). Slo3 proved to be activated by voltage and internal alkalization.

This family of ion channels, because their ability to sense changes in the intracellular ion concentration (H⁺, Na⁺, and Ca²⁺) is unique since establishes a link between the ionic metabolism of the cell and its membrane conductance.

Slo 1

The gene *Slo1* was cloned from the *Drosophila* mutant *Slowpoke*, which has flight problems, mate song defects and

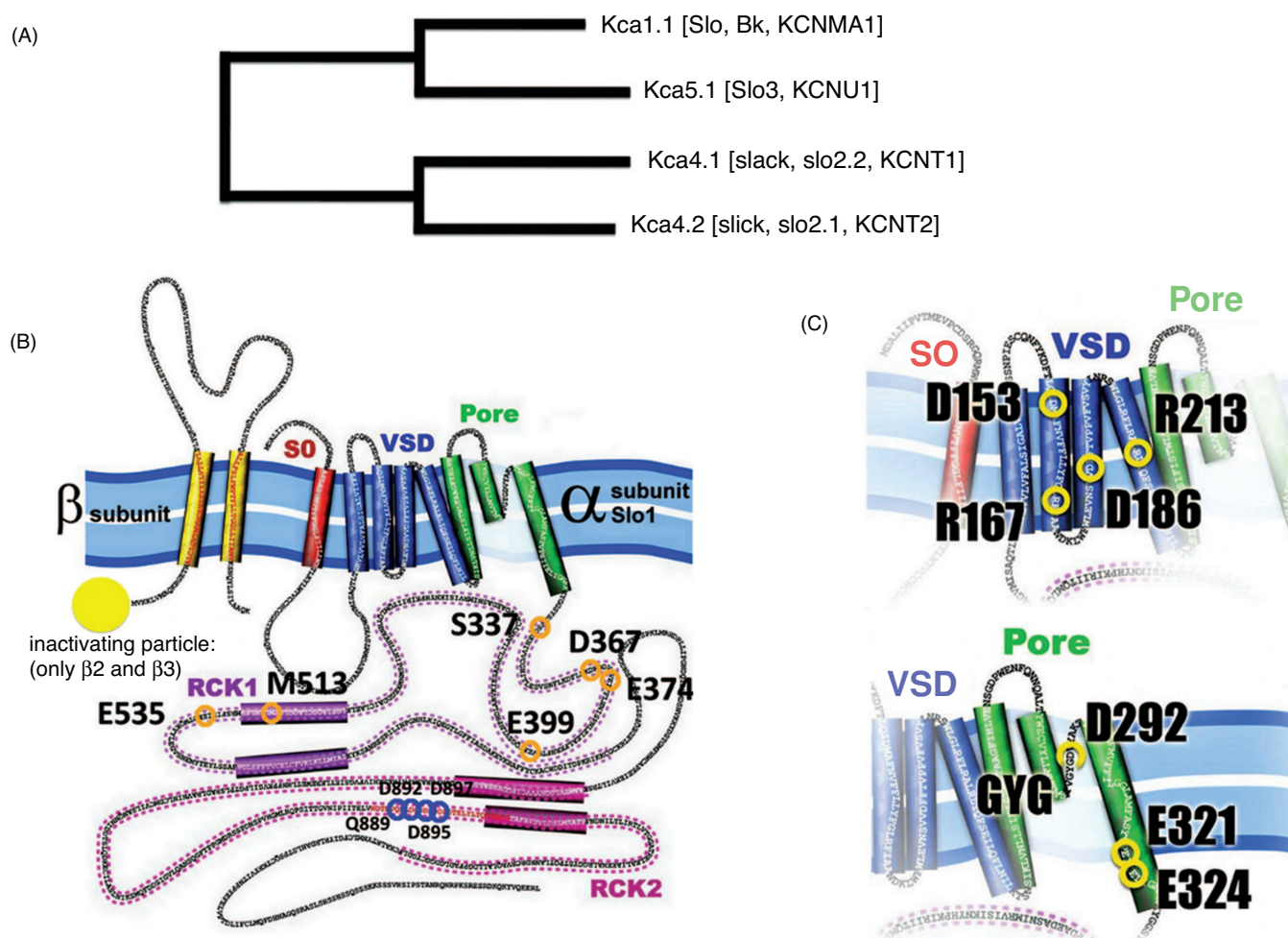


Figure 20 Phylogenetic tree of Slo channels family in mammals and membrane topology of the α - and β -subunits of Slo1 channels. (A) The four genes present in Slo channels families: *Slo*, *Slo2.1*, *Slo2.2*, and *Slo3*. (B) The α -subunit of Slo1 contains seven transmembrane segments divided in two domains [voltage-sensor domain, (VSD) and pore region] that is normally associated to β -subunits consisting of two transmembrane segments. $\beta 2$ and $\beta 3$ have an inactivating particle on their N-terminus able to interact with the channel internal vestibule and block the passage of K⁺ through the channel. The α -subunit contains a long C-terminus domain in which two regulators of K⁺ conductance domains (RCK1 and RCK2) are present. Spread throughout in the BK C-terminus are located the binding sites for Ca²⁺ and Mg²⁺ (for more details on the divalent cation-binding sites see Section "Carboxy terminus"). (C) (Top) The α -subunit has a voltage-sensing domain formed by the S0 to S4 segments. Four charged residues contribute to the channel voltage membrane sensitivity, D153, R167 in S2, D186 in S3, and R213 in S4. (Bottom) The pore region formed by S5, the pore helix, the pore loop, and the S6 transmembrane. Three amino acid residues have been identified in the BK pore as partially responsible for the channel high conductance, D292, E321, and E324.

altered response to heat shock. *Drosophila* muscles of Slowpoke lack a calcium-activated potassium conductance present during early larval stages (127). This gene codes for a protein with homology to voltage-dependent potassium channels, but in addition it has an extra N-terminus segment (S0; Fig. 20B) and in addition to the six TMs segments it has four hydrophobic segments in the C-terminus domain (S7-S10). The S0 segment let the N-terminus facing the extracellular side of the membrane.

When patch clamp and bilayer experiments were performed to record the Slo1 single-channel activity, it was evident that the channel open probability increased when confronted to a membrane depolarization or to an increase in the intracellular Ca²⁺ concentration (Fig. 21A) (296, 356, 409).

This features a study case protein due to its capability of coupling both chemical and electrical stimulus to generate a change in membrane conductance, made of this channel.

Electrophysiological recordings in native cells have shown Slo1 channels with different calcium sensitivities. However, the Slo1 channel is coded by a single gene in mammalian genomes. This channel diversity is possible due to alternative processing of introns, which produce at least 11 splice variants expressed in different tissues and cell types (553). This feature is conserved among evolution, and is observed in mammals, reptiles, birds, and insects (2, 69, 248, 289, 291, 360, 453, 553, 616). When expressed in heterologous expression systems, channels formed by these splice variants present different calcium sensitivities and gating

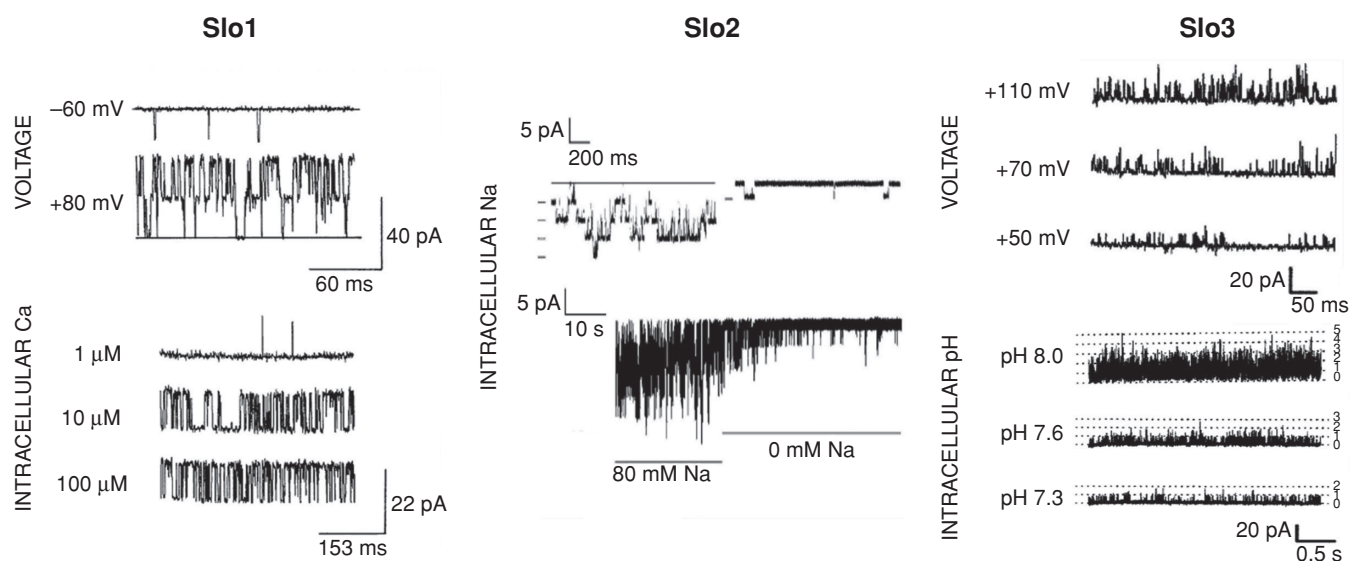


Figure 21 Polymodal activation of Slo channels. (A) Slo1 channel single-channel activity increases its open probability in response to an increase in the membrane voltage. Upper trace was taken at -60 mV. Openings are downward deflections in the current. Lower trace was taken at $+80$ mV. Upward deflections are opening events. The opening of two independent channels can be appreciated in this current record. Open probability also increases with increasing intracellular calcium (1, 10, and 100 μ mol/L) at a fixed voltage ($+60$ mV). (B) Slo2.2 channels single-channel activity increases with high intracellular sodium. Perfusion using 80 mmol/L intracellular sodium elicited four conductance levels, which are reduced to just one with nominal 0 sodium concentration (top). (Bottom) The same type of experiment performed at a compressed time scale. (C) Single-channel recordings of cloned Slo3 increases with the alkalization and depolarizing voltages. Upper, single-channel activity increases at positive potentials. Bottom, single-channel recordings at $+80$ mV at several intracellular pHs.

kinetics, resembling the ones found in native cells. Alternative splicing is responsible in part for the great variety of calcium sensitivities found for Slo1 channels.

Several of these splice variants are produced by “insertions” at the C-terminal and one of the most studied variants is expressed under activation of the hypothalamic-pituitary-adrenal (HPA) axis under stress conditions, reason why it was called STREX (591). Two splice variants produce dominant negative subunits, which retain the channel in subcellular compartments (98, 553, 616). One of these variants corresponds to an insertion of 33 aminoacids in S0 (SV1 subunit) produce a natural dominant negative subunit that reduces the level expression of Slo1 in myometrium.

Diversity of Slo1 channels is vast and it appears as a consequence of metabolic regulation, splicing and/or modulatory β -subunits. The main physiological function of this channel ubiquitously found in a variety of different tissues is to damp excitatory stimuli, like for example, an increase in cytosolic Ca^{2+} or a membrane depolarization (90, 295, 296, 356, 407).

β -subunits of Slo1 channels

Since β -subunits of Slo1 channels escort these channels in most tissues where they are present—the exception is skeletal muscle—and dramatically modify their gating properties, it is convenient to discuss here how these auxiliary subunits modify the gating properties of Slo1 channels.

Regulatory α -subunits share a putative membrane topology, with two TM segments connected by a 120-residue

extracellular “loop” and with NH₂ and COOH terminals oriented toward the cytoplasm (see Fig. 20B). At present, four α -subunits have been cloned in mammals [$\alpha 1$ - $\alpha 4$; (32, 60, 267, 365, 555)]. Sequence similarities are major between $\alpha 1$ - $\alpha 2$ and $\alpha 2$ - $\alpha 3$, respectively. $\alpha 4$ is the most distantly related of all α -subunits.

Changes in biophysical properties of Slo1 channels induced by SLO1 α -subunits

The Slo1 $\beta 1$ -subunit induces an increase of the apparent Ca^{2+} sensitivity, a decrease of the voltage dependence of the Ch, and slowing of the macroscopic kinetics (407, 546, 547) (Fig. 22A and B). Slo1 $\beta 1$ -subunit also modifies the pharmacological properties of the channel (Orio et al. 2002). This subunit is mainly expressed in VSM, but is also found in urinary bladder and in some brain regions. $\beta 2$ increases the Ca^{2+} and voltage sensitivity of Slo1 channels and slows the kinetics of the channel (60, 407) (Fig. 22A and B). Moreover, this subunit induces fast and complete inactivation (586). The N-terminus of the $\beta 2$ -subunit (residues 1–45) blocks the BK channel via interaction with a receptor site in the α -subunit, which becomes accessible once the channel is in the open state (Fig. 22A, third line). $\beta 2$ also induces an instantaneous outward rectification that suggests that the $\beta 2$ external loop approaches the Slo1 pore as to alter the Slo1 ion conduction characteristics (99). It is worth noticing that the N-terminus of $\beta 2$ prevents the surface expression of this subunit and hinders the surface expression of the α -subunit via an endocytic mechanism (333, 615). This subunit is present in kidney, spleen, adrenal

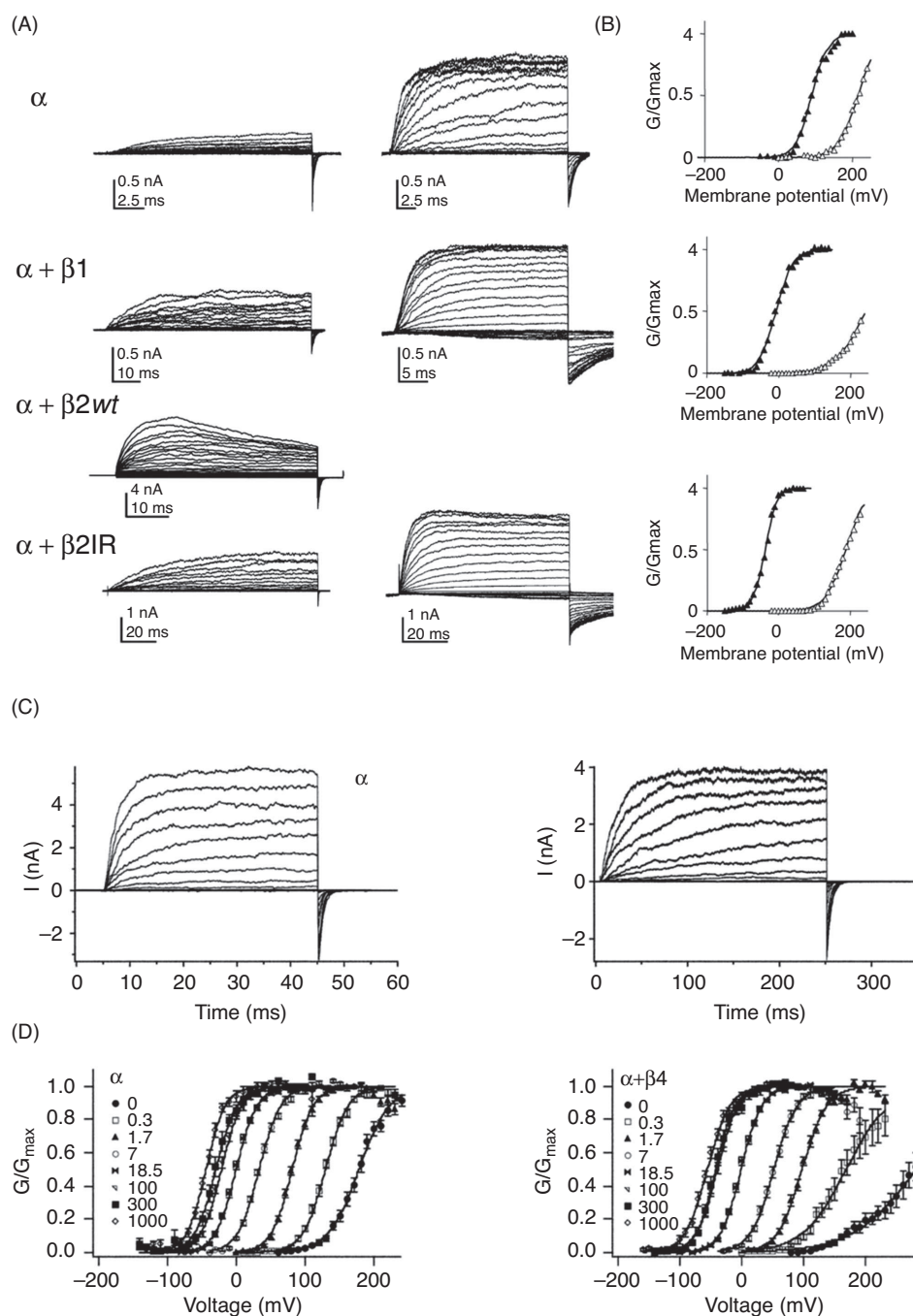


Figure 22 Functional differences between β -subunits. (A) Macroscopic currents were elicited by voltage pulses between -200 and +200 mV at 5 nmol/L (left) and 2.8 μ mol/L (right) intracellular calcium. All currents were recorded in the inside-out configuration. Notice the change in the activation and the deactivation kinetics when $\beta 1$ and $\beta 2^{IR}$ ($\beta 2$ inactivation removed) are coexpressed with the α -subunit. Current records in the third line were obtained by coexpressing the α with the $\beta 2$ -subunit. Notice that currents inactivate. (B) Voltage activation curves obtained from tail currents (the currents measured at the beginning of the repolarizing pulse; -60 mV) of recordings showed in A at 5 nmol/L (open symbols) and 2.8 μ mol/L intracellular calcium (filled symbols) (modified, with permission, from reference 406). (C) Macroscopic currents of $\alpha + \beta 4$ channels (upper), and the activation curves at different calcium concentrations (lower). Notice the slower activation and deactivation kinetic produced by the $\beta 4$ -subunit. (D) Comparison of the voltage activation curves at different Ca^{2+} concentrations between channels formed by expressing the α -subunit alone (left) or by expressing $\alpha + \beta 4$ (adapted, with permission, from reference 564).

chromaffin cells, DRG, and brain (58, 309, 563). $\beta 3a$ – c induce channel inactivation to Slo1 currents and also produce an outward rectification of the open channel currents. The inactivation process is faster than $\beta 2$ -induced inactivation albeit incomplete. The $\beta 3b$ -subunit induces a small and consistent decrease in activation time constants at all Ca^{2+} concentrations, and it does not affect channel deactivation. $\beta 3b$ -subunit confers a non-linearity on instantaneous current-voltage properties that is regulated by the extracellular segment of this subunit (619). This subunit is expressed in adrenal chromaffin cells (587). The human $\beta 4$ -subunit has a complex Ca^{2+} concentration-dependent effect on Slo1 channel current. This subunit decreases apparent Ca^{2+} sensitivity at low Ca^{2+} concentrations but induces an increase in the apparent sensitivity at high Ca^{2+} concentrations (183). Human $\beta 4$ also slows down activation and deactivation kinetics (32, 60) (Fig. 22C and D). This subunit is expressed exclusively in the brain, and is responsible for some of the features of neuronal Slo1 channels as low affinity for scorpion toxins and ethanol sensitivity, (352, 365, 555).

Pharmacology

Slo1 channels are blocked by the scorpion toxin CTX (370) and by the highly selective Slo1 scorpion toxin iberitoxin (IbTX) (74, 153). These scorpion toxins are pore blockers and the group of Miller (414, 415) identify the positively charged side chain of lysine 27 in CTX as the BP. Slo1 channels are also very sensitive to external TEA ($K_D \sim 250 \mu\text{mol/L}$), sensitivity that is due to the presence of a ring of phenylalanines in the neighborhood of the external aspect of the selectivity filter (495, 558).

A number of Slo1 channels openers have been identified including the synthetic benzimidazolone derivatives (NS1619) and the natural modulator dihydrosoyasaponin (reviewed in reference 151). In this regard, we should mention that the compound NS11021 (1-(3,5)-bis-trifluoromethyl-phenyl-3-[4-bromo-2-(1H-tetrazol-5-yl)-phenyl]thiourea) is an Slo1 channel activator with better specificity and ten times higher potency compared to NS1619, one of the most broadly applied Slo1 opener (36).

Tissue distribution and function

Brain

In the CNS Slo1 channels are present in most regions of the mammalian brain and by colocalizing with VDCC they are important in the modulation of neurotransmitter release (Fig. 23A) (131, 156, 449). Colocalization of Slo1 channels with VDCC appears to be essential for Slo1 channel activation since to raise the channel open probability to reasonable values ($P_o \geq 0.5$) at membrane voltages in the range -50 to 0 mV requires values of Ca^{2+} concentration $10 \mu\text{mol/L}$ or more (60, 135, 428) (Fig. 23A). We note here that Slo1 channels form macromolecular complexes with VDCC channels

of the L-, P/Q-, and N-type and that this type of complexes can be reconstituted as a functional Ca^{2+} nanodomain in *Xenopus* oocytes (37, 38, 174). In this type of domains, VDCC channels are able to activate Slo1 channels in the physiological voltage range (Fig. 23B). However, in different neurons, Slo1 channels are fueled by different types of VDCC. N-type of VDCC are involved in the activation of Slo1 channels in hippocampal neurons (351) but P/Q- and T-type of VDCC control the activity of Slo1 channels in Purkinje neurons (123).

In the mammalian brain the Slo1 protein can be found as α -subunits alone or forming $\alpha/\beta 4$ complexes and to a lesser extent as $\alpha/\beta 2$ complexes (e.g., reference 206). In particular, clusters of channels formed by $\alpha/\beta 4$ -subunits are expressed most exclusively in nerve terminal compartments (584).

In neurons, Slo1 channels serve functions like, for example, the repolarization of the action potential (222, 290, 517) and giving origin to the fast phase of the afterhyperpolarization following an action potential (1). The different roles played by Slo1 channels in the nervous system are possible because they show pre- and postsynaptic localizations being likely to find them in soma, dendrites, axons, and synaptic terminals. For example, in neurons from the hippocampus and cerebellum, the Slo1 α -subunit shows a distribution to the axons and presynaptic terminal (477).

In amygdala neurons, Slo1 is responsible of the repolarization and broadening of action potentials without affecting afterhyperpolarization (AHP) (130). In this cell type, the fast afterhyperpolarization (fAHP) is driven by voltage-dependent potassium channels sensitive to 4-AP and DTX but in other cells, as cerebellar Purkinje neurons, Slo1 is responsible only for the AHP (123). In this case, the pronounced AHP induced by Slo1 allows voltage-dependent sodium channels to recover from inactivation and fire the next action potential. Spike broadening during a train of action potentials is a common phenomenon in several neuronal types, and appears as a consequence of cumulative inactivation of voltage-dependent channels that leads to a slower repolarization (6, 150, 335). In hippocampal pyramidal neurons, trains of action potentials show a frequency-dependent spike broadening, which has been attributed to the progressive decrease in Slo1 currents due to Slo1 channel fast inactivation (493). This decrease in the Slo1 current reduces the amplitude of the AHP and the repolarization rate, causing that any successive action potential will have a smaller AHP and a slower repolarization.

During high-frequency (100 Hz) firing periods, Slo1 currents are responsible for the fast repolarization that allows the high spike frequency (177). This Slo1-induced increase in excitability is counterintuitive since in general is thought that potassium channels are involved in *decreasing* the cellular excitability. In this case, Slo1 channels are able to provide a fast repolarization and an AHP large enough to remove the inactivation of sodium channels.

Using $\beta 4^{-/-}$ mice it was possible to show that this subunit is involved in decreasing excitability in the hippocampus dentate gyrus, thus protecting against hyperexcitability that can lead to temporal lobe epilepsy (59). $\beta 4$ knockout

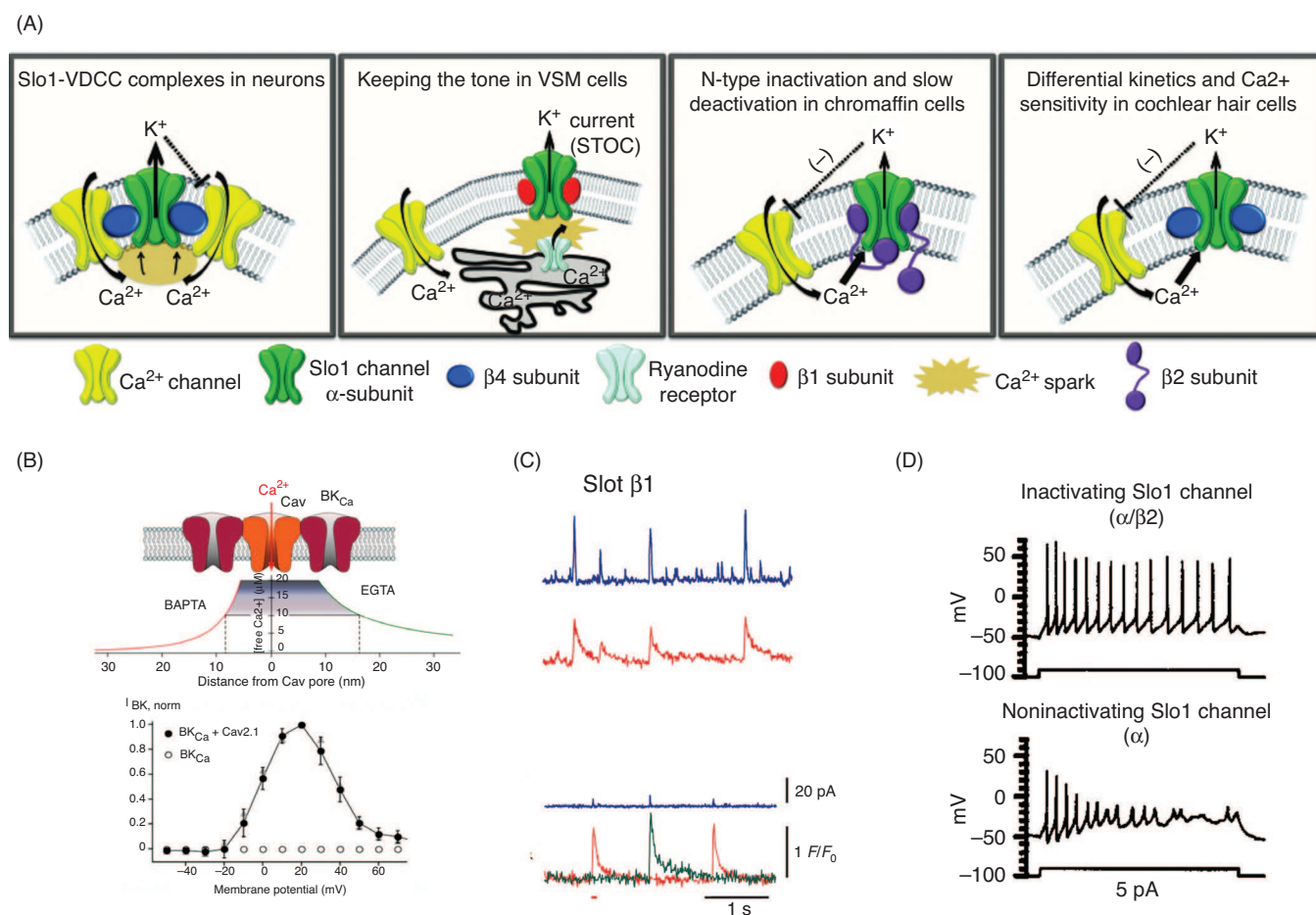


Figure 23 Physiological roles of Slo1 channels. (A) Proposed physiological roles of Slo1 channels. α - and $\beta 1$ -subunits are shown as cartoons. (Adapted, with permission, from reference 407.) (B) Thanks to the close proximity of Slo1 (BK_{Ca}) and voltage-dependent Ca^{2+} channels (VDCC), the increase of Ca^{2+} concentration induced by the opening of VDCC (up to 10 $\mu\text{mol/L}$ in the neighborhood of Slo1 channels) promotes the opening of Slo1 channels (top). (Bottom) Current-voltage relationship obtained in an oocyte expressing only Slo1 (open circles) and coexpressing Slo1 and VDCC. The colocalization of these two channels allows an increase in the K^{+} current that decreases when the potential approaches the reversal potential for Ca^{2+} indicating that K^{+} currents were elicited by the increase in internal Ca^{2+} concentration induced by the VDCC opening. (Adapted, with permission, from reference 131.) (C) In vascular smooth muscle cells, $\beta 1$ -subunits confer the required Ca^{2+} sensitivity for effective coupling between Ca^{2+} sparks and spontaneous outward currents. [Adapted, with permission, from reference 61.] (D) In chromaffin cells, slowed Slo1 deactivation kinetics allows $\beta 2$ -subunit-expressing cells to fire a train of action potentials. (Adapted, with permission, from reference 508.)

mice lack any tonic or clonic behaviors but show paroxysmal synchronous discharges originated in the hippocampus and spreading to the cortex. Action potentials in $\beta 4^{-/-}$ mice were shorter, have an AHP decay faster than those of wt mice and showed very little spike frequency adaptation, all features that allow a higher spike frequency. Addition of the specific blocker paxilline (168) does not affect wt cells, but produce a strong reduction in firing frequency in $\beta 4^{-/-}$ cells, as well as returning action potential width, AHP decay time and interspike interval to wt levels. This result means that under normal conditions, Slo1- $\beta 4$ channel complex in dentate granule cells is not active and it became active in $\beta 4^{-/-}$ animals, possible because the $\beta 4$ -subunit decreases the calcium sensitivity so much that it never opens under physiological conditions. The Slo1 channel became active in $\beta 4^{-/-}$ animals, where sharpens the action potential and support abnormal high-frequency firing.

A mutation in the Slo1 α -subunit has been linked to generalized epilepsy and paroxysmal dyskinesia (119). This is a gain-of-function mutation that promotes an enhanced Slo1 channel activity compared with that of the wild-type channel at the same calcium concentration and voltage. As discussed previously, this apparently counterintuitive result can be explained by the fact that activation of the Slo1 channel induces a faster action potential repolarization and thereby reduced neuronal refractory period. This mutation has helped much in the elucidation of the mechanism that mediates the coupling between Ca^{2+} binding and channel opening (see section on Slo1 channel structure).

It is important to mention here that chronic application of ethanol modulates Slo1 channel function and distribution in neuronal terminal. Chronically applied ethanol also induces a reduction in channel density, membrane clustering, and an increase in channel internalization (reviewed in reference 548).

On the other hand, single-channel experiments, cell and behavioral experiments taking advantage of $\beta 4$ knockout mice strongly suggest that the $\beta 4$ -subunit is the molecular determinant of alcohol tolerance (352).

Smooth muscle

In VSMCs, Slo1 channels provide the adequate regulation of the contractile tone (297). Local Ca^{2+} increases, called Ca^{2+} sparks, generate spontaneous transient outward currents (STOCs), which are generated by Slo1 channels (Fig. 22A and C). This hyperpolarizes the membrane and promotes relaxation (233). In these cells highly Ca^{2+} -sensitive Slo1 channels are formed mostly by α - and $\beta 1$ -subunits. The physiological relevance of $\beta 1$ -subunits in modulating the Ca^{2+} sensitivity of the Slo1 channel was shown with $\beta 1$ -subunit knockout mice (61, 431). The cerebral artery myocytes of these mice exhibited a decrease in the Ca^{2+} sensitivity of the Slo1 channels and a low Ca^{2+} spark-STOC coupling (Fig. 23C). This decreased coupling is responsible for an elevated arterial tone, which leads to an increment in arterial tone and blood pressure.

Role in secreting cells

By acting on target organs such as liver, adrenal gland, and gonads, hormones secreted by electrically excitable cells in the brain are crucial in the regulation of a number of physiological processes including reproduction and stress response. In this regard, adrenal chromaffin cells are a widely studied cell type. Rodent chromaffin cells fire spontaneously and their electrical activity is associated with basal release of catecholamines (386, 630). In this type of cells, L-type VDCC are tightly coupled to Slo1 channels and the action potential firing is modulated by the interaction between these two type of channels (435). In chromaffin cells, Slo1 channels can be either fast inactivating (BK_i) or noninactivating (BK_s) (Fig. 23D). In the former case, inactivation is induced by the amino terminus of the $\beta 2$ -subunit (N-type inactivation). Cells expressing BK_i currents showed a higher firing frequency than BK_s, due to a slower channel deactivation rate that produced an AHP able to remove the inactivation of sodium channels and make the cell fire at high frequencies (508). Slo1 channels formed by $\alpha/\beta 2$ complexes are most closely coupled to VDCC most likely the ones affecting the pacemaker currents (348, 407, 586, 587).

In β -cells, due to the presence of the Slo1 $\beta 2$ -subunit, Slo1 currents activate rapidly and then inactivate and, suggesting that Slo1 channels colocalize with VDCC channels (505). In human β -cells activation of Slo1 channels decreases spike amplitude and addition of iberiotoxin increases insulin secretion by 70% (57). Slo1-knockout mice, on the other hand, are normoglycemic but show a markedly impaired glucose tolerance due to reduced glucose-induced insulin secretion. The glucose-stimulated β -cells from Slo1-knockout mice show broadened action potentials with an afterhyperpolarization greatly reduced (120).

Kidney

The α -subunit of the Slo1 and all the β -subunits subtypes have been found in the nephron (169, 170, 582). In the distal nephron, Slo1 channels are localized in the apical membrane of the principal cells where they mediate flow-stimulated kaliuresis. $\beta 1$ -knockout mice show a reduced fractional excretion of K⁺, decrease glomerular filtration rate, and augmented excretion of Na⁺ in response to acute volume expansion (432). Recalling that Kir1.1 underlies baseline luminal K⁺ secretion (see Kir section), the K⁺ secretion is ablated in the Kir1.1 knockout mouse by the administration of iberiotoxin, a result that strongly suggest that Kir1.1 and Slo1 are responsible for most of the K⁺ secretion in distal tubules. As discussed previously, lack of the $\beta 1$ -subunit leads to hypertension, and this appears to have its origin in an increase vascular tone as well as a renal origin (169, 170).

Cochlea

In the frog, chick, and turtle auditory systems, which have been used as models of study of this sense, frequency tuning is performed almost exclusively by the hair cells (16). Each different hair cell has a characteristic tuning frequency. In these animals, electrical resonance is achieved through the interplay of L-type VDCC and Slo1 channels operating, as, for example, in the turtle, at frequencies from 30 to 600 Hz (137). The opening of L-type VDCC induced by depolarization increases internal Ca^{2+} concentration, which in turn activates Slo1 channels. Activation of Slo1 channels hyperpolarizes the cell, closing Ca^{2+} channels, and promoting the membrane potential oscillation. Subsequent oscillations are damped, because fewer Slo1 channels are recruited in each cycle (17, 137). The number and type of Slo1 channels control the resonant frequency of a particular hair cell. Higher frequencies are present in cells containing a large number of Slo1 channels with faster activation kinetics. The origin of this wide range of Slo1 gating kinetics is not completely clear at present but most probably is accomplished by differential expression of distinct splice variants of the Slo1 α -subunit, together with an expression gradient of α -subunit (137, 248, 291, 441, 453). $\alpha 1$ -subunits add to the system a level of variability that cannot be achieved only with a splice variant expression gradient. It is of interest to note here that, as the frequency range gets wider, more diversity in the Slo1 channel is needed. Thus Fetiplace and Fuchs (137) modeled the electrical tuning in the turtle with five Slo1 splice variants, but in the chicken basilar papilla (150–4000 Hz), they needed a minimum of nine Slo1 splice variants. The main problem in attributing the tonotopic gradient to a differential expression of Slo1 channel splice variants is that they differ only slightly in their gating kinetics (371). The recent results of Miranda-Rottmann et al. (371) argue in favor of the hypothesis that the tonotopic gradient is mainly established on the basis of the gradient in expression of the $\alpha 1$ -subunit and that is this gradient the responsible for the slowing down of Slo1 channels toward the low-frequency apex of the cochlea.

Mitochondria

BK channels are also found in mitochondria (mitoK_{Ca}) where they are present in the inner membrane and contribute to K⁺ uptake (114, 592). Experimental evidence indicates that BK channels in mitochondria are involved in the protection of cardiomyocytes from hypoxia and apparently inhibition of the $\alpha 1$ -subunit mRNA expression contributes to cardioprotection after exposure to chronic hypoxia (28, 56).

Slo2

The Na⁺-activated potassium channel (K_{Na}) was originally described in the cardiomyocytes in the 1980s (251), and subsequently they were identified in brain (117, 118). Due to its fast diffusion rate and the lack of large changes in the bulk concentration, Na⁺ is not commonly thought as a cellular messenger. However, in dendritic domains closer to synaptic inputs, the Na⁺ concentration after a short spike train can increase up to 40 mmol/L and up to 100 mmol/L after high-frequency stimulation similar to the one used to produce long-term potentiation (452). In the axon initial segment, the site of action potential initiation in most central neurons, Na⁺ channels are found at a high density. The opening of these Na⁺ channels promotes a raise in Na⁺ concentration of the order of 3 to 30 times compared to that of the soma (144, 272).

The two main routes of Na⁺ entry to the cell are voltage-dependent Na⁺ channels and glutamate-activated channels of AMPA and NMDA type (48). The K_{Na} channels may serve role of damping the excitatory signal mediated by Na⁺ and glutamate-activated channels helping to avoid the deleterious consequences of the raise in internal Na⁺.

The molecular identity of K_{Na} channels remained elusive until 2003, year in which two independent groups found that mammalian *Slo2* genes code for high-conductance potassium channels sensitive to intracellular sodium (47, 606) (Fig. 21B). Actually, *Slo2* was originally cloned in *C. elegans*, where it codes for a Ca²⁺- and Cl⁻-activated K⁺ channel, mainly expressed in body-wall muscle (605).

In mammals the two *Slo2* paralog, *Slo2.1* and *Slo2.2* code for proteins that give origin to tetrameric channels sensitive to internal Na⁺ and Cl⁻ (466). These channels are also known as Slick (sequence like an intermediate conductance K⁺ channel, *Slo2.1*) and Slack (sequence like a calcium-activated K⁺ channel, *Slo2.2*). Similar to *Slo1*, these channels have a large single-channel conductance [60–180 pS (247, 466)] and *Slo2.2* can coassemble with *Slo1* channels to produce channels with biophysical properties different to those of the parent channels. Moreover, both *Slo2* channels can form heteromeres in heterologous expression systems, with kinetics and unitary conductance different to homomeric channels (96).

Expressed in heterologous systems, *Slo2.1* shows a fast activation, low intrinsic voltage dependence, and an EC₅₀ for Na⁺ of 89 mmol/L. *Slo2.1* shows a basal activity in the absence of Na⁺ and is inhibited by intracellular ATP. *Slo2.2* macroscopic currents show an instantaneous activation and a

slow activating component, the EC₅₀ for Na⁺ is 41 mmol/L and does not show a basal activity in absence of sodium. The chloride dependence is more pronounced in *Slo2.1* than in *Slo2.2*.

In excised patches some of the native K_{Na} are characterized by a fast and strong rundown in single-channel activity (124). In DRG neurons the fast rundown in K_{Na} activity can be reverted by increasing the Na⁺ concentration suggesting that the loss of a diffusible factor responsible for the channels Na⁺ sensitivity (124, 535). A putative NAD⁺ binding is present in *Slo2.1* and *Slo2.2* and addition of NAD⁺ increases the open probability of native K_{Na} and *Slo2.2* channels, indicating that loss of this diffusible factor is the cause of rundown in these channels.

Slo2.2 has several putative PKA and PKC phosphorylation sites. PKA is involved in internalization of channels and PKC increases the activity of *Slo2.2* and decreases it of *Slo2.1* (400, 474). As *Slo1*, *Slo2.2* has several splice variants from which Slack-A and Slack-B are the most frequently found (64).

Na-sensitive channels have a widespread expression in brain (46, 49) and several studies had addressed the roles of K_{Na} channels during action potential repolarization and AHP (reviewed in reference 48). In motoneurons from lamprey spinal cord, it has been reported the existence of both transient and persistent K_{Na} current activated by sodium influx (198). The transient K_{Na} current follows the action potential time course. There is a second persistent component, which disappears when sodium is replaced by lithium. In mammalian neurons only the persistent component has been observed (67). In lamprey motoneurons, the transient K_{Na} current appears at the peak of the action potential before the K_v current, contributing to the early repolarization and setting the spike peak and limiting the duration of the action potential. The K_{Na} component on the AHP is evident after a single-action potential, but is more prominent after spike trains and burst firing (562). The role of the sustained component is unclear at present. In the same cell type Na⁺ influx through AMPA receptors also activated K_{Na} current acting as a negative feedback mechanism, decreasing the magnitude of the excitatory postsynaptic potentials and thus decreasing the excitability (384). In newborn rat motoneurons as well as in neocortical interneurons a K_{Na}-dependent slow AHP was observed after a train of action potentials (146, 460). Under voltage-clamp conditions lithium replacement induces a decrease in the sustained outward potassium current, consistent with the idea that a persistent K_{Na} is responsible for the slow AHP observed in neocortical interneurons. The fact that the K_{Na}-dependent slow AHP in lamprey motoneurons is evidenced after a single-action potential, suggesting that either K_{Na} channels are closer to the sodium influx source or the channel has a high sodium affinity (146, 460).

In several neuronal types, K_{Na} channels are abundantly expressed as evidenced by the high probability to find it in single-channel studies or the big macroscopic current elicited in whole cell recordings (124, 400, 595). In a recent study,

Budelli et al. (67) found that Tetrodotoxin (TTX) application decreases the outward potassium current in 40% to 60%. The potassium current eliminated in this way was not inactivating and depends on the activity of persistent sodium channels. Selective elimination of Slo2.1 and Slo2.2 by RNAi dramatically decreases the effect of TTX.

Slo3

What is unique in Slo3 channels is that they are only found in mammals and remarkably they are only expressed in testis, specifically in developing spermatocytes and mature sperms (473, 484). Slo3 appears to play an important role in sperm capacitation, a process by means of which sperms become competent in fertilizing the ovule. The distinctive feature of Slo3 channel when expressed in heterologous expression systems is that its activity increases by intracellular alkalinization (Fig. 21C). Other key features of Slo3 gating are: (i) maximal P_o increases with increasing pH but to a maximum value of 0.3 and (ii) activation and deactivation kinetics can be fitted to two exponentials (Slo1 is fitted with only one) (625). Slo3 share with Slo1 the high sensitivity for Ba²⁺, TEA, IbTx, and ChTx (537). In the selectivity filter, this channel has a phenylalanine instead of the canonical tyrosine found in most of the potassium channels, which confers a low-permeability discrimination between potassium to sodium ($P_K/P_{Na} \sim 5$ –10, ~ 100 times less than Slo1) (473, 484).

By swapping C-termini between Slo1 and Slo3 it was found that the C-terminus of Slo3 is responsible for proton sensitivity (590). Slo3 is more related to Slo1 than to Slo2, it has seven putative TM domains (with an S0). This high rate of change is a characteristic of genes involved in reproductive functions, possibly creating mechanisms involved in the speciation process (522). Bovine and mouse channels (bSlo3 and mSlo3) show differences in kinetics, voltage dependence, and pH sensitivities; features that were mapped to the C-terminus, one of the domains with the lowest sequence homology between the two channels (473).

In mouse sperm, an outwardly rectifying potassium conductance was identified (K_{sper}) with some of Slo3 features as its pH dependency and pharmacology (355, 387). A potassium conductance and intracellular alkalinization are needed for the phenomenon of capacitation to occur (387). In sperms, the resting membrane potential is driven by intracellular pH through K_{sper} channel (387). At pHi = 6 the K_{sper} is closed and the membrane potential is approximately 0 mV, while at pHi = 7 the channel is open which drives the resting potential to −54 mV. These results show that a proton-inhibited K⁺ conductance is central in setting the membrane potential in sperms. In Slo3^{−/−} mice several defects are evident under capacitation conditions such as impaired motility and failure to undergo achrosomal reaction, resulting in infertile animals (475).

Recently, Yang et al. (596) reported the association of Slo3 and β4-subunit, which was thought exclusively associate to Slo1. In heterologous expression systems, β4-subunit in-

creased Slo3 macroscopic currents by increasing the number of channels in the membrane without affecting other parameters as single-channel conductance or open probability. Both subunits are present in mouse testis, which suggest that this interaction can occur in native cells.

Allosteric models account for most of the Slo1 channel gating properties

In this section, we will emphasize some of the highlights of the two-tiered allosteric model that is commonly used to explain the Slo1 channel activity (reviewed in reference 340). In the absence of Ca²⁺, several closed (4–5) states and several open states (2–3) were necessary to explain the Slo1 single-channel activity (392, 532). Given the large number of closed and open states present in the absence of Ca²⁺, the correlation between adjacent intervals (361) and the fact that the channel is a tetramer (see later), Slo1 channel gating in the absence of internal Ca²⁺ is consistent with the 10-state model indicated in Figure 24A. One of the predictions of this model is that even in the absence of voltage sensor activation, described by the equilibrium constant J , the channel can open through the reaction described by the equilibrium constant L . This prediction was confirmed by Horrigan and Aldrich (216) who found that in the absence of Ca²⁺ and at very negative voltages, the channel can open, albeit with a very low, but measurable, P_o (about 10^{−6}) and a low voltage dependence, z_L , not related to the voltage sensors. On the other hand, a detailed analysis of the gating currents in the absence of Ca²⁺ suggests a two-state model, in which the voltage sensors transit between resting and activated (66) states, suffices to explain the voltage sensor movement (216). The simple behavior the gating charge-voltage [$Q(V)$] curves which are well described by a Boltzmann function, the monoexponential kinetics of the fast component of the gating current, and the lack of a gating current rising phase also are consistent with the kinetic model proposed in Figure 24A in which the voltage sensors act independently. In the allosteric model described in Figure 24A, for each voltage-sensor activated, the equilibrium constant for channel opening, L , is multiply by an allosteric factor D , so the opening process is facilitated as more voltage sensors are activated. The observation that even when all voltage sensor are resting, P_o can be increased by augmenting intracellular Ca²⁺ is the basis for postulating the allosteric kinetic model depicted in Figure 24B under the assumption that there is only one Ca²⁺-binding site per channel subunit (217). In this case, for each Ca²⁺-binding site occupied the equilibrium constant L is multiply by an allosteric factor C . Figure 24A and B define the key feature of Slo1 channels: neither Ca²⁺ nor voltage are strictly necessary for channel activation and Ca²⁺-binding and voltage-sensor activation can act independently to enhance channel opening. Thus, we are in the presence of three processes, Ca²⁺ binding, voltage-sensor activation, and channel opening, which are independent equilibria that interact *allosterically* with each other. In support of the model shown in Figure 24B, Niu and

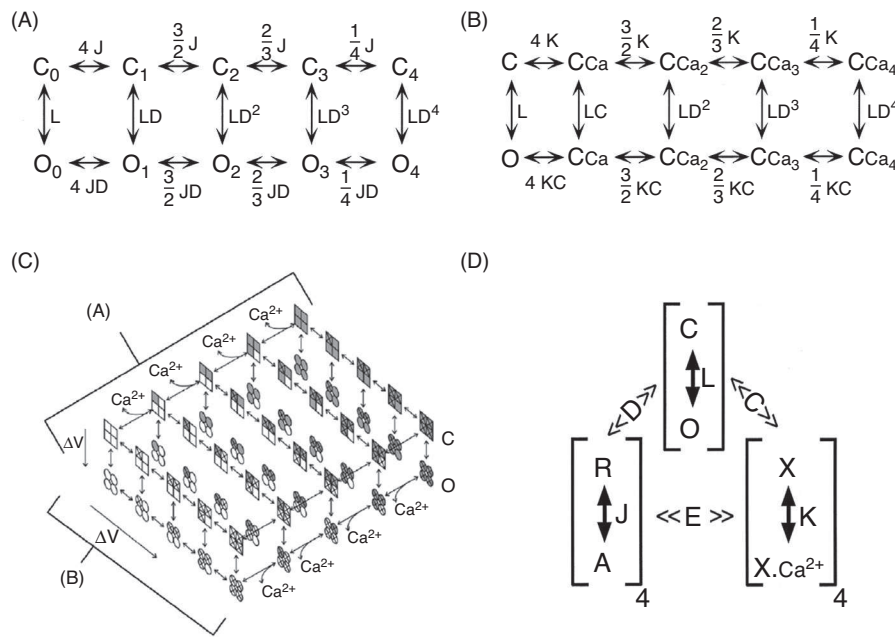
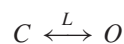


Figure 24 Allosteric models for Slo1 activation by voltage and Ca^{2+} . (A) Allosteric scheme for channel activation by voltage. J is the equilibrium constant governing the equilibrium between resting and active configuration of the voltages sensor. D is the allosteric factor and L is the intrinsic equilibrium for channel opening. Notice that the channel can open when all voltage sensors are in their resting configuration. (Adapted, with permission, from reference 217.) (B) Allosteric kinetic scheme for activation by Ca^{2+} . K is the equilibrium constant for calcium sensor activation and C is an allosteric factor. (C) The combination of A and B produces a two-tiered 50-state kinetic model. [Adapted, with permission, from reference 218.] (D) The complete allosteric model taking into account that Slo1 channels are tetramers and including some interaction between the voltage sensor and Ca^{2+} binding (allosteric factor E). In this type of mechanism neither voltage, nor Ca^{2+} binding is strictly coupled to channel opening, these three processes are independent equilibria that interact allosterically with each other. (Adapted, with permission, from reference 406.)

Magleby (396), using channels with 1, 2, 3, or 4 Ca^{2+} bowls, determined that the Hill coefficient increased in a stepwise fashion as the number of bowl increased from 1 to 4. This observation is consistent with models like the one shown in Figure 24B in which the Ca^{2+} binding to each of the sites is independent, and cooperativity arises as a consequence of the action of the allosteric factor C .

The best compromise between simplicity and reproduction of the voltage and calcium channel dependence in a wide range of voltages and Ca^{2+} concentrations, including very low P_o s, is probably the 50-state two-tiered gating mechanism shown in Figure 24C (89, 455, 456). If some allosteric coupling (E ; Fig. 24D) between Ca^{2+} -binding and voltage-sensor movement is included, the model increases to 70 states (217). The beauty of this model is that it is possible to set experimental conditions to determine some of the different parameters unequivocally. For example, in the absence of Ca^{2+} and at very negative voltages, channel gating kinetics is determined by the transition



and

$$P_o = \frac{O}{O + C} = \frac{1}{1 + L^{-1}}$$

since

$$L \ll 1, \quad P_o \approx L = L_0 e^{(z_L F V / RT)}$$

Thus, under these experimental conditions, we are able to determine two parameters: L_0 and z_L . This exercise allows us to arrive at another important conclusion: for the Slo1 channel, the limiting slope is actually determined by the *lesser* voltage-dependent transition and does not reflect the voltage-sensor charge effectively coupled to channel activation (6, 502).

Slo1 channel structure

The Slo1 channel is a homotetramer of its pore-forming α -subunit is a member of the Kv channels superfamily. As in all other Kv channels, the S4 TM segment is part of an intrinsic voltage sensor (89, 110, 336). Gating and ionic currents in Slo1 channels can be elicited by membrane depolarization in the absence of calcium, suggesting that this is a voltage-dependent channel (217, 514). This divalent cation, by binding to sites contained the regulatory domain for K⁺ conductance (RCK) domains contained in the Slo1 C-terminus, acts as a modulator able to decrease the necessary energy to open the channel, promoting a leftward shift in the open probability (P_o) vs. voltage relationships (reviewed in (340)).

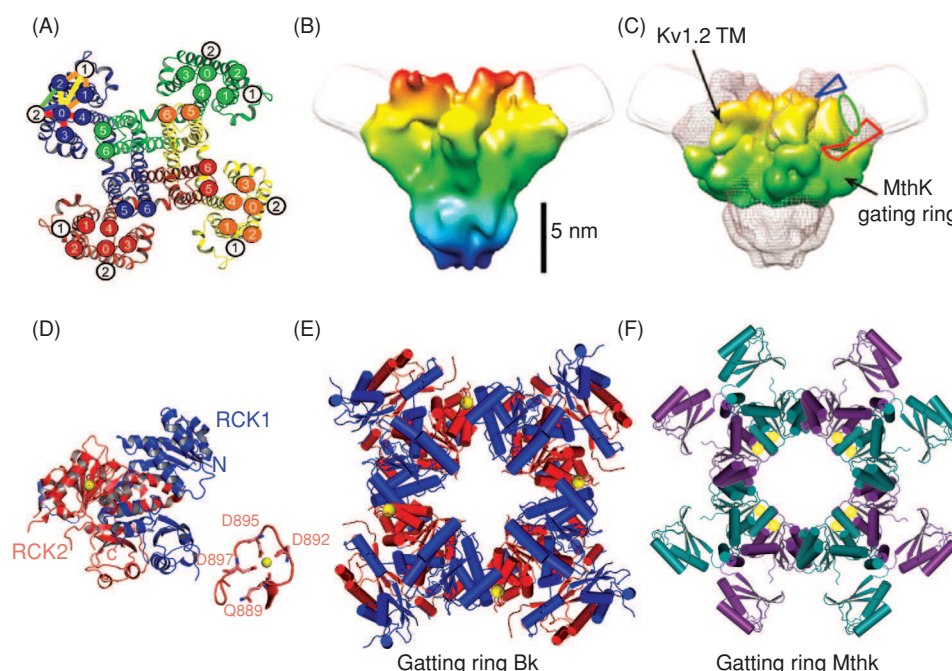


Figure 25 Structural organization of the Slo 1 channel and the crystal structure of the gating ring. (A) Transmembrane segments location using the cysteine cross-linking technique. Kv1.2/Kv2.1 chimera S1 to S6 with superimposed, labeled circles, uniquely colored for each subunit. White numbered circles correspond to TM1 and TM2 of the β 1-subunit. (Adapted, with permission, from reference 565.) (B) Slo 1 20 Å structure resolved with electron cryomicroscopy. The large protrusion at the periphery of the voltage sensor has been suggested to correspond to S0 and the external N-terminus. (C) Superimposed to the Slo1 structure shown in C is the structure of the transmembrane (TM) domains of Kv1.2 and the gating ring of the MthK channel (adapted, with permission, from reference 565). (D) Slo1 channel RCK1 and RCK2 domains of one subunit showing the position of the Ca²⁺-binding site (calcium bowl) in the RCK2 domain. Calcium (yellow ball) is coordinated by D892/D895/D897/Q889 (modified, with permission, from reference 583). (E) Slo1 gating ring at 6 Å resolution. The ring is viewed down the 4-fold symmetry axis with RCK1 in blue and RCK2 in red. Calcium ions are shown as yellow spheres. (F) The open gating ring structure from the MthK channel viewed down the 4-fold axis of symmetry. Notice that a Ca²⁺ binds to the assembly interface in the Slo1 gating ring whereas two Ca²⁺ ions bind to the flexible interface in the MthK gating ring. (Modified, with permission, from reference 607.)

Transmembrane segments: S0, the voltage sensor and the pore

The Slo1 α -subunit contains seven TM segments; an extra one compared with others voltage-dependent K⁺ channels (Kv), and a long C-terminus (364) (Fig. 21B). The minimal molecular component necessary and sufficient for Slo1 activity is its pore-forming α -subunit, and functional channels are formed as tetramers of this protein (495). Tetramerization is driven by an association segment (Slo1-T1 segment) located between the S6 and the α -helix denominated S7 in the intracellular C-terminal region (438). The additional TM segment S0, places the N-terminus toward the extracellular side and adds an extra intracellular linker between the S0 and the S1 compared to Kv channels (364). The exact position of S0 is unknown, but the experiments of Liu et al. (312), using disulfide cross-linking, indicates that S0 lies in close proximity to the S3-S4 loop. S0 is centrally positioned among the extracellular ends of S1 to S4 TM segments (Fig. 25A). A tryptophan scanning mutagenesis study of S0 suggests that the middle and the N-terminus of this TM segment are in direct

contact with the voltage sensor domain (S1-S4) and that this interaction modulates the equilibrium between resting and active states of the channel voltage sensor (274, 489). We note here that, the physical association between the α 1-subunit and the auxiliary β 1-subunit requires the presence of S1, S2, and S3 segments. However, the functional coupling between these two subunits, that is manifested as an apparent increase in the Slo1 Ca²⁺ sensitivity and the Slo1 channel modulation mediated by 17 β -estradiol (556) but not in the changes in gating kinetics, is determined by the Slo1 N-terminus residues (376).

The Slo1 structure recently resolved by electron cryomicroscopy at 17–20 Å, shows a large protrusion at the periphery of the VSD, which as has been suggested should correspond with the additional helix S0 and the extracellular \sim 40 N-terminal residues of Slo1 α -subunit (565) (Fig. 25B and C). As with others Kvs, the α -subunit contain a positively charged TM domain (S4) with one residue directly implicated in the voltage sensing, the R213 [see Fig. 20C (110, 336)]. Unlike other Kvs, a large portion of the gating charge

movement is contributed by residues D153, R167 in S2 and D186 located S3 [Fig. 20C; (336)]. Voltage clamp fluorometry, on the other hand, revealed voltage-dependent conformational changes of the S3-S4 region of R207Q mutant of the Slo1 channel (410, 478) using the same technique found evidence of cooperativity between S2 and S3. Charge neutralization in one segment modifies the effective valence of the other and vice versa, a result explained by Pantazis et al. (410) assuming changes in the dielectric (dynamic field focusing) induced by the creation of aqueous crevices. In Kv channels the VSD is defined as the structure comprised by S1-S4 (238). Most probably, the architecture of the Slo1 VSD would be affected by the presence of the S0 segment and the results of Pantazis et al. (411) appear to confirm this hypothesis.

The pore domain of the channel is assigned to the region contained between S5 and S6 segments, which include the signature sequence of K⁺ channel TVGYG. The external aspect of pore determine the block properties by charibdt toxin (ChTx), iberitoxin (IbTx), and tetraethylammonium (TEA) (339, 370, 379, 495, 558). In general, the architecture of the conduction machinery of Slo1 channels is not different from that of other K⁺ channels but multiple alignments show that the external loop (turret; Fig. 20C) between S5 and the pore helix of Slo1 channels contains several residues more than the other K⁺ channels analyzed (75, 152). This difference in the turret length between Slo1 and Kv channels determines the specificity for only one subfamily of K⁺ channel toxins, alpha-KTx1.x, of the Slo1 channel (152).

Experiments to determine the structural motifs by the high conductance in Slo1 channels (~250 pS) has shown a ring of residues in the inner vestibule entrance in the pore (E321 and E324) that allow to concentrate the K⁺ ions in the inner vestibule trough electrostatic mechanisms doubling the conductance for outward currents with respect to low conductance Kv channels [Fig. 20C (58)]. Also, in the external vestibule near to the selectivity filter, the residue D292 would contribute to concentrate K⁺ ions, increasing the conductance of inward currents (190).

Carboxy terminus

Some K⁺ channels can be activated by a raise in the cytosolic Ca²⁺ and in two cases, the K⁺ channels from the archeon *Methanobacterium thermoautotrophicum* (MthK) (236) and the SLO1 channel, it has been established that the Ca²⁺-binding sites are contained in RCK domains. The structure of the RCK domain of a six TM domain K⁺ channel from *E. coli* solved at 2.4 Å resolution has a Rossmann-fold topology, a very common structural motif found in enzymes and ligand-binding proteins. Rossmann-fold secondary structures are organized into two linked α - α - α - α units and were first identified in a number of NAD⁺-dependent dehydrogenases. This is the type of structure present in the MthK and in the *Drosophila*, mouse and human Slo1 channel (Fig. 25D). The intracellular C-terminus domain, comprising two-thirds of the

protein, contains four hydrophobic segments (S7-S10) and the Ca²⁺- and Mg²⁺-binding sites. As we show later, the C-terminus of Slo1 channels consists of two tandem RCK domains (Figs. 20B and 25E). The RCK domain in the SLO1 channel was initially unveiled by MacKinnon's group (239) by multiple sequence alignment of the SLO1 channel with prokaryotic K⁺ channels and other proteins known to possess the RCK domain structure. We should mention here that based on the primary sequence, C-terminus domains structured as two RCK domains in tandem have been proposed for the K⁺ channels Slo2 and Slo3 (466).

The sequence and predicted secondary structure of the cytoplasmic domain comprised by amino acid residues 339 to 516 in Slo1 that includes the S7 domain, are homologous to a RCK1 domain as that found in a number of K⁺ channels (239). The existence of a second RCK domain (RCK2) contained in the distal part of the C-terminus received support in a structure-based alignment study of the C-terminus of the Slo1 and prokaryotic RCK domains. The structure proposed for Slo1 RCK2 (residues 712 to 999) includes the calcium bowl, and has the characteristic Rossmann-fold topology of RCK domains. In addition, the putative RCK2 undergoes a Ca²⁺-induced change in conformation associated with a α -helix to β -folded structural transition; deletion of the calcium bowl impairs this transition (610).

Recently, two groups determined the x-ray structure of the human SLO1 C-terminus at a 3 and 3.1 Å resolution, respectively (583, 607). The structures obtained confirmed two tandem RCK domains in each SLO1 α -subunit and the deduced tetrameric structure indicated that the SLO1 C-terminus forms a 350 kDa gating ring at the intracellular membrane surface. This study also confirmed that the Ca²⁺ bowl located within the second (RCK2) of the tandem RCK domains forms a Ca²⁺-binding site. This site is located on the outer perimeter of the gating ring, in a region denominated the assembly interface (Fig. 25D and E). Thus, as is the case of the MthK channel, the resulting structure of the SLO1 gating ring is an octamer of RCK domains but different to the MthK channel where each subunit of the tetramer contributes one RCK domain, and another is assembled from solution, both RCK domains in the SLO1 channel are intrinsic to the α -subunit. This structural difference may give origin to the different places to which Ca²⁺ is bound in these two gating rings. In the MthK, Ca²⁺ binds on the "flexible" interface where a cleft between two RCK domains creates the Ca²⁺ binding site (Fig. 25F).

Coupling between Ca²⁺-binding and pore opening

One important question is how the gating ring extracts the free energy of Ca²⁺ binding to open the SLO1 channel gates. It has been proposed that the RCK1-S6 coupling system is contained in the linkers, which behave as a passive spring that applies force to the gates in the absence of cytoplasmic Ca²⁺ to modulate voltage-dependent gating (397). An internal

Ca²⁺ increase changes the force and increases further the Slo1 channel open probability. We notice here that the crystal structure of the MthK-gating ring obtained in the absence of Ca²⁺ and comparison with the structure of the open MthK channel allowed to visualize the open and putative closed conformations of the Ca²⁺ binding domain (601). Calcium binding to each of the RCK domains induces an expansion of the gating ring that in turn can exert a lateral force on the pore opening the channel.

More recently, a clinical problem has come into our help to solve the structures involved in the allosteric coupling between Ca²⁺ binding and Slo1 channel opening (599). A mutation in the neighborhood of the N-terminus of the Slo1 RCK1, D434G, has been associated with human syndrome of generalized epilepsy and paroxysmal dyskinesia. This mutation is inside a region that encompasses the secondary structures β A- α C, hence denominated the AC region, contained in the N-terminus of the SLO1 RCK1 domain and enhances Slo1 channel activity in a manner not related to Ca²⁺ binding. The results indicate that this mutation increases Ca²⁺ sensitivity by augmenting the flexibility of the AC region strongly suggesting that it is or it is part of the coupling system that allows the transformation of chemical energy (Ca²⁺ binding) into mechanical energy (pore opening).

Location and structure of divalent binding sites in the SLO1 RCK domains

Partial deletion or point mutations of the aspartates contained in the calcium bowl in RCK2 produced Slo1 channels that were less sensitive to Ca²⁺ (reviewed in references 90 and 295). Amino acid residues Q889, D892, D895, and D897 in the calcium bowl coordinate the Ca²⁺ ion [(607) Fig. 25D]. The fact that disruption of the Ca²⁺ bowl did not completely eliminate the Slo1 channel sensitivity was a clear demonstration that there was more than one high Ca²⁺-affinity site. The second high-affinity Ca²⁺ sensor was identified on the proximal tail region embedded within the upstream RCK1 domain including residues D367, M513, and E535 (23,583,589,622). Apparently, the Ca²⁺ bowl speeds up channel activation at low Ca²⁺ concentrations whereas the second high-affinity site (D362/D367) modulates both activation and deactivation at [Ca²⁺] more than 10 μ mol/L (620). Surprisingly, the binding of Ca²⁺ to the high-affinity site contained in the RCK1 domain is voltage-dependent whereas at the Ca²⁺ bowl is not (526).

Additional research identified a third lower-affinity divalent cation-sensing domain in the RCK1 able to bind Mg²⁺ as well as Ca²⁺. Mg²⁺ is coordinated at the interface between the voltage-sensor domain and the RCK1 domain to activate Slo1 channels (597). Potential residues contributing to Mg²⁺ coordination are E374 and E399 in RCK1 and D99 in the S1-S2 linker and N172 in the S2-S3 loop. Notably, E374 and E399, and D99 and N172 may come from neighboring subunits to form the Mg²⁺-binding site. The proximity between the Mg²⁺ site and the voltage sensor, on the other hand, en-

ables the electrostatic interaction between the bound Mg²⁺ and R213 contained in the S4 segment that in turn affects the displacement of the voltage-sensor giving an elegant mechanistic explanation to the Mg²⁺ Slo1 channel activation.

C-terminus and ion-binding sites in Slo2 and Slo3

For nematode Slo2 both Ca²⁺ and Cl⁻ are required to induce robust macroscopic K⁺ currents but channel activation is much weaker in the presence of only one of these ions. This is qualitatively similar to what is observed for Slo1, that either Ca²⁺ or voltage is able to open the channel. For the case the *C. elegans* Slo2 channels, it has been postulated the existence of a “chloride bowl” composed of positive residues involved in chloride binding (605). Mutations of several of these positive residues to neutral residues produce channels with reduced sensitivity to Ca²⁺ and charge reversion produced channels insensitive to Ca²⁺ and Cl⁻. However, chimeras between the chloride bowl of Slo2.1 and Slo2.2 (which have different chloride sensitivity) showed no differences with the parental channel Cl⁻ sensitivity, suggesting that the anion site is not located at this position (47). The fact that Ca²⁺ or Cl⁻ alone are unable to generate macroscopic currents and mutations in chloride bowl affect the sensitivity for both ions, suggests that both ions act synergistically to open the channel (605).

The sodium-sensing site in Slo2.2 has been recently mapped to the RCK2 domain, by homology to the sodium site found in G-protein-sensitive inwardly rectifying K⁺ (GIRK) channels (622). Several putative sequences were found in Slo2.2 and finally D818 located in the RCK2 domain was the residue implicated in sodium sensitivity.

For Slo3, the proton-binding site is also located in C-terminal region, evidenced by chimeric channels between Slo1 and Slo3 as explained earlier (590). An allosteric model similar to that proposed for Slo1 channels has been proposed for Slo3 (625).

Small Conductance K⁺ (SKCa, KCa2) Channel Family

KCa2 channels diversity and localization

Small conductance calcium activated potassium channels were originally discovered in red cells. SK channels are so named because they have a small conductance of approximately 10 to 14 pS (50,416) Figure 26. SK channels are potassium channels that are activated by an increase in intracellular calcium. They were first cloned by Kohler et al. (271) and they are divided in three subtypes, KCa2.1 (SKCa1), KCa2.2 (SKCa2), and KCa2.3 (SKCa3), encoded by the genes *KCNN1*, *KCNN2*, and *KCNN3*, respectively (Fig. 27A). This family also includes an “intermediate conductance” channel KCa3.1 (IKCa1; Figs. 1 and Fig. 27A) encoded by the gene *KCNN4*. SKCa1-3 are neuronal and sensible to the bee venom apamin. The intermediate conductance, IKCa1, channel

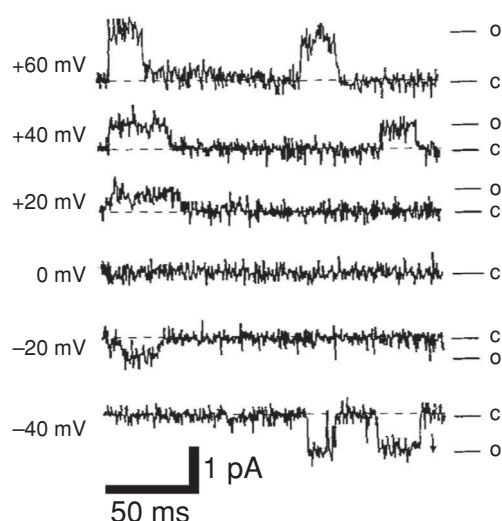


Figure 26 KCa2 channels activation: single-channel currents. Single-channel current from arterial chemoreceptor cells. The inside-out patch containing one observable open channel during 200-ms depolarizations from -80 mV to the indicated membrane potentials. Solutions: 130 mmol/L K, 0.01 mmol/L Ca^{2+} // 130 mmol/L K, 10 mmol/L EGTA. (Adapted, with permission, from reference 149.)

is present mainly in non-neural cells and is not sensitive to apamin. The gene coding for KCa2.1 channel (KCNN1) has 12 exons, with 32 theoretical transcripts, 20 of which have been observed in mouse. Some splice variants can promote the binding of calmodulin to the channel [(621); see later]. The *KCNN4* gene also show alternative processing, producing three splice variants, one of which is expressed in VSM and the other two in endothelial cells (25). In distal colon epithelium, the *KCN4* gene is present in both apical and basolateral membranes. KCa2.1 and KCa2.2 are located in the CNS and KCa2.2 is also located in sensory cells, microglia, and cardiomyocytes. KCa2.3 is located in neurons and glia.

There are also two known isoforms of KCa2.3 channels, one isoform that is insensitive to traditional SK channel blockers and the other that behaves as a dominant negative, preventing the surface expression of all the KCa2.3 subunits (544, 575). The physiological roles of these splice variants are yet to be determined. KCa2 channels are thought to assemble as tetramers because of their similarity with voltage-gated potassium channels (Fig. 27B and C). In expression systems, human KCa2.1 and rat KCa2.2 channels can form functional homomultimers (271), whereas the rat KCa2.1, because of the inability of the C-terminus to mediate trafficking, is unable to reach the cell membrane (35, 105). The 32 splice variants found for KCa2.1 channels encode for at least 16 KCa2.1 polypeptides in the mouse brain. Differences reside in the C-terminus sequence, S6 domain, the calmodulin-binding domain and two predicted binding sites for PDZ¹ domain-containing proteins (499). KCa2.2 subunits can contain either a long or a short N-terminus (518), or lack S3, S4, and S5 TM domains, leading to nonfunctional channels (383).

KCa2.1 and KCa2.2 subunits are primarily expressed in the neocortex, hippocampus, amygdala, cerebellum, and brainstem, whereas KCa2.3 subunits are highly expressed in the midbrain, thalamus, cerebellum, and hypothalamus (see Fig. 29). The calcium sensitivity and wide subcellular distribution confers KCa2.2 channels with the ability to act as feedback regulators in many neuronal processes, including repetitive action potential firing, dendritic calcium rises, spine calcium rises, and endocannabinoid signaling. KCa2.1 and KCa2.2 channels tend to be more important in controlling dendritic integration, synaptic transmission, and synaptic plasticity, whereas KCa2.3 channels appear to be more important in controlling repetitive firing patterns (see Fig. 29).

Calmodulin confers Ca^{2+} sensitivity to KCa2 channels

KCa2 channels have six TM segments and a P loop region (between S5 and S6) containing the characteristic signature sequence GYGD of most K⁺ channels, and intracellular N- and C-termini (Fig. 27B and C). Transmembrane segments of KCa2 channel subtypes are highly homologous and most of the divergence between these channels resides in their C- and N-terminal domains. Although the S4 segment contains two arginines (Fig. 27C), KCa2 channels are voltage independent.

KCa2 channels are highly sensitive to calcium, being activated in the submicromole per liter range (271, 416, 588), and low concentrations of intracellular calcium (EC_{50} of 300–700 nmol/L) induce very fast activation (515). Interestingly, the deactivation time constant is in the orders of tenths of milliseconds and is responsible for the long-lasting changes in membrane potentials, as for example, the medium after hyperpolarization (mAHP) of CA1 hippocampal neurons (488) (Fig. 29a).

In contrast with Slo1 channels that have calcium-binding sites in the α -subunit, KCa2 channels form a stable complex with calmodulin (CaM), a protein that act as the calcium sensor in nearly all eukaryotic cells [Fig. 28; reviewed in Mayle et al. (359)]. In the case of KCa2 channels it is the binding of calcium to calmodulin that leads to channel opening. CaM mediates calcium signaling by protein-protein interactions with other proteins in presence of calcium. CaM has four EF calcium-binding motifs, two located in the N-terminus, and the other two in the C-terminus [reviewed in Weatherall et al. (568)]. Mutant KCa2.2 channels with disrupted C-terminal sites did not show changes in calcium sensitivity (256) indicating that only the two N-terminal EF motifs are necessary for calcium sensitivity. The association of CaM with KCa2 channels is a target of pharmacological agents as the KCa2 activator 1-ethyl-2-benzimidazalinona (1-EBIO). This compound increases the affinity for Ca^{2+} in heterologously expressed channels by one order of magnitude, allowing

¹ PDZ is an acronym combining the first letters of three proteins—post synaptic density protein (PSD95), *Drosophila* disc large tumor suppressor (Dlg1), and zonula occludens-1 protein (zo-1)—which were first discovered to share the domain.

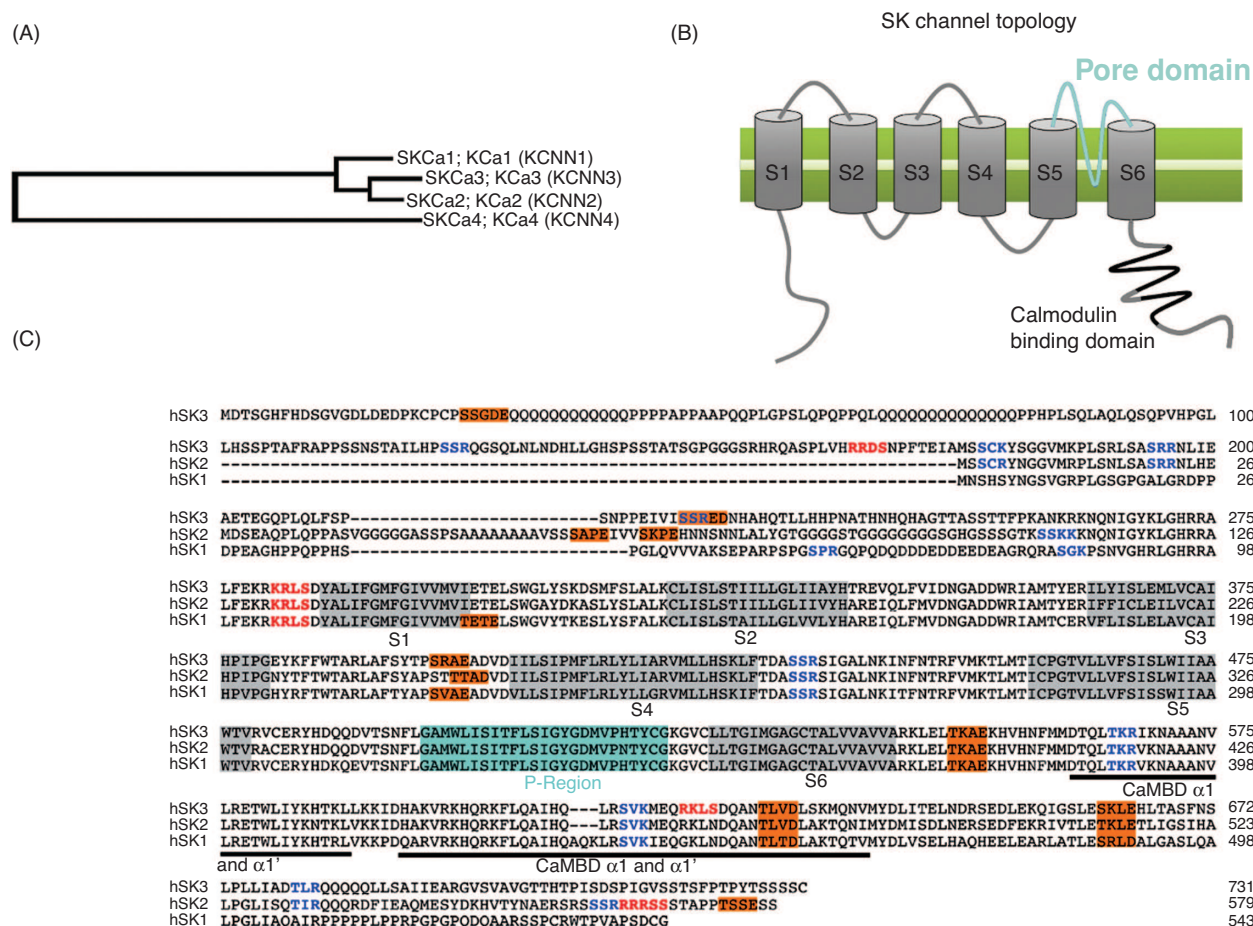


Figure 27 Topology of KCa2 channels and family dendrogram. (A) Dendrogram of the human SK channels genes constructed using t coffee and ClustalW. Genbank accession numbers: NC_000019 (KCNN1), NC_000005 (KCNN2), NC_000001 (KCNN3), and NC_000019 (KCNN4). (B) Proposed topology for KCa2 channels, showing a canonical six-transmembrane segments organization (S1-S6) whence S5 and S6 form the ion-conduction pathway (shown in cyan) and the S4 segment. The intracellular Ca²⁺ regulation is given by the calmodulin-binding domain (CaMBD) located in the C-terminus (black segment). (C) Sequence alignment of the human SK channels (hSK1, hSK2, and hSK3). The transmembrane segments, S1 to S6, are boxed in gray. The pore region (P-Region) is boxed in cyan. The CaMBD is indicated by black bars. Orange boxed amino acids and red residues show different phosphorylation sites conserved along the family. (Adapted, with permission, from reference 424.)

channel activation at Ca²⁺ concentrations as low as 50 nmol/L (423). The main effect of 1-EBIO is to slow down the deactivation without affecting the activation. The effect of EBIO on the calcium sensitivity disappears if the N-terminal EF motifs of CaM are mutated, suggesting that this drug affects the CaM-KCa2 channel interaction.

Once activated, potassium currents through KCa2 channels show inward rectification (271), which in KCa2.2 channels has been attributed to a voltage-dependent block by divalent cations that bind within the selectivity filter (506, 507).

Crystal structure, channel trafficking, and assembly

Crystallographic evidence suggests that four CaM molecules are bound to the channel, within a region in the SK channel

that has no homology with CaM-binding regions in other proteins (486). This CaM-binding domain (CaMBD) is located adjacent to S6, and it has a short and a long α -helix connected by a loop (Fig. 28). In the crystal structure of CaM-CaMBD complex, the α -helices of two CaMBD run antiparallel to each other, making contact with two CaM molecules. Crystallographic and biochemical evidence suggest that in the absence of Ca²⁺, CaM-CaMBD complexes are monomers, which dimerize when calcium is bound (486). It has been hypothesized that when calcium is bound, dimerization of CaMBD produces a conformational change that allows S6 to rotate and open the channel gate (588).

CaM also is important for the sorting of KCa2 channels to the plasma membrane. In IKCa1, the expression of isolated CaMBD prevents the assembly of CaM to the channel, and results in retention of the protein in intracellular organelles that can be overcome by CaM overexpression (246). In the absence of free CaM, channels do not multimerize, causing retention

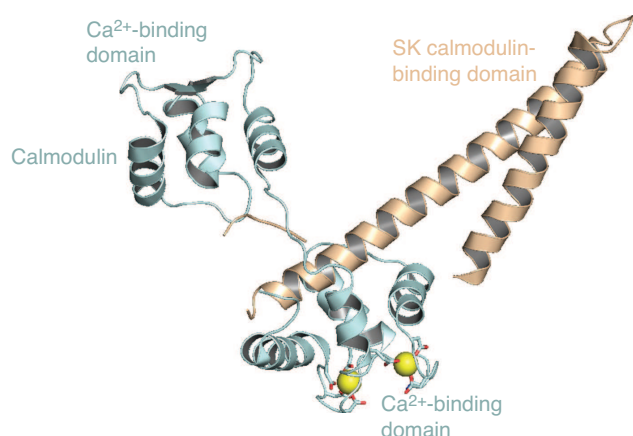


Figure 28 KCa2 channel C-terminal calmodulin-binding domain. Calmodulin protein and KCa2 C-terminal calmodulin-binding domain complex was crystallized at a 1.6 Å resolution (PDB: 1G4Y). Calmodulin protein is shown in cyan with two of the four calcium bowls occupied by Ca²⁺ (yellow balls). The center of the calmodulin molecule is in contact with the KCa2 C-terminal domain (pale brown) (486).

at subcellular locations. In the crystal structure, CaM and CaMBD form saline bridges between residues R464/L467 in KCa2.2 Channels with the double mutation R464E/L467E, have a low affinity for CaM, consistent with these residues being located at the CaM-CaMBD interface (486). This low CaM affinity can be overcome by overexpression of CaM or a CaM mutant unable to bind Ca²⁺ (300). The double mutant R464E/L467E does not express in the membrane by itself but it does when coexpressed with CaM, suffering a robust rundown after patch excision. This rundown is due to CaM washout, and can be rescued if an excess of recombinant CaM is perfused in the bath. This evidence suggests that CaM is essential for channel multimerization at subcellular compartments. However, the channel can be present as tetramers in the plasma membrane in the absence of CaM, but proper function requires the presence of the Ca²⁺-binding protein.

Rat KCa2.1, KCa2.2, and KCa2.3 channels can form functional heteromultimers in expression systems (35,374), while *in vivo*, immunoprecipitation, expression, and pharmacological studies suggest that KCa2.2 and KCa2.3 channels form both homomultimers (422, 463) and heteromultimers (518). KCa2.1 and KCa2.2 channel proteins show distinct subcellular distributions in rat brain regions such as the neocortex and hippocampus, suggesting that they may form homomultimeric channels in these regions (463, 464).

Localization of the KCa2 channel activation gate

The location of the activation gate in KCa2 channels appears to be different to that of Kv channels. Accessibility of MTS reagents to cysteines engineered in Kv channels showed that the K⁺ access to the selectivity filter is controlled by the bundle crossing formed by the intracellular end of the sixth TM domain (S6) of each of the four channel subunits (313). Cysteine residues in the S6 are modified by MTSET at a

faster rate in the open than in closed states, as observed for Kv channels. However, the smaller molecule 2-(aminoethyl) MTS (MTSEA) also modifies a residue located just below the selectivity filter at the same rate irrespective of the channel state (65). This evidence suggests that the gate is located in or very close to the selectivity filter. The state-dependent accessibility changes of S6 can be explained as rotation of the TM helix due to the conformational change that calcium binding to CaM imposes to the channel structure.

Physiological roles

The most explored role for SK channel is its involvement in the mAHP following an action potential. Due to the activation of VDCC during the rising phase of the action potential several types of calcium-activated conductances develop. The fAHP in CA1 neurons is carried by BK channels [(1, 290, 461); see section on Slo channels]. The mAHP is also Ca²⁺-dependent and inhibited by nanomolar concentrations of apamin and it can last tenths to hundred of milliseconds, depending on the neuronal type (186, 427, 434). This long hyperpolarization is responsible for long interburst events as well as determining the firing frequency within a train and its origin resides in a very slow deactivation compared with the channel activation (175, 176, 341).

Potassium channels are involved in the repolarization of action potentials, where there are three phases: the fAHP controlled by Kv and Slo1, the medium AHP which is sensitive to apamin, and the slow whose molecular identity is unknown. The activation of SK channels depends on calcium influx from VDCC during the rising phase of the action potential, and in some system also from intracellular calcium stores.

In several neuronal types as CA1 pyramidal cells, the fAHP is carried by Slo1 channels and is sensitive to IbTX and low TEA concentration (175, 493). The mAHP is also calcium dependent but inhibited by nanomolar concentration of Apamin and can last tenths to hundred of milliseconds, depending on the neuronal type (Fig. 27A) (reviewed in references 54 and 129). This long hyperpolarization is responsible for long interburst events as well as determining the firing frequency within a train (79). The mAHP decays over several hundred milliseconds, consistent with the slow deactivating kinetics observed in heterologous systems (588) (reviewed in references 129 and 515). mAHP is present in cortical structures as neocortex, hippocampus, amygdala; and also in other structures as substantia nigra, hypothalamic nucleus and, *globus pallidus*, *locus ceruleous*, among others (reviewed in reference 129). A prototypical role of SK activation is mAHP in CA1 neurons, where apamin decreases the number of action potentials and decreases the extent of AHP in short trains, without affecting other properties as spike frequency adaptation (516, 554). By using KO animals of the three neuronal SK channels, it was observed that only SK2^{-/-} animals show elimination of mAHP in CA1 pyramidal neurons (509). However, more recent evidence shows that mAHP is mediated by M and H currents (175, 176). The possible explanation for

this discrepancy is that previous studies were performed under voltage-clamp conditions, in which a long (10–50 ms) is used to elicit mAHP, while the recent publications reported current-clamp recordings, in which action potentials last 1 to 2 ms. This difference in depolarization duration can account for an increased calcium influx in voltage-clamp experiments. In this context, is possible that under low-frequency stimulation H and M currents account for mAHP, while SK becomes relevant under higher frequencies where calcium is bigger, or under a calcium spike.

The distal dendrites of CA1 neurons show regenerative events called plateau potentials, which are local membrane depolarizations that do not propagate to adjacent branches (570). This potential is generated by calcium entry through dendritic VDCC. Dendritic SK and Kv4 channels are responsible for maintaining this compartmentalization (70). Local apamin in the distal dendrites increases the plateau potential duration and calcium influx (Fig. 29A); however, do not prevent compartmentalization. Kv4 channels decrease the amplitude of plateau potentials, preventing its propagation to the adjacent branch. Thus, SK conductance controls duration and Kv4 the amplitude of depolarization inhibiting compartmentalization, thus both acting coordinately to regulate synaptic integration.

SK channel block increases the LTP induction after high-frequency stimulation, and improve the performance of spatial learning tasks (509). It is possible that NMDA receptors and KCa2 channels are closely located at dendritic spines, a hot spot for LTP induction, where KCa2 channels decrease the magnitude of depolarization evoked for NMDA channel activation.

Dopaminergic (DA) neurons of the midbrain have a pace-making behavior with a slow (0.6–4.3 Hz) firing rate at physiological conditions (576). Blocking of KCa2 channels leads to an increase, while activation by 1-EBIO produce a decrease in firing frequency. Firing precision is high in this neuronal type, with a low coefficient of variation (CV) and single Gaussian fit of interspike interval (ISI) duration histogram (Fig. 29B). Increasing the number of blocked channels by increasing the concentration of blockers, leads to a decrease in firing precision that is reflected as an increase in the CV and the inability of fit the duration histogram with a single Gaussian (576). Biophysical and pharmacological analysis, single-cell mRNA, and protein-expression profiling strongly suggest that KCa2.3 channels mediate the calcium-dependent afterhyperpolarization in DA neurons (228, 576).

mAHP is blocked when inhibitors of T-type VDCC are presents, suggesting that these types of Ca²⁺ channels are the calcium source needed to activate KCa2 (577). Inhibition of T-type channels decreases mAHP with the same IC₅₀ value estimated for VDCC. In addition, KCa2 current follows the time course of the cumulative inactivation of T-type channels. All these evidences strongly suggests that KCa2 channels are functionally coupled to T-type VDCC. As observed when KCa2 channels are blocked, T-type channel blockage also decreases the precision of firing, seen as an increase in the CV. In a subset of cells with a high basal CV, blockage of

T-type channels leads to an increase in burst firing. Therefore, T-type VDCC stabilizes peacemaking firing and reduce the probability of neurons entering into a burst-firing mode.

In dopaminergic neurons from young animals there is a calcium release from intracellular stores that produces spontaneous miniatures outward currents (SMOCs) through KCa2 channels (88). L-type calcium channel blockers inhibit the large-SMOC and depletion of intracellular calcium stores by ryanodine or cyclopiazonic acid (CPA) eliminates the SMOCs, suggesting that Ca²⁺ influx through VDCC activates a calcium-induced calcium release (CICR), which in turn activates KCa2 channels.

Metabotropic activation of SK, lasting even minutes, has been reported in several cortical structures, all of them mediated by second messengers cascades (reviewed in reference 129).

DA projections in several brain areas are involved in motor functions, working memory, reward, and goal-directed behaviors. Since KCa2 channels control repetitive firing and suppress burst generation in dopaminergic midbrain neurons, these channels play an important role in controlling the amount of dopamine released by these cells.

Cerebellar Purkinje neurons are the only cell type that sends projections out of the cerebellar cortex. This neurons show tonic firing which is maintained by several types of ion channels: transient and resurgent sodium channels, fast activating potassium channels, T-type calcium channels, hyperpolarization activated ion channels, and calcium-activated nonselective cationic conductances (30, 353, 440, 527). Block of Kca2 channels with apamin in tonically firing Purkinje neurons produce a burst-firing behavior, and an increase in CV (Fig. 29C) (580). There is a population of cells that fire in a trimodal pattern consisting of firing, bursting, and silent periods (578). In this group of cells apamin reduces the duration of tonic and bursting periods, without affecting the silent period (580). The calcium entry needed for opening SK channels come through P/Q-type calcium channels (579). In a mice model of cerebellar ataxia that expresses a mutated P/Q-type calcium channel, the precision of firing of Purkinje cell is decreased (561). This is restored by activation KCa2 channels with 1-EBIO, suggesting that the role of P/Q-Type VDCC is to provide a calcium source that leads to the opening of SK channels (579).

By using an action potential as the command waveform in voltage clamp mode, it is possible to record the membrane currents in dissociated Purkinje neurons (527). Analyzing short bursts, during the first ISI the Kv current decays faster than calcium-dependent potassium currents, which do not change much during this period. In successive spikes, Kv current decreases due to cumulative inactivation; however, since Slo1 and SK channel activity is strongly coupled to the activation of VDCC, KCa current remain stable during Purkinje neuron burst activity, being the most important potassium conductance at the end of the ISI. Slo1 currents, as described in previous section, is active in the falling part of action potential, and undergoes a decrease in magnitude after successive

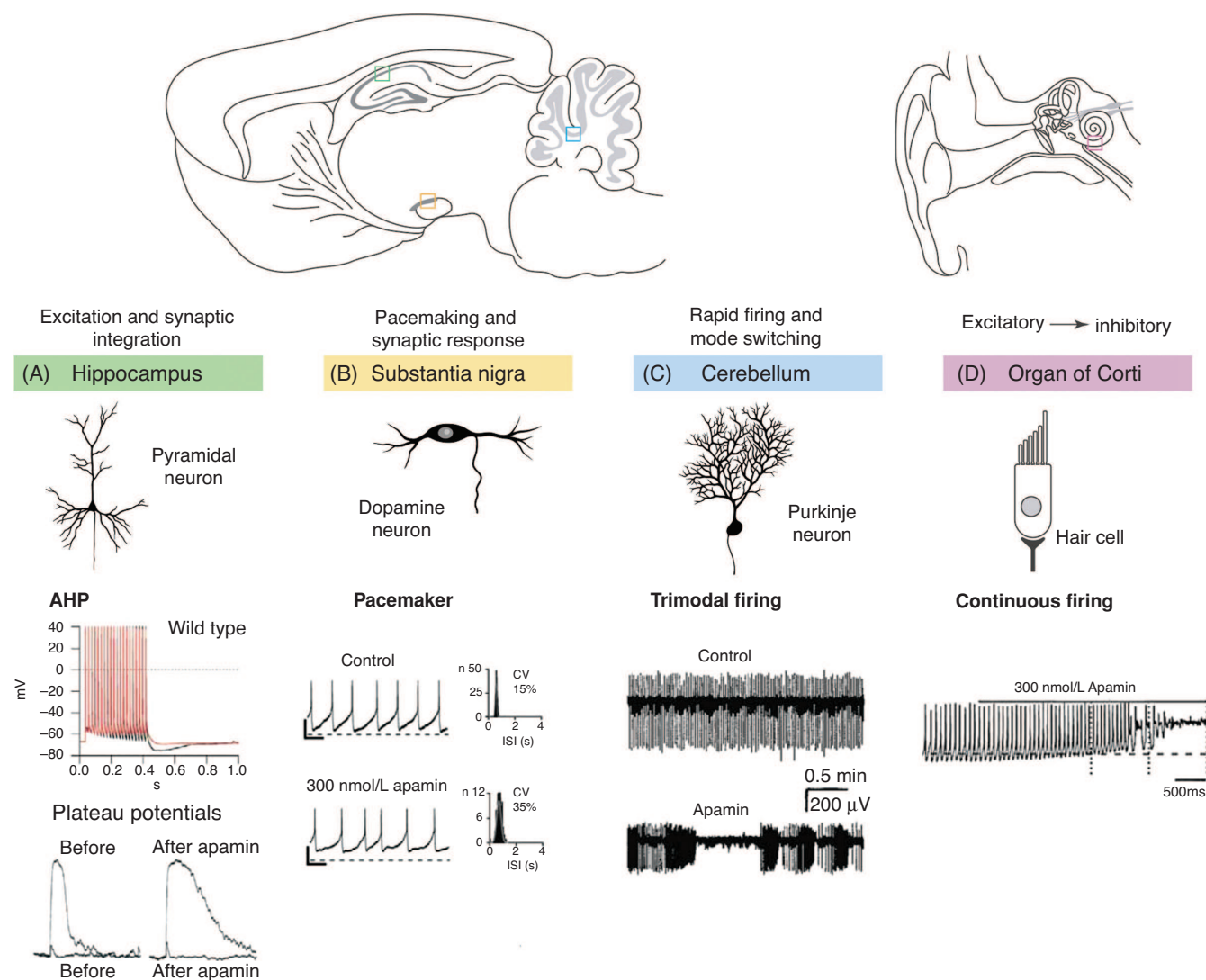


Figure 29 Physiological functions of KCa2 channels. Schematic representation of SK channel function in central nervous system (A) afterhyperpolarization (AHP): CA1 pyramidal neuron whole cell current clamp recording. Twenty action potentials were elicited at 50 Hz in control (black) or apamin (red, 100 nmol/L) bath solutions. The control trace shows the development of an interspike AHP and a posttetanus AHP that is blocked by apamin. Plateau potentials: apamin prolonged the duration of the plateau potential but did not affect the amplitude. (B) Substantia nigra. Pacemaker: perforated-patch current-clamp recording of a dopamine neuron in control or apamin (300 nmol/L) bath solutions. On the left is a 4 s trace representative of a 5-min recording. On the right, the interspike interval (ISI) frequency distribution is plotted for each recording. Apamin significantly decreased the pacemaker precision as shown by the increase in the coefficient of variation (CV). (C) Cerebellum. Trimodal firing: extracellular field recordings of individual cerebellar Purkinje neurons the tonic activity of the cells changed to random bursting when 100 nmol/L apamin was bath applied. (D) Auditory hair cells. Continuous firing: whole cell patch current-clamp recording from inner ear hair cells in the acutely dissected organ of Corti of a P5 rat. Voltage responses induced by a continuous 30 pA depolarizing current from the resting potential of -59 mV are shown. Bath application of 300 nmol/L apamin gradually abolished the evoked action potentials, indicating that KCa2 channel activity is necessary for continued firing. (Modified, with permission, from reference 54.)

action potentials, probably due to inactivation (440). In contrast, KCa2 current increases with successive action potential, possibly due to a calcium increase, which is responsible for the burst termination (527). KCa2 channels blockage with apamin produces a robust increase in burst duration, reinforcing the idea of SK channel as regulators of firing behavior.

In auditory OHCs the IPSPs are due to acetylcholine release. In this cell type the nicotinic acetylcholine receptors (nAChR) contain the $\alpha 9$ -subunit, which confers calcium permeability to these type of channels (126). KCa2 channels

are strongly coupled to nAChR, and the kinetics of IPSPs is determined by KCa2, but not calcium diffusion. Inner hair cells (IHCs) also receive cholinergic afferents but only during early postnatal stages. During this period, a Ca^{2+} -dependent and apamin sensitive potassium conductance is present (349). Apamin increases the firing frequency and reduces the extent of AHP, leading finally to a steady depolarization (Fig. 29D). This means that Kv channels are not sufficient to maintain firing, in contrast to cerebellar Purkinje cells where apamin does not suppress neuron electrical activity.

Pharmacology of SK channels

SK_{Ca} channels are blocked by different pharmacological agents, including the bee toxin apamin (50, 68, 450, 463, 464), tubocurarine, quaternary salts of bicuculline such as bicuculline methiodide and bicuculline methochloride (245, 491), the scorpion toxin scyllatoxin (77, 101), NS8593 (519), dequalinium, UCL1848, and a number of bis-quinolinium cyclophanes (73, 97, 121). More recently, the reversible blockers *N*-methyl-laudanosine (NML) and methyl-noscapine (167, 480), bis-quaternary isoquinoliniums (165), and lipophilic tetrahydroisoquinoline derivatives (166) have been developed. There are also a number of KCa₂ channel openers available. EBIO, which enhances the calcium sensitivity and open probability of SK_{Ca} channels, dichloro-EBIO (DCEBIO), and NS309 (403, 423). Finally, buffering intracellular calcium with high concentrations of 1,2-bis(o-aminophenoxy)ethane-*N,N,N',N'*-tetraacetic acid (BAPTA) or Ethylene glycol tetraacetic acid (EGTA) also blocks activation of SK channels (462, 487).

Apamin-binding site

Blockade of KCa₂ channels by apamin allowed their initial characterization and provided insights into subunit composition due to the differential sensitivity of K⁺ channel subunits to apamin (50, 68, 173, 450). KCa₂ channels are blocked by nanomolar concentrations of the honeybee toxin apamin. KCa_{2.2} is blocked with the highest affinity (27–140 pmol/L), KCa_{2.1} has the lowest affinity (0.7–12 nmol/L), and SKCa₃ has an intermediate affinity (0.6–4 nmol/L) (424). These differences in toxin sensitivities have been used to distinguish between channel types in native systems. Point mutations in the extracellular vestibule of KCa_{2.1} to the residues present in KCa_{2.2} increase the affinity for apamin of KCa_{2.1} to the same levels of KCa_{2.2} channels. The use of chimeras between several KCa_{2.1/2.2} channels, allowed the identification of the extracellular S3-S4 loop as one of the molecular determinants of apamin sensitivity. This finding gives an economical explanation to the fact that some scorpion toxins can strongly displace ¹²⁵I-apamin, without affecting channel ion conduction (492). The binding site for apamin is located in both the pore region, between S5 and S6, and on a serine residue located in the extracellular region between S3 and S4. The lower sensitivity of KCa_{2.1} channels to apamin compared to KCa_{2.2} channels is due to replacement of this serine residue with a threonine on the KCa_{2.1} subunit.

Acknowledgements

The authors thank Drs. John Ewer and Valeria Vasquez for reading and commenting on the manuscript. This work was supported by Chilean Fondecyt grants: 1110430 to R.L., 1120802 to CG, and 1090493 to D.N. The Centro Interdisciplinario de Neurociencia de Valparaíso is a Scientific

Millennium Institute (Programa Iniciativa Científica Milenio del Ministerio de Economía, Fomento y Turismo, Chile).

References

- Adams PR, Constanti A, Brown DA, Clark RB. Intracellular Ca²⁺ activates a fast voltage-sensitive K⁺ current in vertebrate sympathetic neurones. *Nature* 296: 746–749, 1982.
- Adelman JP, Shen KZ, Kavanaugh MP, Warren RA, Wu YN, Lagrutta A, Bond CT, North RA. Calcium-activated potassium channels expressed from cloned complementary DNAs. *Neuron* 9: 209–216, 1992.
- Aggarwal SK, MacKinnon R. Contribution of the S4 segment to gating charge in the Shaker K⁺ channel. *Neuron* 16: 1169–1177, 1996.
- Ahern CA, Horn R. Specificity of charge-carrying residues in the voltage sensor of potassium channels. *J Gen Physiol* 123: 205–216, 2004.
- Ahern CA, Horn R. Focused electric field across the voltage sensor of potassium channels. *Neuron* 48: 25–29, 2005.
- Aldrich RW Jr., Getting PA, Thompson SH. Mechanism of frequency-dependent broadening of molluscan neurone soma spikes. *J Physiol* 291: 531–544, 1979.
- Ando M, Takeuchi S. Immunological identification of an inward rectifier K⁺ channel (Kir4.1) in the intermediate cell (melanocyte) of the cochlear stria vascularis of gerbils and rats. *Cell Tissue Res* 298: 179–183, 1999.
- Anumonwo JM, Lopatin AN. Cardiac strong inward rectifier potassium channels. *J Mol Cell Cardiol* 48: 45–54, 2010.
- Armstrong CM. Inactivation of the potassium conductance and related phenomena caused by quaternary ammonium ion injection in squid axons. *J Gen Physiol* 54: 553–575, 1969.
- Armstrong CM. Interaction of tetraethylammonium ion derivatives with the potassium channels of giant axons. *J Gen Physiol* 58: 413–437, 1971.
- Armstrong CM. Potassium pores of nerve and muscle membranes. *Membranes* 3: 325–358, 1975.
- Armstrong CM, Bezanilla F. Currents related to movement of the gating particles of the sodium channels. *Nature* 242: 459–461, 1973.
- Armstrong CM, Bezanilla F. Charge movement associated with the opening and closing of the activation gates of the Na channels. *J Gen Physiol* 63: 533–552, 1974.
- Armstrong CM, Bezanilla F. Inactivation of the sodium channel. II. Gating current experiments. *J Gen Physiol* 70: 567–590, 1977.
- Armstrong CM, Loboda A. A model for 4-aminopyridine action on K channels: Similarities to tetraethylammonium ion action. *Biophys J* 81: 895–904, 2001.
- Art JJ, Fettiplace R. Variation of membrane properties in hair cells isolated from the turtle cochlea. *J Physiol* 385: 207–242, 1987.
- Art JJ, Wu YC, Fettiplace R. The calcium-activated potassium channels of turtle hair cells. *J Gen Physiol* 105: 49–72, 1995.
- Ashcroft FM, Gribble FM. New windows on the mechanism of action of K(ATP) channel openers. *Trends Pharmacol Sci* 21: 439–445, 2000.
- Ashcroft FM, Rorsman P. Electrophysiology of the pancreatic beta-cell. *Prog Biophys Mol Biol* 54: 87–143, 1989.
- Ashmole I, Vavoulis DV, Stansfeld PJ, Mehta PR, Feng JF, Sutcliffe MJ, Stanfield PR. The response of the tandem pore potassium channel TASK-3 (K2P9.1) to voltage: Gating at the cytoplasmic mouth. *J Physiol* 587: 4769–4783, 2009.
- Atkinson NS, Robertson GA, Ganetzky B. A component of calcium-activated potassium channels encoded by the *Drosophila* slo locus. *Science* 253: 551–555, 1991.
- Bacci A, Huguenard JR, Prince DA. Long-lasting self-inhibition of neocortical interneurons mediated by endocannabinoids. *Nature* 431: 312–316, 2004.
- Bao L, Rapin AM, Holmstrand EC, Cox DH. Elimination of the BK(Ca) channel's high-affinity Ca(2+) sensitivity. *J Gen Physiol* 120: 173–189, 2002.
- Barhanin J, Lesage F, Guillemare E, Fink M, Lazdunski M, Romey G. K(V)LQT1 and Isk (minK) proteins associate to form the IKs cardiac potassium current. *Nature* 384: 78–80, 1996.
- Barmeyer C, Rahner C, Yang Y, Sigworth FJ, Binder HJ, Rajendran VM. Cloning and identification of tissue-specific expression of KCNN4 splice variants in rat colon. *Am J Physiol Cell Physiol* 299: C251–C263, 2010.
- Baukrowitz T, Yellen G. Use-dependent blockers and exit rate of the last ion from the multi-ion pore of a K⁺ channel. *Science* 271: 653–656, 1996.
- Bautista DM, Sigal YM, Milstein AD, Garrison JL, Zorn JA, Tsuruda PR, Nicoll RA, Julius D. Pungent agents from Szechuan peppers excite sensory neurons by inhibiting two-pore potassium channels. *Nat Neurosci* 11: 772–779, 2008.

28. Bautista L, Castro MJ, Lopez-Barneo J, Castellano A. Hypoxia-inducible factor-2 α stabilization and maxi-K⁺ channel β 1-subunit gene repression by hypoxia in cardiac myocytes: Role in preconditioning. *Circ Res* 104: 1364-1372, 2009.
29. Bayliss DA, Barrett PQ. Emerging roles for two-pore-domain potassium channels and their potential therapeutic impact. *Trends Pharmacol Sci* 29: 566-575, 2008.
30. Bean BP. Neurophysiology: Stressful pacemaking. *Nature* 447: 1059-1060, 2007.
31. Beckh S, Pongs O. Members of the RCK potassium channel family are differentially expressed in the rat nervous system. *EMBO J* 9: 777-782, 1990.
32. Behrens R, Nolting A, Reimann F, Schwarz M, Waldschutz R, Pongs O. hKCNMB3 and hKCNMB4, cloning and characterization of two members of the large-conductance calcium-activated potassium channel β subunit family. *FEBS Lett* 474: 99-106, 2000.
33. Ben-Abu Y, Zhou Y, Zilberberg N, Yifrach O. Inverse coupling in leak and voltage-activated K⁺ channel gates underlies distinct roles in electrical signaling. *Nat Struct Mol Biol* 16: 71-79, 2009.
34. Bender K, Wellner-Kienitz MC, Inanobe A, Meyer T, Kurachi Y, Pott L. Overexpression of monomeric and multimeric GIRK4 subunits in rat atrial myocytes removes fast desensitization and reduces inward rectification of muscarinic K(+) current (I(K(ACh))). Evidence for functional homomeric GIRK4 channels. *J Biol Chem* 276: 28873-28880, 2001.
35. Benton DC, Monaghan AS, Hosseini R, Bahia PK, Haylett DG, Moss GW. Small conductance Ca²⁺-activated K⁺ channels formed by the expression of rat SK1 and SK2 genes in HEK 293 cells. *J Physiol* 553: 13-19, 2003.
36. Bentzen BH, Nardi A, Calloe K, Madsen LS, Olesen SP, Grunnet M. The small molecule NS11021 is a potent and specific activator of Ca²⁺-activated big-conductance K⁺ channels. *Mol Pharmacol* 72: 1033-1044, 2007.
37. Berkefeld H, Fakler B. Repolarizing responses of BKCa-Cav complexes are distinctly shaped by their Cav subunits. *J Neurosci* 28: 8238-8245, 2008.
38. Berkefeld H, Sailer CA, Bildl W, Rohde V, Thumfart JO, Eble S, Klugbauer N, Reisinger E, Bischofberger J, Oliver D, Knaus HG, Schulte U, Fakler B. BKCa-Cav channel complexes mediate rapid and localized Ca²⁺-activated K⁺ signaling. *Science* 314: 615-620, 2006.
39. Bezanilla F. How membrane proteins sense voltage. *Nat Rev* 9: 323-332, 2008.
40. Bezanilla F, Armstrong CM. Negative conductance caused by entry of sodium and cesium ions into the potassium channels of squid axons. *J Gen Physiol* 60: 588-608, 1972.
41. Bezanilla F, Armstrong CM. Gating currents of the sodium channels: Three ways to block them. *Science* 183: 753-754, 1974.
42. Bezanilla F, Armstrong CM. Properties of the sodium channel gating current. *Cold Spring Harb Symp Quant Biol* 40: 297-304, 1976.
43. Bezanilla F, Taylor RE, Fernandez JM. Distribution and kinetics of membrane dielectric polarization. I. Long-term inactivation of gating currents. *J Gen Physiol* 79: 21-40, 1982.
44. Bezanilla F, White MM, Taylor RE. Gating currents associated with potassium channel activation. *Nature* 296: 657-659, 1982.
45. Bhalla T, Rosenthal JJ, Holmgren M, Reenan R. Control of human potassium channel inactivation by editing of a small mRNA hairpin. *Nat Struct Mol Biol* 11: 950-956, 2004.
46. Bhattacharjee A, Gan L, Kaczmarek LK. Localization of the Slack potassium channel in the rat central nervous system. *J Comp Neurol* 454: 241-254, 2002.
47. Bhattacharjee A, Joiner WJ, Wu M, Yang Y, Sigworth FJ, Kaczmarek LK. Slick (Slc2.1), a rapidly-gating sodium-activated potassium channel inhibited by ATP. *J Neurosci* 23: 11681-11691, 2003.
48. Bhattacharjee A, Kaczmarek LK. For K⁺ channels, Na⁺ is the new Ca²⁺. *Trends Neurosci* 28: 422-428, 2005.
49. Bhattacharjee A, von Hehn CA, Mei X, Kaczmarek LK. Localization of the Na⁺-activated K⁺ channel Slick in the rat central nervous system. *J Comp Neurol* 484: 80-92, 2005.
50. Blatz AL, Magleby KL. Single ampin-blocked Ca-activated K⁺ channels of small conductance in cultured rat skeletal muscle. *Nature* 323: 718-720, 1986.
51. Bleich M, Schlatter E, Greger R. The luminal K⁺ channel of the thick ascending limb of Henle's loop. *Pflügers Arch* 415: 449-460, 1990.
52. Bockenhauer D, Zilberberg N, Goldstein SA. KCNK2: Reversible conversion of a hippocampal potassium leak into a voltage-dependent channel. *Nat Neurosci* 4: 486-491, 2001.
53. Bond CT, Ammal A, Ashfield R, Blair TA, Gribble F, Khan RN, Lee K, Proks P, Rowe IC, Sakura H, et al. Cloning and functional expression of the cDNA encoding an inwardly-rectifying potassium channel expressed in pancreatic β -cells and in the brain. *FEBS Lett* 367: 61-66, 1995.
54. Bond CT, Maylie J, Adelman JP. SK channels in excitability, pacemaking and synaptic integration. *Curr Opin Neurobiol* 15: 305-311, 2005.
55. Bond CT, Pessia M, Xia XM, Lagrutta A, Kavanaugh MP, Adelman JP. Cloning and expression of a family of inward rectifier potassium channels. *Receptors Channels* 2: 183-191, 1994.
56. Borchert GH, Yang C, Kolar F. Mitochondrial BKCa channels contribute to protection of cardiomyocytes isolated from chronically hypoxic rats. *Am J Physiol Heart Circ Physiol* 300: H507-H513, 2011.
57. Braun M, Ramracheya R, Bengtsson M, Zhang Q, Karanaukaitė J, Partridge C, Johnson PR, Rorsman P. Voltage-gated ion channels in human pancreatic β -cells: Electrophysiological characterization and role in insulin secretion. *Diabetes* 57: 1618-1628, 2008.
58. Brelidze TI, Niu X, Magleby KL. A ring of eight conserved negatively charged amino acids doubles the conductance of BK channels and prevents inward rectification. *Proc Natl Acad Sci U S A* 100: 9017-9022, 2003.
59. Brenner R, Chen QH, Vilaythong A, Toney GM, Noebels JL, Aldrich RW. BK channel β 4 subunit reduces dentate gyrus excitability and protects against temporal lobe seizures. *Nat Neurosci* 8: 1752-1759, 2005.
60. Brenner R, Jegla TJ, Wickenden A, Liu Y, Aldrich RW. Cloning and functional characterization of novel large conductance calcium-activated potassium channel β subunits, hKCNMB3 and hKCNMB4. *J Biol Chem* 275: 6453-6461, 2000.
61. Brenner R, Perez GJ, Bonev AD, Eckman DM, Kosek JC, Wiler SW, Patterson AJ, Nelson MT, Aldrich RW. Vasoregulation by the β 1 subunit of the calcium-activated potassium channel. *Nature* 407: 870-876, 2000.
62. Brock MW, Mathes C, Gilly WF. Selective open-channel block of Shaker (Kv1) potassium channels by s-nitrosodithiothreitol (SNDTT). *J Gen Physiol* 118: 113-134, 2001.
63. Broomand A, Elinder F. Large-scale movement within the voltage-sensor paddle of a potassium channel-support for a helical-screw motion. *Neuron* 59: 770-777, 2008.
64. Brown MR, Kronengold J, Gazula VR, Spiliarakis CG, Flavell RA, von Hehn CA, Bhattacharjee A, Kaczmarek LK. Amino-termini isoforms of the Slack K⁺ channel, regulated by alternative promoters, differentially modulate rhythmic firing and adaptation. *J Physiol* 586: 5161-5179, 2008.
65. Bruening-Wright A, Schumacher MA, Adelman JP, Maylie J. Localization of the activation gate for small conductance Ca²⁺-activated K⁺ channels. *J Neurosci* 22: 6499-6506, 2002.
66. Brünig E, Blumfeldt-Albertus H. *Jasmina und die Lotosblume*. Berlin: Der Kinderbuchverlag, 1986, p. 77.
67. Budelli G, Hage TA, Wei A, Rojas P, Jong YJ, O'Malley K, Salkoff L. Na⁺-activated K⁺ channels express a large delayed outward current in neurons during normal physiology. *Nat Neurosci* 12: 745-750, 2009.
68. Burgess GM, Claret M, Jenkinson DH. Effects of quinine and ampin on the calcium-dependent potassium permeability of mammalian hepatocytes and red cells. *J Physiol* 317: 67-90, 1981.
69. Butler A, Tsunoda S, McCobb DP, Wei A, Salkoff L. mSlo, a complex mouse gene encoding "maxi" calcium-activated potassium channels. *Science* 261: 221-224, 1993.
70. Cai X, Liang CW, Muralidharan S, Kao JP, Tang CM, Thompson SM. Unique roles of SK and Kv4.2 potassium channels in dendritic integration. *Neuron* 44: 351-364, 2004.
71. Campbell DS, Holt CE. Chemotropic responses of retinal growth cones mediated by rapid local protein synthesis and degradation. *Neuron* 32: 1013-1026, 2001.
72. Campos FV, Chanda B, Roux B, Bezanilla F. Two atomic constraints unambiguously position the S4 segment relative to S1 and S2 segments in the closed state of Shaker K channel. *Proc Natl Acad Sci U S A* 104: 7904-7909, 2007.
73. Campos Rosa J, Galanakis D, Piergentili A, Bhandari K, Ganellin CR, Dunn PM, Jenkinson DH. Synthesis, molecular modeling, and pharmacological testing of bis-quinolinium cyclophanes: Potent, non-peptidic blockers of the ampin-sensitive Ca(2+)-activated K(+) channel. *J Med Chem* 43: 420-431, 2000.
74. Candia S, Garcia ML, Latorre R. Mode of action of ibertoxin, a potent blocker of the large conductance Ca(2+)-activated K⁺ channel. *Biophys J* 63: 583-590, 1992.
75. Carvacho I, Gonzalez W, Torres YP, Brauchi S, Alvarez O, Gonzalez-Nilo FD, Latorre R. Intrinsic electrostatic potential in the BK channel pore: Role in determining single channel conductance and block. *J Gen Physiol* 131: 147-161, 2008.
76. Casis O, Olesen SP, Sanguinetti MC. Mechanism of action of a novel human ether-a-go-go-related gene channel activator. *Mol Pharmacol* 69: 658-665, 2006.
77. Castle NA, Strong PN. Identification of two toxins from scorpion (*Leiurus quinquestriatus*) venom which block distinct classes of calcium-activated potassium channel. *FEBS Lett* 209: 117-121, 1986.
78. Catterall WA. Structure and function of voltage-sensitive ion channels. *Science* 242: 50-61, 1988.
79. Cingolani LA, Gymnopoulos M, Boccaccio A, Stocker M, Pedarzani P. Developmental regulation of small-conductance Ca²⁺-activated K⁺

- channel expression and function in rat Purkinje neurons. *J Neurosci* 22: 4456-4467, 2002.
80. Claydon TW, Makary SY, Dibb KM, Boyett MR. The selectivity filter may act as the agonist-activated gate in the G protein-activated Kir3.1/Kir3.4 K⁺ channel. *J Biol Chem* 278: 50654-50663, 2003.
 81. Clement JPt, Kunjilwar K, Gonzalez G, Schwanstecher M, Panten U, Aguilar-Bryan L, Bryan J. Association and stoichiometry of K(ATP) channel subunits. *Neuron* 18: 827-838, 1997.
 82. Cohen A, Ben-Abu Y, Hen S, Zilberberg N. A novel mechanism for human K2P2.1 channel gating. Facilitation of C-type gating by protonation of extracellular histidine residues. *J Biol Chem* 283: 19448-19455, 2008.
 83. Cohen A, Ben-Abu Y, Zilberberg N. Gating the pore of potassium leak channels. *Eur Biophys J* 39: 61-73, 2009.
 84. Cordero-Morales JF, Cuello LG, Zhao Y, Jogini V, Cortes DM, Roux B, Perozo E. Molecular determinants of gating at the potassium-channel selectivity filter. *Nat Struct Mol Biol* 13: 311-318, 2006.
 85. Cordero-Morales JF, Jogini V, Lewis A, Vasquez V, Cortes DM, Roux B, Perozo E. Molecular driving forces determining potassium channel slow inactivation. *Nat Struct Mol Biol* 14: 1062-1069, 2007.
 86. Covarrubias M, Bhattacharji A, De Santiago-Castillo JA, Dougherty K, Kaulin YA, Na-Phuket TR, Wang G. The neuronal Kv4 channel complex. *Neurochem Res* 33: 1558-1567, 2008.
 87. Cuello LG, Jogini V, Cortes DM, Perozo E. Structural mechanism of C-type inactivation in K(+) channels. *Nature* 466: 203-208.
 88. Cui G, Okamoto T, Morikawa H. Spontaneous opening of T-type Ca²⁺ channels contributes to the irregular firing of dopamine neurons in neonatal rats. *J Neurosci* 24: 11079-11087, 2004.
 89. Cui J, Aldrich RW. Allosteric linkage between voltage and Ca(2+)-dependent activation of BK-type mslol K(+) channels. *Biochemistry* 39: 15612-15619, 2000.
 90. Cui J, Yang H, Lee US. Molecular mechanisms of BK channel activation. *Cell Mol Life Sci* 66: 852-875, 2009.
 91. Cha A, Snyder GE, Selvin PR, Bezanilla F. Atomic scale movement of the voltage-sensing region in a potassium channel measured via spectroscopy. *Nature* 402: 809-813, 1999.
 92. Chakrapani S, Cordero-Morales JF, Jogini V, Pan AC, Cortes DM, Roux B, Perozo E. On the structural basis of modal gating behavior in K(+) channels. *Nat Struct Mol Biol* 18: 67-74, 2011.
 93. Chandry KG, Cahalan M, Pennington M, Norton RS, Wulff H, Gutman GA. Potassium channels in T lymphocytes: Toxins to therapeutic immunosuppressants. *Toxicol* 39: 1269-1276, 2001.
 94. Chemin J, Patel A, Duprat F, Zanzouri M, Lazdunski M, Honore E. Lysophosphatidic acid-operated K⁺ channels. *J Biol Chem* 280: 4415-4421, 2005.
 95. Chemin J, Patel AJ, Duprat F, Lauritzen I, Lazdunski M, Honore E. A phospholipid sensor controls mechanogating of the K⁺ channel TREK-1. *EMBO J* 24: 44-53, 2005.
 96. Chen H, Kronengold J, Yan Y, Gazula VR, Brown MR, Ma L, Ferreira G, Yang Y, Bhattacharjee A, Sigworth FJ, Salkoff L, Kaczmarek LK. The N-terminal domain of Slack determines the formation and trafficking of Slack/Slack heteromeric sodium-activated potassium channels. *J Neurosci* 29: 5654-5665, 2009.
 97. Chen JQ, Galanakis D, Ganellin CR, Dunn PM, Jenkinson DH. bis-Quinolium cyclophanes: 8,14-diaz-1,7(1, 4)-diquinolinylnicotetradecaphane (UCL 1848), a highly potent and selective, nonpeptidic blocker of the apamin-sensitive Ca(2+)-activated K(+) channel. *J Med Chem* 43: 3478-3481, 2000.
 98. Chen L, Tian L, MacDonald SH, McClafferty H, Hammond MS, Huibant JM, Ruth P, Knaus HG, Shipston MJ. Functionally diverse complement of large conductance calcium- and voltage-activated potassium channel (BK) alpha-subunits generated from a single site of splicing. *J Biol Chem* 280: 33599-33609, 2005.
 99. Chen M, Gan G, Wu Y, Wang L, Ding J. Lysine-rich extracellular rings formed by hbeta2 subunits confer the outward rectification of BK channels. *PLoS One* 3: e2114, 2008.
 100. Chen X, Yuan LL, Zhao C, Birnbaum SG, Frick A, Jung WE, Schwarz TL, Sweatt JD, Johnston D. Deletion of Kv4.2 gene eliminates dendritic A-type K⁺ current and enhances induction of long-term potentiation in hippocampal CA1 pyramidal neurons. *J Neurosci* 26: 12143-12151, 2006.
 101. Chicchi GG, Gimenez-Gallego G, Ber E, Garcia ML, Winquist R, Casciari MA. Purification and characterization of a unique, potent inhibitor of apamin binding from Leiurus quinquestriatus hebraeus venom. *J Biol Chem* 263: 10192-10197, 1988.
 102. Cho H, Nam GB, Lee SH, Earm YE, Ho WK. Phosphatidylinositol 4,5-bisphosphate is acting as a signal molecule in alpha(1)-adrenergic pathway via the modulation of acetylcholine-activated K(+) channels in mouse atrial myocytes. *J Biol Chem* 276: 159-164, 2001.
 103. Choi KL, Aldrich RW, Yellen G. Tetraethylammonium blockade distinguishes two inactivation mechanisms in voltage-activated K⁺ channels. *Proc Natl Acad Sci U S A* 88: 5092-5095, 1991.
 104. D'Adamo MC, Liu Z, Adelman JP, Maylie J, Pessia M. Episodic ataxia type-1 mutations in the hKv1.1 cytoplasmic pore region alter the gating properties of the channel. *EMBO J* 17: 1200-1207, 1998.
 105. D'Hoedt D, Hirzel K, Pedarzani P, Stocker M. Domain analysis of the calcium-activated potassium channel SK1 from rat brain. Functional expression and toxin sensitivity. *J Biol Chem* 279: 12088-12092, 2004.
 106. Day M, Carr DB, Ulrich S, Ilijic E, Tkatch T, Surmeier DJ. Dendritic excitability of mouse frontal cortex pyramidal neurons is shaped by the interaction among HCN, Kir2, and K leak channels. *J Neurosci* 25: 8776-8787, 2005.
 107. del Camino D, Holmgren M, Liu Y, Yellen G. Blocker protection in the pore of a voltage-gated K⁺ channel and its structural implications. *Nature* 403: 321-325, 2000.
 108. Demo SD, Yellen G. The inactivation gate of the Shaker K⁺ channel behaves like an open-channel blocker. *Neuron* 7: 743-753, 1991.
 109. Dereeper A, Guignon V, Blanc G, Audic S, Buffet S, Chevenet F, Dufayard JF, Guindon S, Lefort V, Lescot M, Claverie JM, Gascuel O. Phylogeny.fr: Robust phylogenetic analysis for the non-specialist. *Nucleic Acids Res* 36: W465-W469, 2008.
 110. Diaz L, Meera P, Amigo J, Stefani E, Alvarez O, Toro L, Latorre R. Role of the S4 segment in a voltage-dependent calcium-sensitive potassium (hSlo) channel. *J Biol Chem* 273: 32430-32436, 1998.
 111. Diness TG, Yeh YH, Qi XY, Chartier D, Tsuji Y, Hansen RS, Olesen SP, Grunnet M, Nattel S. Antiarrhythmic properties of a rapid delayed-rectifier current activator in rabbit models of acquired long QT syndrome. *Cardiovasc Res* 79: 61-69, 2008.
 112. Dobrev D, Friedrich A, Voigt N, Jost N, Wettwer E, Christ T, Knaut M, Ravens U. The G protein-gated potassium current I(K,ACh) is constitutively active in patients with chronic atrial fibrillation. *Circulation* 112: 3697-3706, 2005.
 113. Dougherty K, De Santiago-Castillo JA, Covarrubias M. Gating charge immobilization in Kv4.2 channels: The basis of closed-state inactivation. *J Gen Physiol* 131: 257-273, 2008.
 114. Douglas RM, Lai JC, Bian S, Cummins L, Moczydlowski E, Hadad GG. The calcium-sensitive large-conductance potassium channel (BK/MAXI K) is present in the inner mitochondrial membrane of rat brain. *Neuroscience* 139: 1249-1261, 2006.
 115. Doyle DA, Morais Cabral J, Pfuetzner RA, Kuo A, Gulbis JM, Cohen SL, Chait BT, MacKinnon R. The structure of the potassium channel: Molecular basis of K⁺ conduction and selectivity. *Science* 280: 69-77, 1998.
 116. Doyle ME, Egan JM. Pharmacological agents that directly modulate insulin secretion. *Pharmacol Rev* 55: 105-131, 2003.
 117. Dryer SE. Na(+)-activated K⁺ channels: A new family of large-conductance ion channels. *Trends Neurosci* 17: 155-160, 1994.
 118. Dryer SE, Fujii JT, Martin AR. A Na⁺-activated K⁺ current in cultured brain stem neurones from chicks. *J Physiol* 410: 283-296, 1989.
 119. Du W, Bautista JF, Yang H, Diez-Sampedo A, You SA, Wang L, Kotagal P, Luders HO, Shi J, Cui J, Richerson GB, Wang QK. Calcium-sensitive potassium channelopathy in human epilepsy and paroxysmal movement disorder. *Nat Genet* 37: 733-738, 2005.
 120. Dufer M, Neye Y, Horth K, Krippeit-Drews P, Hennige A, Widmer H, McClafferty H, Shipston MJ, Haring HU, Ruth P, Drews G. BK channels affect glucose homeostasis and cell viability of murine pancreatic beta cells. *Diabetologia* 54: 423-432, 2011.
 121. Dunn PM. Dequalinium, a selective blocker of the slow afterhyperpolarization in rat sympathetic neurones in culture. *Eur J Pharmacol* 252: 189-194, 1994.
 122. Duprat F, Lesage F, Fink M, Reyes R, Heurteaux C, Lazdunski M. TASK, a human background K⁺ channel to sense external pH variations near physiological pH. *EMBO J* 16: 5464-5471, 1997.
 123. Edgerton JR, Reinhart PH. Distinct contributions of small and large conductance Ca²⁺-activated K⁺ channels to rat Purkinje neuron function. *J Physiol* 548: 53-69, 2003.
 124. Egan TM, Dagan D, Kupper J, Levitan IB. Properties and rundown of sodium-activated potassium channels in rat olfactory bulb neurons. *J Neurosci* 12: 1964-1976, 1992.
 125. Eisenman G, Latorre R, Miller C. Multi-ion conduction and selectivity in the high-conductance Ca⁺⁺-activated K⁺ channel from skeletal muscle. *Biophys J* 50: 1025-1034, 1986.
 126. Elgoyhen AB, Johnson DS, Boulter J, Vetter DE, Heinemann S. Alpha 9: an acetylcholine receptor with novel pharmacological properties expressed in rat cochlear hair cells. *Cell* 79: 705-715, 1994.
 127. Elkins T, Ganetzky B, Wu CF. A Drosophila mutation that eliminates a calcium-dependent potassium current. *Proc Natl Acad Sci U S A* 83: 8415-8419, 1986.
 128. Enyedi P, Czirjak G. Molecular background of leak K⁺ currents: Two-pore domain potassium channels. *Physiol Rev* 90: 559-605, 2010.
 129. Faber ES. Functions and modulation of neuronal SK channels. *Cell Biochem Biophys* 55: 127-139, 2009.
 130. Faber ES, Sah P. Physiological role of calcium-activated potassium currents in the rat lateral amygdala. *J Neurosci* 22: 1618-1628, 2002.

131. Fakler B, Adelman JP. Control of K(Ca) channels by calcium nano/microdomains. *Neuron* 59: 873-881, 2008.
132. Fakler B, Schultz JH, Yang J, Schulte U, Brandle U, Zenner HP, Jan LY, Ruppersberg JP. Identification of a titratable lysine residue that determines sensitivity of kidney potassium channels (ROMK) to intracellular pH. *EMBO J* 15: 4093-4099, 1996.
133. Fang Y, Schram G, Romanenko VG, Shi C, Conti L, Vandenberg CA, Davies PF, Nattel S, Levitan I. Functional expression of Kir2.x in human aortic endothelial cells: The dominant role of Kir2.2. *Am J Physiol Cell Physiol* 289: C1134-C1144, 2005.
134. Fernandez-Alacid L, Aguado C, Ciruela F, Martin R, Colon J, Cabanero MJ, Gassmann M, Watanabe M, Shigemoto R, Wickman K, Bettler B, Sanchez-Prieto J, Lujan R. Subcellular compartment-specific molecular diversity of pre- and post-synaptic GABA-activated GIRK channels in Purkinje cells. *J Neurochem* 110: 1363-1376, 2009.
135. Fernandez-Fernandez JM, Tomas M, Vazquez E, Orio P, Latorre R, Senti M, Marrugat J, Valverde MA. Gain-of-function mutation in the KCNMB1 potassium channel subunit is associated with low prevalence of diastolic hypertension. *J Clin Invest* 113: 1032-1039, 2004.
136. Ferrer J, Nichols CG, Makhina EN, Salkoff L, Bernstein J, Gerhard D, Wasson J, Ramanadham S, Permutt A. Pancreatic islet cells express a family of inwardly rectifying K⁺ channel subunits which interact to form G-protein-activated channels. *J Biol Chem* 270: 26086-26091, 1995.
137. Fettiplace R, Fuchs PA. Mechanisms of hair cell tuning. *Annu Rev Physiol* 61: 809-834, 1999.
138. Figueroa KP, Minassian NA, Stevanin G, Waters M, Garibyan V, Forlani S, Strzelczyk A, Burk K, Brice A, Durr A, Papazian DM, Pulst SM. KCNC3: phenotype, mutations, channel biophysics-a study of 260 familial ataxia patients. *Hum Mutat* 31: 191-196.
139. Filosa JA, Bonev AD, Straub SV, Meredith AL, Wilkerson MK, Aldrich RW, Nelson MT. Local potassium signaling couples neuronal activity to vasodilation in the brain. *Nat Neurosci* 9: 1397-1403, 2006.
140. Fink M, Duprat F, Lesage F, Reyes R, Romey G, Heurteaux C, Lazdunski M. Cloning, functional expression and brain localization of a novel unconventional outward rectifier K⁺ channel. *EMBO J* 15: 6854-6862, 1996.
141. Fink M, Lesage F, Duprat F, Heurteaux C, Reyes R, Fosset M, Lazdunski M. A neuronal two P domain K⁺ channel stimulated by arachidonic acid and polyunsaturated fatty acids. *EMBO J* 17: 3297-3308, 1998.
142. FitzHugh R. An electronic model of the nerve membrane for demonstration purposes. *J Appl Physiol* 21: 305-308, 1966a.
143. FitzHugh R. Theoretical effect of temperature on threshold in the Hodgkin-Huxley nerve model. *J Gen Physiol* 49: 989-1005, 1966b.
144. Fleidervish IA, Lasser-Ross N, Gutnick MJ, Ross WN. Na⁺ imaging reveals little difference in action potential-evoked Na⁺ influx between axon and soma. *Nat Neurosci* 13: 852-860, 2010.
145. Fowler CE, Aryal P, Suen KF, Slesinger PA. Evidence for association of GABA(B) receptors with Kir3 channels and regulators of G protein signalling (RGS4) proteins. *J Physiol* 580: 51-65, 2007.
146. Franceschetti S, Lavazza T, Curia G, Aracri P, Panzica F, Sancini G, Avanzini G, Magistretti J. Na⁺-activated K⁺ current contributes to postexcitatory hyperpolarization in neocortical intrinsically bursting neurons. *J Neurophysiol* 89: 2101-2111, 2003.
147. Franks NP, Honore E. The TREK K2P channels and their role in general anaesthesia and neuroprotection. *Trends Pharmacol Sci* 25: 601-608, 2004.
148. Fukushima N. LPA in neural cell development. *J Cell Biochem* 92: 993-1003, 2004.
149. Ganfornina MD, Lopez-Barneo J. Potassium channel types in arterial chemoreceptor cells and their selective modulation by oxygen. *J Gen Physiol* 100: 401-426, 1992.
150. Geiger JR, Jonas P. Dynamic control of presynaptic Ca(2⁺) inflow by fast-inactivating K(+) channels in hippocampal mossy fiber boutons. *Neuron* 28: 927-939, 2000.
151. Ghatta S, Nimmagadda D, Xu X, O'Rourke ST. Large-conductance, calcium-activated potassium channels: Structural and functional implications. *Pharmacol Ther* 110: 103-116, 2006.
152. Giangiacomo KM, Becker J, Garsky C, Schmalhofer W, Garcia ML, Mullmann TJ. Novel alpha-KTx sites in the BK channel and comparative sequence analysis reveal distinguishing features of the BK and KV channel outer pore. *Cell Biochem Biophys* 52: 47-58, 2008.
153. Giangiacomo KM, Garcia ML, McManus OB. Mechanism of iberitoxin block of the large-conductance calcium-activated potassium channel from bovine aortic smooth muscle. *Biochemistry* 31: 6719-6727, 1992.
154. Gil Z, Magleby KL, Silberberg SD. Membrane-pipette interactions underlie delayed voltage activation of mechanosensitive channels in *Xenopus* oocytes. *Biophys J* 76: 3118-3127, 1999.
155. Glauner KS, Mannuzzu LM, Gandhi CS, Isacoff EY. Spectroscopic mapping of voltage sensor movement in the Shaker potassium channel. *Nature* 402: 813-817, 1999.
156. Gola M, Crest M. Colocalization of active KCa channels and Ca2⁺ channels within Ca2⁺ domains in helix neurons. *Neuron* 10: 689-699, 1993.
157. Goldstein SA, Bayliss DA, Kim D, Lesage F, Plant LD, Rajan S. International Union of Pharmacology. LV. Nomenclature and molecular relationships of two-P potassium channels. *Pharmacol Rev* 57: 527-540, 2005.
158. Goldstein SA, Price LA, Rosenthal DN, Pausch MH. ORK1, a potassium-selective leak channel with two pore domains cloned from *Drosophila melanogaster* by expression in *Saccharomyces cerevisiae*. *Proc Natl Acad Sci U S A* 93: 13256-13261, 1996.
159. Gonzalez-Perez V, Neely A, Tapia C, Gonzalez-Gutierrez G, Contreras G, Orio P, Lagos V, Rojas G, Estevez T, Stack K, Naranjo D. Slow inactivation in Shaker K channels is delayed by intracellular tetraethylammonium. *J Gen Physiol* 132: 633-650, 2008.
160. Gonzalez-Perez V, Stack K, Boric K, Naranjo D. Reduced voltage sensitivity in a K⁺-channel voltage sensor by electric field remodeling. *Proc Natl Acad Sci U S A* 107: 5178-5183.
161. Gonzalez C, Koch HP, Drum BM, Larsson HP. Strong cooperativity between subunits in voltage-gated poron channels. *Nature structural & molecular biology* 17: 51-56, 2010.
162. Gonzalez C, Morera FJ, Rosenmann E, Alvarez O, Latorre R. S3b amino acid residues do not shuttle across the bilayer in voltage-dependent Shaker K⁺ channels. *Proc Natl Acad Sci U S A* 102: 5020-5025, 2005.
163. Gonzalez C, Rosenman E, Bezanilla F, Alvarez O, Latorre R. Modulation of the Shaker K(+) channel gating kinetics by the S3-S4 linker. *J Gen Physiol* 115: 193-208, 2000.
164. Gonzalez C, Rosenman E, Bezanilla F, Alvarez O, Latorre R. Periodic perturbations in Shaker K⁺-channel gating kinetics by deletions in the S3-S4 linker. *Proc Natl Acad Sci U S A* 98: 9617-9623, 2001.
165. Graulich A, Dilly S, Farce A, Scuvée-Moreau J, Waroux O, Lamy C, Chavatte P, Seutin V, Liegeois JF. Synthesis and radioligand binding studies of bis-isoquinolinium derivatives as small conductance Ca(2⁺)-activated K(+) channel blockers. *J Med Chem* 50: 5070-5075, 2007.
166. Graulich A, Lamy C, Alleva L, Dilly S, Chavatte P, Wouters J, Seutin V, Liegeois JF. Bis-tetrahydroisoquinoline derivatives: AG525E1, a new step in the search for non-quaternary non-peptidic small conductance Ca(2⁺)-activated K(+) channel blockers. *Bioorg Med Chem Lett* 18: 3440-3445, 2008.
167. Graulich A, Mercier F, Scuvée-Moreau J, Seutin V, Liegeois JF. Synthesis and biological evaluation of N-methyl-laudanosine iodide analogues as potential SK channel blockers. *Bioorg Med Chem* 13: 1201-1209, 2005.
168. Gribkoff VK, Lum-Ragan JT, Boissard CG, Post-Munson DJ, Meanwell NA, Starrett JE Jr., Kozlowski ES, Romine JL, Trojnecki JT, McKay MC, Zhong J, Dworetzky SI. Effects of channel modulators on cloned large-conductance calcium-activated potassium channels. *Mol Pharmacol* 50: 206-217, 1996.
169. Grimm PR, Foutz RM, Brenner R, Sansom SC. Identification and localization of BK-beta subunits in the distal nephron of the mouse kidney. *Am J Physiol Renal Physiol* 293: F350-F359, 2007.
170. Grimm PR, Sansom SC. BK channels and a new form of hypertension. *Kidney Int* 78: 956-962, 2010.
171. Grissmer S, Nguyen AN, Aiyar J, Hanson DC, Mather RJ, Gutman GA, Karmilowicz MJ, Auperin DD, Chandry KG. Pharmacological characterization of five cloned voltage-gated K⁺ channels, types Kv1.1, 1.2, 1.3, 1.5, and 3.1, stably expressed in mammalian cell lines. *Mol Pharmacol* 45: 1227-1234, 1994.
172. Gross GJ, Auchampach JA. Blockade of ATP-sensitive potassium channels prevents myocardial preconditioning in dogs. *Circ Res* 70: 223-233, 1992.
173. Grunnet M, Jespersen T, Angelo K, Frokjaer-Jensen C, Klaerke DA, Olesen SP, Jensen BS. Pharmacological modulation of SK3 channels. *Neuropharmacology* 40: 879-887, 2001.
174. Grunnet M, Kaufmann WA. Coassembly of big conductance Ca2⁺-activated K⁺ channels and L-type voltage-gated Ca2⁺ channels in rat brain. *J Biol Chem* 279: 36445-36453, 2004.
175. Gu N, Hu H, Vervaeke K, Storm JF. SK (KCa2) channels do not control somatic excitability in CA1 pyramidal neurons but can be activated by dendritic excitatory synapses and regulate their impact. *J Neurophysiol* 100: 2589-2604, 2008.
176. Gu N, Vervaeke K, Hu H, Storm JF. Kv7/KCNQ/M and HCN/h, but not KCa2/SK channels, contribute to the somatic medium after hyperpolarization and excitability control in CA1 hippocampal pyramidal cells. *J Physiol* 566: 689-715, 2005.
177. Gu N, Vervaeke K, Storm JF. BK potassium channels facilitate high-frequency firing and cause early spike frequency adaptation in rat CA1 hippocampal pyramidal cells. *J Physiol* 580: 859-882, 2007.
178. Gumina RJ, Pucar D, Bast P, Hodgson DM, Kurtz CE, Dzeja PP, Miki T, Seino S, Terzic A. Knockout of Kir6.2 negates ischemic preconditioning-induced protection of myocardial energetics. *Am J Physiol Heart Circ Physiol* 284: H2106-H2113, 2003.

179. Guo D, Ramu Y, Klem AM, Lu Z. Mechanism of rectification in inward-rectifier K⁺ channels. *J Gen Physiol* 121: 261-275, 2003.
180. Guo W, Li H, Aimond F, Johns DC, Rhodes KJ, Trimmer JS, Nerbonne JM. Role of heteromultimers in the generation of myocardial transient outward K⁺ currents. *Circ Res* 90: 586-593, 2002.
181. Gutman GA, Chandy KG, Grissmer S, Lazdunski M, McKinnon D, Pardo LA, Robertson GA, Rudy B, Sanguinetti MC, Stuhmer W, Wang X. International Union of Pharmacology. LIII. Nomenclature and molecular relationships of voltage-gated potassium channels. *Pharmacol Rev* 57: 473-508, 2005.
182. Guy HR, Seetharamulu P. Molecular model of the action potential sodium channel. *Proc Natl Acad Sci U S A* 83: 508-512, 1986.
183. Ha TS, Heo MS, Park CS. Functional effects of auxiliary beta4-subunit on rat large-conductance Ca(2+)-activated K(+) channel. *Biophys J* 86: 2871-2882, 2004.
184. Hackos DH, Chang TH, Swartz KJ. Scanning the intracellular S6 activation gate in the shaker K⁺ channel. *J Gen Physiol* 119: 521-532, 2002.
185. Hagiwara S, Miyazaki S, Rosenthal NP. Potassium current and the effect of cesium on this current during anomalous rectification of the egg cell membrane of a starfish. *J Gen Physiol* 67: 621-638, 1976.
186. Hallworth NE, Wilson CJ, Bevan MD. Apamin-sensitive small conductance calcium-activated potassium channels, through their selective coupling to voltage-gated calcium channels, are critical determinants of the precision, pace, and pattern of action potential generation in rat subthalamic nucleus neurons in vitro. *J Neurosci* 23: 7525-7542, 2003.
187. Han J, Kang D, Kim D. Functional properties of four splice variants of a human pancreatic tandem-pore K⁺ channel, TALK-1. *Am J Physiol Cell Physiol* 285: C529-C538, 2003.
188. Han X, Light PE, Giles WR, French RJ. Identification and properties of an ATP-sensitive K⁺ current in rabbit sino-atrial node pacemaker cells. *J Physiol* 490(Pt 2): 337-350, 1996.
189. Hansen RS, Diness TG, Christ T, Demnitz J, Ravens U, Olesen SP, Grunnet M. Activation of human ether-a-go-go-related gene potassium channels by the diphenylurea 1,3-bis-(2-hydroxy-5-trifluoromethylphenyl)-urea (NS1643). *Mol Pharmacol* 69: 266-277, 2006.
190. Haug T, Sigg D, Ciani S, Toro L, Stefani E, Olcese R. Regulation of K⁺ flow by a ring of negative charges in the outer pore of BKCa channels. Part I: Aspartate 292 modulates K⁺ conduction by external surface charge effect. *J Gen Physiol* 124: 173-184, 2004.
191. He C, Zhang H, Mirshahi T, Logothetis DE. Identification of a potassium channel site that interacts with G protein betagamma subunits to mediate agonist-induced signaling. *J Biol Chem* 274: 12517-12524, 1999.
192. Hebert SC, Desir G, Giebisch G, Wang W. Molecular diversity and regulation of renal potassium channels. *Physiol Rev* 85: 319-371, 2005.
193. Heginbotham L, Lu Z, Abramson T, MacKinnon R. Mutations in the K⁺ channel signature sequence. *Biophys J* 66: 1061-1067, 1994.
194. Heginbotham L, MacKinnon R. The aromatic binding site for tetraethylammonium ion on potassium channels. *Neuron* 8: 483-491, 1992.
195. Heinemann SH, Rettig J, Graack HR, Pongs O. Functional characterization of Kv channel beta-subunits from rat brain. *J Physiol* 493(Pt 3): 625-633, 1996.
196. Hermansteyne TO, Kihira Y, Misono K, Deitchler A, Yanagawa Y, Misonou H. Immunolocalization of the voltage-gated potassium channel Kv2.2 in GABAergic neurons in the basal forebrain of rats and mice. *J Comp Neurol* 518: 4298-4310.
197. Hervieu GJ, Cluderay JE, Gray CW, Green PJ, Ranson JL, Randall AD, Meadows HJ. Distribution and expression of TREK-1, a two-pore-domain potassium channel, in the adult rat CNS. *Neuroscience* 103: 899-919, 2001.
198. Hess D, Nanou E, El Manira A. Characterization of Na⁺-activated K⁺ currents in larval lamprey spinal cord neurons. *J Neurophysiol* 97: 3484-3493, 2007.
199. Hess P, Tsien RW. Mechanism of ion permeation through calcium channels. *Nature* 309: 453-456, 1984.
200. Hessa T, White SH, von Heijne G. Membrane insertion of a potassium-channel voltage sensor. *Science* 307: 1427, 2005.
201. Heurteaux C, Guy N, Laigle C, Blondeau N, Duprat F, Mazzuca M, Lang-Lazdunski L, Widmann C, Zanzouri M, Romey G, Lazdunski M. TREK-1, a K⁺ channel involved in neuroprotection and general anesthesia. *EMBO J* 23: 2684-2695, 2004.
202. Hibino H, Fujita A, Iwai K, Yamada M, Kurachi Y. Differential assembly of inwardly rectifying K⁺ channel subunits, Kir4.1 and Kir5.1, in brain astrocytes. *J Biol Chem* 279: 44065-44073, 2004.
203. Hibino H, Inanobe A, Furutani K, Murakami S, Findlay I, Kurachi Y. Inwardly rectifying potassium channels: Their structure, function, and physiological roles. *Physiol Rev* 90: 291-366, 2010.
204. Hibino H, Kurachi Y. Molecular and physiological bases of the K⁺ circulation in the mammalian inner ear. *Physiology (Bethesda)* 21: 336-345, 2006.
205. Hibino H, Nin F, Tsuzuki C, Kurachi Y. How is the highly positive endocochlear potential formed? The specific architecture of the stria vascularis and the roles of the ion-transport apparatus. *Pflugers Arch* 459: 521-533, 2010.
206. Hicks GA, Marrion NV. Ca²⁺-dependent inactivation of large conductance Ca²⁺-activated K⁺ (BK) channels in rat hippocampal neurones produced by pore block from an associated particle. *J Physiol* 508(Pt 3): 721-734, 1998.
207. Ho IH, Murrell-Lagnado RD. Molecular determinants for sodium-dependent activation of G protein-gated K⁺ channels. *J Biol Chem* 274: 8639-8648, 1999.
208. Hodgkin AL, Huxley AF. Currents carried by sodium and potassium ions through the membrane of the giant axon of Loligo. *J Physiol* 116: 449-472, 1952a.
209. Hodgkin AL, Huxley AF. A quantitative description of membrane current and its application to conduction and excitation in nerve. *J Physiol* 117: 500-544, 1952b.
210. Hodgkin AL, Keynes RD. The potassium permeability of a giant nerve fibre. *J Physiol* 128: 61-88, 1955.
211. Holmgren M, Shin KS, Yellen G. The activation gate of a voltage-gated K⁺ channel can be trapped in the open state by an intersubunit metal bridge. *Neuron* 21: 617-621, 1998.
212. Holmgren M, Smith PL, Yellen G. Trapping of organic blockers by closing of voltage-dependent K⁺ channels: Evidence for a trap door mechanism of activation gating. *J Gen Physiol* 109: 527-535, 1997.
213. Honore E. The neuronal background K2P channels: Focus on TREK1. *Nat Rev Neurosci* 8: 251-261, 2007.
214. Honore E, Maingret F, Lazdunski M, Patel AJ. An intracellular proton sensor commands lipid- and mechano-gating of the K(+) channel TREK-1. *EMBO J* 21: 2968-2976, 2002.
215. Horn R. Electrifying phosphatases. *Sci STKE* 2005: pe50, 2005.
216. Horrigan FT, Aldrich RW. Allosteric voltage gating of potassium channels II. Msls channel gating charge movement in the absence of Ca(2+). *J Gen Physiol* 114: 305-336, 1999.
217. Horrigan FT, Aldrich RW. Coupling between voltage sensor activation, Ca²⁺ binding and channel opening in large conductance (BK) potassium channels. *J Gen Physiol* 120: 267-305, 2002.
218. Horrigan FT, Cui J, Aldrich RW. Allosteric voltage gating of potassium channels I. Msls ionic currents in the absence of Ca(2+). *J Gen Physiol* 114: 277-304, 1999.
219. Hoshi T, Zagotta WN, Aldrich RW. Biophysical and molecular mechanisms of Shaker potassium channel inactivation. *Science* 250: 533-538, 1990.
220. Hoshi T, Zagotta WN, Aldrich RW. Shaker potassium channel gating. I: Transitions near the open state. *J Gen Physiol* 103: 249-278, 1994.
221. Hoshi T, Zagotta WN, Aldrich RW. Two types of inactivation in Shaker K⁺ channels: Effects of alterations in the carboxy-terminal region. *Neuron* 7: 547-556, 1991.
222. Hu H, Shao LR, Chavoshy S, Gu N, Trieb M, Behrens R, Laake P, Pongs O, Knaus HG, Ottersen OP, Storm JF. Presynaptic Ca²⁺-activated K⁺ channels in glutamatergic hippocampal terminals and their role in spike repolarization and regulation of transmitter release. *J Neurosci* 21: 9585-9597, 2001.
223. Huang CL, Feng S, Hilgemann DW. Direct activation of inward rectifier potassium channels by PIP2 and its stabilization by Gbetagamma. *Nature* 391: 803-806, 1998.
224. Hugnot JP, Salinas M, Lesage F, Guillemare E, de Weille J, Heurteaux C, Mattei MG, Lazdunski M. Kv8.1, a new neuronal potassium channel subunit with specific inhibitory properties towards Shab and Shaw channels. *EMBO J* 15: 3322-3331, 1996.
225. Ilan N, Goldstein SA, Kenko: Single, cloned potassium leak channels are multi-ion pores. *Biophys J* 80: 241-253, 2001.
226. Inagaki N, Gonoi T, Clement JP, Wang CZ, Aguilar-Bryan L, Bryan J, Seino S. A family of sulfonylurea receptors determines the pharmacological properties of ATP-sensitive K⁺ channels. *Neuron* 16: 1011-1017, 1996.
227. Inagaki N, Gonoi T, Clement JP, Namba N, Inazawa J, Gonzalez G, Aguilar-Bryan L, Seino S, Bryan J. Reconstitution of IKATP: An inward rectifier subunit plus the sulfonylurea receptor. *Science* 270: 1166-1170, 1995.
228. Ishii TM, Maylie J, Adelman JP. Determinants of apamin and d-tubocurarine block in SK potassium channels. *J Biol Chem* 272: 23195-23200, 1997.
229. Islas LD, Sigworth FJ. Voltage sensitivity and gating charge in Shaker and Shab family potassium channels. *J Gen Physiol* 114: 723-742, 1999.
230. Islas LD, Sigworth FJ. Electrostatics and the gating pore of Shaker potassium channels. *J Gen Physiol* 117: 69-89, 2001.
231. Ivanina T, Rishal I, Varon D, Mullner C, Frohner-Steinecke B, Schreibmayer W, Dessauer CW, Dascal N. Mapping the Gbetagamma-binding sites in GIRK1 and GIRK2 subunits of the G protein-activated K⁺ channel. *J Biol Chem* 278: 29174-29183, 2003.

232. Iwanir S, Reuveny E. Adrenaline-induced hyperpolarization of mouse pancreatic islet cells is mediated by G protein-gated inwardly rectifying potassium (GIRK) channels. *Pflügers Arch* 456: 1097-1108, 2008.
233. Jaggar JH, Porter VA, Lederer WJ, Nelson MT. Calcium sparks in smooth muscle. *Am J Physiol Cell Physiol* 278: C235-C256, 2000.
234. Jelacic TM, Kennedy ME, Wickman K, Clapham DE. Functional and biochemical evidence for G-protein-gated inwardly rectifying K⁺ (GIRK) channels composed of GIRK2 and GIRK3. *J Biol Chem* 275: 36211-36216, 2000.
235. Jiang X, Bett GC, Li X, Bondarenko VE, Rasmusson RL. C-type inactivation involves a significant decrease in the intracellular aqueous pore volume of Kv1.4 K⁺ channels expressed in *Xenopus* oocytes. *J Physiol* 549: 683-695, 2003.
236. Jiang Y, Lee A, Chen J, Cadene M, Chait BT, MacKinnon R. Crystal structure and mechanism of a calcium-gated potassium channel. *Nature* 417: 515-522, 2002a.
237. Jiang Y, Lee A, Chen J, Cadene M, Chait BT, MacKinnon R. The open pore conformation of potassium channels. *Nature* 417: 523-526, 2002b.
238. Jiang Y, Lee A, Chen J, Ruta V, Cadene M, Chait BT, MacKinnon R. X-ray structure of a voltage-dependent K⁺ channel. *Nature* 423: 33-41, 2003.
239. Jiang Y, Pico A, Cadene M, Chait BT, MacKinnon R. Structure of the RCK domain from the *E. coli* K⁺ channel and demonstration of its presence in the human BK channel. *Neuron* 29: 593-601, 2001.
240. Jiang Y, Ruta V, Chen J, Lee A, MacKinnon R. The principle of gating charge movement in a voltage-dependent K⁺ channel. *Nature* 423: 42-48, 2003.
241. Jin W, Lu Z. A novel high-affinity inhibitor for inward-rectifier K⁺ channels. *Biochemistry* 37: 13291-13299, 1998.
242. Jin W, Lu Z. Synthesis of a stable form of tertiapin: A high-affinity inhibitor for inward-rectifier K⁺ channels. *Biochemistry* 38: 14286-14293, 1999.
243. Jogini V, Roux B. Dynamics of the Kv1.2 voltage-gated K⁺ channel in a membrane environment. *Biophys J* 93: 3070-3082, 2007.
244. Johansson AC, Lindahl E. Amino-acid solvation structure in transmembrane helices from molecular dynamics simulations. *Biophys J* 91: 4450-4463, 2006.
245. Johnson SW, Seutin V. Bicuculline methiodide potentiates NMDA-dependent burst firing in rat dopamine neurons by blocking apamin-sensitive Ca²⁺-activated K⁺ currents. *Neurosci Lett* 231: 13-16, 1997.
246. Joiner WJ, Khanna R, Schlichter LC, Kaczmarek LK. Calmodulin regulates assembly and trafficking of SK4/IK1 Ca²⁺-activated K⁺ channels. *J Biol Chem* 276: 37980-37985, 2001.
247. Joiner WJ, Tang MD, Wang LY, Dworetzky SI, Boissard CG, Gan L, Gribkoff VK, Kaczmarek LK. Formation of intermediate-conductance calcium-activated potassium channels by interaction of Slack and Slo subunits. *Nat Neurosci* 1: 462-469, 1998.
248. Jones EM, Laus C, Fettplace R. Identification of Ca(2+)-activated K⁺ channel splice variants and their distribution in the turtle cochlea. *Proc Biol Sci* 265: 685-692, 1998.
249. Kalman K, Pennington MW, Lanigan MD, Nguyen A, Rauer H, Mahnir V, Paschetto K, Kem WR, Grissmer S, Gutman GA, Christian EP, Cahalan MD, Norton RS, Chandy KG. ShK-Dap22, a potent Kv1.3-specific immunosuppressive polypeptide. *J Biol Chem* 273: 32697-32707, 1998.
250. Kamb A, Iverson LE, Tanouye MA. Molecular characterization of the Shaker, a *Drosophila* gene that encodes a potassium channel. *Cell* 50: 405-413, 1987.
251. Kameyama M, Kakei M, Sato R, Shibasaki T, Matsuda H, Irisawa H. Intracellular Na⁺ activates a K⁺-channel in mammalian cardiac cells. *Nature* 309: 354-356, 1984.
252. Kane GC, Liu XK, Yamada S, Olson TM, Terzic A. Cardiac KATP channels in health and disease. *J Mol Cell Cardiol* 38: 937-943, 2005.
253. Kang D, Choe C, Kim D. Thermosensitivity of the two-pore domain K⁺ channels TREK-2 and TRAAK. *J Physiol* 564: 103-116, 2005.
254. Kang J, Chen XL, Wang H, Ji J, Cheng H, Incardona J, Reynolds W, Viviani F, Tabart M, Rampe D. Discovery of a small molecule activator of the human ether-a-go-go-related gene (HERG) cardiac K⁺ channel. *Mol Pharmacol* 67: 827-836, 2005.
255. Katz B. Les constantes electriques de la membrane du muscle. *Arch Sci Physiol* 3: 285-299, 1949.
256. Keen JE, Khawaled R, Farrens DL, Neelands T, Rivard A, Bond CT, Janowsky A, Fakler B, Adelman JP, Maylie J. Domains responsible for constitutive and Ca(2+)-dependent interactions between calmodulin and small conductance Ca(2+)-activated potassium channels. *J Neurosci* 19: 8830-8838, 1999.
257. Ketchum KA, Joiner WJ, Sellers AJ, Kaczmarek LK, Goldstein SA. A new family of outwardly rectifying potassium channel proteins with two pore domains in tandem. *Nature* 376: 690-695, 1995.
258. Keynes RD, Rojas E. Kinetics and steady-state properties of the charged system controlling sodium conductance in the squid giant axon. *J Physiol* 239: 393-434, 1974.
259. Kihira Y, Hermansteyne TO, Misonou H. Formation of heteromeric Kv2 channels in mammalian brain neurons. *J Biol Chem* 285: 15048-15055.
260. Kim D. Fatty acid-sensitive two-pore domain K⁺ channels. *Trends Pharmacol Sci* 24: 648-654, 2003.
261. Kim D, Clapham DE. Potassium channels in cardiac cells activated by arachidonic acid and phospholipids. *Science* 244: 1174-1176, 1989.
262. Kim D, Fujita A, Horio Y, Kurachi Y. Cloning and functional expression of a novel cardiac two-pore background K⁺ channel (cTBK-1). *Circ Res* 82: 513-518, 1998.
263. Kim Y, Bang H, Kim D. TASK-3, a new member of the tandem pore K(+) channel family. *J Biol Chem* 275: 9340-9347, 2000.
264. Kim Y, Gnatenco C, Bang H, Kim D. Localization of TREK-2 K⁺ channel domains that regulate channel kinetics and sensitivity to pressure, fatty acids and pH. *Pflügers Arch* 442: 952-960, 2001.
265. Klement G, Nilsson J, Arhem P, Elinder F. A tyrosine substitution in the cavity wall of a k channel induces an inverted inactivation. *Biophys J* 94: 3014-3022, 2008.
266. Klemic KG, Kirsch GE, Jones SW. U-type inactivation of Kv3.1 and Shaker potassium channels. *Biophys J* 81: 814-826, 2001.
267. Knaus HG, Folander K, Garcia-Calvo M, Garcia ML, Kaczorowski GJ, Smith M, Swanson R. Primary sequence and immunological characterization of beta-subunit of high conductance Ca(2+)-activated K⁺ channel from smooth muscle. *J Biol Chem* 269: 17274-17278, 1994.
268. Knot HJ, Zimmermann PA, Nelson MT. Extracellular K(+) induced hyperpolarizations and dilatations of rat coronary and cerebral arteries involve inward rectifier K(+) channels. *J Physiol* 492(Pt 2): 419-430, 1996.
269. Kobrinisky E, Mirshahi T, Zhang H, Jin T, Logothetis DE. Receptor-mediated hydrolysis of plasma membrane messenger PIP2 leads to K⁺-current desensitization. *Nat Cell Biol* 2: 507-514, 2000.
270. Kofuji P, Davidson N, Lester HA. Evidence that neuronal G-protein-gated inwardly rectifying K⁺ channels are activated by G beta gamma subunits and function as heteromultimers. *Proc Natl Acad Sci U S A* 92: 6542-6546, 1995.
271. Kohler M, Hirschberg B, Bond CT, Kinzie JM, Marrion NV, Maylie J, Adelman JP. Small-conductance, calcium-activated potassium channels from mammalian brain. *Science* 273: 1709-1714, 1996.
272. Kole MH, Ilsechner SU, Kampa BM, Williams SR, Ruben PC, Stuart GJ. Action potential generation requires a high sodium channel density in the axon initial segment. *Nat Neurosci* 11: 178-186, 2008.
273. Kollwe A, Lau AY, Sullivan A, Roux B, Goldstein SA. A structural model for K2P potassium channels based on 23 pairs of interacting sites and continuum electrostatics. *J Gen Physiol* 134: 53-68, 2009.
274. Koval OM, Fan Y, Rothberg BS. A role for the S0 transmembrane segment in voltage-dependent gating of BK channels. *J Gen Physiol* 129: 209-220, 2007.
275. Koyrakh L, Lujan R, Colon J, Karschin C, Kurachi Y, Karschin A, Wickman K. Molecular and cellular diversity of neuronal G-protein-gated potassium channels. *J Neurosci* 25: 11468-11478, 2005.
276. Krapivinsky G, Gordon EA, Wickman K, Velimirovic B, Krapivinsky L, Clapham DE. The G-protein-gated atrial K⁺ channel IKACH is a heteromultimer of two inwardly rectifying K(+) channel proteins. *Nature* 374: 135-141, 1995.
277. Krapivinsky G, Medina I, Eng L, Krapivinsky L, Yang Y, Clapham DE. A novel inward rectifier K⁺ channel with unique pore properties. *Neuron* 20: 995-1005, 1998.
278. Krepiy D, Mihailescu M, Freites JA, Schow EV, Worcester DL, Gawrisch K, Tobias DJ, White SH, Swartz KJ. Structure and hydration of membranes embedded with voltage-sensing domains. *Nature* 462: 473-479, 2009.
279. Kreusch A, Pfaffinger PJ, Stevens CF, Choe S. Crystal structure of the tetramerization domain of the Shaker potassium channel. *Nature* 392: 945-948, 1998.
280. Kubo Y, Adelman JP, Clapham DE, Jan LY, Karschin A, Kurachi Y, Lazdunski M, Nichols CG, Seino S, Vandenberg CA. International Union of Pharmacology. LIV. Nomenclature and molecular relationships of inwardly rectifying potassium channels. *Pharmacol Rev* 57: 509-526, 2005.
281. Kubo Y, Murata Y. Control of rectification and permeation by two distinct sites after the second transmembrane region in Kir2.1 K⁺ channel. *J Physiol* 531: 645-660, 2001.
282. Kung C. A possible unifying principle for mechanosensation. *Nature* 436: 647-654, 2005.
283. Kunkel MT, Peralta EG. Identification of domains conferring G protein regulation on inward rectifier potassium channels. *Cell* 83: 443-449, 1995.
284. Kuo A, Gulbis JM, Antcliff JF, Rahman T, Lowe ED, Zimmer J, Cuthbertson J, Ashcroft FM, Ezaki T, Doyle DA. Crystal structure of the potassium channel KirBac1.1 in the closed state. *Science* 300: 1922-1926, 2003.
285. Kurachi Y, Ito H, Sugimoto T, Katada T, Ui M. Activation of atrial muscarinic K⁺ channels by low concentrations of beta gamma subunits of rat brain G protein. *Pflügers Arch* 413: 325-327, 1989.

286. Kurachi Y, Nakajima T, Sugimoto T. On the mechanism of activation of muscarinic K⁺ channels by adenosine in isolated atrial cells: Involvement of GTP-binding proteins. *Pflügers Arch* 407: 264-274, 1986.
287. Kurata HT, Doerksen KW, Eldstrom JR, Rezazadeh S, Fedida D. Separation of P/C- and U-type inactivation pathways in Kv1.5 potassium channels. *J Physiol* 568: 31-46, 2005.
288. Kwan HY, Leung PC, Huang Y, Yao X. Depletion of intracellular Ca²⁺ stores sensitizes the flow-induced Ca²⁺ influx in rat endothelial cells. *Circ Res* 92: 286-292, 2003.
289. Lagrutta A, Shen KZ, North RA, Adelman JP. Functional differences among alternatively spliced variants of Slowpoke, a Drosophila calcium-activated potassium channel. *J Biol Chem* 269: 20347-20351, 1994.
290. Lancaster B, Nicoll RA. Properties of two calcium-activated hyperpolarizations in rat hippocampal neurones. *J Physiol* 389: 187-203, 1987.
291. Langer P, Grunder S, Rusch A. Expression of Ca²⁺-activated BK channel mRNA and its splice variants in the rat cochlea. *J Comp Neurol* 455: 198-209, 2003.
292. Larsen AP, Bentzen BH, Grunnet M. Differential effects of Kv11.1 activators on Kv11.1a, Kv11.1b and Kv11.1a/Kv11.1b channels. *Br J Pharmacol* 161: 614-628, 2010.
293. Larsson HP, Baker OS, Dhillon DS, Isacoff EY. Transmembrane movement of the shaker K⁺ channel S4. *Neuron* 16: 387-397, 1996.
294. Larsson HP, Elinder F. A conserved glutamate is important for slow inactivation in K⁺ channels. *Neuron* 27: 573-583, 2000.
295. Latorre R, Morera FJ, Zaelzer C. Allosteric interactions and the modular nature of the voltage- and Ca²⁺-activated (BK) channel. *J Physiol* 588: 3141-3148, 2010.
296. Latorre R, Vergara C, Hidalgo C. Reconstitution in planar lipid bilayers of a Ca²⁺-dependent K⁺ channel from transverse tubule membranes isolated from rabbit skeletal muscle. *Proc Natl Acad Sci U S A* 79: 805-809, 1982.
297. Ledoux J, Werner ME, Brayden JE, Nelson MT. Calcium-activated potassium channels and the regulation of vascular tone. *Physiology (Bethesda)* 21: 69-78, 2006.
298. Lee K, Dixon AK, Richardson PJ, Pinnock RD. Glucose-receptive neurones in the rat ventromedial hypothalamus express KATP channels composed of Kir6.1 and SUR1 subunits. *J Physiol* 515(Pt 2): 439-452, 1999.
299. Lee SY, Banerjee A, MacKinnon R. Two separate interfaces between the voltage sensor and pore are required for the function of voltage-dependent K⁺ channels. *PLoS Biol* 7: e47, 2009.
300. Lee WS, Ngo-Anh TJ, Bruening-Wright A, Maylie J, Adelman JP. Small conductance Ca²⁺-activated K⁺ channels and calmodulin: Cell surface expression and gating. *J Biol Chem* 278: 25940-25946, 2003.
301. Lei Q, Talley EM, Bayliss DA. Receptor-mediated inhibition of G protein-coupled inwardly rectifying potassium channels involves G(alpha)q family subunits, phospholipase C, and a readily diffusible messenger. *J Biol Chem* 276: 16720-16730, 2001.
302. Leonoudakis D, Gray AT, Winegar BD, Kindler CH, Harada M, Taylor DM, Chavez RA, Forsayeth JR, Yost CS. An open rectifier potassium channel with two pore domains in tandem cloned from rat cerebellum. *J Neurosci* 18: 868-877, 1998.
303. Lesage F, Guillemare E, Fink M, Duprat F, Heurteaux C, Fosset M, Romey G, Barhanin J, Lazdunski M. Molecular properties of neuronal G-protein-activated inwardly rectifying K⁺ channels. *J Biol Chem* 270: 28660-28667, 1995.
304. Lesage F, Guillemare E, Fink M, Duprat F, Lazdunski M, Romey G, Barhanin J, TWIK-1, a ubiquitous human weakly inward rectifying K⁺ channel with a novel structure. *EMBO J* 15: 1004-1011, 1996.
305. Lesage F, Lazdunski M. Molecular and functional properties of two-pore-domain potassium channels. *Am J Physiol Renal Physiol* 279: F793-F801, 2000.
306. Lesage F, Reyes R, Fink M, Duprat F, Guillemare E, Lazdunski M. Dimerization of TWIK-1 K⁺ channel subunits via a disulfide bridge. *EMBO J* 15: 6400-6407, 1996.
307. Li-Smerin Y, Hackos DH, Swartz KJ. alpha-helical structural elements within the voltage-sensing domains of a K⁺ channel. *J Gen Physiol* 115: 33-50, 2000.
308. Li M, Jan YN, Jan LY. Specification of subunit assembly by the hydrophilic amino-terminal domain of the Shaker potassium channel. *Science* 257: 1225-1230, 1992.
309. Li W, Gao SB, Lv CX, Wu Y, Guo ZH, Ding JP, Xu T. Characterization of voltage- and Ca²⁺-activated K⁺ channels in rat dorsal root ganglion neurons. *J Cell Physiol* 122: 348-357, 2007.
310. Lichter-Konecki U, Mangin JM, Gordish-Dressman H, Hoffman EP, Gallo V. Gene expression profiling of astrocytes from hyperammonemic mice reveals altered pathways for water and potassium homeostasis in vivo. *Glia* 56: 365-377, 2008.
311. Liman ER, Tytgat J, Hess P. Subunit stoichiometry of a mammalian K⁺ channel determined by construction of multimeric cDNAs. *Neuron* 9: 861-871, 1992.
312. Liu G, Zakharov SI, Yang L, Deng SX, Landry DW, Karlin A, Marx SO. Position and role of the BK channel alpha subunit S0 helix inferred from disulfide crosslinking. *J Gen Physiol* 131: 537-548, 2008.
313. Liu Y, Holmgren M, Jurman ME, Yellen G. Gated access to the pore of a voltage-dependent K⁺ channel. *Neuron* 19: 175-184, 1997.
314. Lodge NJ, Li YW. Ion channels as potential targets for the treatment of depression. *Curr Opin Drug Discov Devel* 11: 633-641, 2008.
315. Logothetis DE, Kurachi Y, Galper J, Neer EJ, Clapham DE. The beta gamma subunits of GTP-binding proteins activate the muscarinic K⁺ channel in heart. *Nature* 325: 321-326, 1987.
316. Long SB, Campbell EB, MacKinnon R. Crystal structure of a mammalian voltage-dependent Shaker family K⁺ channel. *Science* 309: 897-903, 2005a.
317. Long SB, Campbell EB, MacKinnon R. Voltage sensor of Kv1.2: Structural basis of electromechanical coupling. *Science* 309: 903-908, 2005b.
318. Long SB, Tao X, Campbell EB, MacKinnon R. Atomic structure of a voltage-dependent K⁺ channel in a lipid membrane-like environment. *Nature* 450: 376-382, 2007.
319. Lopatin AN, Makhina EN, Nichols CG. Potassium channel block by cytoplasmic polyamines as the mechanism of intrinsic rectification. *Nature* 372: 366-369, 1994.
320. Lopatin AN, Makhina EN, Nichols CG. The mechanism of inward rectification of potassium channels: "Long-pore plugging" by cytoplasmic polyamines. *J Gen Physiol* 106: 923-955, 1995.
321. Lopatin AN, Nichols CG. [K⁺] dependence of open-channel conductance in cloned inward rectifier potassium channels (IRK1, Kir2.1). *Biophys J* 71: 682-694, 1996.
322. Lopes CM, Gallagher PG, Buck ME, Butler MH, Goldstein SA. Proton block and voltage gating are potassium-dependent in the cardiac leak channel Kcnk3. *J Biol Chem* 275: 16969-16978, 2000.
323. Lopes CM, Zhang H, Rohacs T, Jin T, Yang J, Logothetis DE. Alterations in conserved Kir channel-PIP2 interactions underlie channelopathies. *Neuron* 34: 933-944, 2002.
324. Lopez-Barneo J, Hoshi T, Heinemann SH, Aldrich RW. Effects of external cations and mutations in the pore region on C-type inactivation of Shaker potassium channels. *Receptors Channels* 1: 61-71, 1993.
325. Lu Z. Mechanism of rectification in inward-rectifier K⁺ channels. *Annu Rev Physiol* 66: 103-129, 2004.
326. Lu Z, Klem AM, Ramu Y. Ion conduction pore is conserved among potassium channels. *Nature* 413: 809-813, 2001.
327. Lu Z, Klem AM, Ramu Y. Coupling between voltage sensors and activation gate in voltage-gated K⁺ channels. *J Gen Physiol* 120: 663-676, 2002.
328. Lu Z, MacKinnon R. Electrostatic tuning of Mg²⁺ affinity in an inward-rectifier K⁺ channel. *Nature* 371: 243-246, 1994.
329. Lu Z, MacKinnon R. Probing a potassium channel pore with an engineered protonatable site. *Biochemistry* 34: 13133-13138, 1995.
330. Lujan R, Maylie J, Adelman JP. New sites of action for GIRK and SK channels. *Nat Rev Neurosci* 10: 475-480, 2009.
331. Luscher C, Jan LY, Stoffel M, Malenka RC, Nicoll RA. G protein-coupled inwardly rectifying K⁺ channels (GIRKs) mediate postsynaptic but not presynaptic transmitter actions in hippocampal neurons. *Neuron* 19: 687-695, 1997.
332. Luscher C, Slesinger PA. Emerging roles for G protein-gated inwardly rectifying potassium (GIRK) channels in health and disease. *Nat Rev Neurosci* 11: 301-315, 2010.
333. Lv C, Chen M, Gan G, Wang L, Xu T, Ding J. Four-turn alpha-helical segment prevents surface expression of the auxiliary hbeta2 subunit of BK-type channel. *J Biol Chem* 283: 2709-2715, 2008.
334. Ma D, Tang XD, Rogers TB, Welling PA. An andersen-Tawil syndrome mutation in Kir2.1 (V302M) alters the G-loop cytoplasmic K⁺ conduction pathway. *J Biol Chem* 282: 5781-5789, 2007.
335. Ma M, Koester J. The role of K⁺ currents in frequency-dependent spike broadening in Aplysia R20 neurons: A dynamic-clamp analysis. *J Neurosci* 16: 4089-4101, 1996.
336. Ma Z, Lou XJ, Horrigan FT. Role of charged residues in the S1-S4 voltage sensor of BK channels. *J Gen Physiol* 127: 309-328, 2006.
337. MacKinnon R. Determination of the subunit stoichiometry of a voltage-activated potassium channel. *Nature* 350: 232-235, 1991.
338. MacKinnon R. Structural biology. Membrane protein insertion and stability. *Science* 307: 1425-1426, 2005.
339. MacKinnon R, Miller C. Mutant potassium channels with altered binding of charybdotoxin, a pore-blocking peptide inhibitor. *Science* 245: 1382-1385, 1989.
340. Magleby KL. Gating mechanism of BK (Slo1) channels: So near, yet so far. *J Gen Physiol* 121: 81-96, 2003.
341. Maher BJ, MacKinnon RL II, Bai J, Chapman ER, Kelly PT. Activation of postsynaptic Ca(2+) stores modulates glutamate receptor cycling in hippocampal neurons. *J Neurophysiol* 93: 178-188, 2005.
342. Maingret F, Honore E, Lazdunski M, Patel AJ. Molecular basis of the voltage-dependent gating of TREK-1, a mechano-sensitive K⁺ channel. *Biochem Biophys Res Commun* 292: 339-346, 2002.

343. Maingret F, Lauritzen I, Patel AJ, Heurteaux C, Reyes R, Lesage F, Lazdunski M, Honore E. TREK-1 is a heat-activated background K⁺ channel. *EMBO J* 19: 2483-2491, 2000.
344. Maingret F, Patel AJ, Lesage F, Lazdunski M, Honore E. Lysophospholipids open the two-pore domain mechano-gated K⁺ channels TREK-1 and TRAAK. *J Biol Chem* 275: 10128-10133, 2000.
345. Maingret F, Patel AJ, Lesage F, Lazdunski M, Honore E. Mechano- or acid stimulation, two interactive modes of activation of the TREK-1 potassium channel. *J Biol Chem* 274: 26691-26696, 1999.
346. Malin SA, Nerbonne JM. Delayed rectifier K⁺ currents, IK, are encoded by Kv2 alpha-subunits and regulate tonic firing in mammalian sympathetic neurons. *J Neurosci* 22: 10094-10105, 2002.
347. Mao J, Wang X, Chen F, Wang R, Rojas A, Shi Y, Piao H, Jiang C. Molecular basis for the inhibition of G protein-coupled inward rectifier K⁺ channels by protein kinase C. *Proc Natl Acad Sci U S A* 101: 1087-1092, 2004.
348. Marcantoni A, Vandaal DH, Mahapatra S, Carabelli V, Sinnegger-Brauns MJ, Striessnig J, Carbone E. Loss of Cav1.3 channels reveals the critical role of L-type and BK channel coupling in pacemaking mouse adrenal chromaffin cells. *J Neurosci* 30: 491-504, 2010.
349. Marcotti W, Johnson SL, Kros CJ. A transiently expressed SK current sustains and modulates action potential activity in immature mouse inner hair cells. *J Physiol* 560: 691-708, 2004.
350. Marcus DC, Wu T, Wangemann P, Kofuji P. KCNJ10 (Kir4.1) potassium channel knockout abolishes endocochlear potential. *Am J Physiol Cell Physiol* 282: C403-C407, 2002.
351. Marrión NV, Tavalin SJ. Selective activation of Ca²⁺-activated K⁺ channels by co-localized Ca²⁺ channels in hippocampal neurons. *Nature* 395: 900-905, 1998.
352. Martin GE, Hendrickson LM, Penta KL, Friesen RM, Pietrzykowski AZ, Tapper AR, Treisman SN. Identification of a BK channel auxiliary protein controlling molecular and behavioral tolerance to alcohol. *Proc Natl Acad Sci U S A* 105: 17543-17548, 2008.
353. Martina M, Yao GL, Bean BP. Properties and functional role of voltage-dependent potassium channels in dendrites of rat cerebellar Purkinje neurons. *J Neurosci* 23: 5698-5707, 2003.
354. Martinac B. Mechanosensitive ion channels: Molecules of mechanotransduction. *J Cell Sci* 117: 2449-2460, 2004.
355. Martinez-Lopez P, Santi CM, Trevino CL, Ocampo-Gutierrez AY, Acevedo JJ, Alisio A, Salkoff LB, Darszon A. Mouse sperm K⁺ currents stimulated by pH and cAMP possibly coded by Slo3 channels. *Biochem Biophys Res Commun* 381: 204-209, 2009.
356. Marty A. Ca-dependent K channels with large unitary conductance in chromaffin cell membranes. *Nature* 291: 497-500, 1981.
357. Mathur R, Zheng J, Yan Y, Sigworth FJ. Role of the S3-S4 linker in Shaker potassium channel activation. *J Gen Physiol* 109: 191-199, 1997.
358. Matsuda H, Saigusa A, Irisawa H. Ohmic conductance through the inwardly rectifying K channel and blocking by internal Mg²⁺. *Nature* 325: 156-159, 1987.
359. Maylie J, Bond CT, Herson PS, Lee WS, Adelman JP. Small conductance Ca²⁺-activated K⁺ channels and calmodulin. *J Physiol* 554: 255-261, 2004.
360. McCobb DP, Fowler NL, Featherstone T, Lingle CJ, Saito M, Krause JE, Salkoff L. A human calcium-activated potassium channel gene expressed in vascular smooth muscle. *Am J Physiol* 269: H767-H777, 1995.
361. McManus OB, Blatz AL, Magleby KL. Inverse relationship of the durations of adjacent open and shut intervals for C1 and K channels. *Nature* 317: 625-627, 1985.
362. Medhurst AD, Rennie G, Chapman CG, Meadows H, Duckworth MD, Kelsell RE, Gloger, II, Pangalos MN. Distribution analysis of human two pore domain potassium channels in tissues of the central nervous system and periphery. *Brain Res Mol Brain Res* 86: 101-114, 2001.
363. Medina I, Krapivinsky G, Arnold S, Kovoor P, Krapivinsky L, Clapham DE. A switch mechanism for G beta gamma activation of I(KACh). *J Biol Chem* 275: 29709-29716, 2000.
364. Meera P, Wallner M, Song M, Toro L. Large conductance voltage- and calcium-dependent K⁺ channel, a distinct member of voltage-dependent ion channels with seven N-terminal transmembrane segments (S0-S6), an extracellular N terminus, and an intracellular (S9-S10) C terminus. *Proc Natl Acad Sci U S A* 94: 14066-14071, 1997.
365. Meera P, Wallner M, Toro L. A neuronal beta subunit (KCMB4) makes the large conductance, voltage- and Ca²⁺-activated K⁺ channel resistant to charybdotoxin and iberiotoxin. *Proc Natl Acad Sci U S A* 97: 5562-5567, 2000.
366. Mi H, Deerinck TJ, Jones M, Ellisman MH, Schwarz TL. Inwardly rectifying K⁺ channels that may participate in K⁺ buffering are localized in microvilli of Schwann cells. *J Neurosci* 16: 2421-2429, 1996.
367. Mikhailov MV, Campbell JD, de Wet H, Shimomura K, Zadek B, Collins RF, Sansom MS, Ford RC, Ashcroft FM. 3-D structural and functional characterization of the purified KATP channel complex Kir6.2-SUR1. *EMBO J* 24: 4166-4175, 2005.
368. Miki T, Liss B, Minami K, Shiuchi T, Saraya A, Kashima Y, Horiuchi M, Ashcroft F, Minokoshi Y, Roeper J, Seino S. ATP-sensitive K⁺ channels in the hypothalamus are essential for the maintenance of glucose homeostasis. *Nat Neurosci* 4: 507-512, 2001.
369. Miller C. See potassium run. *Nature* 414: 23-24, 2001.
370. Miller C, Moczydlowski E, Latorre R, Phillips M. Charybdotoxin, a protein inhibitor of single Ca²⁺-activated K⁺ channels from mammalian skeletal muscle. *Nature* 313: 316-318, 1985.
371. Miranda-Rottmann S, Kozlov AS, Hudspeth AJ. Highly specific alternative splicing of transcripts encoding BK channels in the chicken's cochlea is a minor determinant of the tonotopic gradient. *Mol Cell Biol* 30: 3646-3660, 2010.
372. Mohapatra DP, Park KS, Trimmer JS. Dynamic regulation of the voltage-gated Kv2.1 potassium channel by multisite phosphorylation. *Biochem Soc Trans* 35: 1064-1068, 2007.
373. Molina A, Castellano AG, Lopez-Barneo J. Pore mutations in Shaker K⁺ channels distinguish between the sites of tetraethylammonium blockade and C-type inactivation. *J Physiol* 499(Pt 2): 361-367, 1997.
374. Monaghan AS, Benton DC, Bahia PK, Hosseini R, Shah YA, Haylett DG, Moss GW. The SK3 subunit of small conductance Ca²⁺-activated K⁺ channels interacts with both SK1 and SK2 subunits in a heterologous expression system. *J Biol Chem* 279: 1003-1009, 2004.
375. Morais-Cabral JH, Zhou Y, MacKinnon R. Energetic optimization of ion conduction rate by the K⁺ selectivity filter. *Nature* 414: 37-42, 2001.
376. Morrow JP, Zakharov SI, Liu G, Yang L, Sok AJ, Marx SO. Defining the BK channel domains required for beta1-subunit modulation. *Proc Natl Acad Sci U S A* 103: 5096-5101, 2006.
377. Moulton G, Attwood TK, Parry-Smith DJ, Packer JC. Phylogenomic analysis and evolution of the potassium channel gene family. *Receptors Channels* 9: 363-377, 2003.
378. Mullins FM, Stepanovic SZ, Desai RR, George AL Jr., Balser JR. Extracellular sodium interacts with the HERG channel at an outer pore site. *J Gen Physiol* 120: 517-537, 2002.
379. Mullmann TJ, Munujos P, Garcia ML, Giangiacomo KM. Electrostatic mutations in iberiotoxin as a unique tool for probing the electrostatic structure of the maxi-K channel outer vestibule. *Biochemistry* 38: 2395-2402, 1999.
380. Mullner C, Vorobiov D, Bera AK, Uezono Y, Yakubovich D, Frohnwieser-Steinecker B, Dascal N, Schreibmayer W. Heterologous facilitation of G protein-activated K⁺ channels by beta-adrenergic stimulation via cAMP-dependent protein kinase. *J Gen Physiol* 115: 547-558, 2000.
381. Murakoshi H, Trimmer JS. Identification of the Kv2.1 K⁺ channel as a major component of the delayed rectifier K⁺ current in rat hippocampal neurons. *J Neurosci* 19: 1728-1735, 1999.
382. Murata Y, Iwasaki H, Sasaki M, Inaba K, Okamura Y. Phosphoinositide phosphatase activity coupled to an intrinsic voltage sensor. *Nature* 435: 1239-1243, 2005.
383. Murthy SR, Teodorescu G, Nijholt IM, Dolga AM, Grissmer S, Spiess J, Blank T. Identification and characterization of a novel, shorter isoform of the small conductance Ca²⁺-activated K⁺ channel SK2. *J Neurochem* 106: 2312-2321, 2008.
384. Nanou E, El Manira A. A postsynaptic negative feedback mediated by coupling between AMPA receptors and Na⁺-activated K⁺ channels in spinal cord neurones. *Eur J Neurosci* 25: 445-450, 2007.
385. Naranjo D, Latorre R. Ion conduction in substates of the batrachotoxin-modified Na⁺ channel from toad skeletal muscle. *Biophys J* 64: 1038-1050, 1993.
386. Nassar-Gentina V, Pollard HB, Rojas E. Electrical activity in chromaffin cells of intact mouse adrenal gland. *Am J Physiol* 254: C675-C683, 1988.
387. Navarro B, Kirichok Y, Clapham DE. KSper, a pH-sensitive K⁺ current that controls sperm membrane potential. *Proc Natl Acad Sci U S A* 104: 7688-7692, 2007.
388. Neusch C, Papadopoulos N, Muller M, Maletzki I, Winter SM, Hirrlinger J, Handschuh M, Bahr M, Richter DW, Kirchhoff F, Hulsman S. Lack of the Kir4.1 channel subunit abolishes K⁺ buffering properties of astrocytes in the ventral respiratory group: Impact on extracellular K⁺ regulation. *J Neurophysiol* 95: 1843-1852, 2006.
389. Newman EA. Regional specialization of retinal glial cell membrane. *Nature* 309: 155-157, 1984.
390. Nichols CG, Lederer WJ. Adenosine triphosphate-sensitive potassium channels in the cardiovascular system. *Am J Physiol* 261: H1675-H1686, 1991.
391. Niemeyer MI, Gonzalez-Nilo FD, Zuniga L, Gonzalez W, Cid LP, Sepulveda FV. Neutralization of a single arginine residue gates open a two-pore domain, alkali-activated K⁺ channel. *Proc Natl Acad Sci U S A* 104: 666-671, 2007.
392. Nimigean CM, Magleby KL. Functional coupling of the beta(1) subunit to the large conductance Ca(2+)-activated K(+) channel in the absence of Ca(2+). Increased Ca(2+) sensitivity from a Ca(2+)-independent mechanism. *J Gen Physiol* 115: 719-736, 2000.

393. Nin F, Hibino H, Doi K, Suzuki T, Hisa Y, Kurachi Y. The endocochlear potential depends on two K⁺ diffusion potentials and an electrical barrier in the stria vascularis of the inner ear. *Proc Natl Acad Sci U S A* 105: 1751-1756, 2008.
394. Nishida M, Cadene M, Chait BT, MacKinnon R. Crystal structure of a Kir3.1-prokaryotic Kir channel chimera. *EMBO J* 26: 4005-4015, 2007.
395. Nishida M, MacKinnon R. Structural basis of inward rectification: Cytoplasmic pore of the G protein-gated inward rectifier GIRK1 at 1.8 Å resolution. *Cell* 111: 957-965, 2002.
396. Niu X, Magleby KL. Stepwise contribution of each subunit to the cooperative activation of BK channels by Ca²⁺. *Proc Natl Acad Sci U S A* 99: 11441-11446, 2002.
397. Niu X, Qian X, Magleby KL. Linker-gating ring complex as passive spring and Ca(2+)-dependent machine for a voltage- and Ca(2+)-activated potassium channel. *Neuron* 42: 745-756, 2004.
398. Noda M, Shimizu S, Tanabe T, Takai T, Kayano T, Ikeda T, Takahashi H, Nakayama H, Kanaoka Y, Minamino N, et al. Primary structure of Electrophorus electricus sodium channel deduced from cDNA sequence. *Nature* 312: 121-127, 1984.
399. Noma A. ATP-regulated K⁺ channels in cardiac muscle. *Nature* 305: 147-148, 1983.
400. Nuwer MO, Picchione KE, Bhattacharjee A. PKA-induced internalization of slack KNa channels produces dorsal root ganglion neuron hyperexcitability. *J Neurosci* 30: 14165-14172, 2010.
401. Okamura Y. Biodiversity of voltage sensor domain proteins. *Pflugers Arch* 454: 361-371, 2007.
402. Olcese R, Latorre R, Toro L, Bezanilla F, Stefani E. Correlation between charge movement and ionic current during slow inactivation in Shaker K⁺ channels. *J Gen Physiol* 110: 579-589, 1997.
403. Olesen SP, Munch E, Moldt P, Drejer J. Selective activation of Ca(2+)-dependent K⁺ channels by novel benzimidazolone. *Eur J Pharmacol* 251: 53-59, 1994.
404. Oliva C, Gonzalez V, Naranjo D. Slow inactivation in voltage gated potassium channels is insensitive to the binding of pore occluding peptide toxins. *Biophys J* 89: 1009-1019, 2005.
405. Ordway RW, Walsh JV Jr., Singer JJ. Arachidonic acid and other fatty acids directly activate potassium channels in smooth muscle cells. *Science* 244: 1176-1179, 1989.
406. Orio P, Latorre R. Differential effects of beta 1 and beta 2 subunits on BK channel activity. *J Gen Physiol* 125: 395-411, 2005.
407. Orio P, Rojas P, Ferreira G, Latorre R. New disguises for an old channel: MaxiK channel beta-subunits. *News Physiol Sci* 17: 156-161, 2002.
408. Ottuschytsch N, Raes A, Van Hoorick D, Snyders DJ. Obligatory heterotetramerization of three previously uncharacterized Kv channel alpha-subunits identified in the human genome. *Proc Natl Acad Sci U S A* 99: 7986-7991, 2002.
409. Pallotta BS, Magleby KL, Barrett JN. Single channel recordings of Ca²⁺-activated K⁺ currents in rat muscle cell culture. *Nature* 293: 471-474, 1981.
410. Pantazis A, Gudzenko V, Savalli N, Sigg D, Olcese R. Operation of the voltage sensor of a human voltage- and Ca²⁺-activated K⁺ channel. *Proc Natl Acad Sci U S A* 107: 4459-4464, 2010.
411. Pantazis A, Kohanteb AP, Olcese R. Relative motion of transmembrane segments S0 and S4 during voltage sensor activation in the human BK(Ca) channel. *J Gen Physiol* 136: 645-657, 2010.
412. Papazian DM, Schwarz TL, Tempel BL, Jan YN, Jan LY. Cloning of genomic and complementary DNA from Shaker, a putative potassium channel gene from Drosophila. *Science* 237: 749-753, 1987.
413. Pardo LA, Suhmer W. Eag1 as a cancer target. *Expert Opin Ther Targets* 12: 837-843, 2008.
414. Park CS, Miller C. Interaction of charybdotoxin with permeant ions inside the pore of a K⁺ channel. *Neuron* 9: 307-313, 1992a.
415. Park CS, Miller C. Mapping function to structure in a channel-blocking peptide: Electrostatic mutants of charybdotoxin. *Biochemistry* 31: 7749-7755, 1992b.
416. Park YB. Ion selectivity and gating of small conductance Ca(2+)-activated K⁺ channels in cultured rat adrenal chromaffin cells. *J Physiol* 481(Pt 3): 555-570, 1994.
417. Patel AJ, Honore E. Molecular physiology of oxygen-sensitive potassium channels. *Eur Respir J* 18: 221-227, 2001.
418. Patel AJ, Honore E, Maingret F, Lesage F, Fink M, Duprat F, Lazdunski M. A mammalian two pore domain mechano-gated S-like K⁺ channel. *EMBO J* 17: 4283-4290, 1998.
419. Patel AJ, Lazdunski M, Honore E. Lipid and mechano-gated 2P domain K(+) channels. *Curr Opin Cell Biol* 13: 422-428, 2001.
420. Patel SP, Campbell DL. Transient outward potassium current, 'Ito', phenotypes in the mammalian left ventricle: Underlying molecular, cellular and biophysical mechanisms. *J Physiol* 569: 7-39, 2005.
421. Pearson WL, Nichols CG. Block of the Kir2.1 channel pore by alkylamine analogues of endogenous polyamines. *J Gen Physiol* 112: 351-363, 1998.
422. Pedarzani P, Kulik A, Muller M, Ballanyi K, Stocker M. Molecular determinants of Ca²⁺-dependent K⁺ channel function in rat dorsal vagal neurones. *J Physiol* 527(Pt 2): 283-290, 2000.
423. Pedarzani P, Mosbacher J, Rivard A, Cingolani LA, Oliver D, Stocker M, Adelman JP, Fakler B. Control of electrical activity in central neurons by modulating the gating of small conductance Ca²⁺-activated K⁺ channels. *J Biol Chem* 276: 9762-9769, 2001.
424. Pedarzani P, Stocker M. Molecular and cellular basis of small- and intermediate-conductance, calcium-activated potassium channel function in the brain. *Cell Mol Life Sci* 65: 3196-3217, 2008.
425. Pegan S, Arrabit C, Zhou W, Kwiatkowski W, Collins A, Slesinger PA, Choe S. Cytoplasmic domain structures of Kir2.1 and Kir3.1 show sites for modulating gating and rectification. *Nat Neurosci* 8: 279-287, 2005.
426. Peleg S, Varon D, Ivanina T, Dessauer CW, Dascal N. G(alpha) (i) controls the gating of the G protein-activated K(+) channel, GIRK. *Neuron* 33: 87-99, 2002.
427. Pennefather P, Lancaster B, Adams PR, Nicoll RA. Two distinct Ca-dependent K currents in bullfrog sympathetic ganglion cells. *Proc Natl Acad Sci U S A* 82: 3040-3044, 1985.
428. Perez GJ, Bonev AD, Nelson MT. Micromolar Ca(2+) from sparks activates Ca(2+)-sensitive K(+) channels in rat cerebral artery smooth muscle. *Am J Physiol Cell Physiol* 281: C1769-C1775, 2001.
429. Pessia M, Imbrici P, D'Adamo MC, Salvatore L, Tucker SJ. Differential pH sensitivity of Kir4.1 and Kir4.2 potassium channels and their modulation by heteropolymerisation with Kir5.1. *J Physiol* 532: 359-367, 2001.
430. Plant LD, Rajan S, Goldstein SA. K2P channels and their protein partners. *Curr Opin Neurobiol* 15: 326-333, 2005.
431. Pluger S, Faulhaber J, Furstenau M, Lohn M, Waldschutz R, Gollasch M, Haller H, Luft FC, Ehmke H, Pongs O. Mice with disrupted BK channel beta1 subunit gene feature abnormal Ca(2+) spark/STOC coupling and elevated blood pressure. *Circ Res* 87: E53-E60, 2000.
432. Pluznick JL, Wei P, Carmines PK, Sansom SC. Renal fluid and electrolyte handling in BKCa-beta1-/- mice. *Am J Physiol Renal Physiol* 284: F1274-F1279, 2003.
433. Posson DJ, Ge P, Miller C, Bezanilla F, Selvin PR. Small vertical movement of a K⁺ channel voltage sensor measured with luminescence energy transfer. *Nature* 436: 848-851, 2005.
434. Power JM, Sah P. Competition between calcium-activated K⁺ channels determines cholinergic action on firing properties of basolateral amygdala projection neurons. *J Neurosci* 28: 3209-3220, 2008.
435. Prakriya M, Lingle CJ. BK channel activation by brief depolarizations requires Ca²⁺ influx through L- and Q-type Ca²⁺ channels in rat chromaffin cells. *J Neurophysiol* 81: 2267-2278, 1999.
436. Preisig-Muller R, Schlichthorl G, Goerge T, Heinen S, Bruggemann A, Rajan S, Derst C, Veh RW, Daut J. Heteromerization of Kir2.x potassium channels contributes to the phenotype of Andersen's syndrome. *Proc Natl Acad Sci U S A* 99: 7774-7779, 2002.
437. Prole DL, Lima PA, Marrion NV. Mechanisms underlying modulation of neuronal KCNQ2/KCNQ3 potassium channels by extracellular protons. *J Gen Physiol* 122: 775-793, 2003.
438. Quirk JC, Reinhart PH. Identification of a novel tetramerization domain in large conductance K(ca) channels. *Neuron* 32: 13-23, 2001.
439. Rajan S, Wischmeyer E, Xin Liu G, Preisig-Muller R, Daut J, Karschin A, Derst C. TASK-3, a novel tandem pore domain acid-sensitive K⁺ channel. An extracellular histidine as pH sensor. *J Biol Chem* 275: 16650-16657, 2000.
440. Raman IM, Bean BP. Ionic currents underlying spontaneous action potentials in isolated cerebellar Purkinje neurons. *J Neurosci* 19: 1663-1674, 1999.
441. Ramanathan K, Michael TH, Jiang GJ, Hiel H, Fuchs PA. A molecular mechanism for electrical tuning of cochlear hair cells. *Science* 283: 215-217, 1999.
442. Ramsey IS, Moran MM, Chong JA, Clapham DE. A voltage-gated proton-selective channel lacking the pore domain. *Nature* 440: 1213-1216, 2006.
443. Ramu Y, Xu Y, Lu Z. Enzymatic activation of voltage-gated potassium channels. *Nature* 442: 696-699, 2006.
444. Rangaraju S, Chi V, Pennington MW, Chandy KG. Kv1.3 potassium channels as a therapeutic target in multiple sclerosis. *Expert Opin Ther Targets* 13: 909-924, 2009.
445. Ravindran A, Kwiecinski H, Alvarez O, Eisenman G, Moczydlowski E. Modeling ion permeation through batrachotoxin-modified Na⁺ channels from rat skeletal muscle with a multi-ion pore. *Biophys J* 61: 494-508, 1992.
446. Rettig J, Heinemann SH, Wunder F, Lorra C, Parcej DN, Dolly JO, Pongs O. Inactivation properties of voltage-gated K⁺ channels altered by presence of beta-subunit. *Nature* 369: 289-294, 1994.
447. Riven I, Kalmanzon E, Segev L, Reuveny E. Conformational rearrangements associated with the gating of the G protein-coupled potassium channel revealed by FRET microscopy. *Neuron* 38: 225-235, 2003.

448. Roberds SL, Tamkun MM. Cloning and tissue-specific expression of five voltage-gated potassium channel cDNAs expressed in rat heart. *Proc Natl Acad Sci U S A* 88: 1798-1802, 1991.
449. Robitaille R, Charlton MP. Presynaptic calcium signals and transmitter release are modulated by calcium-activated potassium channels. *J Neurosci* 12: 297-305, 1992.
450. Romey G, Hugues M, Schmid-Antomarchi H, Lazdunski M. Apamin: A specific toxin to study a class of Ca²⁺-dependent K⁺ channels. *J Physiol (Paris)* 79: 259-264, 1984.
451. Rorsman P, Bokvist K, Ammal C, Arkhammar P, Berggren PO, Larsson O, Wahlander K. Activation by adrenaline of a low-conductance G protein-dependent K⁺ channel in mouse pancreatic B cells. *Nature* 349: 77-79, 1991.
452. Rose CR, Konnerth A. NMDA receptor-mediated Na⁺ signals in spines and dendrites. *J Neurosci* 21: 4207-4214, 2001.
453. Rosenblatt KP, Sun ZP, Heller S, Hudspeth AJ. Distribution of Ca²⁺-activated K⁺ channel isoforms along the tonotopic gradient of the chicken's cochlea. *Neuron* 19: 1061-1075, 1997.
454. Rosenhouse-Dantsker A, Sui JL, Zhao Q, Rusinova R, Rodriguez-Menchaca AA, Zhang Z, Logothetis DE. A sodium-mediated structural switch that controls the sensitivity of Kir channels to PtdIns(4,5)P(2). *Nat Chem Biol* 4: 624-631, 2008.
455. Rothberg BS, Magleby KL. Gating kinetics of single large-conductance Ca²⁺-activated K⁺ channels in high Ca²⁺ suggest a two-tiered allosteric gating mechanism. *J Gen Physiol* 114: 93-124, 1999.
456. Rothberg BS, Magleby KL. Voltage and Ca²⁺ activation of single large-conductance Ca²⁺-activated K⁺ channels described by a two-tiered allosteric gating mechanism. *J Gen Physiol* 116: 75-99, 2000.
457. Ruta V, Chen J, MacKinnon R. Calibrated measurement of gating-charge arginine displacement in the KvAP voltage-dependent K⁺ channel. *Cell* 123: 463-475, 2005.
458. Ruta V, MacKinnon R. Localization of the voltage-sensor toxin receptor on KvAP. *Biochemistry* 43: 10071-10079, 2004.
459. Sabbadini M, Yost CS. Molecular biology of background K channels: Insights from K(2P) knockout mice. *J Mol Biol* 385: 1331-1344, 2009.
460. Safronov BV, Vogel W. Properties and functions of Na(+)-activated K⁺ channels in the soma of rat motoneurons. *J Physiol* 497(Pt 3): 727-734, 1996.
461. Sah P. Role of calcium influx and buffering in the kinetics of Ca(2+)-activated K⁺ current in rat vagal motoneurons. *J Neurophysiol* 68: 2237-2247, 1992.
462. Sah P. Ca(2+)-activated K⁺ currents in neurones: Types, physiological roles and modulation. *Trends Neurosci* 19: 150-154, 1996.
463. Sailer CA, Hu H, Kaufmann WA, Trieb M, Schwarzer C, Storm JF, Knaus HG. Regional differences in distribution and functional expression of small-conductance Ca²⁺-activated K⁺ channels in rat brain. *J Neurosci* 22: 9698-9707, 2002.
464. Sailer CA, Kaufmann WA, Marksteiner J, Knaus HG. Comparative immunohistochemical distribution of three small-conductance Ca²⁺-activated potassium channel subunits, SK1, SK2, and SK3 in mouse brain. *Mol Cell Neurosci* 26: 458-469, 2004.
465. Sali A, Blundell TL. Comparative protein modelling by satisfaction of spatial restraints. *J Mol Biol* 234: 779-815, 1993.
466. Salkoff L, Butler A, Ferreira G, Santi C, Wei A. High-conductance potassium channels of the SLO family. *Nat Rev Neurosci* 7: 921-931, 2006.
467. Salkoff L, Wei AD, Baban B, Butler A, Fawcett G, Ferreira G, Santi CM. Potassium channels in *C. elegans*. *WormBook* 1-15, 2005.
468. Sandoz G, Thummler S, Duprat F, Feliciangeli S, Vinh J, Escoubas P, Guy N, Lazdunski M, Lesage F. AKAP150, a switch to convert mechano-, pH- and arachidonic acid-sensitive TREK K(+) channels into open leak channels. *EMBO J* 25: 5864-5872, 2006.
469. Sandtner W, Szendroedi J, Zarrabi T, Zebenedi E, Hilber K, Glaaser I, Fozzard HA, Dudley SC, Todt H. Lidocaine: A foot in the door of the inner vestibule prevents ultra-slow inactivation of a voltage-gated sodium channel. *Mol Pharmacol* 66: 648-657, 2004.
470. Sanguinetti MC, Curran ME, Zou A, Shen J, Spector PS, Atkinson DL, Keating MT. Coassembly of K(V)LQT1 and minK (IsK) proteins to form cardiac I(Ks) potassium channel. *Nature* 384: 80-83, 1996.
471. Sanguinetti MC, Jiang C, Curran ME, Keating MT. A mechanistic link between an inherited and an acquired cardiac arrhythmia: HERG encodes the IKr potassium channel. *Cell* 81: 299-307, 1995.
472. Sano Y, Mochizuki S, Miyake A, Kitada C, Inamura K, Yokoi H, Nozawa K, Matsushima H, Furuichi K. Molecular cloning and characterization of Kv6.3, a novel modulatory subunit for voltage-gated K(+) channel Kv2.1. *FEBS Lett* 512: 230-234, 2002.
473. Santi CM, Butler A, Kuhn J, Wei A, Salkoff L. Bovine and mouse SLO3 K⁺ channels: Evolutionary divergence points to an RCK1 region of critical function. *J Biol Chem* 284: 21589-21598, 2009.
474. Santi CM, Ferreira G, Yang B, Gazula VR, Butler A, Wei A, Kaczmarek LK, Salkoff L. Opposite regulation of Slick and Slack K⁺ channels by neuromodulators. *J Neurosci* 26: 5059-5068, 2006.
475. Santi CM, Martinez-Lopez P, de la Vega-Beltran JL, Butler A, Alisio A, Darszon A, Salkoff L. The SLO3 sperm-specific potassium channel plays a vital role in male fertility. *FEBS Lett* 584: 1041-1046, 2010.
476. Sasaki M, Takagi M, Okamura Y. A voltage sensor-domain protein is a voltage-gated proton channel. *Science* 312: 589-592, 2006.
477. Sausbier U, Sausbier M, Sailer CA, Arntz C, Knaus HG, Neuhuber W, Ruth P. Ca²⁺-activated K⁺ channels of the BK-type in the mouse brain. *Histochem Cell Biol* 125: 725-741, 2006.
478. Savalli N, Kondratiev A, Toro L, Olcese R. Voltage-dependent conformational changes in human Ca(2+)- and voltage-activated K(+) channel, revealed by voltage-clamp fluorometry. *Proc Natl Acad Sci U S A* 103: 12619-12624, 2006.
479. Scanziani M. GABA spillover activates postsynaptic GABA(B) receptors to control rhythmic hippocampal activity. *Neuron* 25: 673-681, 2000.
480. Scuvée-Moreau J, Bolland A, Graulich A, Van Overmeire L, D'Hoedt D, Graulich-Lorge F, Thomas E, Abras A, Stocker M, Liegeois JF, Seutin V. Electrophysiological characterization of the SK channel blockers methyl-laudanosine and methyl-noscapine in cell lines and rat brain slices. *Br J Pharmacol* 143: 753-764, 2004.
481. Schmidt D, Jiang QX, MacKinnon R. Phospholipids and the origin of cationic gating charges in voltage sensors. *Nature* 444: 775-779, 2006.
482. Schoppa NE, McCormack K, Tanouye MA, Sigworth FJ. The size of gating charge in wild-type and mutant Shaker potassium channels. *Science* 255: 1712-1715, 1992.
483. Schoppa NE, Sigworth FJ. Activation of Shaker potassium channels. III. An activation gating model for wild-type and V2 mutant channels. *J Gen Physiol* 111: 313-342, 1998.
484. Schreiber M, Wei A, Yuan A, Gaut J, Saito M, Salkoff L. Slo3, a novel pH-sensitive K⁺ channel from mammalian spermatocytes. *J Biol Chem* 273: 3509-3516, 1998.
485. Schrempf H, Schmidt O, Kummerlen R, Hinnah S, Muller D, Betzler M, Steinkamp T, Wagner R. A prokaryotic potassium ion channel with two predicted transmembrane segments from *Streptomyces lividans*. *EMBO J* 14: 5170-5178, 1995.
486. Schumacher MA, Rivard AF, Bachinger HP, Adelman JP. Structure of the gating domain of a Ca²⁺-activated K⁺ channel complexed with Ca²⁺/calmodulin. *Nature* 410: 1120-1124, 2001.
487. Schwartzkroin PA, Stafstrom CE. Effects of EGTA on the calcium-activated afterhyperpolarization in hippocampal CA3 pyramidal cells. *Science* 210: 1125-1126, 1980.
488. Schwandt PC, Spain WJ, Foehring RC, Stafstrom CE, Chubb MC, Crill WE. Multiple potassium conductances and their functions in neurons from cat sensorimotor cortex in vitro. *J Neurophysiol* 59: 424-449, 1988.
489. Semenova NP, Abarca-Heidemann K, Loranc E, Rothberg BS. Bi-mane fluorescence scanning suggests secondary structure near the S3-S4 linker of BK channels. *J Biol Chem* 284: 10684-10693, 2009.
490. Seoh SA, Sigg D, Papazian DM, Bezanilla F. Voltage-sensing residues in the S2 and S4 segments of the Shaker K⁺ channel. *Neuron* 16: 1159-1167, 1996.
491. Seutin V, Johnson SW. Recent advances in the pharmacology of quaternary salts of bicuculline. *Trends Pharmacol Sci* 20: 268-270, 1999.
492. Shakkottai VG, Regaya I, Wulff H, Fajloun Z, Tomita H, Fathallah M, Cahalan MD, Gargus JJ, Sabatier JM, Chandy KG. Design and characterization of a highly selective peptide inhibitor of the small conductance calcium-activated K⁺ channel, SkCa2. *J Biol Chem* 276: 43145-43151, 2001.
493. Shao LR, Halvorsrud R, Borg-Graham L, Storm JF. The role of BK-type Ca²⁺-dependent K⁺ channels in spike broadening during repetitive firing in rat hippocampal pyramidal cells. *J Physiol* 521(Pt 1): 135-146, 1999.
494. Sharon D, Vorobiov D, Dascal N. Positive and negative coupling of the metabotropic glutamate receptors to a G protein-activated K⁺ channel, GIRK, in *Xenopus* oocytes. *J Gen Physiol* 109: 477-490, 1997.
495. Shen KZ, Lagrutta A, Davies NW, Standen NB, Adelman JP, North RA. Tetraethylammonium block of Slowpoke calcium-activated potassium channels expressed in *Xenopus* oocytes: Evidence for tetrameric channel formation. *Pflügers Arch* 426: 440-445, 1994.
496. Shieh RC, Chang JC, Arreola J. Interaction of Ba²⁺ with the pores of the cloned inward rectifier K⁺ channels Kir2.1 expressed in *Xenopus* oocytes. *Biophys J* 75: 2313-2322, 1998.
497. Shin HG, Lu Z. Mechanism of the voltage sensitivity of IRK1 inward-rectifier K⁺ channel block by the polyamine spermine. *J Gen Physiol* 125: 413-426, 2005.
498. Shin KS, Maertens C, Proenza C, Rothberg BS, Yellen G. Inactivation in HCN channels results from reclosure of the activation gate: Desensitization to voltage. *Neuron* 41: 737-744, 2004.
499. Shmukler BE, Bond CT, Wilhelm S, Bruening-Wright A, Maylie J, Adelman JP, Alper SL. Structure and complex transcription pattern of the mouse SK1 K(Ca) channel gene, KCNN1. *Biochim Biophys Acta* 1518: 36-46, 2001.

500. Shyng S, Nichols CG. Octameric stoichiometry of the KATP channel complex. *J Gen Physiol* 110: 655-664, 1997.
501. Sieg A, Su J, Munoz A, Buchenau M, Nakazaki M, Aguilar-Bryan L, Bryan J, Ullrich S. Epinephrine-induced hyperpolarization of islet cells without KATP channels. *Am J Physiol Endocrinol Metab* 286: E463-E471, 2004.
502. Sigg D, Bezanilla F. Total charge movement per channel. The relation between gating charge displacement and the voltage sensitivity of activation. *J Gen Physiol* 109: 27-39, 1997.
503. Signorini S, Liao YJ, Duncan SA, Jan LY, Stoffel M. Normal cerebellar development but susceptibility to seizures in mice lacking G protein-coupled, inwardly rectifying K⁺ channel GIRK2. *Proc Natl Acad Sci U S A* 94: 923-927, 1997.
504. Slesinger PA, Reuveny E, Jan YN, Jan LY. Identification of structural elements involved in G protein gating of the GIRK1 potassium channel. *Neuron* 15: 1145-1156, 1995.
505. Smith PA, Bokvist K, Arkhammar P, Berggren PO, Rorsman P. Delayed rectifying and calcium-activated K⁺ channels and their significance for action potential repolarization in mouse pancreatic beta-cells. *J Gen Physiol* 95: 1041-1059, 1990.
506. Soh H, Park CS. Inwardly rectifying current-voltage relationship of small-conductance Ca²⁺-activated K⁺ channels rendered by intracellular divalent cation blockade. *Biophys J* 80: 2207-2215, 2001.
507. Soh H, Park CS. Localization of divalent cation-binding site in the pore of a small conductance Ca(2+)-activated K(+) channel and its role in determining current-voltage relationship. *Biophys J* 83: 2528-2538, 2002.
508. Solaro CR, Prakriya M, Ding JP, Lingle CJ. Inactivating and noninactivating Ca(2+)- and voltage-dependent K⁺ current in rat adrenal chromaffin cells. *J Neurosci* 15: 6110-6123, 1995.
509. Stackman RW, Hammond RS, Linardatos E, Gerlach A, Maylie J, Adelman JP, Tzounopoulos T. Small conductance Ca²⁺-activated K⁺ channels modulate synaptic plasticity and memory encoding. *J Neurosci* 22: 10163-10171, 2002.
510. Stanfield PR, Davies NW, Shelton PA, Sutcliffe MJ, Khan IA, Brammar WJ, Conley EC. A single aspartate residue is involved in both intrinsic gating and blockage by Mg²⁺ of the inward rectifier, IRK1. *J Physiol* 478(Pt 1): 1-6, 1994.
511. Starace DM, Bezanilla F. Histidine scanning mutagenesis of basic residues of the S4 segment of the shaker k⁺ channel. *J Gen Physiol* 117: 469-490, 2001.
512. Starace DM, Bezanilla F. A proton pore in a potassium channel voltage sensor reveals a focused electric field. *Nature* 427: 548-553, 2004.
513. Starace DM, Stefani E, Bezanilla F. Voltage-dependent proton transport by the voltage sensor of the Shaker K⁺ channel. *Neuron* 19: 1319-1327, 1997.
514. Stefani E, Ottolia M, Noceti F, Olcese R, Wallner M, Latorre R, Toro L. Voltage-controlled gating in a large conductance Ca²⁺-sensitive K⁺-channel (hsl). *Proc Natl Acad Sci U S A* 94: 5427-5431, 1997.
515. Stocker M, Hirzel K, D'Hoedt D, Pedarzani P. Matching molecules to function: Neuronal Ca²⁺-activated K⁺ channels and afterhyperpolarizations. *Toxicon* 43: 933-949, 2004.
516. Stocker M, Krause M, Pedarzani P. An apamin-sensitive Ca²⁺-activated K⁺ current in hippocampal pyramidal neurons. *Proc Natl Acad Sci U S A* 96: 4662-4667, 1999.
517. Storm JF. Action potential repolarization and a fast after-hyperpolarization in rat hippocampal pyramidal cells. *J Physiol* 385: 733-759, 1987.
518. Strassmaier T, Bond CT, Sailer CA, Knaus HG, Maylie J, Adelman JP. A novel isoform of SK2 assemblies with other SK subunits in mouse brain. *J Biol Chem* 280: 21231-21236, 2005.
519. Strobaek D, Hougaard C, Johansen TH, Sorensen US, Nielsen EO, Nielsen KS, Taylor RD, Pedarzani P, Christophersen P. Inhibitory gating modulation of small conductance Ca²⁺-activated K⁺ channels by the synthetic compound (R)-N-(benzimidazol-2-yl)-1,2,3,4-tetrahydro-1-naphthylamine (NS8593) reduces afterhyperpolarizing current in hippocampal CA1 neurons. *Mol Pharmacol* 70: 1771-1782, 2006.
520. Sui JL, Chan KW, Logothetis DE. Na⁺ activation of the muscarinic K⁺ channel by a G-protein-independent mechanism. *J Gen Physiol* 108: 381-391, 1996.
521. Sui JL, Petit-Jacques J, Logothetis DE. Activation of the atrial KACH channel by the betagamma subunits of G proteins or intracellular Na⁺ ions depends on the presence of phosphatidylinositol phosphates. *Proc Natl Acad Sci U S A* 95: 1307-1312, 1998.
522. Swanson WJ, Vacquier VD. The rapid evolution of reproductive proteins. *Nat Rev Genet* 3: 137-144, 2002.
523. Swartz KJ. Towards a structural view of gating in potassium channels. *Nat Rev Neurosci* 5: 905-916, 2004.
524. Swartz KJ. Sensing voltage across lipid membranes. *Nature* 456: 891-897, 2008.
525. Swartz KJ, MacKinnon R. An inhibitor of the Kv2.1 potassium channel isolated from the venom of a Chilean tarantula. *Neuron* 15: 941-949, 1995.
526. Sweet TB, Cox DH. Measuring the influence of the BKCa {beta}1 subunit on Ca²⁺ binding to the BKCa channel. *J Gen Physiol* 133: 139-150, 2009.
527. Swensen AM, Bean BP. Ionic mechanisms of burst firing in dissociated Purkinje neurons. *J Neurosci* 23: 9650-9663, 2003.
528. Taglialatela M, Wible BA, Caporaso R, Brown AM. Specification of pore properties by the carboxyl terminus of inwardly rectifying K⁺ channels. *Science* 264: 844-847, 1994.
529. Takano K, Yasufuku-Takano J, Kozasa T, Singer WD, Nakajima S, Nakajima Y. Gq/11 and PLC-beta 1 mediate the substance P-induced inhibition of an inward rectifier K⁺ channel in brain neurons. *J Neurophysiol* 76: 2131-2136, 1996.
530. Takano M, Kuratomi S. Regulation of cardiac inwardly rectifying potassium channels by membrane lipid metabolism. *Prog Biophys Mol Biol* 81: 67-79, 2003.
531. Takeuchi S, Ando M, Kakigi A. Mechanism generating endocochlear potential: Role played by intermediate cells in stria vascularis. *Biophys J* 79: 2572-2582, 2000.
532. Talukder G, Aldrich RW. Complex voltage-dependent behavior of single unliganded calcium-sensitive potassium channels. *Biophys J* 78: 761-772, 2000.
533. Talley EM, Lei Q, Sirois JE, Bayliss DA. TASK-1, a two-pore domain K⁺ channel, is modulated by multiple neurotransmitters in motoneurons. *Neuron* 25: 399-410, 2000.
534. Talley EM, Solorzano G, Lei Q, Kim D, Bayliss DA. Cns distribution of members of the two-pore-domain (KCNK) potassium channel family. *J Neurosci* 21: 7491-7505, 2001.
535. Tamsett TJ, Picchione KE, Bhattacharjee A. NAD⁺ activates KNa channels in dorsal root ganglion neurons. *J Neurosci* 29: 5127-5134, 2009.
536. Tanemoto M, Kittaka N, Inanobe A, Kurachi Y. In vivo formation of a proton-sensitive K⁺ channel by heteromeric subunit assembly of Kir5.1 with Kir4.1. *J Physiol* 525(Pt 3): 587-592, 2000.
537. Tang QY, Zhang Z, Xia XM, Lingle CJ. Block of mouse Slo1 and Slo3 K⁺ channels by CTX, IbTX, TEA, 4-AP and quinidine. *Channels (Austin)* 4: 22-41, 2010.
538. Tang X, Schmidt TM, Perez-Leighton CE, Kofuji P. Inwardly rectifying potassium channel Kir4.1 is responsible for the native inward potassium conductance of satellite glial cells in sensory ganglia. *Neuroscience* 166: 397-407, 2010.
539. Tao X, Avalos JL, Chen J, MacKinnon R. Crystal structure of the eukaryotic strong inward-rectifier K⁺ channel Kir2.2 at 3.1 Å resolution. *Science* 326: 1668-1674, 2009.
540. Tiwari-Woodruff SK, Lin MA, Schulteis CT, Papazian DM. Voltage-dependent structural interactions in the Shaker K(+) channel. *J Gen Physiol* 115: 123-138, 2000.
541. Tiwari-Woodruff SK, Schulteis CT, Mock AF, Papazian DM. Electrostatic interactions between transmembrane segments mediate folding of Shaker K⁺ channel subunits. *Biophys J* 72: 1489-1500, 1997.
542. Tombola F, Pathak MM, Gorostiza P, Isacoff EY. The twisted ion-permeation pathway of a resting voltage-sensing domain. *Nature* 445: 546-549, 2007.
543. Tombola F, Pathak MM, Isacoff EY. Voltage-sensing arginines in a potassium channel permeate and occlude cation-selective pores. *Neuron* 45: 379-388, 2005.
544. Tomita H, Shakkottai VG, Gutman GA, Sun G, Bunney WE, Cahalan MD, Chandy KG, Gargus JJ. Novel truncated isoform of SK3 potassium channel is a potent dominant-negative regulator of SK currents: Implications in schizophrenia. *Mol Psychiatry* 8: 524-535, 2003.
545. Topert C, Doring F, Wischmeyer E, Karschin C, Brockhaus J, Ballanyi K, Derst C, Karschin A. Kir2.4: A novel K⁺ inward rectifier channel associated with motoneurons of cranial nerve nuclei. *J Neurosci* 18: 4096-4105, 1998.
546. Toro L, Wallner M, Meera P, Tanaka Y. Maxi-K(Ca), a unique member of the voltage-gated K channel superfamily. *News Physiol Sci* 13: 112-117, 1998.
547. Torres YP, Morera FJ, Carvacho I, Latorre R. A marriage of convenience: Beta-subunits and voltage-dependent K⁺ channels. *J Biol Chem* 282: 24485-24489, 2007.
548. Treisman SN, Martin GE. BK Channels: Mediators and models for alcohol tolerance. *Trends Neurosci* 32: 629-637, 2009.
549. Treptow W, Tarek M. Environment of the gating charges in the Kv1.2 Shaker potassium channel. *Biophys J* 90: L64-L66, 2006.
550. Trimmer JS. Immunological identification and characterization of a delayed rectifier K⁺ channel polypeptide in rat brain. *Proc Natl Acad Sci U S A* 88: 10764-10768, 1991.
551. Tristani-Firouzi M, Jensen JL, Donaldson MR, Sansone V, Meola G, Hahn A, Bendahhou S, Kwiecinski H, Fidzianska A, Plaster N, Fu YH, Ptacek LJ, Tawil R. Functional and clinical characterization of KCNJ2

- mutations associated with LQT7 (Andersen syndrome). *J Clin Invest* 110: 381-388, 2002.
552. Tsaur ML, Sheng M, Lowenstein DH, Jan YN, Jan LY. Differential expression of K⁺ channel mRNAs in the rat brain and down-regulation in the hippocampus following seizures. *Neuron* 8: 1055-1067, 1992.
 553. Tseng-Crank J, Foster CD, Krause JD, Mertz R, Godinot N, DiChiara TJ, Reinhart PH. Cloning, expression, and distribution of functionally distinct Ca(2+)-activated K⁺ channel isoforms from human brain. *Neuron* 13: 1315-1330, 1994.
 554. Tzounopoulos T, Stackman R. Enhancing synaptic plasticity and memory: A role for small-conductance Ca(2+)-activated K⁺ channels. *Neuroscientist* 9: 434-439, 2003.
 555. Uebele VN, Lagrutta A, Wade T, Figueroa DJ, Liu Y, McKenna E, Austin CP, Bennett PB, Swanson R. Cloning and functional expression of two families of beta-subunits of the large conductance calcium-activated K⁺ channel. *J Biol Chem* 275: 23211-23218, 2000.
 556. Valverde MA, Rojas P, Amigo J, Cosmelli D, Orio P, Bahamonde MI, Mann GE, Vergara C, Latorre R. Acute activation of Maxi-K channels (hSlo) by estradiol binding to the beta subunit. *Science* 285: 1929-1931, 1999.
 557. Vanderberg C. Inward rectification in a potassium channel in cardiac ventricular cells depends on internal magnesium ions. *Proc Natl Acad Sci U S A* 84: 307-320, 1987.
 558. Vergara C, Moczydlowski E, Latorre R. Conduction, blockade and gating in a Ca-activated K channel incorporated into planar lipid bilayers. *Biophys J* 45: 73-76, 1984.
 559. Villalba-Galea CA, Miceli F, Taglialatela M, Bezanilla F. Coupling between the voltage-sensing and phosphatase domains of Ci-VSP. *J Gen Physiol* 134: 5-14, 2009.
 560. Villalba-Galea CA, Sandtner W, Starace DM, Bezanilla F. S4-based voltage sensors have three major conformations. *Proc Natl Acad Sci U S A* 105: 17600-17607, 2008.
 561. Walter JT, Alvina K, Womack MD, Chevez C, Khodakhah K. Decreases in the precision of Purkinje cell pacemaking cause cerebellar dysfunction and ataxia. *Nat Neurosci* 9: 389-397, 2006.
 562. Wallen P, Robertson B, Cangiano L, Low P, Bhattacharjee A, Kaczmarek LK, Grillner S. Sodium-dependent potassium channels of a Slack-like subtype contribute to the slow afterhyperpolarization in lamprey spinal neurons. *J Physiol* 585: 75-90, 2007.
 563. Wallner M, Meera P, Toro L. Molecular basis of fast inactivation in voltage and Ca2+-activated K⁺ channels: A transmembrane beta-subunit homolog. *Proc Natl Acad Sci U S A* 96: 4137-4142, 1999.
 564. Wang B, Rothberg BS, Brenner R. Mechanism of beta4 subunit modulation of BK channels. *J Gen Physiol* 127: 449-465, 2006.
 565. Wang L, Sigworth FJ. Structure of the BK potassium channel in a lipid membrane from electron cryomicroscopy. *Nature* 461: 292-295, 2009.
 566. Wang WH, Giebisch G. Regulation of potassium (K) handling in the renal collecting duct. *Pflügers Arch* 458: 157-168, 2009.
 567. Wang X, Xu R, Abernathy G, Taylor J, Alzghoul MB, Hannon K, Hockerman GH, Pond AL. Kv11.1 channel subunit composition includes MinK and varies developmentally in mouse cardiac muscle. *Dev Dyn* 237: 2430-2437, 2008.
 568. Weatherall KL, Goodchild SJ, Jane DE, Marrion NV. Small conductance calcium-activated potassium channels: From structure to function. *Prog Neurobiol* 91: 242-255, 2010.
 569. Wei AD, Gutman GA, Aldrich R, Chandy KG, Grissmer S, Wulff H. International Union of Pharmacology. LII. Nomenclature and molecular relationships of calcium-activated potassium channels. *Pharmacol Rev* 57: 463-472, 2005.
 570. Wei DS, Mei YA, Bagal A, Kao JP, Thompson SM, Tang CM. Compartmentalized and binary behavior of terminal dendrites in hippocampal pyramidal neurons. *Science* 293: 2272-2275, 2001.
 571. Wellman GC, Bevan JA. Barium inhibits the endothelium-dependent component of flow but not acetylcholine-induced relaxation in isolated rabbit cerebral arteries. *J Pharmacol Exp Ther* 274: 47-53, 1995.
 572. White MM, Bezanilla F. Activation of squid axon K⁺ channels. Ionic and gating current studies. *J Gen Physiol* 85: 539-554, 1985.
 573. Wible BA, Taglialatela M, Ficker E, Brown AM. Gating of inwardly rectifying K⁺ channels localized to a single negatively charged residue. *Nature* 371: 246-249, 1994.
 574. Wickman K, Clapham DE. Ion channel regulation by G proteins. *Physiol Rev* 75: 865-885, 1995.
 575. Wittekindt OH, Dreker T, Morris-Rosendahl DJ, Lehmann-Horn F, Grissmer S. A novel non-neuronal hSK3 isoform with a dominant-negative effect on hSK3 currents. *Cell Physiol Biochem* 14: 23-30, 2004.
 576. Wolfart J, Neuhoff H, Franz O, Roeper J. Differential expression of the small-conductance, calcium-activated potassium channel SK3 is critical for pacemaker control in dopaminergic midbrain neurons. *J Neurosci* 21: 3443-3456, 2001.
 577. Wolfart J, Roeper J. Selective coupling of T-type calcium channels to SK potassium channels prevents intrinsic bursting in dopaminergic midbrain neurons. *J Neurosci* 22: 3404-3413, 2002.
 578. Womack M, Khodakhah K. Active contribution of dendrites to the tonic and trimodal patterns of activity in cerebellar Purkinje neurons. *J Neurosci* 22: 10603-10612, 2002.
 579. Womack MD, Chevez C, Khodakhah K. Calcium-activated potassium channels are selectively coupled to P/Q-type calcium channels in cerebellar Purkinje neurons. *J Neurosci* 24: 8818-8822, 2004.
 580. Womack MD, Khodakhah K. Somatic and dendritic small-conductance calcium-activated potassium channels regulate the output of cerebellar Purkinje neurons. *J Neurosci* 23: 2600-2607, 2003.
 581. Woodhull AM. Ionic blockage of sodium channels in nerve. *J Gen Physiol* 61: 687-708, 1973.
 582. Wu RS, Marx SO. The BK potassium channel in the vascular smooth muscle and kidney: Alpha- and beta-subunits. *Kidney Int* 78: 963-974, 2010.
 583. Wu Y, Yang Y, Ye S, Jiang Y. Structure of the gating ring from the human large-conductance Ca(2+)-gated K(+) channel. *Nature* 466: 393-397, 2010.
 584. Wynne PM, Puig SI, Martin GE, Treistman SN. Compartmentalized beta subunit distribution determines characteristics and ethanol sensitivity of somatic, dendritic, and terminal large-conductance calcium-activated potassium channels in the rat central nervous system. *J Pharmacol Exp Ther* 329: 978-986, 2009.
 585. Xia XM, Ding JP, Lingle CJ. Molecular basis for the inactivation of Ca2+- and voltage-dependent BK channels in adrenal chromaffin cells and rat insulinoma tumor cells. *J Neurosci* 19: 5255-5264, 1999.
 586. Xia XM, Ding JP, Lingle CJ. Inactivation of BK channels by the NH2 terminus of the beta2 auxiliary subunit: An essential role of a terminal peptide segment of three hydrophobic residues. *J Gen Physiol* 121: 125-148, 2003.
 587. Xia XM, Ding JP, Zeng XH, Duan KL, Lingle CJ. Rectification and rapid activation at low Ca2+ of Ca2+-activated, voltage-dependent BK currents: Consequences of rapid inactivation by a novel beta subunit. *J Neurosci* 20: 4890-4903, 2000.
 588. Xia XM, Fakler B, Rivard A, Wayman G, Johnson-Pais T, Keen JE, Ishii T, Hirschberg B, Bond CT, Lutsenko S, Maylie J, Adelman JP. Mechanism of calcium gating in small-conductance calcium-activated potassium channels. *Nature* 395: 503-507, 1998.
 589. Xia XM, Zeng X, Lingle CJ. Multiple regulatory sites in large-conductance calcium-activated potassium channels. *Nature* 418: 880-884, 2002.
 590. Xia XM, Zhang X, Lingle CJ. Ligand-dependent activation of Slo family channels is defined by interchangeable cytosolic domains. *J Neurosci* 24: 5585-5591, 2004.
 591. Xie J, McCobb DP. Control of alternative splicing of potassium channels by stress hormones. *Science* 280: 443-446, 1998.
 592. Xu W, Liu Y, Wang S, McDonald T, Van Eyk JE, Sidor A, O'Rourke B. Cytoprotective role of Ca2+-activated K⁺ channels in the cardiac inner mitochondrial membrane. *Science* 298: 1029-1033, 2002.
 593. Xu Y, Ramu Y, Lu Z. Removal of phospho-head groups of membrane lipids immobilizes voltage sensors of K⁺ channels. *Nature* 451: 826-829, 2008.
 594. Xu Y, Shin HG, Szep S, Lu Z. Physical determinants of strong voltage sensitivity of K(+) channel block. *Nat Struct Mol Biol* 16: 1252-1258, 2009.
 595. Yang B, Gribkoff VK, Pan J, Damagnez V, Dworetzky SI, Boissard CG, Bhattacharjee A, Yan Y, Sigworth FJ, Kaczmarek LK. Pharmacological activation and inhibition of Slack (Slo2.2) channels. *Neuropharmacology* 51: 896-906, 2006.
 596. Yang CT, Zeng XH, Xia XM, Lingle CJ. Interactions between beta subunits of the KCNMB family and Slo3: Beta4 selectively modulates Slo3 expression and function. *PLoS One* 4: e6135, 2009.
 597. Yang H, Shi J, Zhang G, Yang J, Delaloye K, Cui J. Activation of Slo1 BK channels by Mg2+ coordinated between the voltage sensor and RCK1 domains. *Nat Struct Mol Biol* 15: 1152-1159, 2008.
 598. Yang J, Jan YN, Jan LY. Control of rectification and permeation by residues in two distinct domains in an inward rectifier K⁺ channel. *Neuron* 14: 1047-1054, 1995.
 599. Yang J, Krishnamoorthy G, Saxena A, Zhang G, Shi J, Yang H, Delaloye K, Sept D, Cui J. An epilepsy/dyskinesia-associated mutation enhances BK channel activation by potentiating Ca2+ sensing. *Neuron* 66: 871-883, 2010.
 600. Yang N, George AL Jr., Horn R. Molecular basis of charge movement in voltage-gated sodium channels. *Neuron* 16: 113-122, 1996.
 601. Ye S, Li Y, Chen L, Jiang Y. Crystal structures of a ligand-free MthK gating ring: Insights into the ligand gating mechanism of K⁺ channels. *Cell* 126: 1161-1173, 2006.
 602. Ye X, Fukushima N, Kingsbury MA, Chun J. Lysophosphatidic acid in neural signaling. *Neuroreport* 13: 2169-2175, 2002.

603. Yellen G. The moving parts of voltage-gated ion channels. *Q Rev Biophys* 31: 239-295, 1998.
604. Yoshimoto Y, Fukuyama Y, Horio Y, Inanobe A, Gotoh M, Kurachi Y. Somatostatin induces hyperpolarization in pancreatic islet alpha cells by activating a G protein-gated K⁺ channel. *FEBS Lett* 444: 265-269, 1999.
605. Yuan A, Dourado M, Butler A, Walton N, Wei A, Salkoff L. SLO-2, a K⁺ channel with an unusual Cl⁻ dependence. *Nat Neurosci* 3: 771-779, 2000.
606. Yuan A, Santi CM, Wei A, Wang ZW, Pollak K, Nonet M, Kaczmarek L, Crowder CM, Salkoff L. The sodium-activated potassium channel is encoded by a member of the Slo gene family. *Neuron* 37: 765-773, 2003.
607. Yuan P, Leonetti MD, Pico AR, Hsiung Y, Mackinnon R. Structure of the Human BK Channel Ca²⁺-Activation Apparatus at 3.0 Å Resolution. *Science* 329: 182-186, 2010.
608. Yuill KH, Stansfeld PJ, Ashmole I, Sutcliffe MJ, Stanfield PR. The selectivity, voltage-dependence and acid sensitivity of the tandem pore potassium channel TASK-1: Contributions of the pore domains. *Pflügers Arch* 455: 333-348, 2007.
609. Yusaf SP, Wray D, Sivaprasadarao A. Measurement of the movement of the S4 segment during the activation of a voltage-gated potassium channel. *Pflügers Arch* 433: 91-97, 1996.
610. Yusifov T, Savalli N, Gandhi CS, Ottolia M, Olcese R. The RCK2 domain of the human BKCa channel is a calcium sensor. *Proc Natl Acad Sci U S A* 105: 376-381, 2008.
611. Zagha E, Manita S, Ross WN, Rudy B. Dendritic Kv3.3 potassium channels in cerebellar purkinje cells regulate generation and spatial dynamics of dendritic Ca²⁺ spikes. *J Neurophysiol* 103: 3516-3525.
612. Zagotta WN, Hoshi T, Aldrich RW. Restoration of inactivation in mutants of Shaker potassium channels by a peptide derived from ShB. *Science* 250: 568-571, 1990.
613. Zagotta WN, Hoshi T, Aldrich RW. Shaker potassium channel gating. III: Evaluation of kinetic models for activation. *J Gen Physiol* 103: 321-362, 1994.
614. Zagotta WN, Hoshi T, Dittman J, Aldrich RW. Shaker potassium channel gating. II: Transitions in the activation pathway. *J Gen Physiol* 103: 279-319, 1994.
615. Zarei MM, Song M, Wilson RJ, Cox N, Colom LV, Knaus HG, Stefani E, Toro L. Endocytic trafficking signals in KCNMB2 regulate surface expression of a large conductance voltage and Ca(2+)-activated K⁺ channel. *Neuroscience* 147: 80-89, 2007.
616. Zarei MM, Zhu N, Alioua A, Eghbali M, Stefani E, Toro L. A novel MaxiK splice variant exhibits dominant-negative properties for surface expression. *J Biol Chem* 276: 16232-16239, 2001.
617. Zaritsky JJ, Redell JB, Tempel BL, Schwarz TL. The consequences of disrupting cardiac inwardly rectifying K(+) current (I(K1)) as revealed by the targeted deletion of the murine Kir2.1 and Kir2.2 genes. *J Physiol* 533: 697-710, 2001.
618. Zawar C, Plant TD, Schirra C, Konnerth A, Neumcke B. Cell-type specific expression of ATP-sensitive potassium channels in the rat hippocampus. *J Physiol* 514(Pt 2): 327-341, 1999.
619. Zeng XH, Xia XM, Lingle CJ. Redox-sensitive extracellular gates formed by auxiliary beta subunits of calcium-activated potassium channels. *Nat Struct Biol* 10: 448-454, 2003.
620. Zeng XH, Xia XM, Lingle CJ. Divalent cation sensitivity of BK channel activation supports the existence of three distinct binding sites. *J Gen Physiol* 125: 273-286, 2005.
621. Zhang BM, Kohli V, Adachi R, Lopez JA, Udden MM, Sullivan R. Calmodulin binding to the C-terminus of the small-conductance Ca²⁺-activated K⁺ channel hSK1 is affected by alternative splicing. *Biochemistry* 40: 3189-3195, 2001.
622. Zhang G, Huang SY, Yang J, Shi J, Yang X, Moller A, Zou X, Cui J. Ion sensing in the RCK1 domain of BK channels. *Proc Natl Acad Sci U S A* 107: 18700-18705, 2010.
623. Zhang PC, Keleshian AM, Sachs F. Voltage-induced membrane movement. *Nature* 413: 428-432, 2001.
624. Zhang X, Bertaso F, Yoo JW, Baumgartel K, Clancy SM, Lee V, Cienfuegos C, Wilmot C, Avis J, Hunyh T, Daguia C, Schmedt C, Noebels J, Jegla T. Deletion of the potassium channel Kv12.2 causes hippocampal hyperexcitability and epilepsy. *Nat Neurosci* 13: 1056-1058.
625. Zhang X, Zeng X, Lingle CJ. Slo3 K⁺ channels: Voltage and pH dependence of macroscopic currents. *J Gen Physiol* 128: 317-336, 2006.
626. Zhang Y, Gao F, Popov VL, Wen JW, Hamill OP. Mechanically gated channel activity in cytoskeleton-deficient plasma membrane blebs and vesicles from *Xenopus* oocytes. *J Physiol* 523(Pt 1): 117-130, 2000.
627. Zheng J, Sigworth FJ. Intermediate conductances during deactivation of heteromultimeric Shaker potassium channels. *J Gen Physiol* 112: 457-474, 1998.
628. Zhou Y, MacKinnon R. The occupancy of ions in the K⁺ selectivity filter: Charge balance and coupling of ion binding to a protein conformational change underlie high conduction rates. *J Mol Biol* 333: 965-975, 2003.
629. Zhou Y, Morais-Cabral JH, Kaufman A, MacKinnon R. Chemistry of ion coordination and hydration revealed by a K⁺ channel-Fab complex at 2.0 Å resolution. *Nature* 414: 43-48, 2001.
630. Zhou Z, Misler S. Action potential-induced quantal secretion of catecholamines from rat adrenal chromaffin cells. *J Biol Chem* 270: 3498-3505, 1995.
631. Zilberberg N, Ilan N, Goldstein SA. KCNK0: Opening and closing the 2-P-domain potassium leak channel entails "C-type" gating of the outer pore. *Neuron* 32: 635-648, 2001.
632. Zingman LV, Hodgson DM, Bast PH, Kane GC, Perez-Terzic C, Gumina RJ, Pucar D, Bienengraeber M, Dzeja PP, Miki T, Seino S, Alekseev AE, Terzic A. Kir6.2 is required for adaptation to stress. *Proc Natl Acad Sci U S A* 99: 13278-13283, 2002.
633. Zobel C, Cho HC, Nguyen TT, Pekhletski R, Diaz RJ, Wilson GJ, Backx PH. Molecular dissection of the inward rectifier potassium current (IK1) in rabbit cardiomyocytes: Evidence for heteromeric co-assembly of Kir2.1 and Kir2.2. *J Physiol* 550: 365-372, 2003.
634. Zou A, Lin Z, Humble M, Creech CD, Wagoner PK, Krafte D, Jegla TJ, Wickenden AD. Distribution and functional properties of human KCNH8 (Elk1) potassium channels. *Am J Physiol Cell Physiol* 285: C1356-C1366, 2003.